



Pervaporation for the separation of transesterification reaction mixtures

Wenqi LI

Supervisor:

Prof. Patricia Luis Alconero (UCLouvain)

Prof. Damien Debecker (UCLouvain)

Members of the Examination Committee:

Prof. Laurent Delannay (Chairman)

Prof. Bart Van der Bruggen (KUL)

Prof. Juray De Wilde (UCLouvain)

Prof. Patrick Gerin (UCLouvain)

Prof. Pieter Vandezande (VITO)

Dissertation presented in partial
fulfilment of the requirements for
the degree of PhD in Science of
Engineering and Technology

January 2019

Abstract

The increasing demand of raw materials and the risk of sources depletion are becoming the motivation for the development of new bio-based routes of synthesis of chemicals. The use non-renewable natural resources, such as fossil fuels, and the generation of greenhouse gases lead to severe environmental problems. However, one of the challenges of using renewable biomass resources to produce building molecules is to achieve an efficient and economically affordable purification step due to the complexity of the mixture and high cost of separation. Separation processes such as distillation and liquid-liquid extraction have been proposed to purify target compounds from bio-based sources. However, the high energetic cost associated with those processes is directing the current research towards the development of other alternatives. Membrane technology appears in this context in the form of pervaporation as a potential solution to minimize the energy consumption of the separation process. Pervaporation achieves the separation of challenging liquid-liquid mixtures, except non-volatile compounds. In this thesis, organic liquid mixtures from three model transesterification reactions, typically performed in the production of bio-based chemicals, were studied for the application of pervaporation separation, involving commercial membranes, self-made PEEK membranes and supported ionic liquid membranes.

The application of pervaporation for the separation of multicomponent mixtures may involve coupling effects among components and the membrane, which could increase or decrease the permeance of the target compound. The first organic mixtures from two transesterification reactions, the transesterification reaction between methyl acetate and butanol to produce methanol and butyl acetate (mixture 1), and the transesterification reaction between methanol and ethyl acetate to produce ethanol and methyl acetate (mixture 2), are studied for pervaporation separation. Both reactions are of utmost interest in the chemical industry and present high cost of separation due to the presence of azeotropic mixtures (*i.e.*, methanol/methyl acetate; butanol/butyl acetate; ethanol/ethyl acetate). The separation performance of four commercial membranes (*i.e.*, PERVAP 1255-30, PERVAP 4155-40, PERVAP 1255-50, PERVAP 4155-80) from Sulzer Chemtech, Switzerland, is evaluated. The effect of the feed concentration and the temperature on the separation performance was

studied in terms of permeance and selectivity. Results from mixture M1 indicated that the methanol is enriched in the permeates of the membranes 1255-30, 4155-40 and 1255-50 with a separation factor (methanol to butyl acetate) of 6-10. However, for the membrane 4155-80, butanol is enriched in the permeate with a separation factor (butanol to butyl acetate) around 7.5 at 40 °C. Since butanol is a reagent in the reaction, there is not practical interest in using this membrane for the separation. Regarding mixture M2, results showed that methanol is enriched in the permeate for all the membranes. The separation factor (methanol to ethyl acetate) can reach 4.5-9.5. These commercial membranes can be successfully applied in the separation of methanol from mixture M2. Coupling effects were observed when the permeance of pure solvents was compared with that of the components in the mixture. The coupling effects were analyzed by the Hansen solubility approach. It is proved that Hansen solubility parameters is a useful tool to predict potential coupling effects.

In addition, glycerol carbonate is a platform molecule with a large range of applications. It can be synthesized from glycerol by transesterification with dimethyl carbonate, which is considered a bio-based path of synthesis since glycerol is generated during the production of biodiesel. The purification of the reaction products is quite challenging and costly using conventional separation technology, since methanol (by-product) and dimethyl carbonate (in excess) form an azeotropic mixture. In this thesis, pervaporation is presented as a technological alternative to separate the multicomponent mixture composed of methanol, glycerol, dimethyl carbonate and glycerol carbonate, *i.e.*, reactants and products of the reaction of synthesis of glycerol carbonate. The separation performance of the four commercial membranes PERVAP 1255-30, PERVAP 4155-40, PERVAP 1255-50, PERVAP 4155-80 from Sulzer Chemtech, Switzerland, were evaluated. The effect of temperature (30°C, 45°C, and 60°C \pm 2 °C) on the separation performance was also studied in terms of transmembrane flux, separation factor, permeance and selectivity. Results show that the membranes cannot permeate glycerol and glycerol carbonate (not detected in the permeate), and permeate methanol and dimethyl carbonate, with higher selectivity for methanol (around 6, methanol to DMC for the membrane 1255-50 at 45 °C). In addition, the performance of pervaporation separation was compared with that obtained by distillation via the McCabe-Thiele diagram, showing the technical advantage of

pervaporation. It proves that pervaporation has a better efficiency compared to simple flash distillation.

The PVA commercial membrane can only permeate DMC and methanol. Therefore, in the following work, a dense membrane prepared by using a modified poly ether ether ketone (PEEK-WC) polymer was studied for the pervaporation separation of a binary mixture dimethyl carbonate (DMC) and methanol. Contact angle and mechanical measurements were carried out to study the properties of the membrane as well as SEM analysis to evaluate the surface morphology. The swelling degree of the membrane was studied at different concentrations of methanol. Thus, the membrane is more favorable to be swollen by DMC than methanol. When tested in a pervaporation process by varying methanol concentration and feed temperature, the transmembrane flux was found to be temperature dependent with a value of $0.14 \text{ kg/m}^2\cdot\text{h}$ at low concentration of methanol (10 mol%) with its highest separation factor being 13.4 (selective to methanol) at 30°C . The flux increased with the increase of the temperature, but the separation factor decreased. Using high concentration of methanol resulted in a high permeance of DMC due to a dragging effect caused by intermolecular interaction. Selectivity results showed that the composition of the mixture had a strong influence on the membrane performance.

Supported ionic liquid membranes (SILMs) may achieve better mass transport. Thus, two supported ionic liquid membranes based on ionic liquids 1-octyl-3-methylimidazole bis(trifluoromethanesulfonyl)imide [OMIM][NTf₂] and 1-octyl-1-methylpyrrolidine bis(trifluoromethanesulfonyl)imide [OMPyrr][NTf₂] were prepared and studied for the pervaporation separation of binary mixture dimethyl carbonate (DMC) and methanol. The SEM analysis was carried out to evaluate the surface morphology of porous membrane before and after impregnating and after their pervaporation separation applications. When tested in a pervaporation separation process by varying methanol concentration, the performance of SILMs was found to be highly concentration dependent. At low concentration of methanol (0.2 molar fraction), the SILMs tend to permeate DMC for both membranes. In general, The SILM based on [OMIM][NTf₂] shows a better performance than that of [OMPyrr][NTf₂]. The optimal transmembrane flux of [OMIM][NTf₂] based membrane was found with a value of $0.739 \text{ kg/m}^2\cdot\text{h}$, the membrane is more selective to permeate DMC with a high selectivity of 67 and separation factor 21 at 30°C . At high concentration of methanol, the permeance of

methanol increases due to dragging effects. However, the production cost of ionic liquids may be a limitation for a real application, hence, an economic evaluation should be further considered.

Table of Contents

Abstract.....	i
Table of Contents	v
List of abbreviations and symbols	ix
Chapter 1. Introduction	1
1.1 Context	2
1.2 Motivation and scope of the thesis	4
1.2.1 Transesterification reactions	4
1.2.2 Challenge of pervaporation in organic-organic separation	7
1.3 Theory to describe coupling effects	9
1.3.1 Hansen solubility theory.....	9
1.3.2 Flory-Huggins solution theory	12
1.3.3 Kamlet-Taft solvation parameters.....	13
1.4 Membrane performance evaluation	13
1.5 Objective and research questions	16
1.6 Thesis outline	17
Chapter 2. Literature review	19
2.1 Introduction.....	20
2.2 Fundamentals of pervaporation.....	23
2.3 Factors affecting pervaporation membrane performance	24
2.3.1 Membrane performance evaluation parameters	24
2.3.2 Influence of feed composition on membrane performance	25
2.3.3 Effect of temperature on membrane performance	29
2.3.4 Effect of membrane thickness on membrane performance.....	32
2.4 Coupling effects in pervaporation.....	35
2.5 Pervaporation membranes	40
2.6 Pervaporation-distillation hybrid processes in bio-based mixture separation.....	57
2.7 Reaction-pervaporation hybrid processes in bio-based mixture separation	61
2.8 Conclusion.....	65
Chapter 3. Materials and methods	66
3.1 Introduction	67
3.2 Chemicals	68
3.3 Membranes	68
3.3.1 Commercial membranes from SULZER.....	68

3.3.2 Self-made PEEK-WC membranes	70
3.3.3 Supported ionic liquid membranes	70
3.4 Pervaporation setup.....	72
3.4.1 3” round cell from Sulzer Chemtech (Sulzer unit).....	72
3.4.2 DeltaE s.r.l cell.....	73
3.5 Pervaporation experiments.....	75
3.5.1 Experiments performed with the Sulzer Unit	75
3.5.2 Experiments performed with the DeltaE s.r.l cell for binary mixtures of dimethyl carbonate and methanol (reaction 3).....	76
3.6 Gas chromatography analysis	77
3.6.1 Reaction 1 and reaction 2.....	77
3.6.2 Reaction 3.....	77
3.6.3 Samples from the experiments of supported ionic liquid membranes.....	78
3.7 Membrane characterization.....	78
3.7.1 Measurement of membrane sorption	78
3.7.2 Contact angle measurement.....	78
3.7.3 Mechanical test	79
3.7.4 Scanning electron microscopy (SEM) analysis.....	79
Chapter 4. Application of pervaporation in the production of butyl acetate and methyl acetate	80
4.1 Introduction	81
4.2 Sorption experiments	81
4.3 Pervaporation on pure solution	83
4.4 Pervaporation of mixtures	87
4.4.1 Effect of the feed composition.....	87
4.4.2 Effect of variation of the activity coefficient within the membrane	93
4.5 Conclusions	96
Chapter 5. Application of pervaporation in the production of glycerol carbonate	98
5.1 Introduction	99
5.2 Results and discussion.....	99
5.2.1 Pervaporation performance.....	99
5.3.2 Membrane performance.....	105
5.3.3 McCabe-Thiele separation diagram	110
5.4 Conclusions	112
Chapter 6. Sorption and pervaporation study of methanol/dimethyl carbonate mixture with poly(etheretherketone) (PEEK-WC) membrane.....	114
6.1 Introduction	115

6.2 Results and discussion.....	116
6.2.1 Membrane characterization: contact angle, mechanical test and SEM analysis	116
6.2.2 Sorption degree measurement	118
6.2.3 Coupling effects.....	118
6.2.4 Pervaporation performance.....	121
6.2.5 Membrane performance.....	123
6.3 Conclusions	128
Chapter 7. Pervaporation separation of methanol/dimethyl carbonate mixture by using supported ionic liquid membranes.....	129
7.1 Introduction	130
7.2 Results and discussion.....	132
7.2.1 SEM analysis	132
7.2.2 Pervaporation separation performance.....	134
7.2.3 Membrane stability.....	136
7.2.4 Comparison of DMC/methanol pervaporation separation in literature	137
7.3 Conclusions	138
Chapter 8. Conclusion and Future work	139
8.1 Summary and general conclusions	140
8.2 Future work	142
Appendices	146
Chapter 1	146
A1.1. Summarizing of the chemical structure and relevant properties of the mixture components.....	146
A1.2. Summarizing of the chemical structure of membrane materials	150
Chapter 3	151
A3.1. Reynolds number in the membrane cell estimation.....	151
Chapter 4	152
A4.1. Overall average transmembrane flux of different types of membranes for mixture M1 at 30 °C, 40 °C and 50 °C.....	152
A4.2. The separation factor of different types of membranes for the mixture M1 at 30 °C, 40 °C and 50 °C; (a) 1255-30 membrane, (b) 4155-40 membrane, (c) 1255-50 membrane and (d) 4155-80 membrane	153
A4.3. Transmembrane flux of different types of membrane for the mixture M2 at 30°C, 40°C and 50°C.....	154
A4.4. The separation factor of different types of membranes for mixture M2 at different temperature (a) 1255-30 membrane, (b) 4155-40 membrane, (c) 1255-50 membrane and (d) 4155-80 membrane	155

A4.5. Hansen solubility sphere for PVA and pure components and mixtures at 40 °C	156
A4.6. Hansen solubility sphere for PVA and pure components and mixtures at 50 °C	157
A4.7. Calculated Hansen solubility parameters of each component at 40 °C	158
A4.8. Calculated Hansen solubility parameters of each component at 50 °C	159
Chapter 6	160
A6.1. Partial flux of methanol and DMC for different concentrations.....	160
Terminology	161
References	162
Curriculum Vitae	184

List of abbreviations and symbols

M1: Mixture of Methyl acetate/Butanol//Butyl acetate/Methanol

M2: Mixture of Ethyl acetate/Methanol/Methyl acetate/Ethanol

M3: Mixture of Glycerol/Dimethyl carbonate/Glycerol carbonate/Methanol

A : the membrane active surface area (m^2)

E_P : the permeation activation energy (J/mol)

$E_{i,D}$: is activation energy for diffusion (J/mol)

ΔG^E : free energy of binary mixing (J/mol)

P_i^0 : vapor pressure (Pa)

$\Delta H_{i,S}$: the heat of solution or enthalpy of dissolution (J)

J : the permeation flux ($\text{kg/m}^2\cdot\text{h}$)

J_0 : pre-exponential factor

R : gas constant ($8.314 \text{ J/mol}\cdot\text{K}$)

R_a : the distance between the solvent and the center of polymer solubility sphere ($\text{MPa}^{1/2}$)

R_0 : interaction radius of polymer

T : temperature (K).

Δt : the collecting time (h)

x_i : mole fraction of each component

w : the weight of permeate (kg)

$S_{i,0}$ and $D_{i,0}$: temperature independent pre-exponential coefficients.

α : coefficient of thermal expansion ($^\circ\text{C}^{-1}$)

α_i : activity

$\alpha_{i/j}$: selectivity

$\beta_{i/j}$: separation factor

γ_i : activity coefficient

v : the volume fraction of the component in the binary phase,

Chapter 1. Introduction

1.1 Context

Membrane technology has achieved widely applications for separation and purification, such as in water treatment, food production and bio-chemical processes among others. Membrane separation can be generally classified according to the driving force: membrane separation with hydrostatic pressure difference as the driving force, such as microfiltration, ultrafiltration, nanofiltration and reverse osmosis; membrane separation with concentration differences as the driving force, such as dialysis, gas separation, forward osmosis and pervaporation; and membrane separation with an electrical potential difference as driving force, such as electrodialysis¹. Among these, pervaporation is a promising membrane-based technology for the separation of liquid mixtures, in which vacuum is applied in the permeate side to enhance the driving force for the separation (*i.e.*, difference in partial pressure between the feed and permeate sides). If compared to distillation or evaporation, pervaporation is a low energy consumption process because the pervaporation separation mechanism is not based on relative volatility as distillation. The separation depends on the interaction of permeants and membrane materials and only a fraction of the permeants permeate through the membrane with a phase transition (liquid to vapor)^{2,3}. Hence, lower energy consumption is required compared to distillation. In addition, pervaporation can also work at the temperature which is the optimal temperature for reaction⁴. Several studies have already confirmed the energetic advantage when using pervaporation instead of distillation, as stand-alone technology or in hybrid processes⁵. In addition, if compared to solvent extraction, which may be considered a low energy consumption process as well, it does not involve the use of toxic and/or flammable and usually expensive solvents. Pervaporation has been applied to different areas, such as organic-organic separations⁶, waste water treatment⁷, esterification reactions^{8,9} or alcohol dehydration¹⁰.

Pervaporation technology has been proposed in many studies as an alternative technology to separate azeotrope mixtures because the separation is not based on the thermodynamic liquid-vapour equilibrium but only depends on the interaction of the membrane and the permeants. The membrane provides selectivity for the compounds and determines which compounds can diffuse through it according to their affinity with the membrane. The driving force is then the gradient of chemical potential on both

sides of the membrane. Hence, the sorption and diffusion of components within the membrane determines the permeate composition¹¹. In addition, if pervaporation is integrated with equilibrium-limited reactions, it can improve the reaction yield *via* the selective removal of one of the products in the reaction mixture, thereby shifting the reaction equilibrium according to the principle of Le Châtelier-Braun. The integration of reaction and membrane separation has been extensively described by Van der Bruggen¹². These are alternatives to reactive distillation, in which the reaction and separation are also integrated. However, in reactive distillation, the separation is carried out in a traditional way using a distillation column. It is generally not the most straightforward solution because most systems of practical interest contain binary and ternary azeotropes. In addition, even when the intrinsic challenges related to the mixtures involved can be solved, reactive distillation still has the fundamental disadvantage that energy requirements related to the separation are high. Thus, novel separation processes should be developed.

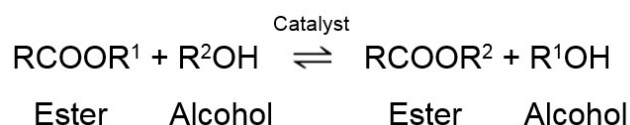
Pervaporation has thus emerged as a straightforward technology to separate streams produced during biochemical conversions, such as the production of bio-ethanol. Many studies have focused on the use of pervaporation for esterification reactions. The idea of using a pervaporation module to remove water from an esterification reaction was suggested for the first time in 1988 by Kita *et al.*¹³. The usual pathway to produce an ester is through the reaction of an acid and an alcohol, with water as the by-product. These are equilibrium reactions in which a (nearly) complete conversion can be obtained by selectively removing water through a hydrophilic pervaporation membrane. The separation of water from a mixture of organic compounds is relatively undemanding, because it is similar to the most developed application of pervaporation, *i.e.*, solvent dehydration. Many reactions, usually esterification reactions, have been studied in this context during the last decade¹⁴. The most reported esterification reaction by far is the reaction of ethanol with acetic acid to yield ethyl acetate and water^{15,16}. However, a challenge in which pervaporation is being developed is for transesterification reactions. In this case, the separation is between an ester and an alcohol (in the reaction medium), which is a difficult organic-organic separation that currently is being done by reactive distillation, at high cost. These reactions are important in, for example, the production of biodiesel. Reactive distillation has been studied and experimented already in an early stage¹⁷. It has been shown that reactive

distillation alone may not lead to a full conversion for reactions with low reaction rate¹⁸. Using pervaporation in transesterification reactions is a niche of current research^{19,20, 21} and it is the main motivation of this thesis.

1.2 Motivation and scope of the thesis

1.2.1 Transesterification reactions

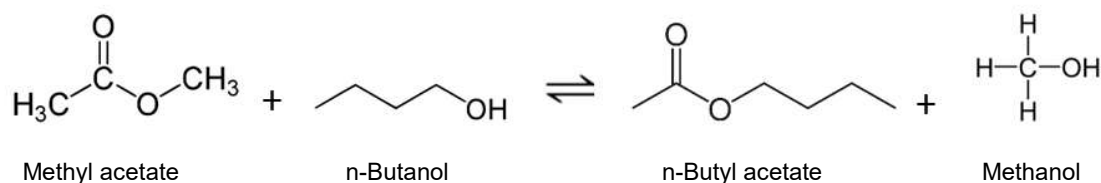
Transesterification reactions have been extensively studied in both laboratory and industry. A transesterification reaction involves the displacement of an organic group of an alcohol with an organic group of an ester²². Transesterification reactions are thus common in the synthesis of esters and can be expressed by the following general reaction equation:



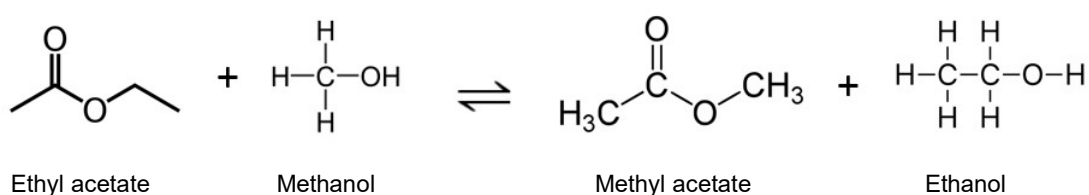
The development of renewable energy sources is critical throughout the globe because of the energy crisis caused by the depletion of petroleum reserves and the environmental concerns associated with CO₂ emissions. Nowadays, biofuels, mainly biodiesel and bioethanol production are important sources of bioenergy, which are attracting great interest as alternative energy sources derived from biomass, and they have been growing dramatically as a sulfur-free, non-toxic and biodegradable additive for fuels²³. The transesterification process of plants, vegetable oil, animal fats or dairy waste scum has been widely studied as alternative routes to obtain biodiesel, a mixture of fatty acid methyl/ethyl esters^{24–26}.

In order to advance in the understanding of organic-organic separations using pervaporation, three model transesterification reactions are studied in this thesis: i) the reaction between methyl acetate and n-butanol to produce n-butyl acetate, with methanol as by-product, ii) the reaction between methanol and ethyl acetate to produce methyl acetate, with ethanol as by-product, and iii) the reaction of glycerol and dimethyl carbonate (DMC) to produce glycerol carbonate, with methanol as by-product.

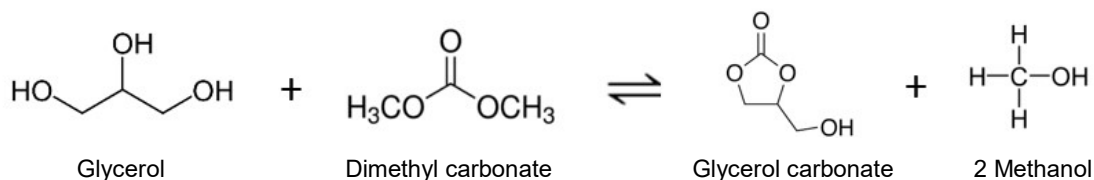
Reaction 1: transesterification reaction of methyl acetate and n-butanol to yield n-butyl acetate and methanol:



Reaction 2: transesterification of ethyl acetate and methanol to produce methyl acetate and ethanol:



Reaction 3: Transesterification reaction of glycerol and dimethyl carbonate to produce glycerol carbonate. Methanol is considered byproduct in this reaction:



Reactions 1 and 2 are characterized by a low conversion (chemical equilibrium constant close to unity) and the formation of two pairs of azeotropes: methyl acetate/methanol and butanol/butyl acetate in reaction 1, and methyl acetate/methanol and ethyl acetate/ethanol in reaction 2. Due to the high cost of separation by means of conventional methods such as distillation, pervaporation seems to be a more effective approach to consider.

Reaction 1 has been the focus of attention of several researchers since the product butyl acetate is an important and useful solvent for various applications, e.g., paint and coating manufacture and lacquer industry, and methanol is the feedstock of poly-vinyl-alcohol. For example, Jimenez *et al.*²⁷ evaluated the recovery of a mixture of methanol and 30 wt% methyl acetate from the poly(vinyl alcohol) process. This mixture was

concentrated to ~ 80 wt% methyl acetate, then it was reacted with n-butanol to produce butyl acetate by reactive distillation. O-xylene is applied as an entrainer in order to overcome the azeotrope. By combining reactive distillation and extractive distillation, a high purity of butyl acetate and high conversion of n-butanol can be achieved, however, this approach showed no economic advantage¹¹.

Reaction 2 is considered as a model reaction for the development of different catalysts for transesterification reactions^{28–30}. In this reaction, the product methyl acetate is one of the compounds in the production of biodiesel. In addition, this transesterification reaction contains a quaternary organic mixture with two azeotropes (methyl acetate/methanol and ethyl acetate/ethanol), thus, pressure swing distillation has been proposed for breaking the azeotropes and achieving separation^{31,32}. This process requires two distillation columns in which the components of the feed stream and recycle stream from the second column are separated at a specific pressure at the first column. Then, the azeotropic mixture at the bottom is separated by a second column that operates at a different pressure. This technique consumes a lot of energy and presents high capital costs.

Reaction 3 is of great interest in the chemical industry because glycerol can be an inexpensive bio-based product from the production of biodiesel. The production of biodiesel in 2006 reached 6.5 million m³³³. As a consequence, the production of biobased glycerol - a co-product of biodiesel production, representing 10 wt% of the total its production^{34–36} – has also encountered a massive increase, leading to a dramatic decrease of its value in the market from 900-950 USD/ton in 2013 to 240 USD/ton in 2014³⁷. Extensive research has been performed to convert glycerol into other value-added chemicals such as 1,3-propanediol, polyglycerols, polyurethanes, lactates, acrolein or bioethanol^{38–44}. Glycerol carbonate is one of these products and can be extremely valuable because of its low toxicity, good water solubility and biodegradability, and it can also be used as an intermediate for the production of other chemicals. Some of its applications include: solvent in the manufacture of cosmetics and pharmaceuticals, lubricating oil, solvent in lithium ion batteries and surfactant^{45,46}. Different routes can lead to the synthesis of glycerol carbonate and they have been reviewed recently⁴⁵. For example, glycerol carbonate can be prepared from glycerol and phosgene using metallic catalysts, but this process is obviously difficult to implement due to toxicity issues⁴⁷. Another route consists in a carbonation reaction

between urea and glycerol under low pressure (40-50 mbar) to shift the equilibrium and generate glycerol carbonate. The separation of the by-product ammonia is then necessary⁴⁸. Glycerol can also react with CO₂ using zeolite/Sn catalysts to obtain glycerol carbonate, but the conversion is low (max. 32% with catalyst Purosiv)⁴⁹. Finally, one direct way to produce glycerol carbonate is *via* a transesterification reaction of glycerol generally using either ethylene carbonate or dimethyl carbonate as reactants. When the former compound is used^{50,51}, the separation can be difficult because the by-product (ethylene glycol) has high boiling point (197.3 °C)⁵². On the other hand, the use of dimethyl carbonate (DMC) leads to methanol as a by-product, as indicated by Reaction 3⁵²⁻⁶⁰. It is a simple route to produce glycerol carbonate, and dimethyl carbonate is a renewable green chemical with environmentally sustainable applications⁶¹⁻⁶³. Since it is a transesterification reaction, the production yield is enhanced by using an excess of dimethyl carbonate. The boiling point of dimethyl carbonate and methanol is 90.3 °C and 64.7 °C, respectively. Thus, the use of distillation as a separation method seems to be more appealing here than for the process for glycerol carbonate synthesis involving ethylene carbonate (b.p. 243°C under atmospheric pressure) and ethylene glycol (197.3°C). In this case, however, the major challenge is the formation of an azeotropic mixture at a composition ratio of 30/70 (wt%/wt%) in DMC/methanol, making distillation energetically very unfavourable. The separation of this reaction mixture has been studied by using azeotropic distillation⁶⁴, reactive distillation and extractive distillation⁶⁵. The summarizing of the chemical structure and relevant properties of the mixture components and membrane materials are given in Appendix A1.1 and A1.2.

1.2.2 Challenge of pervaporation in organic-organic separation

The application of pervaporation to separate azeotropic mixtures has been studied and its technical feasibility is proved⁶⁶. In pervaporation, the membrane is a selective barrier that determines which molecules can pass through. The interaction between the molecules and the membrane results in the solubility and diffusivity of the component and determines if the molecules can pass through the membrane from the feed side to the permeate side. Hence, the presence of an azeotrope has no impact on the separation due to its different separation mechanism compared with distillation⁶⁷. However, the separation of organic-organic mixtures by using pervaporation is still a challenge when it comes to finding membranes able to separate two similar organic

compounds. One of the reasons of the poor selectivity of the membranes for organic-organic mixtures is caused by coupling effects. The transport mechanism of solution-diffusion can be considered for pervaporation, consisting of three stages: 1) the molecules are adsorbed on the membrane at the feed side, 2) the molecules diffuse through the membrane, and 3) the molecules are desorbed as vapor phase at the permeate side⁶⁸. Therefore, the permeation can be described in terms of solubility and diffusivity. The solubility is a thermodynamic property. In multi-component mixtures, there are interactions that influence activity coefficients between each component, and interactions between each component and the membrane⁶⁹. These will affect the amount of each component present in the membrane. The driving force is calculated from the activity coefficient and mole fraction of the component in the feed liquid⁷⁰. According to the work by Binning *et al.*⁷¹, the polymer film under permeation can be divided in two zones: the solution phase zone and the vapor phase zone. Selectivity in separating mixtures occurs at the two interfaces. The phase transition from liquid phase to vapor phase takes place within the polymer film. Therefore, the activity coefficient and mole fraction of the component liquid inside the membrane are different from those in the feed liquid due to the interaction between the component and membrane material. Hence, the real activity coefficients located at the interface of solution phase zone and vapor phase zone should be taken into account. As a result, the interface of a liquid phase and a vapor phase inside the membrane will affect this driving force. However, most of the recent research is assuming that the activity coefficients of the feed solution can be applied without taking the interaction between the solution and polymer into account. On the other hand, diffusivity is a kinetic property. When one component diffuses through the membrane faster than other components, a drag effect may occur. Fast compounds can drag slow compounds diffusing together through the membrane, leading to coupling effects. A mutual drag coefficient can be introduced to describe two coupled diffusion flows⁷². However, preferential sorption is the prerequisite to the preferential permeation⁷³. Hence, the solubility factor plays an important role on the performance of pervaporation polymeric membranes. The Hansen solubility parameters approach is a useful method to predict the solubility behavior of the solvent and polymers. For instance, the solubility of polymer and pure substance can be predicted by the Hansen solubility parameter to select appropriate solvent. In the literature^{74,75}, Hansen solubility parameters have been used extensively for the interpretation the

interaction and affinity between polymer and penetrants. Only data of the interaction of pure components were used and compared for the interpretation of coupling effects. Actually, the solubility of pure solvent and mixture may be different. The study of solubility parameter of mixture is missing. In this work, a detailed study is carried out in order to determine how the differences in solubility of a mixture and a pure substance influence the performance of pervaporation process.

The measurement of coupling effects is difficult due to coupled fluxes, in which the presence of one component can affect the transport rate of the other⁷⁶. Therefore, many studies have been carried out for binary⁷⁷ or ternary⁷⁸ systems, but the studies of multicomponent mixtures with four components⁷⁹ are scarce. Research results show that coupling effects are different in different scenarios. For example, She *et al.*⁸⁰ observed no coupling effects in pervaporation of dilute flavor organics. However, Raisi *et al.*⁸¹ found that coupling effects cannot be neglected when the presence of some aroma compounds has influence on the permeation of other aroma compounds. The pervaporation performance of alcohol - ester mixtures has been investigated by Luis *et al.*^{19,82}. However, coupling effects are not systematically studied. Thus, a deeper understanding of when and how coupling effects take place in organic-organic mixture is important.

Therefore, in this thesis, a depth study of the separation of binary and quaternary mixtures involved in the transesterification reactions indicated above using pervaporation is performed. Different membranes are studied, including commercial membranes intended for organic-organic separations as well as self-made membranes. The synthesized membranes were made of modified poly ether ether ketone (poly(oxa-p-phenylene-3,3-phthalido-p-phenylene-oxy-phenylene)), tested with the binary mixture dimethyl carbonate and methanol. Furthermore, supported ionic liquid membranes were also prepared aiming at decreasing the mass transfer resistance caused by the membrane while increasing the selectivity of the latter binary mixture.

1.3 Theory to describe coupling effects

1.3.1 Hansen solubility theory

In order to describe coupling effects, the Hansen solubility theory is applied in this thesis. Hansen⁸³ proposed an approach based on solubility parameters to predict the

solubility of components into a polymer. In pervaporation, Hansen solubility parameters are used for studying the interaction between molecules and the membrane material and their affinity, which have been widely applied in the selection of materials for membranes. The basis of the approach is to introduce three main parameters: a dispersion component, a polar component and a hydrogen bonding component, leading to a three dimensional space that is represented by a sphere. The center of the sphere is determined by the Hansen solubility parameters of the polymer and the radius of the sphere is called interaction radius, which is typically determined experimentally and reported in the literature⁸⁴. In this way, a spherical solubility region is developed in the three dimensional space. A component can be more favorable to be sorbed by the membrane if the solubility parameters of the component is located in three dimensional sphere of the membrane material.

A polymer may be soluble in a solvent or blend solvent (mixture) if the Hansen solubility parameters of the solvent are located inside the polymer solubility sphere. The distance of the pure solvent or a mixture of solvents from the center of the polymer solubility sphere is calculated by following equation⁸⁴:

$$R_a = [4(\delta_{Ds} - \delta_{Dp})^2 + (\delta_{Ps} - \delta_{Pp})^2 + (\delta_{Hs} - \delta_{Hp})^2]^{1/2} \quad (1-1)$$

where R_a is the distance between the solvent and the center of polymer solubility sphere ($\text{MPa}^{1/2}$), and δ refers to the Hansen solubility parameters. The first subscript, D , P and H , refer to the Hansen component: dispersion component, polar component and hydrogen bonding component, respectively; the second subscript, s and p , refer to the solvent and polymer, respectively. The difference of solubility parameters $\Delta\delta_{(s-p)}$ should be smaller than the interaction radius of polymer (R_0), then the solute could be sorbed by this polymer. The applied Sulzer commercial membranes in this work is polyvinyl alcohol, the interaction radius of polyvinyl alcohol is 10.9. The representation of Hansen solubility parameters in the 3D space is shown in Figure 1-1.

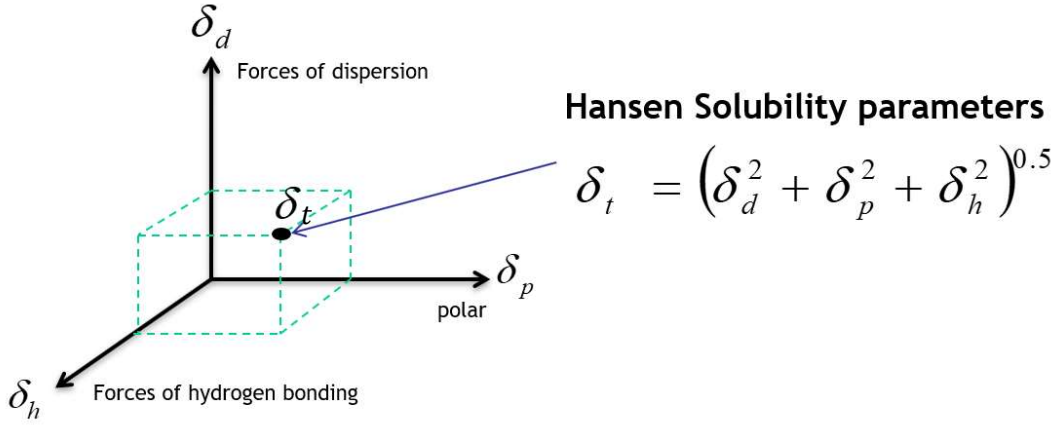


Figure 1-1. Representation of Hansen solubility parameters in the 3D space

For liquids, the change of Hansen solubility parameters due to the temperature effect can be calculated by Eq. (1-2) to (1-4) ⁸⁴:

$$\frac{d\delta_D}{dT} = -1.25 \cdot \alpha \cdot \delta_D \quad (1-2)$$

$$\frac{d\delta_P}{dT} = -0.5 \cdot \alpha \cdot \delta_P \quad (1-3)$$

$$\frac{d\delta_H}{dT} = -\delta_H \cdot (1.22 \times 10^{-3} + 0.5 \cdot \alpha) \quad (1-4)$$

where α is the coefficient of thermal expansion ($^{\circ}\text{C}^{-1}$).

The Hansen solubility parameters of the blended solvents were estimated by Eq. (1-5), suggested by Barton *et al.*⁸⁵ for calculating Hildebrand solubility parameters:

$$\bar{\delta}_k = \sum_i \phi_i \delta_{ki} \quad (1-5)$$

the subscripts k indicate the D, P and H Hansen components (dispersion component, polar component and hydrogen bonding component, respectively). ϕ_i is the volume fraction of the different pure solvents in the mixture.

The Hansen solubility parameters play an important role in the analysis of the interactions between the membrane polymer material and solvents since the solubility parameters of pure components and their mixtures are completely different. A pure component rejected by a membrane can be present in the permeate when the feed

solution is a mixture due to the change of solubility properties, resulting in coupling effects⁸⁶. Therefore, the variation of solubility parameters caused by different compositions in the feed mixture is not negligible.

1.3.2 Flory-Huggins solution theory

The difference of the activity of the components within the membrane has a contribution in causing coupling effects⁶⁹. The Flory-Huggins solution theory can be used to estimate the liquid-liquid and liquid-membrane interactions. The Flory-Huggins theory has been extended to multiple components. The Gibbs free energy of mixing is calculated as follows⁸⁷:

$$\frac{\Delta G}{RT} = \left(\sum_i \frac{\Phi_i}{m_i} \ln \Phi_i + \sum_i \sum_{j < i} \chi_{ij} \Phi_i \Phi_j \right) \sum_i n_i m_i \quad (1-6)$$

The activity coefficient of a component can be derived as:

$$\ln \gamma_i = \ln \frac{\Phi_i}{x_i} + 1 - m_i \left(\sum_{j=1}^n \frac{\Phi_j}{m_j} - \sum_{j=1}^n \Phi_j \chi_{ij} + \sum_{j=1}^n \sum_{k > j}^n \chi_{jk} \Phi_i \Phi_j \right) \quad (1-7)$$

Since the mixture is a quaternary system, indices 1-4 indicates four components in the mixture and 5 indicates the membrane-polymer (PVA). Thus, i refers to 5 components, x_i is the mole fraction of each component. m_i is the characteristic size of component i , which is related to the degree of polymerization. ϕ_1 - ϕ_5 is the mole fractions on a segment basis, it is calculated by:

$$\Phi_i = \frac{w_i v_i}{\sum_j w_j v_j} \quad (1-8)$$

where v is the specific volume (m^3/kg) and w is the mass fraction.

Therefore, the activity can be calculated as:

$$a_i = x_i \gamma_i \quad (1-9)$$

The above equations show that the activity of a component within the membrane is affected by the interaction between each component and the component-membrane material.

For the binary interaction between solvents, the interaction parameter χ_{ij} is temperature dependent and it can be calculated by⁷³

$$\chi_{ij} = \frac{1}{x_i v_j} \left[x_i \ln \frac{x_i}{v_i} + x_j \ln \frac{x_j}{v_j} + \frac{\Delta G^E}{RT} \right] \quad (1-10)$$

where x is the mole fraction of a component in the binary phase, v is the volume fraction of the component in the binary phase, ΔG^E is the excess free energy of binary mixing (J/mol).

1.3.3 Kamlet-Taft solvation parameters

Kamlet-Taft solvation parameters describe the dipolarity-polarizability of the solvents⁸⁸. It contains three parameters: α hydrogen bond donor, β hydrogen bond acceptor and π^* dipolarity/polarizability. It shows the structural and physicochemical properties of ionic liquids and solvents.

1.4 Membrane performance evaluation

The membrane performance is evaluated by the transmembrane flux, separation factor, permeance and selectivity. During the experiment, the transmembrane flux is determined by weighing the mass of permeate over time by using a balance with precision of 10^{-4} g (Mettler-Toledo, AE200, Belgium). The transmembrane flux J ($\text{kg/m}^2\cdot\text{h}$) was determined by the following equation:

$$J = \frac{w}{\Delta t \times A} \quad (1-11)$$

where A is the membrane active surface area (m^2), Δt is the collecting time (h) and w is the weight of permeate (kg).

The concentration in the feed and permeate can be measured by analytical methods, such as gas chromatography. Therefore, the experimental flux for each component (J_i) can be determined by following equation⁸²:

$$J_i = J \times y_i \quad (1-12)$$

where y_i is the molar fraction component i in the permeate side.

The permeance, $\frac{P_i}{l}$, can be calculated as follows:

$$\frac{P_i}{l} = \frac{j_i}{(x_i \times \gamma_i \times P_i^0 - y_i \times P_p)} \quad (1-13)$$

Eq. 1-13 shows that the permeance is calculated by dividing the molar flux by the driving force. Therefore, the impact of driving force is removed and the membrane performance can be evaluated. The permeance is typically expressed in GPU (1 GPU = $1 \times 10^{-6} \text{ cm}^3 \text{ (STP)}/(\text{cm}^2 \text{ s cmHg}) = 7.5005 \times 10^{-12} \text{ m s}^{-1} \text{ Pa}^{-1}$).

The activity coefficient of each component γ_i and the vapor pressure P_i^0 were calculated by Aspen Plus. The total pressure at the permeate side P_p is determined experimentally during the experiment. The composition of the permeate (y_i) and feed (x_i) solutions are determined by gas chromatography (see section 3.6).

The separation factor $\beta_{i/j}$ is defined as the ratio between the molar concentration of each component (i, j) in the permeate (y_i, y_j) and feed (x_i, x_j) solutions:

$$\beta_{i/j} = \frac{y_i/y_j}{x_i/x_j} \quad (1-14)$$

As the transmembrane flux and separation factor are influenced by the operation conditions, such as feed concentration, permeate pressure and feed temperature, the transmembrane flux and separation factor cannot reflect the affinity between molecules and membrane materials. Therefore, permeability or permeance and selectivity are introduced in order to eliminate the impact of the driving force⁷⁰. As a result, these parameters are related to the intrinsic separation properties of the membrane.

The selectivity $\alpha_{i/j}$ of the membrane is given by the ratio of permeances (or permeabilities):

$$\alpha_{i/j} = \frac{P_i/l}{P_j/l} = \frac{P_i}{P_j} \quad (1-15)$$

If the value of $\alpha_{i/j}$ is larger than 1, it indicates that the membrane is more favourable to permeate component i than component j ¹⁹.

The temperature effect on the transmembrane flux can be investigated by an Arrhenius-type equation:

$$J = J_0 \exp\left(-\frac{E_p}{RT}\right) \quad (1-16)$$

which can be also written as

$$\ln J_p = -\frac{E_p}{RT} + \ln J_0 \quad (1-17)$$

where E_p is the permeation activation energy (J/mol) and J is the permeation flux (kg/m²·h), J_0 is the pre-exponential factor, R is the gas constant (8.314 J/mol·K) and T is temperature (K). E_p and J_0 can be calculated graphically through the fitting $\ln J_p$ vs. $1/T$.

The transport rate of the permeant passing through the membrane depends on sorption and diffusion according to the solution-diffusion model, therefore, the permeability is the product of the diffusion coefficient and the sorption coefficient⁸⁹:

$$P_i = D_i \times S_i \quad (1-18)$$

where D_i and S_i are the diffusion coefficient and solubility coefficients of component i in the membrane, respectively. Both of them are temperature dependent. Considering an Arrhenius-type equation, they are expressed by⁸⁹:

$$S_i = S_{i,0} \exp\left(\frac{-\Delta H_{i,S}}{RT}\right) \quad (1-19)$$

$$D_i = D_{i,0} \exp\left(\frac{-E_{i,D}}{RT}\right) \quad (1-20)$$

where $S_{i,0}$ and $D_{i,0}$ are temperature-independent pre-exponential coefficients. $\Delta H_{i,S}$ is the heat of solution or enthalpy of dissolution. $E_{i,D}$ is activation energy for diffusion. Using equation $P_i = D_i \times S_i$

$$P_i = D_{i,0} S_{i,0} \exp\left(-\frac{E_{i,D} + \Delta H_{i,S}}{RT}\right) \quad (1-21)$$

Therefore, the activation energy of permeation is expressed by the following equation⁹⁰:

$$E_{i,P} = E_{i,D} + \Delta H_{i,S} \quad (1-22)$$

The increase of temperature improves diffusion; therefore, the activation energy of diffusion $E_{i,D}$ is usually positive. This is the energy to produce free volume between the polymer chains, which allows the permeant molecule to diffuse through and jump from one created free volume to another⁹¹. The heat of solution is the heat generated or absorbed during the sorption process, which also depends on the sorption mechanisms dominated during the sorption process⁹². If the sorption follows Henry's law, the sorption process will be endothermic because a site has to be formed before the molecule can be sorbed by that site. Otherwise, in the case of Langmuir sorption, the molecule can be sorbed by a site that already exists in the polymer matrix and presents exothermic sorption. A low activation energy indicates that the molecules have to overcome a low energy barrier for the permeation through the membrane.

In order to evaluate the temperature effect on the permeance, an Arrhenius-type equation is applied as follows⁸²:

$$\frac{P_i}{l} = \frac{P_{i,\infty}}{l} \times \exp\left(-\frac{1000 \times E_a}{RT}\right) \quad (1-23)$$

where P_i/l is the permeance of the component i , $P_{i,\infty}/l$ is the pre-exponential factor of permeance and E_a is the activation energy. The effect of temperature on the permeance is estimated in terms of the activation energy. From the equations above, it can be observed that an increase of temperature accelerates diffusion and, as a consequence, the activation energy of diffusion $E_{i,D}$ is usually positive.

1.5 Objective and research questions

The general objective of this thesis is to separate organic liquid mixtures from transesterification reactions using pervaporation, understanding the mechanisms

behind the separation, such as sorption and diffusion through the membrane and possible coupling effects. The study focuses on the following objectives:

1. Development of an in-depth experimental study of the separation of products and/or reagents in three model transesterification reactions as mentioned in section 1.2, and determination of the potential application of pervaporation as stand-alone technology using current commercial membranes.
2. Development of novel polymeric membranes as well as supported liquid membranes and experimental determination of the pervaporation performance.
3. Investigating the coupling effect resulting from the interaction among liquid molecules and between those and the membrane material.

In this thesis, the following research questions have been proposed:

- Are commercial membranes able to achieve the separation of the studied transesterification mixtures?
- Do PEEK-based membranes have appropriate properties and high performance for the separation of the studied mixtures?
- What is the effect of the temperature and feed composition on the flux and selectivity?
- Is it possible to apply theories based on solubility parameters, which is commonly used in material screening, to predict potential coupling effects in the separation?
- Does the intermolecular interaction have impact on the permeation behaviour?
- How is the performance of novel supported ionic liquid membranes compared to available membranes in the literature for the separation of methanol/DMC?

1.6 Thesis outline

The content of this thesis is organized as follows: Chapter 1 represents the general introduction and objectives of this thesis. Chapter 2 is a literature study on pervaporation separation of organic liquid mixtures in the context of bio-based applications. The motivation of this chapter is to have an overview of the application of pervaporation in this field, including the important factors affecting on pervaporation separation performance, membrane materials and application of pervaporation

(distillation pervaporation hybrid processes and reaction pervaporation hybrid processes). Chapter 3 describes the experimental set-up, materials, analytical methods, calculation of performance parameters, preparation of PEEK-based membranes and supported ionic liquid membranes and experimental procedures. In Chapter 4, the application of pervaporation in the production of butyl acetate and methyl acetate is shown, using current novel commercial membranes. The impact of coupling effects in organic-organic separation was investigated. Chapter 5 presents the study of the application of commercial membranes on the separation of a quaternary mixture resulting from the synthesis of glycerol carbonate. The obtained permeate only contains dimethyl carbonate and methanol. Therefore, in Chapter 6, the separation of binary organic mixture, dimethyl carbonate and methanol, is studied. In this case, a novel type of PEEK membrane is introduced, because the literature suggests that it could be a suitable material for permeating methanol. In addition, in order to have improved mass transfer, supported ionic liquid membranes (SILMs) were introduced. Chapter 7 illustrates the performance of SILMs for the separation of the binary mixture dimethyl carbonate/methanol. Chapter 8 gives a general conclusion of this work and suggests future work and perspectives.

Chapter 2. Literature review

Based on:

Wenqi Li, Julien Estager, Jean-Christophe M. Monbaliu, Damien P. Debecker, Patricia Luis, Separation of bio-based chemicals using pervaporation: a review.

2.1 Introduction

With the increase of population and economic development, the sustainable demand of raw materials across the world becomes a key challenge for the future. In 2015, five priorities for the UN Sustainable Development Goals were mentioned in order to implement the 17 sustainable development Goals⁹³. Climate change is one of the main priorities, thus, research on the substitution of crude oil has been carried out since the late 90s due to the price hiking⁹⁴. Recently, there are many efforts to develop new technologies to produce renewable resources in order to replace petroleum-based materials. The ultimate goal is to ensure a sustainable future while protecting the environment and reducing pollution.

The application of non-renewable natural resources, such as fossil fuels, is classified in two categories: energy applications and non-energy applications⁹⁵. The typical example of energy applications is power generation from fossil fuels, which has led to a rapid growth in greenhouse gas emissions. On the other hand, non-energy applications are mainly those oriented to the synthesis of organic chemicals and polymers of great importance to our daily life due to their wide use. These materials can be used in electronics, packaging, construction, sports industry, textile industry, pharmaceutical industry, plastics industry, food industry, etc. The majority of organic chemicals and polymers are refined from non-renewable natural resources to produce ethylene, ammonia, methanol, bitumen, lubricants, aromatics, etc. These products are important building blocks and intermediates for further conversion to different specialty chemicals with specific functions and attributes.

In 2000, the share of non-energy applications from non-renewable resources was 13.2% in OCED countries⁹⁶. In the work by Shen *et al.* (2009)⁹⁷, it is concluded that 9% of all fossil fuel and 16% of oil products are used for non-energy applications and around 330 million tons of feedstock chemicals and polymers of global petrochemical production are produced every year. Thus, the use of renewable resources is a key to decrease greenhouse gas emissions from non-renewable raw materials and prevent climate change⁹⁸.

In the report “Industrial material use of biomass basic data for Germany, Europe and the World” elaborated by Achim *et al.*⁹⁹, it is discussed that most of the feedstock of

chemicals and polymers obtained from petrochemical production can be also derived from renewable raw materials, such as starch, chemical pulp, proteins, glycerol, natural fibers, medicinal plants, etc. These extracted or biochemical converted raw materials can be applied in different fields, for instance, in the chemical industry, oleo-chemistry, textile industry, pharmaceutical and cosmetics industry and so on. However, the chemical feedstock of bio-based renewable raw materials is still not able to replace those produced by petrochemical production, because the production cost is one of the major concerns.

Biomass is a complex heterogeneous mixture of organics and inorganics that contains all kinds of solids and liquids mixtures¹⁰⁰; a biorefinery is a facility to convert biomass into a series of products, including bio-fuel, specialty chemicals and other valuable intermediates¹⁰¹. This process can be analogous to traditional petroleum refinery, which produces different types of fuels, energy and chemicals from crude oil¹⁰². For example, biodiesel may be produced from different natural sources, such as oils/fats and alcohols, through a transesterification reaction with a base, acid or enzymatic catalyst.

Among the entire processes, separation and purification of mixtures of bio-based chemicals is of great importance to produce the chemicals with the desired purity level for future applications in the industry. Many reactions, such as transesterification reactions, produce multicomponent mixtures. It is necessary to have a separation process to separate the desired chemicals from the mixture. The complexity of the mixture and the separation can be a challenging task, not only technically but also economically. Physical separations, evaporation, distillation, extraction, adsorption, crystallization and membrane technology are nowadays major technologies for separation. Membrane technology is one of the promising separation technologies due to its low energy consumption and environmental friendly process. In addition, membrane separation processes can be carried out at low temperature in order to preserve temperature sensitive chemicals.

Among different types of membrane processes, pervaporation is a promising technology for liquid-liquid separation: organic-water mixtures and organic-organic solvent mixtures. The selective separation of organic mixtures is a challenging issue in the chemical industry. Most industrial scale separation processes, such as

conventional distillation, are energy intensive processes, and sometimes a large quantity of waste is generated¹⁰³. Solvent extraction is a lower energy consumption process, but the choice of the solvent has some specific requirements: toxicity, flammability, selectivity and economy. Therefore, pervaporation has been considered as an alternative solution because no additional solvents are required. It has been applied for various mixtures, such as organic-organic separations⁶, waste water treatment⁷, dehydration for esterification reactions^{8,9} and alcohol dehydration¹⁰. In addition, pervaporation has been also combined with a reactor leading to a reaction-separation hybrid process in order to improve the conversion of especially equilibrium-limited reactions. The pervaporation membrane can selectively remove a product or by-product from the reaction mixture, shifting the reaction to a higher production yield based on Le Châtelier-Braun principle. Besides, pervaporation has the advantage of separating azeotropic mixtures because the separation mechanism is not based on the thermodynamic equilibrium but on the interaction between molecules and the membrane material. Consequently, the separation performance of pervaporation highly depends on the affinity of the molecules for the membrane materials.

Pervaporation membranes are commonly nonporous dense membranes that act as a barrier to provide selectivity for the mixed compounds¹¹. During the process, the liquid feed mixture is transported by a pump and contacts the active layer of the membrane. On the other side of the membrane, vacuum is applied in order to have larger driving force. Therefore, the driving force of pervaporation is the difference of the gradient of chemical potential on both sides of the membrane. A phase transformation, from liquid phase to vapor phase, takes place inside the membrane. The molecules diffuse through the membrane and then desorb on the permeate side. The solution-diffusion model is widely employed to describe mass transport in pervaporation⁶⁸. It considers three steps: sorption, diffusion and desorption. Many factors influence the mass transport in pervaporation, such as temperature, membrane thickness, concentration, etc.

In general, pervaporation separation has been studied widely. Different reviews on pervaporation separation are available, which cover several aspects of pervaporation, such as the use of polymeric membranes in pervaporation¹⁰⁴, pervaporation in biorefinery applications¹⁰⁵, separation of organic-organic mixtures and pervaporation on fermentation processes¹⁰⁶. In this literature study, the objective is to give a

comprehensive overview on recent advances of the pervaporation separation of renewable bio-based chemicals. A discussion on the pervaporation performance and coupling effects during the separation is included, as well as the description of hybrid processes in the separation of bio-based chemicals.

2.2 Fundamentals of pervaporation

Pervaporation is a separation process in which the membrane is in contact with a homogeneous liquid (feed side) and vacuum is applied in the other side of the membrane (permeate side). Differently to gas permeation, in pervaporation, the feed is liquid and it is absorbed into the polymer membrane, thus, the membrane is partially wetted by the solution, which may produce membrane swelling⁷¹. Figure 2-1 shows the liquid phase zone and the vapor phase zone in the membrane when the membrane is under operation.

The principle of membrane transport can be interpreted by two models. These two models are the pore-flow model¹⁰⁷ and the solution-diffusion model¹⁰⁸. The pore flow model contains three steps: (1) The liquid transport from the pore inlet to the liquid-vapor phase boundary; (2) the liquid evaporated at the phase boundary; (3) vapor phase transport from the phase boundary to the pore outlet. This model is common to describe the mass transport in porous membranes, such as ultrafiltration and microfiltration membranes. For pervaporation, the solution-diffusion model is extensively used¹⁰⁹. The solution-diffusion model consists of three steps as well: (1) sorption of the penetrant molecules in the liquid at feed side of the surface of the membrane; (2) the penetrant molecules diffuse through the membrane; and (3) desorption of the permeate in vapor phase at the permeate side of the surface of the membrane. Hence, the solution diffusion model is widely accepted and applied for the interpretation of transport mechanisms in pervaporation as the chemical potential gradient within the membrane is expressed by the concentration gradient. A detailed derivation of equations of this model can be found in the work of Wijmans⁶⁸. It is generally assumed that a thermodynamic equilibrium is present at the interface of membrane and feed liquid. Thus, the transmembrane transport can be written as:

$$J_i = \frac{P_i^G}{l} (p_{i,o} - p_{i,v}) \quad (2-1)$$

where J_i is the partial flux of component i , P_i^G is permeability coefficient, $p_{i,o}$ is the partial vapor pressure of i in equilibrium with the feed liquid. $p_{i,v}$ is the pressure at the permeate side. From the equation, it can be seen that the driving force can be simplified by expressing it in terms of the difference of partial pressure across the membrane. The vapor pressure of the components in the feed is an important factor to determine the performance of permeation. The effect of pressure on the transmembrane flux has been studied by Thompson: a higher transmembrane flux can be obtained when the pressure in the permeate side is decreased¹¹⁰.

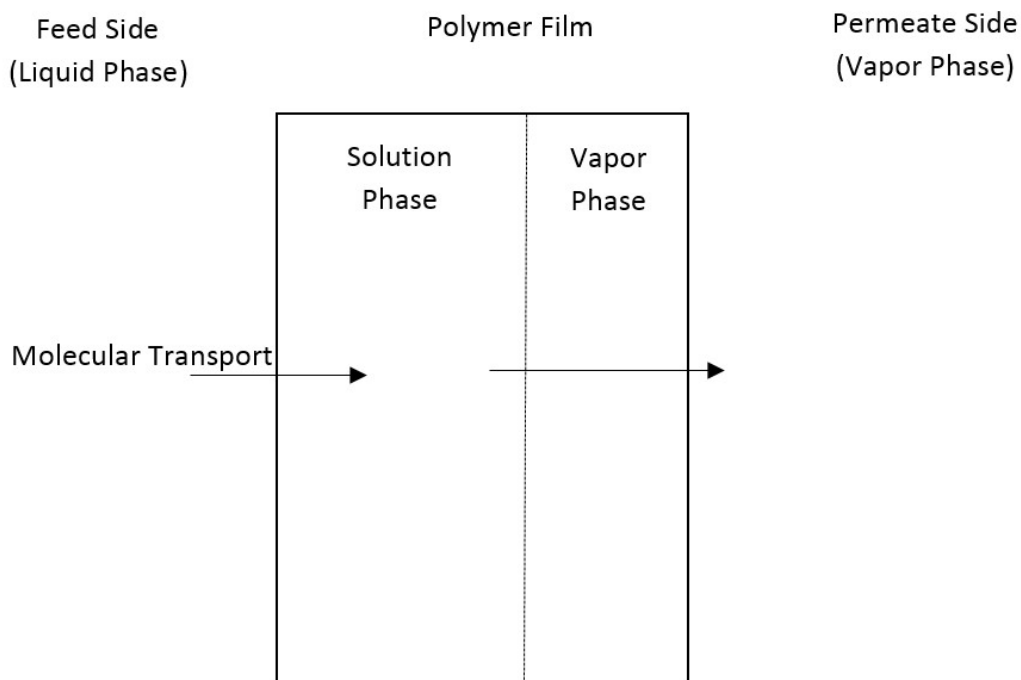


Figure 2-1. A liquid phase zone and a vapor phase zone are distinguished inside the membrane

2.3 Factors affecting pervaporation membrane performance

2.3.1 Membrane performance evaluation parameters

The experimental performance of separation *via* pervaporation is typically evaluated by studying the transmembrane flux, separation factor, permeance (or permeability) and selectivity. The detailed calculation of these parameters can be found in section 1.4.

2.3.2 Influence of feed composition on membrane performance

2.3.2.1 Influence on polymeric membrane swelling and plasticization

Polymeric membrane swelling is a phenomenon in which solvents diffuse into polymer chains and expand the polymer network¹¹¹. As the polymer-polymer interaction is stronger than the polymer-solvent interaction, the dissolution of polymeric membrane does not occur. In the separation of bio-based chemicals with pervaporation, when a liquid mixture contacts the membrane, the components can usually cause a swelling effect on the polymer membrane resulting in an increase of the free volume within the polymeric membrane matrix. The membrane swelling phenomenon has an important impact on the membrane performance, affecting the permeability of components and the selectivity. For example, water can cause membrane swelling during dehydrating processes. In the study of hybrid membranes of ZIF-L and ZIF-8 for dehydrating bio-ethanol¹¹², the membrane experienced excessive swelling at high water concentration; both water and ethanol flux were increased due to the raise of water concentration in the mixture. It is observed that the ethanol flux increases dramatically when a high water concentration is presented in the mixture. Ethanol is more sensitive to the expansion of polymer chain spacing because the ethanol molecule has a larger kinetic diameter¹¹³. As a result, the separation factor decreases with the increase of water concentration. In addition, the permeance of water and ethanol also increases with the increase of water concentration in the mixture, whereas the selectivity decreases.

The plasticization effect may occur due to the increase of the membrane swelling degree produced by the solvents. The presence of specific chemicals inside the membrane can change the mechanical properties of a given polymer and lead to a more flexible membrane and increase the diffusivity of the permeant^{114,115}. Hence, membrane swelling can result in plasticization. The concentration of the mixture has an influence on the plasticization effect due to the interaction between specific chemicals and membrane. For example, in the work by Cao *et al.*¹¹⁶, the separation of methanol/MTBE with a cellulose triacetate membrane was studied to break the azeotropes (68 wt% MTBE in methanol) in the context of bio-MTBE production (gasoline oxygenate from the reaction between bio-methanol and isobutene in order to decrease automotive carbon monoxide emissions)¹¹⁷. During the pervaporation of

the methanol/MTBE mixture with a concentration of methanol in the feed of 13.04 wt%, 19.41 wt% and 37.52 wt%, the observed plasticization effect enhanced when the methanol concentration increased in the mixture, resulting in an enhancement of the permeation of MTBE due to the increased free volume. Particularly on the feed side, a significant phase transition of polymer from glassy to rubbery takes place. As a result, the polymer plasticization effect becomes serious due to excessive membrane swelling, it increases the polymer chain spacing dramatically and more free volume can be created due to creep of polymer chains. This effect facilitates the permeation of MTBE through the membrane leading to more permeation of compounds through the membrane¹¹⁸. The plasticization effect has a great negative impact on the performance of the pervaporation membrane in terms of selectivity or separation factor. It is important to know that membrane swelling can lead to plasticization, but it does not necessarily occur.

As excessive membrane swelling leads to a lower membrane separation performance, research was carried out to reduce the membrane swelling effect. The swelling effect can be counterbalanced by introducing another polymer to form a blend membrane. In the separation of the mixture ethanol/ETBE with polypyrrolidinone based blend membrane with N-[3-(trimethylamoniopropyl)] methacrylamidemethylsulfate (TMA)¹¹⁹, pyrrolidinone was found to increase strongly the membrane affinity for ethanol. However, the membrane could be swollen severely by ethanol. As a result, a coupling transport phenomenon was observed: the higher the ethanol concentration in the feed, the higher the ether flux through the copolymer membrane, leading to a selectivity drop. When TMA polymer was introduced in the copolymer membrane, the TMA crosslinking effect prevented membrane swelling because of ammonium sulfate residues in TMA, due to its strong polar feature of the material. Therefore, a low concentration of pyrrolidinone content and a high TMA content in the membrane can reduce the swelling effect. Pure pyrrolidinone suffered severe swollen by excess of ethanol. Yet, the higher amount of TMA in the copolymer membrane also resulted in a lower overall transmembrane flux but improving membrane selectivity.

2.3.2.2 Modification of solubility parameters of the mixture

The basic theory of Hansen solubility parameters has been illustrated in section 1.3.1. As solubility parameters depend on the composition of the mixture, the position of the solubility parameters of a mixture mapping on the three dimensional space shifts from their pure solution. Therefore, when shifting towards to the center of the polymer sphere, the mixture is more favourable to be sorbed by the membrane. In the case of the pervaporation separation of an organic liquid-water mixture by a copolymer membrane (polydimethylsiloxane and ladder-like phenylsilsesquioxane)¹²⁰, it was found that the transmembrane flux and separation factor follow the trend methanol < ethanol < 2-propanol < acetone < THF. This sequence corresponds to the decrease of solubility parameters of these organic compounds regardless of their molecular size. Therefore, in this case, the permeation behaviour is determined by the solubility parameters of the organic compounds; the molecular size is less important. In other words, according to the solution diffusion model, sorption is more dominant than diffusion in the permeation of these organic compounds.

The solubility parameter also indicates the affinity between the organic compound and the polymer, and it has an inseparable relationship with membrane swelling¹²¹. Yamaguchi *et al.*¹²² studied the solubility of a polymethyl acrylate membrane prepared by plasma graft polymerization for 54 organic compounds and water. These organic compounds and water were classified as soluble and insoluble component mixtures for the membrane. In the separation of a benzene-cyclohexane mixture, according to the solubility parameter prediction, the polymethyl acrylate membrane shows high affinity to benzene over a large concentration range. However, the transmembrane flux increases and the separation factor decreases with the increase of benzene concentration in the feed since the solubility parameter of the mixture was getting closer to the center of polymethyl acrylate polymer three dimensional sphere. This indicates that the mixture has more affinity to the polymeric membrane, especially benzene, because it has a high concentration in the mixture. As a result, the degree of membrane swelling increased due to the higher benzene concentration in the mixture. Furthermore, plasticization of the polymeric membrane can take place. Consequently, the selectivity of the pervaporation membrane was reduced by plasticization effects due to the increase of the benzene concentration in the mixture.

In summary, solubility parameters are a useful tool not only to screen and to select membrane materials for a targeted separation of bio-based chemicals, but also to predict possible affinities between the membrane material and components, and the potential of membrane swelling.

2.3.1.3 Influence on pH of the feed

Organic acids, such as formic acid, acetic acid, lactic acid, propionic acid or butanoic acid, are important bio-based raw material for synthesizing other useful materials. A large number of catalytic systems have been developed to convert biomass (including cellulose, lignin, etc.) into organic acids, which can be used in chemical industries directly or act as building blocks for further applications^{123,124}. The pH becomes an important factor in the application of the permeation of organic acids in pervaporation. The pH level in the feed solution determines the degree of dissociation of each organic acid. Therefore, the permeation of an undissociated (uncharged) compound only depends on the interaction between the compound and the membrane material (for example, a polar or non-polar membrane). On the other hand, the dissociated (charged) form would not be able to diffuse through pervaporation membranes^{125,126}. At low pH level, the organic acids are mainly not dissociated, whereas the proportion of dissociated organic acids increases when the pH in the mixture increases.

In Overington's works¹²⁷, pervaporation was used to separate organic acids (acetic acid, butanoic acid, hexanoic acid and octanoic acid), ketones (2-heptanone and 2-nonanone) and esters (ethyl butanoate, ethyl hexanoate and ethyl octanoate) in mixtures. At low pH (2.5-3.5), more than 94% organic acids was in the non-dissociated form in the feed mixture and the enrichment factor (the ratio of a component's concentration in the permeate to its concentration in the feed) was the highest for these organic acids. When the pH level increased from 2.5 to 4.8 and further increases up to 7, more and more organic acids were dissociated, and a lower enrichment factor was observed. At pH 7, the enrichment factor of these organic acids was decreased by 84% due to their dissociation. As less organic acids can be adsorbed by the hydrophobic polydimethylsiloxane membrane due to the dissociation at high pH, the competition between permeants for the sites in the membrane becomes less. This situation would be more favourable to esters and ketones to be permeated through the membrane. Organic acids were concentrated more effectively when the pH remained below 3.5.

Therefore, pervaporation permeation performance can be altered due to the sorption and diffusion behaviour caused by the chemical environment, for example, the presence of acidic conditions.

In other cases, a low pH may not be preferred for the pervaporation separation. A silicalite membrane is an ethanol permselective membrane and exhibits a good separation performance for ethanol/water mixture¹²⁸. This membrane can be directly applied to produce highly concentrated bioethanol from fermentation via fermentation-pervaporation. However, the pervaporation performance could be deteriorated due to the presence of succinic acid, which can be absorbed by silicalite membrane. Ikegami *et al.* studied the pervaporation performance of the ternary mixture ethanol/water/succinic acid by using silicalite membrane double-coated with silicone rubbers¹²⁹. The ethanol permeation decreased dramatically when the pH is below 5 because the concentration of non-dissociated succinic acid is increased proportionally at lower pH. As a result, more non-dissociated succinic acid can be absorbed by silicalite membrane resulting in drastically decreasing ethanol permeation.

2.3.3 Effect of temperature on membrane performance

Temperature is one of the most important factors affecting the membrane performance. The interpretation of the effect of temperature can be done by analysing the activation energy. The basic theory and calculation of activation energy has been discussed in section 1.4. The dehydration of butyl acetate is one of the typical examples for the impact of activation energy on the permeation behaviour. The temperature variation has influence on the activation energy of water and butyl acetate when polyvinyl alcohol (PVA) and chitosan (CS) blend membrane was used¹³⁰. The blend membrane polyvinyl alcohol and chitosan gave a better separation performance at high temperature (70 °C). The activation energy of water was 23.77 kJ/mol, and -56.44 kJ/mol for butyl acetate, respectively. The activation energy illustrates the sensitivity of molecule permeation to the temperature. As the activation energy of water is positive, it indicates that the permeation behaviour of water is dominated by diffusion. However, for butyl acetate it is negative, which means that the permeation behaviour is controlled by sorption: a higher temperature is not in favour of molecular permeation. As a result, the permeance of water increased linearly and the butyl acetate decreased with the rise in temperature. Due to this contradictory permeation behaviour, the separation

performance is significantly improved at higher temperature. Another typical example was performed by Adymkanov *et al.*¹³¹. They studied the temperature effect on the permeation for water, ethanol and butanol from 30 to 50 °C. It shows that the activation energy is an important factor that determines selectivity. As water has a higher activation energy than alcohols in a PIM-1 membrane, the selectivity of this hydrophobic membrane tends to worsen with increasing of temperature.

Apart from the temperature effect, the composition in the mixture can have an impact on the activation energy as well. In the ethanol purification from methanol using a polybenzoxazineimide (PBOI) membrane¹³², the activation energy of methanol is generally lower than that of ethanol (Table 2-1).

The methanol molecules have to overcome a lower energy barrier for the permeation through the membrane than ethanol. Therefore, the membrane shows a better permeation to methanol. On the other hand, when the concentration of methanol increases in the feed, the activation energy of methanol decreases. From Table 2-1, it can be seen that the activation energy of methanol is the highest at 20 wt% and the lowest at 5 wt% of methanol in the feed at the same temperature, respectively. An increase in temperature and methanol concentration are therefore more pronounced for methanol permeation.

As indicated in section 1.4, the transmembrane flux and separation factor depend on the driving force, which can be expressed as (see Eq. (1-13)):

$$\text{driving force} = x_i \times \gamma_i \times P_i^0 - y_i \times P_p \quad (2-2)$$

where x_i is the molar fraction in the feed, γ_i is the activity coefficient, y_i is the permeate molar fraction and P_p is the total pressure at the permeate side. P_i^0 is the saturated vapor pressure, which were determined from the Antoine equation:

$$P_i^0 = 10^{A - \frac{B}{C+T}} \quad (2-3)$$

where P_i^0 is the vapor pressure, T is temperature and A , B and C are component-specific constants.

Table 2-1. Activation energy of methanol and ethanol permeation. Reprinted with permission from Pulyalina *et al.*¹³².

Feed composition (wt%)		Activation energy of permeation E_p (kJ/mol)	
Methanol	Ethanol	Methanol	Ethanol
5	80	14.5	17.0
10	90	14.0	15.0
20	80	12.5	13.5

From the Antoine equation, it can be seen that when the temperature increases, the saturated vapor pressure also increases. As a result, upon a temperature increase, the driving force is improved. Hence, an increase of temperature can have a positive impact on the transmembrane flux. In the permeate side, the partial pressure is extremely low, thus, the term $y_i \times P_p$ in Eq. (2-2) is normally negligible. For example, pervaporation is applied for removing water from esterification reaction lactic acid and ethanol to enhance the yield of ethyl acetate via chitosan-TEOS membrane¹³³. The vapor pressure of all penetrants increased with increasing the temperature. As a result, the partial pressure gradient across the membrane is increased and enhanced the driving force of each penetrant. However, the partial flux of ethanol increases more than that of water because ethanol is more volatile than water.

In some cases, the effect of temperature on the transmembrane flux and permeance is opposite¹⁹: Increasing the temperature leads to an increase in transmembrane flux, but a decrease of permeance. It is important to understand the relation between transmembrane flux and permeance. The transmembrane flux and separation factor depend on the operational conditions related to the driving force. However, the permeance and selectivity reveal the real interaction between the molecules and membrane materials. A high permeance indicates that the affinity between certain molecules and the membrane material is high and the membrane is more favourable to permeate this molecule. Therefore, when a novel application for the pervaporation separation for bio-based chemical mixtures is developed, the evaluation of the thermodynamic properties of the target mixture and intrinsic properties of the membrane for separating the mixture are essential. Luis *et al.*⁸² studied a quaternary mixture composed of methanol, methyl acetate, butanol and butyl acetate as a case

study. A procedure is proposed in order to evaluate the separation potential of pervaporation membranes: 1) Evaluation of the driving force of each compound: the compounds with the largest driving force can be determined as target compounds for permeation; 2) determining the permeances and selectivities of membranes experimentally; the optimal situation is when the membrane can enhance the permeation of the compounds with highest driving force in step 1; 3) a McCabe-Thiele separation diagram is set up for comparing the separation properties of pervaporation membranes and performance with distillation. With this procedure, it can be concluded whether the pervaporation process is able to achieve the best performance under optimal conditions. The ideal situation would be that the membrane permeates the target components and these components have the largest driving force. As a result, the feasibility of applying pervaporation can be determined.

2.3.4 Effect of membrane thickness on membrane performance

The membrane thickness is also an important factor determining the performance of pervaporation membrane separation of bio-based chemical mixtures. The general conclusion reported in several studies is that a thicker membrane reduces the flux but increases the selectivity.

In pervaporation, the decrease of selectivity could be observed when thickness of the membrane is reduced. An example is the study by Brun *et al.* on 1,3-butadiene¹³⁴, which is an important intermediate for synthesizing other materials and it is a commodity having large market. Traditionally, it is a by-product of stream cracking of naphtha of petroleum for the production of ethylene. Due to the sustainable concern of consumption of fossil stock, the renewable route to produce 1,3-butadiene from bio-butanol is proposed¹³⁵. The purification process includes the separation of 1,3-butadiene and the intermediate product isobutene which is generated during butanol dehydration. In the separation by pervaporation of a mixture of 1,3-butadiene and isobutene (60/40 volume fraction), it was found that the transmembrane flux was inversely proportional to the nitrile rubber membrane thickness (12 – 500 μm)¹³⁴. The selectivity was independent on the membrane thickness when the thickness is above 100 μm . The interpretation of this observation is that the membrane material is an elastomer and made up of very thin grains. Therefore, highly tortuous micro-pores are

present inside the membrane material. When the membrane thickness is comparable to the size of thin grains, a micro-pore diffusion can occur.

The defects inside the membrane also have a strong influence on the performance of a thin membrane. The biological route to produce acetic acid involves fermentation; the purification process involves to remove water as it is a by-product¹³⁶. In the work of dehydration of acetic acid by using polysulfone (PSf), poly (vinyl chloride) (PVC), and polyacrylonitrile (PAN) membranes, a linear relationship was found between the total flux and the reciprocal membrane thickness¹³⁷. Regarding the selectivity, it was dependent of the membrane thickness when it is thinner than 15 μm . Below this thickness, the selectivity decreases with the decrease of membrane thickness. This phenomenon is explained by the formation of defects during pervaporation, regardless of polymer morphology or transport coupling. When a critical strain of polymeric material has been reached, crazes and cracks can be formed. In a chemically active environment, the formation of crazes can be intensified because the polymeric materials undergo plasticization and the surface energy for the formation of craze is lower. The transportation through these solvent-induced craze defects can be described by Knudsen flow.

A similar observation was made for chitosan membranes for the separation of water-ethanol mixtures¹³⁸. The results showed that the transmembrane flux does not always follow Fick's law and that selectivity is a function of membrane thickness when it is less than 30 μm . On the other hand, a higher and constant selectivity can be observed when the membrane thickness is higher than 50 μm . The selectivity begins to decrease when the membrane thickness is decreasing below this level. Hence, a minimum membrane thickness (critical thickness) is essential to determine the intrinsic selectivity of the membrane. Furthermore, the partial flux of each component shows a reversely proportional relationship to the membrane thickness when the membrane thickness is higher than critical thickness. A non-Fickian behaviour of partial flux is observed at low membrane thickness (smaller than critical thickness); a lower membrane thickness yields a higher partial flux. This phenomenon is interpreted by the growth of crazes in the direction of diffusion when the liquid is enriching at the tip of crazes. Crazes are fine crack-like striations, which were affected by solvents, surface treatment and various environmental agents¹³⁹. Koops *et al.* suggested that a minimum membrane thickness has to be determined in order to stop the growth of crazes, because part of

the flux is caused by crazes¹³⁷. The lack of mechanical stability of the membrane can lead to a breakthrough of the crazes. The growth of crazes is easier in thinner membranes, hence, the overall membrane flux of a thinner membrane increases and the selectivity decreases when a significant breakthrough of crazes occurs¹⁴⁰.

Besides, Kanti *et al.*¹⁴¹ tested different thicknesses from 25 to 190 μm of blend membranes of chitosan and sodium alginate. These membranes were studied for the dehydration of a mixture of ethanol-water (95.4wt%-4.6wt%). It was found that the flux is gradually decreasing with an increase of membrane thickness at the same operation conditions because the diffusion rate decreases when the membrane thickness increases. On the other hand, the selectivity increased dramatically (from 436.3 to 2118.5) with increasing membrane thickness. The variation of selectivity with membrane thickness was related to membrane swelling and plasticization. A thinner membrane active layer may be swollen and plasticized, and allow all the permeating components in feed solution diffuse through the membrane layer unrestrictedly. In opposition to a thicker membrane, when the membrane is only partially swollen and plasticized, the thickness of a non-swollen layer increases with the entire membrane thickness leading to an increasing of mass transfer resistance inside the membrane. As the non-swollen layer gives a restrictive barrier and only allows certain penetrants to diffuse through resulting in a decreasing flux and enhancing the selectivity. Similar phenomena were also observed in the separation of water acetamide by a chitosan membrane¹⁴².

On the other hand, a thicker membrane can enhance the mass transfer resistance resulting in a decrease of the flux. In the separation of a methanol/MTBE mixture, Villaluenga *et al.* studied the mass transfer behavior in terms of the resistance-in-series model with a cellulose acetate membrane and poly(2,6-dimethyl-1,4-phenylene oxide) membrane¹⁴³. It was found that the liquid membrane boundary layer resistance was larger than the membrane resistance when a thinner membrane was applied. With the increase of membrane thickness, the membrane resistance became a dominant factor on mass transfer in the membrane; the liquid membrane boundary layer resistance was lower than the membrane resistance. For the cellulose acetate membrane, this membrane thickness is between 23-33 μm and for the poly(2,6-dimethyl-1,4-phenylene oxide) membrane, it is around 38 μm . When the membrane thickness is

larger than these values, the membrane resistance became a dominant factor on mass transfer in the membrane.

As discussed above, an optimal membrane thickness is important to the performance of pervaporation separation for the separation of molecular mixtures. In order to have an intrinsic membrane selectivity, a minimum membrane thickness has to be determined. On the other hand, a thicker membrane active layer can decrease the transmembrane flux.

2.4 Coupling effects in pervaporation

Coupling effects are an important phenomenon observed frequently in pervaporation. The mass transport in the membrane is a complicated process due to the interactions among permeants and between the permeants and the membrane material. Coupling effects are difficult to measure quantitatively, but it is possible to obtain indirect information from the partial flux of each component or sorption and desorption experiments¹⁴⁴. In pervaporation, this effect is not negligible.

Different factors lead to the occurrence of coupling transport. Some of the causes have been mentioned in Chapter 2.3: coupling transport phenomena can be related to membrane thickness, craze defects in thinner membrane, membrane swelling, and plasticization. One important observation is that coupling effects can relate to the composition of the feed. Bio-based aroma compounds are often produced via microbial bioconversion¹⁴⁵. In the work of Raisi *et al.*, different groups of aroma compounds (3-methylbutanal, isopentyl acetate, n-hexanol and α -ionone) mixture were studied⁸¹. From binary mixtures, each aroma compound was mixed with de-ionized water to make a dilute aroma/water mixture. For ternary mixtures, the feed was prepared by mixing two aroma compounds and de-ionized water. No obvious coupling effect was observed at low aroma concentration (<200 ppm). The aroma molecules are separated by large quantities of water in dilute solutions. The interactions among aroma molecules are too small to influence their permeation behaviour. Therefore, the coupling effect is not significant at low aroma concentrations in the feed solution. At relatively high concentration, coupling effects were observed for 3-methylbutanal/n-hexanol/water and 3-methylbutanal/ α -ionone/water mixtures. It was shown that 3-methylbutanal can enhance the permeation of n-hexanol and α -ionone. In addition,

isopentyl acetate showed a strong coupling effect for all aroma compounds (3-methylbutanal, n-hexanol and α -ionone) mixtures. The partial flux of these aroma compounds was increased compared with their binary mixture with water. According to the diffusion-solution model, the sorption of molecules in the polymeric membrane depends on the affinity between the permeants and membrane materials. The affinity can be expressed by solubility parameters. It is found that the order of solubility parameters of each aroma compounds and PDMS membrane is as follows: isopentyl acetate > 3-methylbutanal > n-hexanol > water. This indicates that isopentyl acetate and 3-methylbutanal have a high sorption degree in PDMS membrane¹⁴⁶. Therefore, the presence of these components in the feed solution results in swelling effects due to their high sorption degree. As a result, the n-hexanol and α -ionone permeation fluxes through the membrane are enhanced.

It is also found that some organics can modify the polymer phase and change the solubility of other organics¹⁴⁶. This phenomenon is often observed during separation on bio-synthesized alcohol mixtures. The solubility of n-butanol decreased when other alcohols were presented in the mixture. It is caused by the formation of clusters of alcohol molecules via hydrogen bonds, which modify the polymer phase. Consequently, the solubility of n-butanol in the polymer material (poly(octyl)methylsiloxane (POMS)) is reduced.

The free volume inside the membrane is an important factor determining coupling effects. In the literature, studies of free volume show that the microscopic change of the membrane results in membrane swelling^{147–150}. Coupling effects can also be reduced by varying the free volume size or by creating artificial free volume.

The relationship between the free volume in polymeric membranes and transport properties has been studied in different processes, such as gas separation^{148,149} and pervaporation^{147,151–153}. The free volumes are disordered voids with the size between 0.1 – 0.5 nm in the polymer matrix which are randomly created by thermal motions of polymer chain. It is considered an important factor on the transport of penetrants through polymeric membranes and has a significant influence on the separation of small molecules, such as water or alcohols. Pervaporation involves the contact between the membrane and a liquid feed, of which the composition may vary with time. The free volume in the membrane can change with process time because the degree

of membrane swelling can evolve over time. A swollen membrane can have a much higher free volume than a dry membrane, therefore, a wet pervaporation membrane can have a strong impact on the diffusion inside the membrane. In an early study on effect of water-swollen poly vinyl alcohol membrane¹⁵⁰, it was found that the expansion of free volume experiences three stages. Initially (concentration of water < 8 wt%), the mean size of free volume is not significantly changed because the water molecules bind to the hydroxyl groups of PVA. With the increase of water concentration up to 30 wt%, the mean radius of free volume starts to increase because the water molecules expand the inter/intra chain distance of PVA. When the water concentration reaches 30 wt%, the free volume expansion reaches its maximum size. The change of free volume size is reversible. Satyanarayana *et al.* investigated the free volume size of a water soaked and a dried membrane (PERVAP 2210). It was shown that the free volume is reversible if a dry membrane experiences sorption followed by drying¹⁵⁴. However, the sorption degree of a used membrane was almost 50% lower than that of a fresh membrane.

As the expansion of the free volume can reduce the selectivity of pervaporation membranes – resulting in a so-called “coupling effect”, a solution is to introduce inorganic and rigid particles in the polymer to inhibit the expansion of free volume. Li *et al.* studied the influence of adding zeolite 13X into a polyimide (BAPP-BODA) membrane¹⁵³. It was found that the resulting free volume radius was between the free volumes of pure BAPP-BODA (2.85 Å) and zeolite 13X (4.08 Å). In addition, the number of free volume cavities was reduced after introducing zeolite into the polymer matrix. The free volume radius distribution of the hybrid membrane was within the range of the kinetic radius of water (1.2 Å) and isopropanol (3.86 Å). By introducing zeolite 13X into the polyimide membrane, the expansion of the free volume caused by membrane swelling was significantly inhibited. The permeation increases with increasing of 13X zeolite content into the polyimide membrane due to the molecular sieving effect and hydrophilicity of the zeolite 13X; however, the separation factor is constant in the permeate for a 90 wt% aqueous isopropanol mixture (Figure 2-2).

A similar study was carried out by Shi *et al.*¹⁵². ZIF-8 nano-particles were added into a polybenzimidazole (PBI) membrane for the separation of a mixture of alcohols and water. The swelling degree of the membrane in the presence of water, methanol and ethanol solutions was decreased after introducing ZIF-8 particles into the PBI

membrane. In addition, it was found that the swelling caused by water was subdued significantly due to the hydrophobic property of ZIF-8 particles. Comparing the performance of PBI membrane with and without ZIF-8 particles, it was observed that ZIF-8 addition can suppress the changes of membrane structures, which is otherwise caused by ethanol swelling. The free volume diameter of PBI/ZIF-8 membrane (swollen by ethanol) is smaller than that of PBI membrane (4.9 Å vs. 5.9 Å), which was linked to the better selectivity of the hybrid membrane.

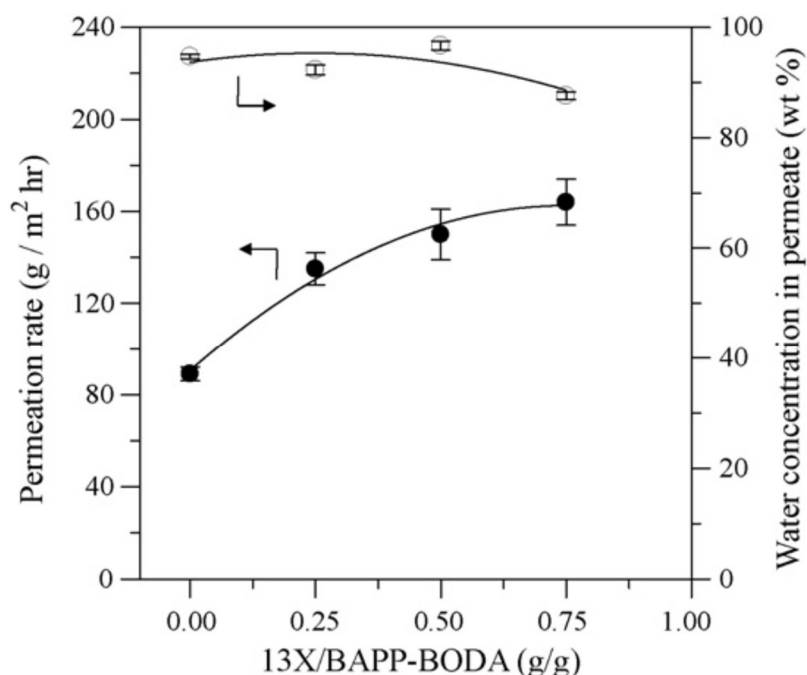


Figure 2-2. Effect of zeolite 13X content on pervaporation separation of 90 wt% aqueous isopropanol mixture for the BAPP–BODA/13X hybrid membranes at 25 °C. Reprinting with permission from Li *et al.*¹⁵³

In some cases, such as in biofuel production, it is required to remove toxic products, such as low molecular weight alcohols ethanol and butanol, while the medium of the fermentation water has to be retained by the membrane. These bio-alcohols are larger than water; thus, a hydrophobic membrane should be applied in order to achieve a high permeability and selectivity. In the work of Petzetakis *et al.*¹⁵¹, an artificial free volume inside cross-linked PDMS membrane was created based on the self-assembly of polyethylene-*b*-polydimethylsiloxane-*b*-polyethylene triblock copolymers (EDE) for purifying ethanol/water and butanol/water by pervaporation. The experimental results (Figure 2-3) showed that the improvement of permeability of butanol and ethanol is significantly dependent on the amount of artificial free volume. The selectivity was

improved by increasing the free volume created in the PDMS membrane because the artificially created free volume is more hydrophobic than the original cross-linked PDMS. Therefore, the transport of less polar molecules butanol is more enhanced by the artificial free volume. One important feature is that the improvement of permeability EDE/PDMS copolymer membrane is not subject to the sacrifice of selectivity^{155,156}.

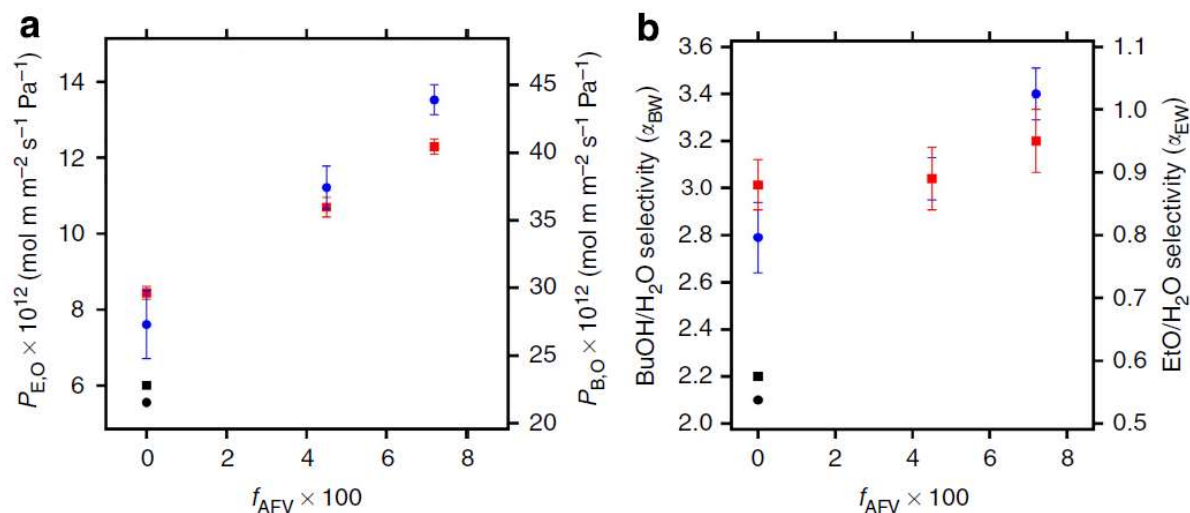


Figure 2-3. Membrane separation permeability and selectivity for butanol and ethanol. (a) Butanol permeability (right ordinate) and ethanol permeability (left ordinate) as a function of artificial free-volume, f_{AFV} , (bottom ordinate). Blue circles: butanol and red squares: ethanol are introduced EDE in cross-linked PDMS membrane; black circle: butanol and black square: ethanol are permeability by cross-linked PDMS membrane. (b) Butanol/water (left) and ethanol/water (right) selectivity as a function of artificial free-volume f_{AFV} (bottom ordinate). Blue circles: butanol/water and red squares: ethanol/water are selectivity by EDE membranes; black circle: butanol/water and black square: ethanol/water are selectivity by cross-linked PDMS membrane. Reprinting with permission from Petzetakis *et al.*¹⁵¹

The physicochemical interaction between the membrane-molecules and molecules-molecules of the system can lead to drag effect during pervaporation. Huang *et al.* studied the ethanol-water system by using PERVAP 2510 membrane. Results showed that this membrane gives very poor separation performance with separation factor 14-16 for water¹⁵⁷. However, the separation factor obtained for water over isopropyl alcohol is between 300-1400 with 2-15 wt% of water under 60-100 °C. For butanol-water system, the separation factor is even higher than isopropyl alcohol-water system. One of the reason is that ethanol and water can form stronger interaction coming from hydrogen bonding (O-H...O) and thus result in a considerable mutual-dragging effect^{158,159}. On the other hand, Huang *et al.* also applied zeolite silicalite-1 for ethanol-

water mixture. It was concluded that the presence of sinusoidal channels in silicalite-1 can possibly drag the transport of penetrants resulting in the decrease of ethanol permeance.

Sommer *et al.* investigated the water-alcohols (methanol, ethanol, isopropanol and n-butanol) permeation behavior by using silica membrane (made by ECN)¹⁶⁰. By comparing their partial flux, the smaller alcohol molecules, such as methanol and ethanol, are being dragged across the membrane with water. However, the bigger and more hydrophobic alcohols (isopropanol and n-butanol) show less effect. There is a more or less pronounced drag effect for all alcohols. Similarly, Ten Elshof *et al.* studied water-organic binary mixtures (methanol, N,N-dimethyl formamide (DMF) and 1,4-dioxane) containing 5-22 wt% water by using silica membranes¹⁶¹. In that work, it was found that the flux of methanol is dominated by a drag effect by the larger water flux. Besides alcohols, Koops *et al.* found that the permeation was influenced by the interaction between acetic acid and water due to their strong hydrogen bonding¹⁶². Hence, the faster permeating water molecules has impact on the relatively slow permeating acetic acid molecules. Consequently, the acetic acid molecules can be dragged across the membrane by water flux due to intermolecular interaction.

As discussed above, drag effect resulting from the interaction of molecules and molecules, *e.g.* intermolecular interaction, is an important factor to influence permeation performance. A strong drag effect can influence flux and separation factor. Currently, the majority study of drag effect in the literature is based on water-alcohol mixtures or water-organic mixture because the intermolecular interaction for organic-organic mixture could be more complex.

2.5 Pervaporation membranes

Compared with other pervaporation applications, the use of pervaporation for separating bio-based mixtures may be more challenging due to the complexity of the feed composition, requiring usually multiple separation steps. In recent years, research has been carried out to develop novel membranes to separate different liquid-liquid mixtures. Table 2-2 is a summary of application of pervaporation membranes for different separations. In general, the separation based on the mixture can be divided in two types: water-organic (dehydration) and organic-organic mixtures. Dehydration

involves the separation of water from organic components, for example, the mixture of acids, alcohols, esters and water from esterification and transesterification reactions. The application of dehydration in pervaporation has been achieved in industrial applications for the removal of water from an organic phase¹⁶³. The membranes produced by SULZER, PolyAn, have been commercially available for dehydration processes. These commercial membranes, based on polyvinyl alcohol, and polyimides materials, are able to permeate water with high flux and selectivity by modifying the chemical composition and structure properties to improve the hydrophilicity of the membranes.

The application of pervaporation technology for the separation of organic–organic mixtures is less commercialized. Many studies have been carried out for the separation of various organic mixtures. From Table 2-2, it can be seen that the membranes can be generally classified into three types based on the membrane materials: inorganic, organic and inorganic-organic hybrid membranes.

Organic membranes

Organic membranes, mainly synthesized from polymers, are the most studied and widely applied in pervaporation. A low mechanical resistance and thermal stability are the shortcomings of organic membranes. In addition, the tradeoff between permeability and selectivity is very common in the application of organic membranes. However, the organic membranes are still attractive and applied for many separation processes due to their low cost and flexible and easy membrane synthesis.

In some cases, the problem of chemical resistance can limit the application of organic membranes. Some polymer materials can appear as good candidates for a given separation, but cannot be applied in other mixtures because they react with some components of the mixture. For instance, polybenzimidazole (PBI) is a good membrane material for pervaporation dehydration, but it has a tendency to form PBI-acid, which limits its application for the separation in acidic mixtures. Wang *et al.* developed a novel two-step sulfonation modification technique and investigated the performance in dehydration of acetic acid¹⁶⁴. Sulfonated polybenzimidazole (SPBI) is prepared by sulfonation with sulfuric acid followed by a thermal treatment at 450 °C in order to develop a stable membrane made of SPBI with good acid resistance. By

comparing SPBI and PBI membranes at 50/50 wt% water/acetic acid mixture, the sulfonated PBI membrane (2.5 wt% H_2SO_4 , 450 °C, 30s) gave a flux of 168 $\text{g/m}^2\cdot\text{h}$ with a separation factor of 6631, while the pristine PBI membrane only gives 100 $\text{g/m}^2\cdot\text{h}$ flux with a separation factor of 7. With the sulfonated membrane, the separation performance is better than with conventional distillation and other polymeric membranes in the literature.

Inorganic membranes

Inorganic membranes have a low swelling degree, good mechanical properties and a good chemical and thermal resistance comparing with organic membranes. However, they suffer from a higher cost and are difficult to fabricate into defect free membranes. Zeolite and silica are very common ceramic membranes. The materials for preparing silica membranes are SiO_2 , $\text{SiO}_2\text{-TiO}_2$, $\text{SiO}_2\text{-ZrO}_2$, etc. They are stable at high temperature and acidic environment. The silica-based membranes prepared by sol-gel processing are highly permeable and selective. This method offers great advantage on the controlling of pore sizes.

The sol-gel processing begins with the hydrolysis of alkoxysilane precursors (e.g. Tetraethyl orthosilicate). The precursors first react with water to replace the alkoxy groups with hydroxyl groups by using acid (HCl) or base (NaOH) catalyst. Then, condensation reaction takes place between hydroxyl groups and between a hydroxyl group and alkoxy group forming SiO_2 sol with siloxane bond. Then the SiO_2 sol is coated on the support layer to form a thin silica gel layer and finally, the coated silica membrane is dried or calcined at high temperature to form desire silica structure. The pore size and the structure of silica networks has strong impact on the final obtained membranes. Hence, the synthesis conditions, such as concentration of precursors and catalysts, the ratio of water to precursor, are important factors. In the book of Brinker & Scherer, it is illustrated that silica sol-gel obtained via acid-catalysts has a polymeric structure and a colloidal structure via base-catalysts¹⁶⁵. In addition, a high water to precursor ratio can improve the degree of hydrolysis of alkoxy group, leading to a higher degree of condensation reaction and a denser silica network can be obtained¹⁶⁶.

The application of silica membrane for pervaporation can be found in dehydration of alcohols^{167,168}, dehydration of acids^{169,170} and separation of organic-organic mixtures¹⁷¹.

The silica membrane exhibits a high and stable water flux ($5.4 \text{ kg/m}^2\cdot\text{h}$) in IPA/water mixture by silica-zirconia membranes with separation factor 2500 under the condition 10 wt% water in the feed at 75°C ¹⁶⁷. Silica membranes are promising to apply for the dehydration of acetic acid solutions due to its high stability contacting acidic solution. For example, a separation factor 450 and water flux $0.9 \text{ kg/m}^2\cdot\text{h}$ can be achieved by silica membrane under the condition 10 mol% water/acidic acid mixture at 70°C ¹⁶⁹.

Zeolites are a mixture of silicates-alumino with different compositions of silicon to aluminium ratio. The ratio of $\text{SiO}_2/\text{Al}_2\text{O}_3$ is an important factor for the performance of inorganic membranes. The zeolites form crystalline structure and pore size can achieve several nanometers. It is found that a low silicon to aluminium ratio can improve the hydrophilicity of the membrane leading to a preferential sorption of water inside pores¹⁷². However, the stability of zeolite membranes under acidic environment is a challenge¹⁷³. The zeolite membranes can be destructed by hydrolysis reaction resulting from acidic environment, such as Si-O and Al-O bonds in zeolite are dissociated. Furthermore, the silica-alumina layer is dissolved into the solution. Consequently, the zeolite membranes lose their selectivity. Acid-stable zeolite membranes are improved by increasing $\text{SiO}_2/\text{Al}_2\text{O}_3$ ratio by trading off hydrophilicity. For example, ZSM-5 zeolite membranes were studied for the separation acetic acid/water and acetic acid/ethanol/water/ethyl acetate¹⁷⁴. It was found that a higher Si/Al ratio can decrease the hydrophilicity of the membrane. However, the acid-stable ZSM-5 membrane still has an acceptable water permeability in target mixtures. The water content in permeates can achieve 99.5 wt% in both binary and quaternary mixtures¹⁷⁴.

Organic-inorganic hybrid membrane

Organic-inorganic hybrid membranes present interesting properties for pervaporation applications because of their thermal stability, good mechanical strength and chemical resistance. The major applications of hybrid membranes can be found in dehydration. Ma *et al.*¹³³ studied organic-inorganic hybrid membranes prepared from the sol-gel polycondensation of tetraethoxysilane (TEOS) within chitosan (CS) aqueous solution. The membranes were studied for the pervaporation-assisted esterification of lactic acid and ethanol. Chitosan is one of the interesting membrane materials to be studied extensively because of its hydrophilicity¹⁷⁵. However, the low thermal stability and low

mechanical resistance are the main shortcomings of chitosan. By introducing TEOS, the hydrophilicity of the membrane and thermal stability are improved. TEOS-CS hybrid membranes have a high selectivity to water in the separation of water from an aqueous ethanol mixture. With the combination of batch reactor (reaction between lactic acid and ethanol to produce ethyl acetate and byproduct water) and the assistance of pervaporation, water can be preferentially removed from the reaction mixture due to the high hydrophilicity of the membrane, enhancing the yield of ethyl lactate for the esterification reaction of ethanol and lactic acid.

In the recovery of bio-based furfural, the performance of a $\text{Zn}_2(\text{bim})_4$ (bim=benzimidazole ion) and PMPS (polymethylphenylsiloxane) hybrid membrane improves the stability comparing with a pure PMPS membrane¹⁷⁶. At the same operational conditions, the hybrid membrane has a better membrane flux and separation factor than the pure PMPS due to introducing $\text{Zn}_2(\text{bim})_4$ crystals. The presence of $\text{Zn}_2(\text{bim})_4$ can reduce the membrane swelling effect.

Other advanced organic-inorganic membranes were also developed. For instance, Liu *et al.* fabricated a ZIF-8-silicone membrane on a stainless-steel-mesh by using a Plugging-Filling method¹⁷⁷. In the first plugging step, the ZIF-8 nanoparticles were plugged in HOSSM (hierarchically ordered stainless-steel-mesh). Then, the plugged HOSSM was dip-coated in the solution (1.0 g of polymethylphenylsiloxane (PMPS), 0.1 g tetraethyl orthosilicate and 0.01 g dibutyltin diaurate dissolved in 4.0 g of *i*-octane). The membrane shows a high separation performance (53.3 separation factor) in the recovery of 1.0 wt% furfural from water.

In recent advances in membrane synthesis, the study of organic-inorganic hybrid membrane is more attractive than inorganic membranes because the preparation of inorganic membrane is not only expensive but also it is difficult to achieve a defect free membrane.

In addition, the polarity of the permeant and of the membrane material, should be taken into account when selecting membrane materials. The polarity determines the hydrophilicity and hydrophobicity of the membrane materials. In the case of removing water for producing high purity solvents, a highly hydrophilic polymer will be the first option for the application. For example, in the study of a poly(dimethylsiloxane) and

polyolefin composite membrane for dehydration of ethyl acetate and ethanol, the experimental results show that the membrane was not selective to ethanol because it is a polar solvent. With non-polar organic ethyl acetate, and ethyl acetate enrichment in the permeate and the membrane gives a high selectivity (20-60)¹⁷⁸.

The mechanical strength, chemical resistance and thermal stability of a membrane in aqueous solutions are important issues for the application of pervaporation as well. For instance, polyacrylic acid (PAA), polyvinyl alcohol (PVA) and chitosan are suitable polymeric materials for dehydration by pervaporation to produce high purity alcohols. However, these materials do not have strong mechanical properties and lack stability in aqueous solution due to excessive membrane swelling. As a result, the selectivity of these membranes decreases dramatically during pervaporation. Thus, the application of these polymers is limited¹⁷⁹⁻¹⁸¹. Alternative membrane preparation methods are therefore required. For example, in the preparation of polybenzoxazole membranes, in-situ thermal conversion of hydroxyl-containing polyimide precursors method is applied. An aromatic polyimide can be converted to polybenzoxazole through thermal rearrangement between 350-500 °C under vacuum or in inert gas environment¹⁸⁰.

Table 2-2. The application of pervaporation on the separation of liquid mixtures

Materials	Mixture	Membrane material	Flux ($\text{kg m}^{-2} \text{h}^{-1}$)	Separation factor	Permeance (GPU)	Selectivity	Ref.
acetic acid	acetic acid water	Polyphenylsulfone (PPSU)	-	2-24	Water: 2000-25000 Acetic acid: 50-1500	5-38	182
	acetic acid/ethanol/water/ethyl acetate	ZSM-5 zeolite	1.24-2.36	130-2070	-	-	183
	acetic acid water	polyphenylsulfone-based membranes, modified with silica nanoparticles	0.76-2.34	-	Water: ~4000-7000 Acetic acid: ~500-1000	2.9-5.7	184

Table 2-2. The application of pervaporation on the separation of liquid mixtures (Cont.)

Materials	Mixture	Membrane material	Flux ($\text{kg m}^{-2} \text{h}^{-1}$)	Separation factor	Permeance (GPU)	Selectivity	Ref.
acetic acid	acetic acid water	polyelectrolytes complex (PEC)/11-phosphotungstic acid hydrate (PW11) hybrid membrane (PEC/PW11)	0.44	144	-	-	185
	acetic acid water	Composite membranes of sodium alginate active layer and microporous polypropylene substrate	0.653	631	-	-	186
	acetic acid water	Polycrystalline silicalite membranes ZSM-5 zeolite crystals	0.22	59	-	-	187

Table 2-2. The application of pervaporation on the separation of liquid mixtures (Cont.)

Materials	Mixture	Membrane material	Flux (kg m⁻² h⁻¹)	Separation factor	Permeance (GPU)	Selectivity	Ref.
acetic acid	acetic acid water	Sulfonated polybenzimidazole membranes	0.207	5461	-	-	164
isopropanol	Isopropanol water (85 wt% isopropanol)	polybenzoxazole (C-TR-PBO)	0.09	-	-	4019	188
ethyl tert-butyl ether	Ethyl tert-butyl ether/ethanol	CA-g-PLA copolymers	0.01447-0.02177	46-396	-	-	189
furfural	Furfural/water	Zn ₂ (bim) ₄ -PMPS	2.05-2.15	19.1-19.5	-	-	190
	Furfural/water	Metal-organic framework ZIF-8 nanocomposite	0.67-1.8	17.6-53.3	-	~5-15	177
	Furfural/water	HTPB-based hydrophobic polyurethaneurea membranes	0.003-0.022	100-600	-	-	191

Table 2-2. The application of pervaporation on the separation of liquid mixtures (Cont.)

Materials	Mixture	Membrane material	Flux ($\text{kg m}^{-2} \text{h}^{-1}$)	Separation factor	Permeance (GPU)	Selectivity	Ref.
1,4-dioxane	1,4-dioxane/water	Chitosan and nylon 66 blend	0.028-0.118	767-1123	-	-	192
Tetrahydrofuran	THF/water (0.56 wt% water)	acrylamide and 2-hydroxyethyl methacrylate blend	0.57	216	-	-	193
isobutyl propionate	Propionic acid /isobutyl alcohol/isobutyl propionate/water	polyvinyl alcohol–polyethersulphone (PVA–PES) (Only conversion reported: Improved from 60% to 90%)	-	-	-	-	194

Table 2-2. The application of pervaporation on the separation of liquid mixtures (Cont.)

Materials	Mixture	Membrane material	Flux ($\text{kg m}^{-2} \text{h}^{-1}$)	Separation factor	Permeance (GPU)	Selectivity	Ref.
Ethyl lactate	ethyl lactate/ ethanol/lactic acid/water	Commercial membrane PERVAP® 2201 (Only conversion reported: Achieve ~90%)	-	-	-	-	195
	ethyl lactate/ ethanol/lactic acid/water	Tetraethoxysilane (TEOS)- chitosan hybrid membrane	~0.05-0.284	~460-700	-	~18-36	196
isopropyl lactate	lactic acid/ isopropanol/ isopropyl lactate/water.	Polyvinyl alcohol- polyether sulfone (PVA-PES) (Only conversion reported: Improved from 51% to 86%)	-	-	-	-	9

Table 2-2. The application of pervaporation on the separation of liquid mixtures (Cont.)

Materials	Mixture	Membrane material	Flux ($\text{kg m}^{-2} \text{h}^{-1}$)	Separation factor	Permeance (GPU)	Selectivity	Ref.
ethylene glycol	ethylene glycol/water	poly(vinyl alcohol) (PVA) and a MOF with hydrophilic sulfonic acid group ($\text{SO}_3\text{H-MIL-101-Cr}$) coated by a thin and uniform polydopamine (PD) layer	0.540	2864	-	68.1	197
	ethylene glycol/water	PVA and γ -mercaptopropyltrimethoxysilane (MPTMS)	0.067-0.2	50-311	-	-	198
	ethylene glycol/water (80 wt% EG)	Chitosan–poly(acrylic acid) polyelectrolyte complex membranes	0.216	105	-	-	199
	ethylene glycol/water (90 wt% EG)	Poly (vinyl alcohol)/hyperbranched polyester membrane	0.04377	312	-	-	200

Table 2-2. The application of pervaporation on the separation of liquid mixtures (Cont.)

Materials	Mixture	Membrane material	Flux ($\text{kg m}^{-2} \text{h}^{-1}$)	Separation factor	Permeance (GPU)	Selectivity	Ref.
ethylene glycol	ethylene glycol/water	composite membranes comprising of polyamide and polydopamine	~0.081-0.429	196-388	-	-	201
cyclohexane	Ethanol/cyclohexane (30.5 wt% /69.5 wt%)	Ethylene-chlorotrifluoroethylene	0.45-1.7	15-31	-	-	202
styrene	styrene/ethylbenzene	Poly(hexamethylene sebacate) (PHS)	0.05-0.15	2.2-5.8	-	-	203
n-butyl acetate	n-butyl acetate/ n-butanol/ water	polyvinyl alcohol (PVA) and chitosan (CS)	~0.683-1.5	~1500-4800	-	-	130
n-butyl acetate	n-butyl acetate/water	polyvinyl alcohol (PVA) and chitosan (CS)	~0.4-0.6	27000 (25 wt% CS)	-	-	130

Table 2-2. The application of pervaporation on the separation of liquid mixtures (Cont.)

Materials	Mixture	Membrane material	Flux (kg m⁻² h⁻¹)	Separation factor	Permeance (GPU)	Selectivity	Ref.
1,3-propanediol	1,3-propanediol–water	Allylcyclohexylamine functionalized siloxane polymer	0.0055–0.0058	9-15	-	-	204
methyl anthranilate	flavor compound of concord grapes	polydimethoxysiloxane-polycarbonate	0.055-0.102	4-10	-	-	205
ethyl lactate	water/ethanol/ethyl lactate/lactic acid	PERVAP® 2201	~0.2-3	~600	-	-	206
acetic acid	acetic acid/water	Sodium alginate/polyaniline polyion complex membrane	0.04-0.07	359.33-441	-	-	207
succinate	succinic acid/ ethanol/ diethyl succinate/water	GFT-1005 membrane	1-5.8	-	-	-	208

Table 2-2. The application of pervaporation on the separation of liquid mixtures (Cont.)

Materials	Mixture	Membrane material	Flux ($\text{kg m}^{-2} \text{h}^{-1}$)	Separation factor	Permeance (GPU)	Selectivity	Ref.
ethyl levulinate synthesis from ethanol and levulinic acid	ethyl levulinate /ethanol/levulinic acid/water	catalytic composite membrane consists of two layers: the top layer is the catalytic layer coated with $\text{SO}_4^{2-}/\text{ZrO}_2$ catalyst, the bottom layer is the dense hydroxyethyl cellulose membrane	2.3	30-65	-	-	209
xylene	O-xylene/P- xylene	polyurethane–zeolite composite membranes	0.07-0.46	0.76-1.37	-	-	210
dimethylformamide	dimethylformamide/water	Sodium alginate/poly(vinyl alcohol) alloy membranes	0.9-1.1	20-30	-	-	211

Except for the membranes reviewed above, supported ionic liquid membranes (SILMs) also attract attention for liquid-liquid separation. Ionic liquids have good chemical and thermal stabilities and a negligible vapor pressure²¹². SILMs have been studied widely for gas separation and purification, such as SO₂/CO₂ separation and natural gas purification^{213,214}. Even though research on the application of SILMs in pervaporation is still limited, some progress has been achieved and some applications related to the separation of bio-based mixture by using pervaporation proved to be successful (See Table 2-3). Compared with dense membranes, SILMs can have a better mass transfer because the diffusion coefficient in liquids is much higher than in solids²¹⁵. A discussion of fundamentals and recent advances in SILMs technology is given by Lozano *et al.*²¹⁶ and Wang *et al.*²¹⁷.

Table 2-3. The application of SILMs via pervaporation on the separation of bio-based chemicals

Mixtures	IL	Supported membranes	Ref.
1-phenylethanol, 1-phenylethyl propionate, Vinyl propionate and Propionic acid	[BMIm][PF6]	Nylon	223
	[OMIm][PF6]	Nylon	223
	[BMIm][PF4]	Nylon	223
	[OMIm][PF4]	Nylon	223
	[BMIm][NTf2]	Nylon	223
	[OMIm][NTf2]	nylon	223

Table 2-3. The application of SILMs via pervaporation on the separation of liquid-liquid mixtures (Cont.)

Mixtures	IL	Supported membranes	Ref.
Vinyl buyrate, butanol, butyl butyrate, butyric acid	[BMIm][PF6]	PVDF, PTFE, PC, Nylon	218 219 220 221
	[OMIm][PF6]	Nylon	218 219 220 221
	[BMIm][PF4]	Nylon	219 220 221
	[OMIm][PF4]	Nylon	219 220 221
	[BMIm][NTf2]	Nylon	219 221
	[OMIm][NTf2]	Nylon	219 221
	[BMIm][Cl]	Nylon	220
Vinyl acetate, Vinyl propionate, Vinyl butyrate, Vinyl laurate, Methyl acetate, Methyl propionate, Butyl butyrate, Ethyl decanoate, Metanol, Propanol, Butanol, 1-Octanol, Acetic acid, Propionic acid, Butyric acid, Lauric acid	[BMIm][PF6]	Nylon	219
	[OMIm][PF6]	Nylon	219
	[BMIm][PF4]	Nylon	222
	[OMIm][PF4]	Nylon	222

2.6 Pervaporation-distillation hybrid processes in bio-based mixture separation

In the past decade, membranes have been widely applied in the chemical industry for purification processes. Pervaporation has often been compared with other purification technologies, such as distillation and liquid-liquid extraction. As reviewed above, many studies have proved that it is an environmentally friendly and cost-effective purification technology. It is a suitable technology for dehydration of a product (ethanol, butanol, isopropanol, etc.) or separating the mixture forming azeotrope with water, such as some esterification reactions. However, stand-alone pervaporation is rare because the composition of the permeate may not have the required product purity or environmental standards. In most cases, pervaporation is combined with other processes to improve the overall efficiency of the entire process. In recent years, hundreds of research papers have been published on pervaporation hybrid processes for different types of mixtures. Two major types of installations are reported in the literature. The first one is pervaporation combined with distillation for separation and purification. For instance, ETBE is an attractive bio-ether used as additive in bio-fuels due to its beneficial effect on fuel combustion and reduction of hydrocarbon emissions. The bio-ETBE can be synthesized from the reaction of bio-ethanol and isobutene over a catalyst, such as Amberlyst 15 (A15)²²⁴. In the production of ETBE, pervaporation plays an important role for breaking the azeotrope²²⁵. The elimination of the excess of alcohol in the mixture cannot be achieved with conventional distillation; the final ETBE product can not achieve the required purity due to the contamination by residual alcohol in the product. Pervaporation-distillation and reactive distillation were compared for the production of ETBE²²⁶. In the pervaporation distillation hybrid process, the purity of ETBE is up to 95.2 wt% and the permeate, enriched with ethanol, is recycled to the reactor. Compared with reactive distillation, the purity of ETBE obtained from reactive distillation (97.3 wt%) is higher than by the pervaporation-distillation process (95.2 wt%), but the energy consumption of the pervaporation-distillation hybrid process is 465 kWh per ton of product compared with 1205 kWh per ton of product in reactive distillation. The pervaporation-distillation scheme is shown in Figure 2-4.

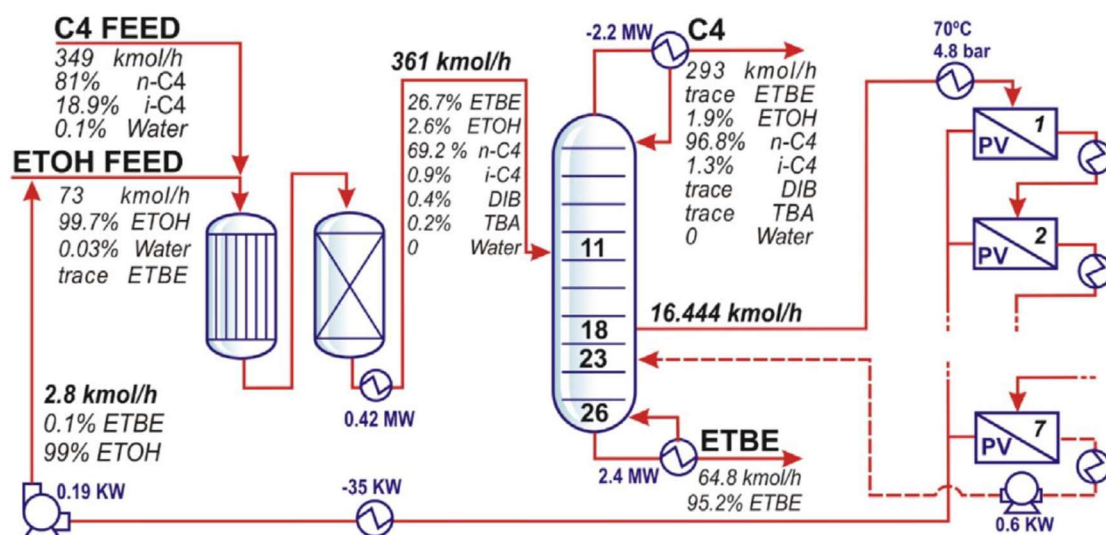


Figure 2-4. Schematic diagram of the pervaporation integrated hybrid process for production of ETBE. Reprinted with permission from Norkobilov *et al.*²²⁶

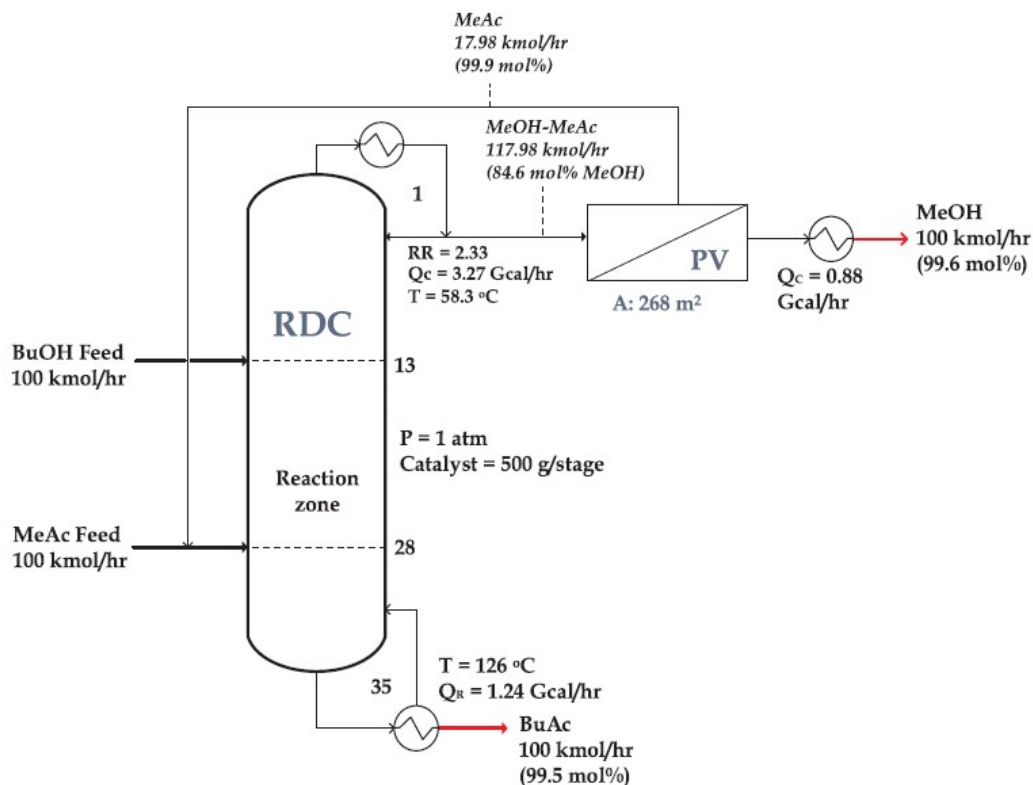


Figure 2-5. A connection of hybrid reactive distillation with high selectivity pervaporation. Reprinted with permission from Harvianto *et al.*²¹

The bio-based butyl acetate can be produced by reacting bio-butanol and methyl acetate. Jimenez *et al.* proposed a new process combining extractive and reactive distillation for the production of butyl acetate²⁷. Although this process can produce high purity butyl acetate, the economic analysis shows it is not profitable¹¹. In the work of

Gregorius *et al.* a reactive distillation combined with pervaporation (polyimide-6 membrane) was applied for the production of butyl acetate using the same starting reactants (Figure 2-5)^{21,227}. The azeotrope of methanol and methyl acetate was broken by pervaporation. The methyl acetate obtained from the pervaporation retentate is redirected as feed solution to the reactive distillation. As a result, a high purity of methyl acetate was obtained, along with a high conversion in the reactive distillation column. The energy consumption can be reduced by up to 71% by this process. This is a very promising process, since the overall cost of the butyl acetate production is markedly reduced compared with conventional process.

In order to study a real application of hybrid processes, Danilo *et al.* screened commercial membranes for the pervaporation-distillation hybrid process for the separation of methanol and methyl acetate²²⁸. It was shown that the best commercial membranes were Poly Al TypM1 (Produced by PolyAl) and Pervap 2256 (produced by Sulzer) membranes. Both membranes permeate methanol and reduce the overall cost of separation at optimal conditions.

As discussed above, the pervaporation-distillation hybrid system presents a decisive advantage in terms of energy consumption compared with other separation processes. In the separation of azeotropic mixtures, the pervaporation-distillation hybrid has the additional advantage of being able to break the azeotrope as the pervaporation separation is based on the affinity of molecules and membrane materials instead of thermodynamic vapor-liquid equilibrium in reactive distillation.

Figure 2-6 shows a novel concept proposed by Fontalvo *et al.*²²⁹, in which pervaporation is integrated a single distillation column. In this process, a section of packing or trays in a distillation column is replaced by a coated ceramic hollow fibre membrane. The permeate is removed from the lumen side of the ceramic membranes. The reboiler provides the energy for separation by pervaporation separation. In the separation of a mixture of organic compounds (MTBE, 1-butene, and methanol), it was shown that the optimal separation of methanol can be achieved. The pervaporation section in the distillation column located at stage 20 gave the largest driving force for removing methanol by pervaporation because the methanol activity is the largest at this stage. For the same membrane area, a higher amount of methanol can be permeate through the membrane because methanol liquid activity is the highest at this

stage. Therefore, a maximum driving force was achieved. Compared with pervaporation-distillation systems where the pervaporation unit is separated from the distillation system, there are several advantages. First, the energy consumption for pervaporation can be reduced greatly. The condensation of the vapor in the distillation can release latent heat, which can be supplied to the pervaporation process. Second, the vapor and liquid phase are in contact in the pervaporation section, therefore, the vapor can enhance turbulence in the liquid phase, which can improve the mass and heat transfer between the liquid and the membrane surface. In addition, less membrane area is required comparing to external pervaporation. Therefore, the energy consumption and membrane cost can be reduced.

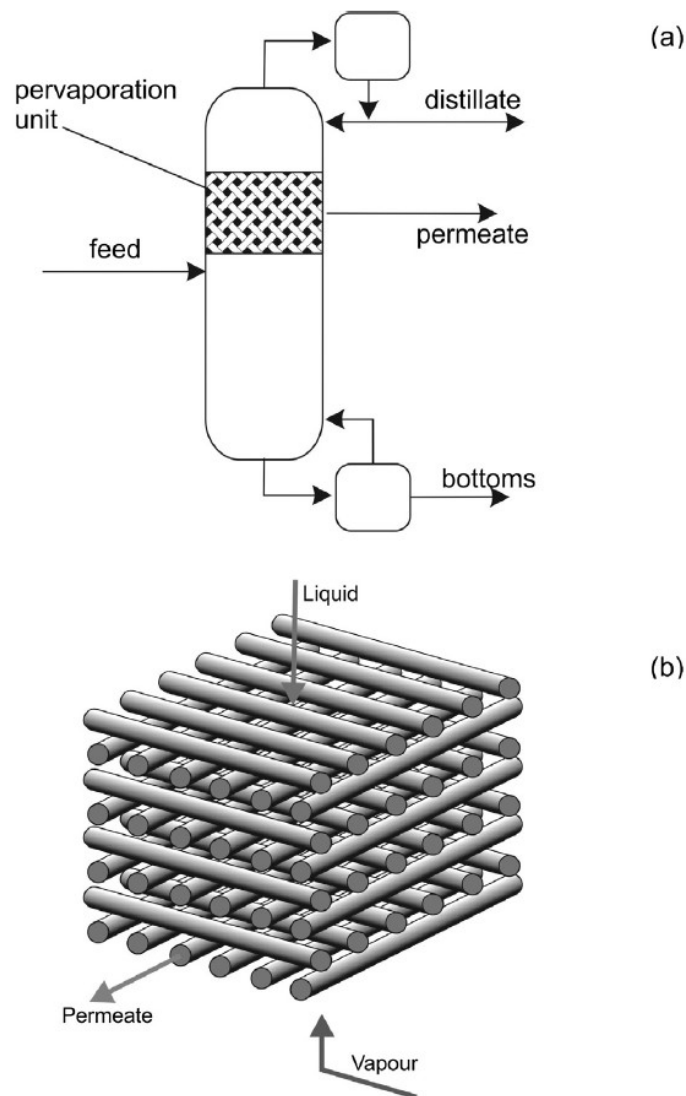


Figure 2-6. Hybrid distillation–pervaporation system in a single column (a), ceramic hollow fibre membrane packed section in an integrated distillation pervaporation unit (b). Reprinted with permission from Fontalvo *et al.*²²⁹

2.7 Reaction-pervaporation hybrid processes in bio-based mixture separation

Pervaporation can be combined with a reactor to form a reaction-separation hybrid process. The advantage of such combination is that one of the products/by-products can be removed by pervaporation. By doing so, an equilibrated reaction can be shifted towards the products, thereby improving the yields according the principle of Le Châtelier-Braun. Biobutanol is an important alternative to gasoline or fuel additive due to its higher energy content and low volatility in comparison with bioethanol. Furthermore, the current combustion engines can use biobutanol as fuel directly. In the production of biobutanol via fermentation²³⁰, lignocellulose is a more economical feedstock than sugar based fermentation. However, the presence of the by-product furfural in the reaction mixture can reduce the yield because furfural is the microbial inhibitory compounds for fermentation²³¹. The pervaporation process in the biobutanol production plays two functions: detoxification and separation of butanol. In the detoxification process, In the detoxification process, 94.5% of the furfural by-product produced by SSB (sweet sorghum bagasse) hydrolyzed by dilute acetic acid could be removed via pervaporation²³⁰. In addition, the mixture of butanol-acetone-ethanol was separated by pervaporation. As a result, the pervaporation process was found attractive to the production of biobutanol and biochemical furfural.

Dehydration is a crucial step to purify various types of bio-based products. In a recent study focused on the production of isopropyl lactate, the esterification of lactic acid by iso-propanol was coupled with pervaporation⁹. By removing water through a PVA-PES membrane during the reaction, the conversion of lactic acid was increased from 51% up to 86%. Commercial membranes for pervaporation dehydration are now available in the market and give a good performance on the separation processes²³². For example, the commercial hydrophilic membrane PERVAP 2201 (Sulzer) was applied in the synthesis of ethyl acetate from the esterification reaction of ethanol and lactic acid. The conversion of lactic acid was much higher than in the conventional reactor (limited by equilibrium) because the by-product water was removed selectively during the reaction, which shifted the thermodynamic equilibrium. Furthermore, the conversion of lactic acid related to the ratio of membrane area vs. initial reaction volume. A higher ratio led to a higher conversion.

Assabumrungrat *et al.* compared the performance of pervaporation (PVA membrane)-reactor operated under continuous stirred tank reactor (CSTR) and plug flow reactor (PFR) for the reaction tert-butyl alcohol (TBA) and ethanol to produce Ethyl tert-Butyl Ether (ETBE) by a zeolite catalyst²³³. Comparing with conventional semi-batch reactor, pervaporation-reactor has better yield due to selective removal of water from the reaction mixture. The performance of PFR offers higher yield than CSTR in wide range of operational conditions. It is concluded that it is desire to operate at low temperature with a high ratio of membrane area to catalyst weight.

Feng *et al.* simulated a batch reactor integrated with a pervaporation unit for removing water from esterification mixtures²³⁴. It was found that a complete conversion of one reactant can be achieved when the other one is in excess. The joint effect of membrane area (A), initial volume of reaction mixture (V_0) and membrane permeability (ω) determine the reactor performance. It turns out that the higher the value of $\omega(A / V_0)$, the higher the conversion at a given reaction time. Hence, low permeability can be made up by increasing membrane area. However, when $\omega(A / V_0) = 1 \text{ h}^{-1}$, the reactor performance reaches its upper limit. In addition, temperature is an important factor because it influences reaction rate and membrane permeability.

The study of application of commercial membranes on pervaporation-reaction processes has been performed. Even though the quantity is still limited, it shows this application can be potentially achieved in industrial scale. In Table 2-4, it shows that the conversions are improved when a pervaporation is coupled with reactor. Pervaporation has distinctive advantage to improve conversion and it has great potential in industrial applications.

Table 2-4. The application of commercial membranes on pervaporation-reaction hybrid process

Reaction	Catalyst	Membrane	Conversion (Without PV)	Conversion (With PV)	Ref
Lactic acid + ethanol produces Ethyl lactate	Amberlyst 15	PERVAP 2201	Lactic acid conversion 0.21	Lactic acid conversion 0.88	195
Acetic acid + benzyl alcohol produces benzyl acetate	p-toluene-sulphonic acid	PERVAP 1005	Acetic acid conversion 0.45	Acetic acid conversion 0.6	235
Acetic acid + isopropanol produces isopropyl acetate	Amberlyst 15	PERVAP 2201	isopropanol conversion 0.66	isopropanol conversion 0.78	236
Acrylic acid + n-butanol produces n-Butyl acrylate	Amberlyst 131	PERVAP 2201	Acrylic acid conversion 0.68	Acrylic acid conversion 0.96	8
Propionic acid + isopropyl alcohol produces isopropyl propionate	p-toluene-sulphonic acid	PERVAP 2201	Acrylic acid conversion 0.69	Acrylic acid conversion 0.98	237

Table 2-4. The application of commercial membranes on pervaporation-reaction hybrid process (Cont.)

Reaction	Catalyst	Membrane	Conversion (Without PV)	Conversion (With PV)	Ref
Methyl ricinoleate + trimethylolpropane produces trimethylolpropane ricinoleate	Lipomod-34P	Polydimethyl siloxane (PDMS) (Medicone)	Methyl ricinoleate conversion 0.41	Methyl ricinoleate conversion 0.88	20
Lactic acid + isopropanol produces isopropyl lactate	Sulphuric acid	PVA-PES (Permionics)	Lactic acid conversion 51%	Lactic acid conversion 86%	9
Propionic acid + isobutyl alcohol produces isobutyl propionate	Cenosphere (composed of SiO ₂ , Al ₂ O ₃ and Fe ₂ O ₃)	PVA-PES (Permionics)	Propionic acid conversion 67%	Propionic acid conversion 88%	238
Lactic acid + butanol produces butyl acetate	Sulphuric acid	PVA-PES (Permionics)	Lactic acid conversion 66%	Lactic acid conversion 88%	239
Acetic acid + isopropanol produces isopropyl acetate	Amberlyst 15	PERVAP 2201	Acetate acid conversion 73.8%	Acetate acid conversion 98.8%	240

2.8 Conclusion

The application of pervaporation on the separation of liquid-liquid mixtures has been studied extensively and applied on industrial scale. The most prominent example is dehydration. The literature shows the great potential of pervaporation for the separation or purification of bio-based products. Particularly for dehydration, such as water removal from mixtures from esterification and fermentation, the membrane can achieve a good separation and commercial membranes are available.

In addition, pervaporation can be a good alternative solution for breaking azeotropic mixtures since the separation mechanism of pervaporation is only dependent on the molecule-molecule interaction and the molecule-membrane materials interaction regardless the thermodynamic equilibrium.

Nevertheless, stand-alone pervaporation is still not viable due to the lack of membranes available for the separation. The development of novel membranes is the key for the success for the purification of bio-based chemicals *via* pervaporation. Both a high selectivity and a high transmembrane flux are desired, but a better selectivity is more important than flux for the sake of separation. The low flux can be solved by simply using a larger membrane area or a different membrane configuration, for instance asymmetric membranes to enhance the flux. A more selective membrane is attractive for real industrial applications on the purification of bio-based chemicals *via* pervaporation. In addition, it can be seen that the hybrid system can give not only a reduction of energy consumption during the separation process but also an improvement of the conversion when connected with reactor. Compared with alternative separation process, such as reactive distillation, the energy consumption of pervaporation is more competitive in the bio-molecule purification process, which reduces the overall cost.

In summary, pervaporation is an attractive membrane separation technology for bio-based chemicals for real industrial applications due to the merits mentioned in this chapter.

Chapter 3. Materials and methods

3.1 Introduction

In this section, the materials/chemicals and methods applied in performing this PhD thesis are included. The experimental setup (the pervaporation separation unit) is described in detail as well as the calculations to obtain the permeance and selectivity of membranes, and the theory behind coupling effects. In addition, the analytical techniques are also described.

3.2 Chemicals

The chemicals used to perform all the experimental work were: methanol (>99%), n-butanol (>99.9%), butyl acetate (>99.7%), ethanol (>99.0%) and ethyl acetate (>99.8%), supplied by VWR PROLABO®, Belgium; methyl acetate (>99.0%) was supplied by Merck, Germany; glycerol (bidistilled) from VWR PROLABO Chemicals, France, purity $\geq 99.5\%$; dimethyl carbonate from ThermoFisher (Kandel) GmbH, Germany, purity $\geq 99\%$; Sodium aluminate NaAlO_2 , from Carlo Erba, Italy, purity ≥ 98 (used as catalyst for the transesterification reaction to produce glycerol carbonate)⁵³.

The chemicals used for the preparation of self-made polymeric membranes and the corresponding experiments to determine the membrane performance were: dimethyl carbonate (ReagentPlus®, 99%) and methanol (purity 99.8%), purchased from Sigma-Aldrich; the polymer (poly(oxa-p-phenylene-3,3-phthalido-p-phenylene-oxy-phenylene), namely PEEK-WC, was purchased from Chanchung Institute of Applied Chemistry (China). The solvent chloroform (anhydrous, $\geq 99\%$, containing 0.5-1.0% ethanol as stabilizer) was obtained from Sigma-Aldrich.

The materials and chemicals used for the preparation of supported ionic liquid membranes and corresponding experiments to determine the membrane performance were: the support membrane is a polyacrylonitrile (PAN) flat ultrafiltration hydrophilic membrane, which was purchased from Synder Filtration (USA); Dimethyl carbonate (purity >99%) and methanol (purity >99.8%) were purchased from VWR International and Alfa Aesar, respectively; Lithium bis(trifluoromethanesulfonyl)imide (purity >99%) was purchased from Abcr GmbH, Germany; 1-octyl-3-methylimidazole (purity 99%) was purchased from Alfa Aesar and 1-octyl-1-methylpyrrolidine (purity >98%) was purchased from Acros Organics.

3.3 Membranes

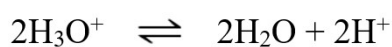
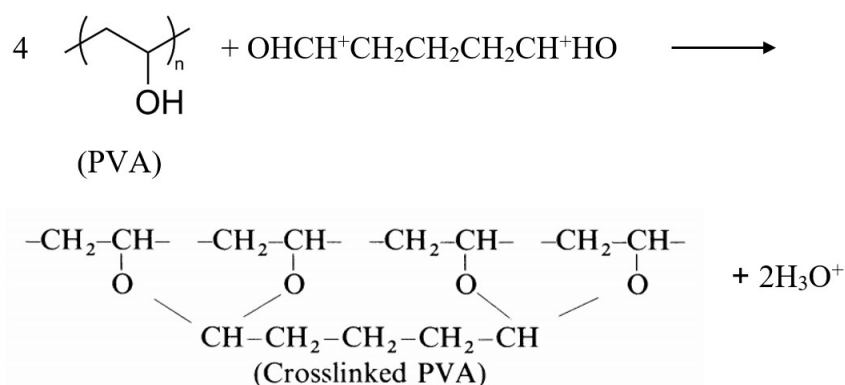
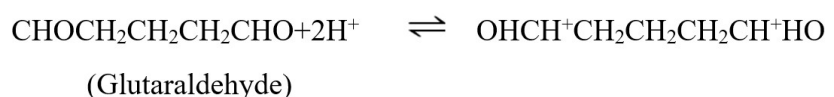
3.3.1 Commercial membranes from SULZER

The commercial membranes Pervap 1255-30, 4155-40, 1255-50 and 4155-80 manufactured by Sulzer Chemtech GmbH (Germany) were studied in this work. According to the information obtained from the supplier, they are composite membranes containing three layers. The top layer is the active layer of the membranes,

containing polyvinyl alcohol (PVA) with a thickness of 0.5-5 μm . In the middle, there was a porous support layer with a thickness of 70-100 μm made of polyacrylonitrile. Finally, at the bottom of the membrane, mechanical support layer with a thickness of 100-150 μm was made of polyphenylene sulfide polymer. The information of thickness of active layer of these commercial membranes is not provided by the supplier. It is known that the PVA content in different types of membranes are different and the supplier indicates that the last notation number expresses the degree of crosslinking: the higher the number, the higher the degree of crosslinking. Hence, the 4155-80 membrane has the highest degree of crosslinking than the other ones, followed by 1255-50, 4155-40 and 1255-30. The membranes were immersed in the feed solution for 24 hours before running a pervaporation experiment. In the membrane swelling test, the mechanical support layer (polyphenylene sulfide) was stripped from the membrane manually by using knife and tweezers.

The reaction mechanism of crosslinking of PVA membrane using a crosslinking agent glutaraldehyde and sulfuric acid as a catalyst has been studied by Kim *et al.*²⁴¹.

The crosslinking reaction is expressed as follows:



The concentration of glutaraldehyde determines the degree of crosslinking with a linear relationship, an increase of degree of crosslinking respects to the increase of glutaraldehyde concentration²⁴². However, the mass ratio of glutaraldehyde/PVA with 0.01 can achieve highest crosslinking density, further increase glutaraldehyde concentration results in the branching of PVA instead of crosslinking²⁴³.

3.3.2 Self-made PEEK-WC membranes

The polymer PEEK-WC (poly(oxa-p-phenylene-3,3-phthalido-p-phenylene-oxy-phenylene) (2 g) was dissolved in chloroform (18 g) by magnetically stirring overnight to allow its complete dissolution at room temperature²⁴⁴. The solution was then casted on a glass plate by means of a manual casting knife (thickness 250 μm). After solvent evaporation, the casted film was immersed in a coagulation bath containing distilled water in order to detach the obtained dense membranes. Then, they were dried in an oven at 40 °C for 24 hours. The thickness of membrane PEEK-WC was $250 \pm 0.5 \mu\text{m}$ with 3 measurements. The preparation of membrane is shown in Figure 3-1.

3.3.3 Supported ionic liquid membranes

A hydrophilic PAN flat sheet membrane was used as the support membrane, it is purchased from Synder Filtration (U. S. A.). All the SILMs used through this study were prepared by the following immobilization procedure: a commercial circular flat sheet ultrafiltration membrane (PAN) was placed inside the membrane cell. The ionic liquid was added on top of the membrane with a pipette. The quantity of the added ILs was enough to cover the surface of the porous membrane homogeneously and completely. An O-ring was installed on the circular membrane and gently pressed down on the membrane. Then, the membrane cell was closed by lifting it from the holder and inserting the bottom part into the upper part of the cell, so that both parts fit smoothly into each other. Finally, the cell was fixed and tightened by closing the bolts. A vacuum from a rotatory pump (50 mbar) was applied for 2 hours to remove all of the air from the pores of the membrane and suck the ionic liquids into the pores. When the immobilization was completed, the excess of IL on the membrane surface was removed carefully using a tissue. To determine the amount of ionic liquid immobilized in the support membrane, all the membranes were weighted before and after

impregnation with an analytical balance (AE 260 mettler toledo, Belgium). The thickness of the prepared SILM is around $200 \pm 0.5 \mu\text{m}$ with 3 measurements.

Polyacrylonitrile (PAN) is chemically stable and PAN ultrafiltration membranes can be prepared via phase inversion process²⁴⁵. It shows excellent mechanical and chemical stability²⁴⁶. According to the information provided by supplier, the porosity is 60% - 70% and contact angle is 81° . The amount of ionic liquid immobilization is $67.7 \pm 1.4 \text{ g/m}^2$ for [OMIM][NTf₂] and $69.6 \pm 1.25 \text{ g/m}^2$ for [OMPyrr][NTf₂], respectively.

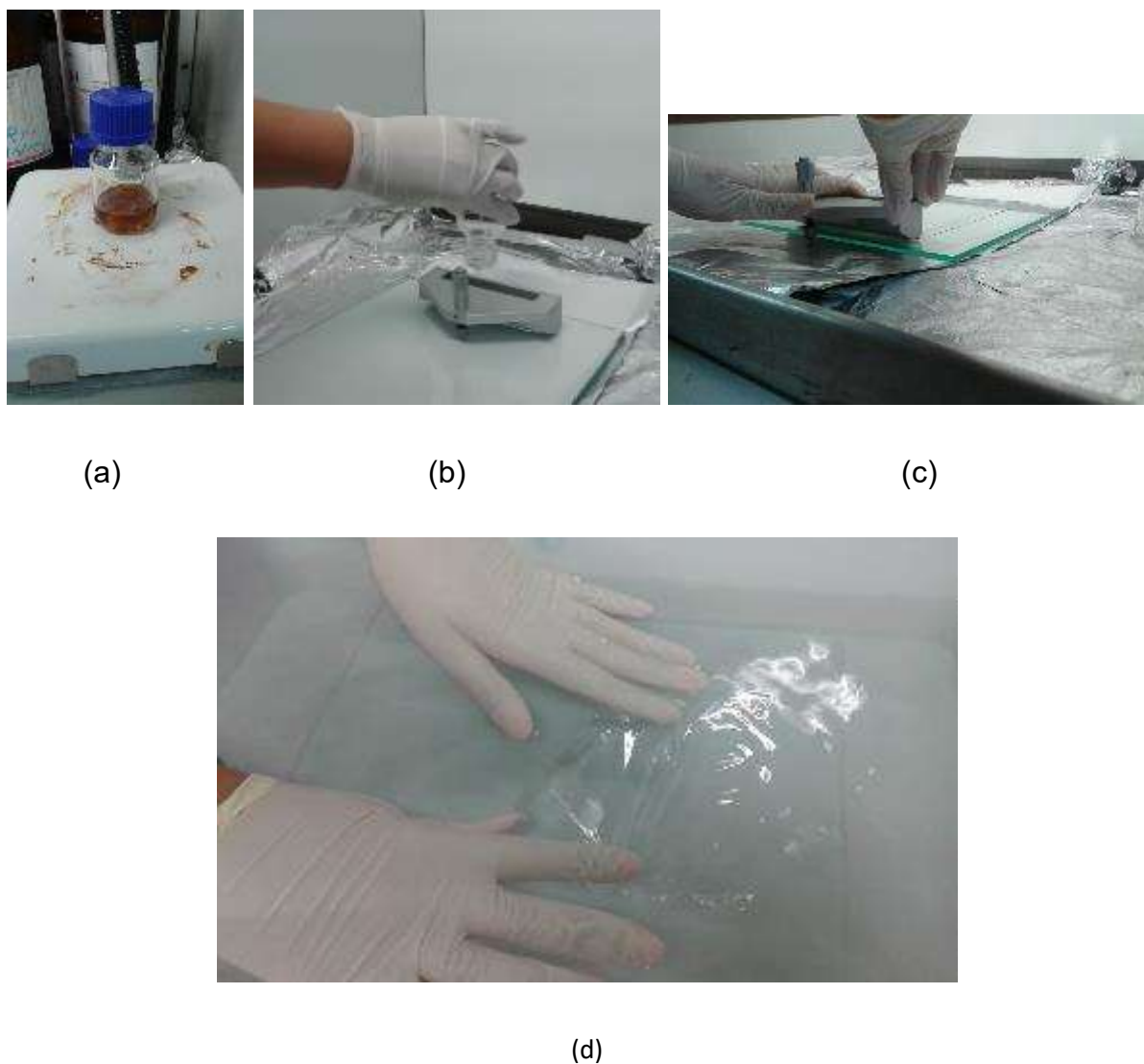


Figure 3-1. PEEK membrane preparation: (a) Preparation of polymer solution; (b) Casting on a glass plate; (c) after evaporation; (d) detach membrane from glass plate.

3.4 Pervaporation setup

In this work, two pervaporation units were used for the pervaporation laboratory tests.

3.4.1 3" round cell from Sulzer Chemtech (Sulzer unit)

Pervaporation experiments were carried out using a pervaporation laboratory test unit with a 3" round cell from Sulzer Chemtech, Switzerland. The schematic representation and photo of the pervaporation laboratory test unit and the 3" round cell from Sulzer Chemtech, Switzerland, is shown in Figure 3-2. The experimental temperature (temperature in the membrane cell) was kept at desired temperature by a heating circulator (Julabo model ME, Germany). The vacuum pressure at the permeate side is 8-12 mbar provided by a vacuum pump. A flat sheet membrane with a diameter of 7.0 cm (active area of 38.48 cm²) was installed in the membrane cell. All tested membranes were immersed in the feed solution for 24 hours before the experiment was carried out. When the experiment started, the set-up was allowed to stabilize for two hours before the samples of permeate were collected. The feed solution was transported and recirculated by using a centrifugal pump with a peripheral impeller (Speck Pimpen Systemtechnik GmbH, Germany) and the flow rate was between 70-80 L/h. With this high flow rate, the estimated Reynolds number reached 12550 in the membrane cell, according to the calculations shown in Appendix A3.1. Concentration polarization is a phenomenon produced by concentration gradients at the membrane and the liquid feed interface due to the selective transportation of some species through the membrane. The impact of concentration polarization may be enhanced due to the increase in membrane permselectivity. However, concentration polarization is unlikely to have a strong impact on the pervaporation separation performance when the feed concentration is high²⁴⁷. Therefore, a turbulent flow in the membrane cell can be achieved in order to reduce the concentration polarization effect. The permeate was collected every 30 minutes or 60 minutes, depending on the amount of permeate collected. The feed sample was collected and analyzed at the beginning of the experiment and every 2 hours. A constant value of feed concentration was observed, which indicates that no chemical reaction took place during the experiment and a pseudo steady state could be kept due to the recycling of the retentate. The analysis of concentration was performed by gas chromatography, according to section 3.6.

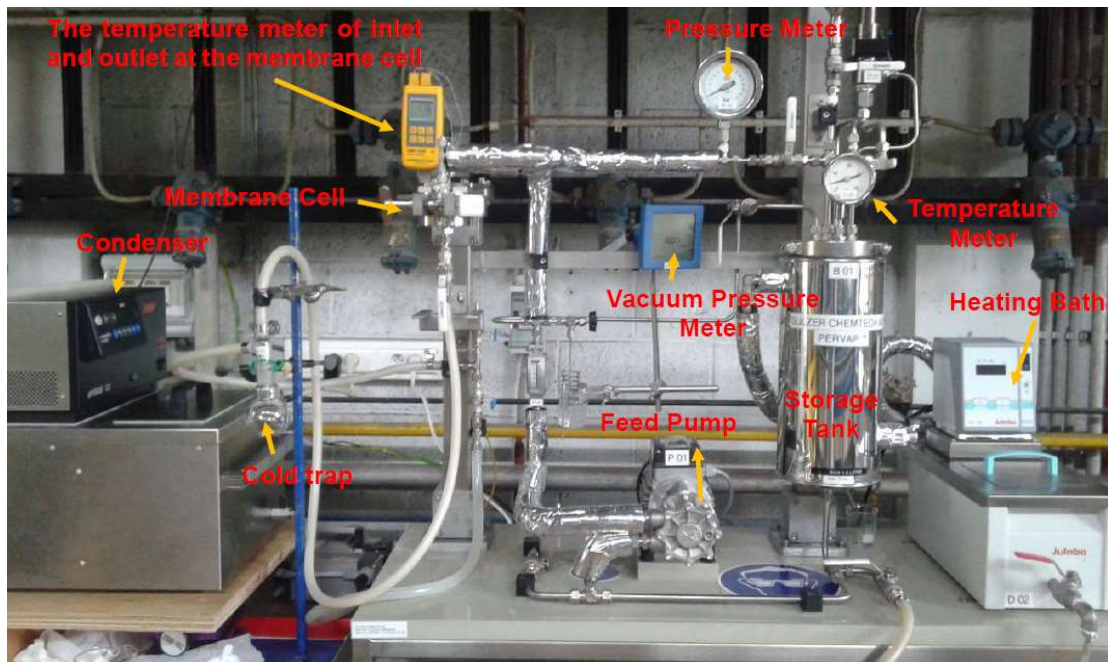
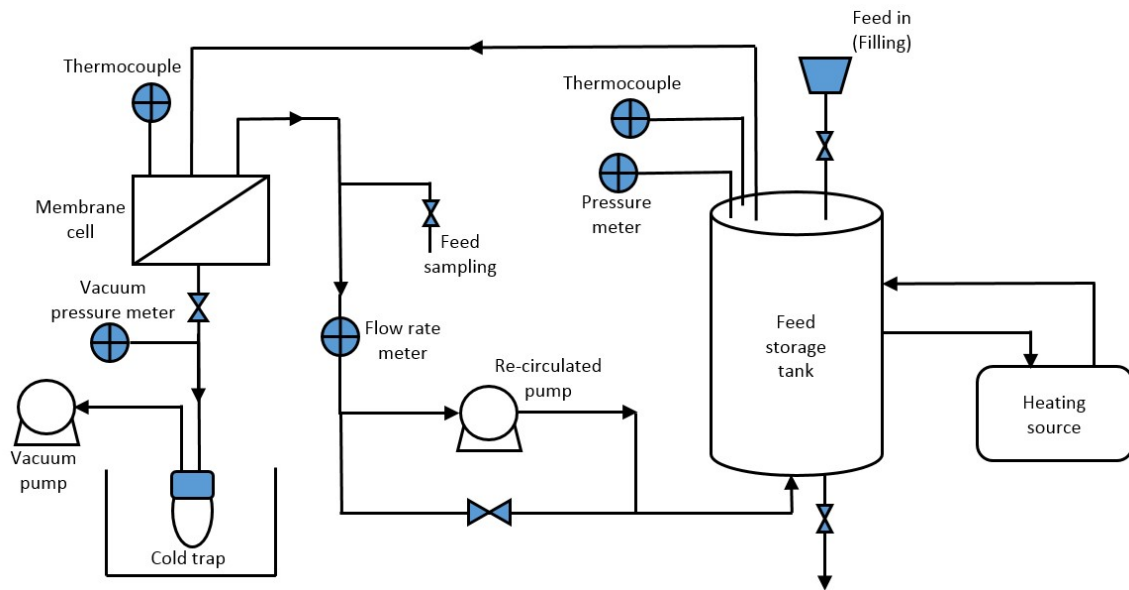


Figure 3-2. Schematic representation of the pervaporation experimental equipment

3.4.2 DeltaE s.r.l cell

The second pervaporation unit used in this thesis was produced by DeltaE s.r.l., Italy. The scheme and photo of the experimental set-up is presented in Figure 3-3. It is composed of a stainless feed tank with inner diameter 89 mm, an overhead stirrer, a heating circulator and a vacuum pump. The principle of this pervaporation experimental set-up is the same as the 3" round cell from Sulzer. An overhead stirrer was installed with a rotation speed of 40 rpm in order to avoid concentration and

temperature polarization on the surface of the membrane. The estimated Reynolds number is within the range from 4110.85 to 4851.40 in the membrane cell. Hence, turbulent flow conditions are achieved. In this setup, the feed solution is confined in the membrane cell, involving no cross flow over the membrane, which is a key difference with the pervaporation unit from Sulzer (section 3.4.1). The vapor permeate was condensed and collected in a “U” type glass trap immersed in a liquid nitrogen tank.

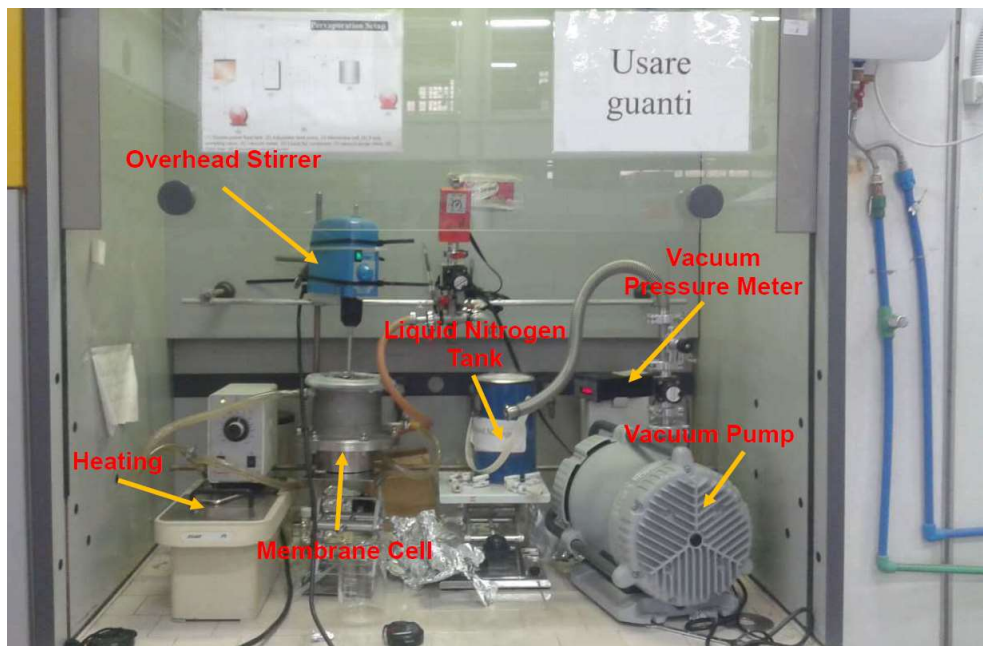
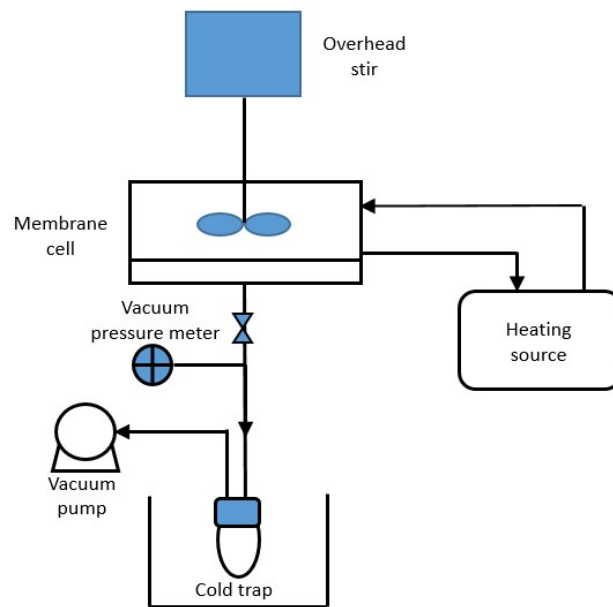


Figure 3-3. Scheme of the pervaporation experimental set-up

3.5 Pervaporation experiments

3.5.1 Experiments performed with the Sulzer Unit

3.5.1.1 Quaternary mixture of reaction 1 and reaction 2

For reaction 1 and reaction 2, two different quaternary mixtures were prepared as feed solutions: 1) methyl acetate, n-butanol, butyl acetate and methanol, named mixture M1; and 2) ethyl acetate, methanol, methyl acetate and ethanol, named mixture M2. Both mixtures were stored in a 1.5-liter stainless steel feed tank. In the poly(vinyl alcohol) production, the mixture of methyl acetate (0.2 molar fraction) and methanol is a by-product. Jimenez *et al.*²⁷ designed a new process route to recover methyl acetate from a feed solution composed of (mole fraction): 0.2 (methyl acetate), 0.15 (n-butyl acetate), 0.35 (methanol) and 0.3 (n-butanol). This composition was also studied in this thesis as the mixture M1 in order to have a real industry scenario. For mixture M2, in the work of Dossin *et al.*³⁰, the molar ratio of methanol/ethyl acetate is 0.1-10. In order to make a comparison with the mixture M1, the same organic solvents are kept the same molar fraction in the mixture M2. Therefore, the concentration of methyl acetate and methanol in mixture M2 is kept the same as those in mixture M1. The mole fraction of ethyl acetate and ethanol is 0.15 and 0.3, respectively. In this work, each experiment was carried out twice in order to check the reproducibility of experimental results. The analysis of concentration was performed by a Shimadzu GC-14A gas chromatograph as indicated in section 3.6.1.

3.5.1.2 Quaternary mixture of reaction 3

The feed solution corresponds to the mixture of the transesterification reaction between glycerol and dimethyl carbonate (reaction 3). The initial mixture before the reaction starts is biphasic (mixture of glycerol and DMC). The molar fraction of the initial mixture is 1:2 in glycerol/DMC, an excess of dimethyl carbonate being used both to favour the kinetics of the reaction and to force the equilibrium towards the formation of glycerol carbonate. Noteworthy, glycerol is a relatively viscous liquid, and using more dimethyl carbonate can improve the mixing between reagents and the catalyst. Glycerol (678.75 g), DMC (1386.74 g) and the catalyst NaAlO₂ (18.83 g) are mixed in a 2500 mL round bottom flask glass reactor equipped with a magnetic stirrer and heated in an oil bath. The reaction was run for 30 min at 90 °C. After reaction, the

mixture was filtered in order to remove the fine powder catalysts. The final concentration of the filtered mixture is determined by gas chromatography (see section 3.6.2). After filtration, the mixture is a monophasic system with a molar ratio of 0.075/0.291/0.193/0.44 in glycerol/DMC/glycerol carbonate/methanol. A calibration curve is obtained by performing GC analysis of samples of known concentrations. Three trials were done for each of the data points. This information was then used to estimate the error bars. The standard deviation is ± 0.03 . Theoretically, the reaction stoichiometry of glycerol carbonate and methanol is 1:2. Experimentally, the molar fraction of glycerol carbonate and methanol was $0.193(\pm 0.03):0.44(\pm 0.03)$. This mixture is the feed solution for the pervaporation experiments.

3.5.1.3 Binary mixture DMC and methanol via SILMs

The experimental temperature in the membrane cell was kept at 30 °C (± 2 °C). The temperature was maintained by a heating circulator (Julabo, Germany). A vacuum pump was used at the permeate side giving a vacuum pressure of 1-2 mbar. The prepared supported ionic liquid membranes were placed in the membrane cell and the surface area of installed supported ionic liquid membrane was 38.48 cm² (diameter 7.0 cm). The sampling of the permeate was collected after two hours running of the system in order to reach stable conditions. The sample of permeate was weighed every 60 minutes. The concentration of samples was analyzed every 120 minutes by means of gas chromatography as indicated in section 3.6.3. The prepared membranes were tested with different composition of binary mixtures methanol/DMC. The feed compositions were 0.2, 0.5, 0.8 mole fraction of methanol.

3.5.2 Experiments performed with the DeltaE s.r.l cell for binary mixtures of dimethyl carbonate and methanol (reaction 3)

From the experimental results shown in chapter 5, it was decided to focus on the separation of the binary mixture dimethyl carbonate and methanol. The feed solution (around 100 mL) was poured in a stainless steel feed tank with an inner diameter of 89 mm. The feed compositions of 0.1, 0.3, 0.5, 0.7, 0.9 mole fraction of methanol were studied. When the experiment started, the system was run for two hours in order to achieve quasi static steady state before the sample of the permeate was collected. An overhead stirrer was installed with a rotation speed of 40 rpm in order to avoid

concentration and temperature polarization on the membrane surface. A heating circulator was employed to maintain the experimental temperature of the feed solution at 30, 40, 50 or 60 °C (± 2 °C). The prepared membrane was contacted with different compositions of binary mixtures methanol/DMC. The prepared PEEK-WC membrane was immersed in the feed solution for 24 hours before the start of the experiments. The permeate was collected every 60 minutes and the composition of the permeate was analysed by means of an Abbe 60 type direct reading refractometer (Bellingham+Stanley Ltd., UK) at 25 °C.

3.6 Gas chromatography analysis

3.6.1 Reaction 1 and reaction 2

A gas chromatograph (Shimadzu GC-14A) was applied for determining the composition of permeate and feed solution from reaction 1 and reaction 2. The mobile phase was helium. The packed column is Stabilwax (Length: 30 m, Internal Diameter: 0.32 mm, DF: 1.0 μ m) and equipped with a FID (flame ionisation detector). The initial injection temperature was 200 °C and the detector temperature was 250 °C. The parameters of the headspace (injection of vapor) are: the temperature was 80 °C, the temperature of the needle was 100 °C and the injection time was 0.02 minutes.

3.6.2 Reaction 3

The reaction products before and after pervaporation of reaction 3 were analyzed by gas chromatography (GC-456 SCION BRUKER) equipped with a flame ionization detector, split/splitless injection unit and a capillary column (DB-WAX, 30 m, 0.25 mm, 0.25 μ m). Helium was used as the carrier gas. The injection was performed in split mode with a split ratio of 100:1. Initially, the oven temperature was set at 80°C and it was increased at the rate of 15°C /min until it reached 240°C. Then, it was maintained at this temperature for 15 min. The FID and injection temperatures were fixed at 270°C and 300°C, respectively. The molar fractions of the organic compounds based on a calibration curve were obtained from the analysis of the gas chromatograph.

3.6.3 Samples from the experiments of supported ionic liquid membranes

The composition of feed and permeates were analyzed by gas chromatography (Interscience TRACE 1300) equipped with a flame ionization detector (FID), split/splitless injection (SSL) unit, thermal conductivity detector (TCD) and a capillary column (Stabilwax, 30 m, 0.32 mm, 1 μ m). The carrier gas was helium and the injection was performed in split mode with a split ratio of 100. Initially, the oven temperature was set at 50°C and it was increased at the rate of 20°C /min until it reached 150 °C. Then, it was maintained at this temperature for 1 min. The FID and injection temperatures were 250°C and 300°C, respectively.

3.7 Membrane characterization

3.7.1 Measurement of membrane sorption

Sorption measurements were performed in the separation of binary mixtures methanol/DMC using PEEK membranes. Three membrane pieces were immersed and weighed in pure solvents as well as in methanol/DMC mixtures with a combination of 0.1, 0.3, 0.5, 0.7, and 0.9 molar fraction at room temperature (25 °C) for 7 days so that the membrane and solution reached sorption equilibrium. After achieving sorption equilibrium, the membranes were taken out from the solution. The excess of liquid on the membrane surface was removed immediately by using tissue paper. After cleaning, the membrane was weighed on a high precision balance (Mettler-Toledo, AE200, Belgium) with a precision of +/- 0.0001 g. The sorption degree of the membrane was then calculated by the following equation²⁴⁸:

$$SD = \frac{m_w - m_d}{m_d} \times 100\% \quad (3-1)$$

where m is the mass of membrane (g); subscripts w and d refer to the membrane after sorption (wet) and before sorption (dry), respectively.

3.7.2 Contact angle measurement

Wettability is the ease of spreading of a liquid on a solid surface. It is determined by contact angle measurements. The contact angle (θ) with water is obtained by measuring the angle between the solid-liquid interface and the liquid-vapor interface.

When $\theta < 90^\circ$, the membrane is defined hydrophilic. Otherwise, the membrane surface is hydrophobic. The contact angle of the membrane surface was measured by an optical instrument (Nordtest srl, G-I, Italy) at room temperature and the measurements were repeated three times. A water droplet generated by a needle was dropped on the membrane surface and the contact angle was measured immediately.

3.7.3 Mechanical test

For PEEK membranes, mechanical tests were performed using a Zwick/Roell testing machine single column model Z2.5, equipped with a 50 N maximum load cell (BTC-FR2.5TN-D09, Germany). Each membrane sample (1 cm x 5 cm) was stretched unidirectionally at the constant rate of 5 mm/min until its break.

3.7.4 Scanning electron microscopy (SEM) analysis

The morphology of the prepared PEEK membranes (top, bottom and cross-section) was evaluated by scanning electron microscopy (Zeiss, EVO MA10). Before the analyses, all the samples were sputter coated with a thin layer of gold (Quorum Q150 RS) to make them conductive.

For supported ionic liquid membranes, in order to qualify the quality of impregnation (if they were filled up with ILs), the morphology of the cross section before (raw PAN membrane) and after adding the ILs was analyzed by SEM (Zeiss, ULTRA). Before analysis, all the samples were sputter coated with a thin layer of gold (BALZERS UNION FL 9460 BALZERS SCD 030) to make them conductive. SILMs were cut in small rectangular pieces and immersed into liquid nitrogen. As the polymeric material from which they are made up is very brittle at such low temperatures, samples were broken without deforming the cross section.

Chapter 4. Application of pervaporation in the production of butyl acetate and methyl acetate

Based on:

Wenqi Li, Patricia Luis, Understanding coupling effects in pervaporation of multi-component mixtures, *Separation and Purification Technology* 197 (2018) 95–106.

4.1 Introduction

In this chapter, commercial membranes for organic-organic separations from Sulzer were used at different temperatures and different concentrations of the feed solution. The performance of each membrane is evaluated for the two model transesterification mixtures produced in reaction 1 and reaction 2. The mixture from reaction 1 (methyl acetate, butyl acetate, butanol and methanol mixture) refers to mixture M1 and the mixture from reaction 2 (ethyl acetate, methyl acetate, ethanol and methanol mixture) refers to mixture M2. Since strong coupling effects were observed, the objective of the work was oriented to determine the origin of component interactions. Firstly, coupling effects were evaluated by studying and comparing the solubility of pure substances and mixtures in the polymeric membrane, based on the Hansen solubility theory. Secondly, the variation of activities within the membrane was investigated, following the Flory-Huggins theory.

In this chapter, the following scientific question will be studied:

- Is it possible to apply theories based on solubility parameters, which is commonly used in material screening, to predict potential coupling effects in the separation?

4.2 Sorption experiments

Figure 4-1 shows the sorption experimental data, which is the average of three samples, and the standard deviation. An increase of the membrane weight after immersion in pure solution and in the different mixtures is observed. For pure solution, the membranes sorb preferentially more alcohols than esters with butyl acetate as exception. The sorption degree follows: butanol > butyl acetate > ethanol > methanol > methyl acetate \approx ethyl acetate. Methyl acetate and ethyl acetate have a very low sorption degree. Comparing the two mixtures, mixture M1 leads to a larger weight increase than the mixture M2. This could be caused by the presence of butyl acetate in the mixture 1. In pervaporation, polymer-solvent interactions combine sorption and membrane swelling in liquid media. When the polymeric membranes swell, the swelling of polymers involves either mutual solution of miscible substances, *e.g.*, the penetrants and the polymer, or solution of the low molecular penetrants in the polymer. The affinity between the penetrant and the polymer determines the concentration of

penetrant in the polymeric membrane. In either case, a higher solubility of the penetrants in the polymeric membrane leads to an enhanced chain mobility which increases the diffusivity of penetrant²⁴⁹. On the other hand, a more swollen polymeric membrane can permit a relatively large molecules diffuse through²⁵⁰. Therefore, the transmembrane flux can increase due to the swelling effect. Contrarily, the membrane selectivity can decrease because larger molecules can pass through the membrane. For this reason, it is important to be aware of the impact of swelling effects caused by the interaction between the penetrant and the polymer²⁵¹. The sorption of penetrants by polymer is caused by the equilibrium between the chemical potentials of the penetrants in the system²⁵². Therefore, it is important to immerse the membranes in the feed solution prior to perform the experiment.

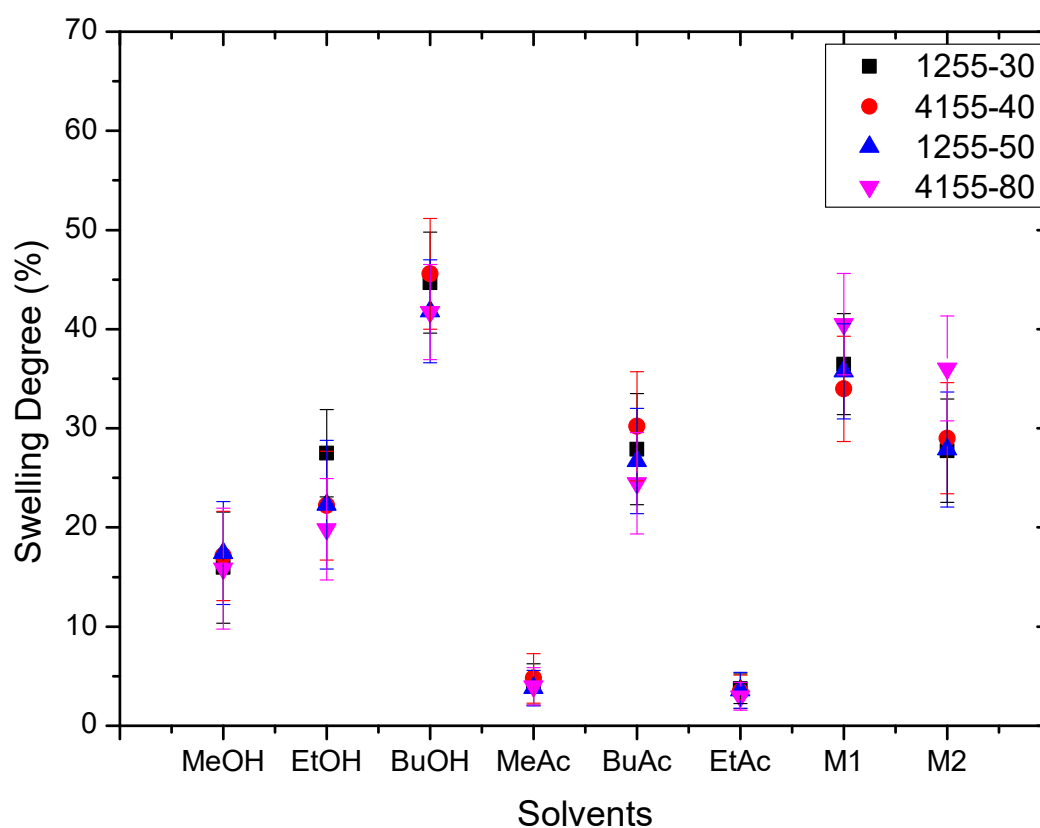


Figure 4-1. Sorption degree after immersion of membranes in the pure solution, in the mixture of methyl acetate (MeAc), butyl acetate (BuAc), butanol (BuOH) and methanol (MeOH) with molar fraction 0.2/0.15/0.3/0.35 (mixture M1), and mixture of methyl acetate (MeAc), ethyl acetate (EtAc), ethanol (EtOH) and methanol (MeOH) with molar fraction 0.2/0.15/0.3/0.35 (mixture M2)

4.3 Pervaporation on pure solution

During the pervaporation experiments, the experiments of pure solution and mixture were performed twice. The transmembrane flux is the average of both experiments. The reproducibility of the results is calculated in terms of standard deviation based on two experimental measurements. In order to detect coupling effects in multicomponent mixtures, it is necessary to determine the permeance of each compound when they are alone in the feed. The results of the transmembrane flux of each pure compound through the studied membranes at different temperatures are shown in Figure 4-2. The driving force for mass transport is strongly affected by the concentration and the vapor pressure of the compound²⁵³. As a result, the transmembrane flux cannot reflect the real interaction/affinity between compounds and the membrane material. Thus, the permeance is key to eliminate the influence of the applied driving force, shown in Figure 4-3. For pure solution, the selectivity has been calculated as the ratio of the permeance of each pure compound related to the permeance of methanol.

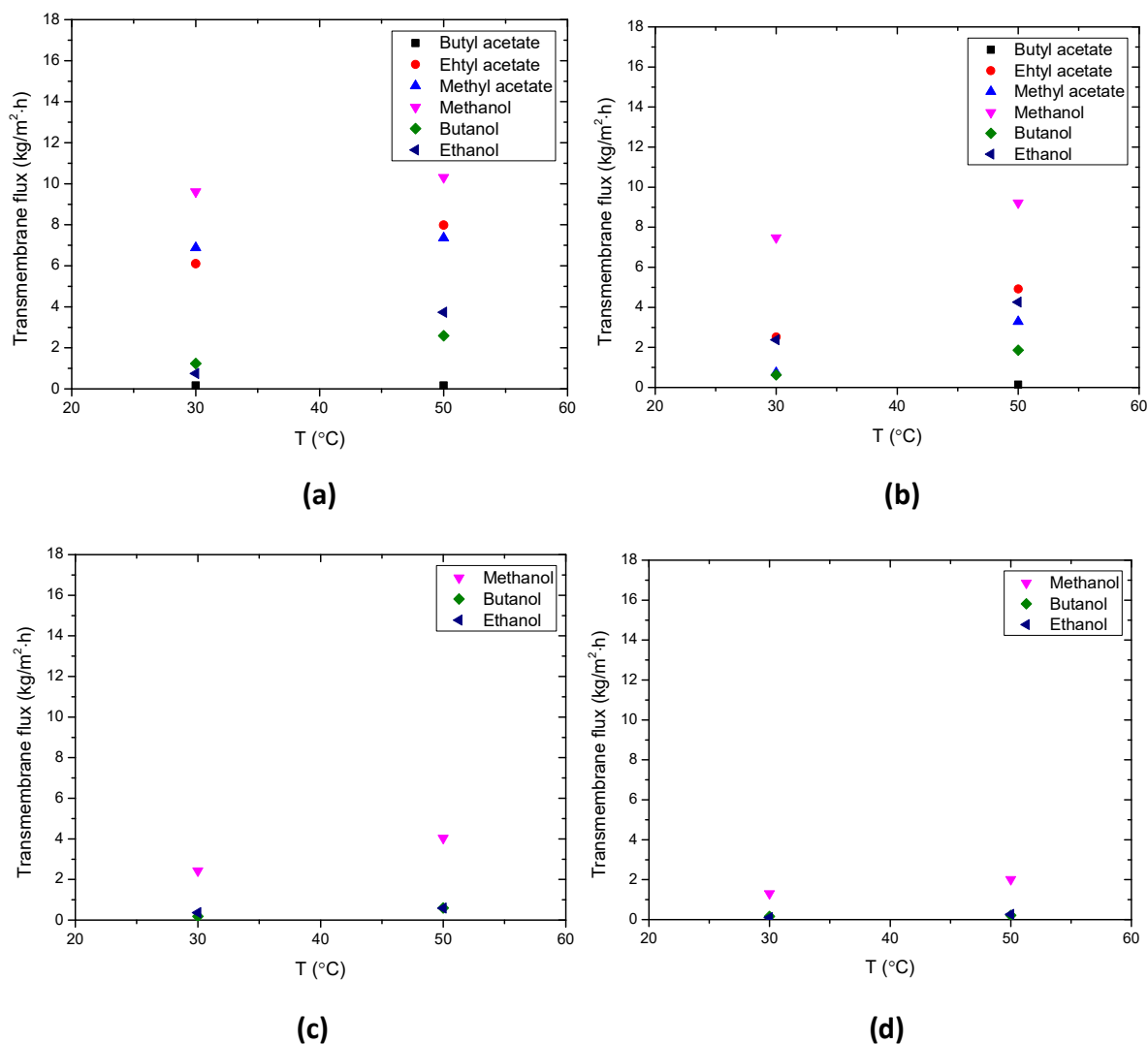
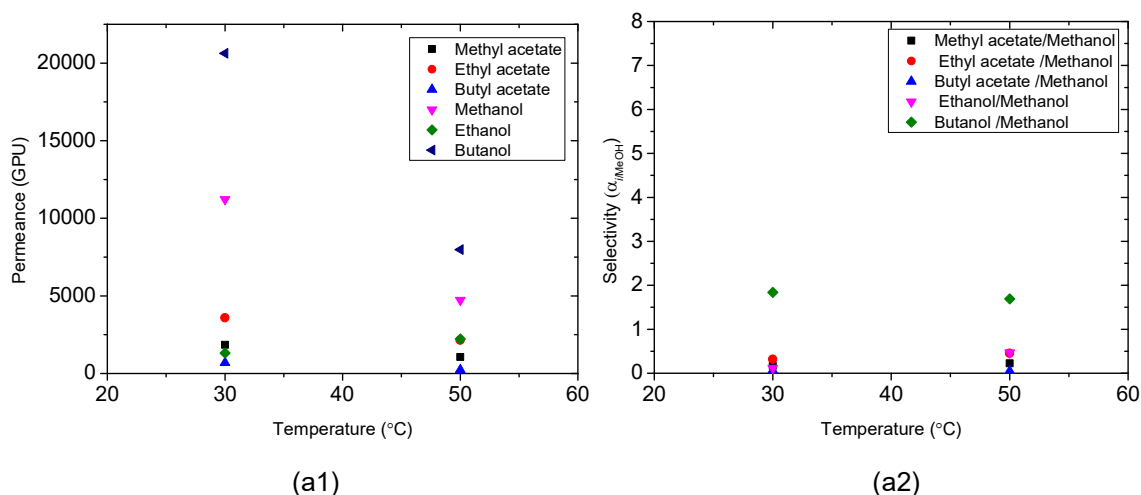


Figure 4-2. Transmembrane flux of pure compounds, (a) 1255-30 membrane; (b) 4155-40 membrane; (c) 1255-50 membrane; (d) 4155-80 membrane

In Figure 4-3, it can be observed that all the membranes can permeate the alcohols and follow the preferential permeability sequence of butanol, methanol, and ethanol at different temperatures. The membrane 4155-40 can permeate butyl acetate only at higher experimental temperature (334 GPU at 50 °C) and the membranes 1255-50 and 4155-80 do not permeate methyl acetate, ethyl acetate and butyl acetate (permeate was not produced during the experiment). From the experimental evaluation of sorption by alcohols shown in section 4.2, it was observed that the membranes can sorb all alcohols, which is in good agreement with the pervaporation results (all the alcohols can be permeated). Methanol has the highest transmembrane flux due to its high vapor pressure and small molecule size (Figure 4-2). However, when looking at permeance in Figure 4-3 to remove the effect of the driving force, it is clear that butanol has the highest permeance, followed by methanol and ethanol.

In addition, the membranes 1255-50 and 4155-80 are very selective to alcohols and do not allow the permeance of esters. This result is also consistent with the result obtained from sorption of pure solutions of methyl acetate and ethyl acetate due to the low sorption degree. However, butyl acetate does not follow this trend. These membranes preferentially sorb butyl acetate but no permeate was obtained. This phenomenon confronts the pervaporation results with the sorption results. The explanation could be related to the membrane-solvent interaction and the membrane structure. The membranes 4155-80 and 1255-50 have less free volume for permeation comparing with the other two types of membranes because only certain size of molecules can diffuse easily through the membrane. According to the solution-diffusion model, the permeants have to be sorbed by the polymeric membrane, then diffuse through the membrane due to the difference of partial pressure across the membrane⁷³. Therefore, after sorption, if the free volume is large as may be in the membrane 1255-30, larger molecular size compounds (such as butyl acetate, which has largest molecular size among all compounds) can diffuse through the membrane. On the contrary, when the free volume is small, the large molecules cannot diffuse through the membrane, as happens in the membranes 1255-50 and 4155-80, in which only alcohols can diffuse due to their small molecular size. On the other hand, the mobility of polymer chains and the free volume can allow faster diffusion by increasing temperature. Therefore, butyl acetate was not observed in the permeate of the membrane 1255-40 at 30 °C but it was observed at 50 °C. In addition, the permeance of butyl acetate is much lower than that of methanol and ethanol, but it has higher sorption degree than these two alcohols. Thus, diffusion is the limiting factor of the permeance of this compound through the membrane.



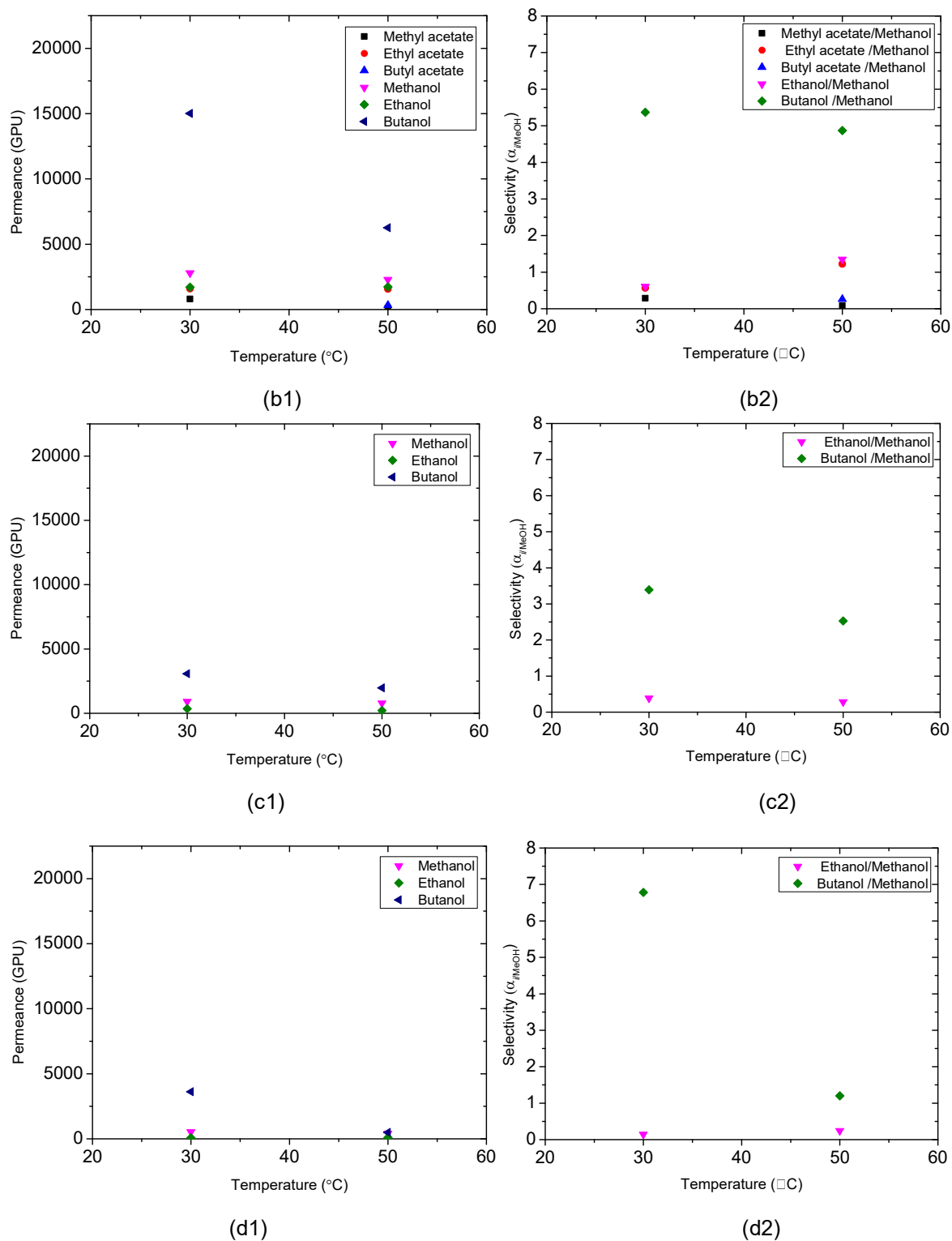
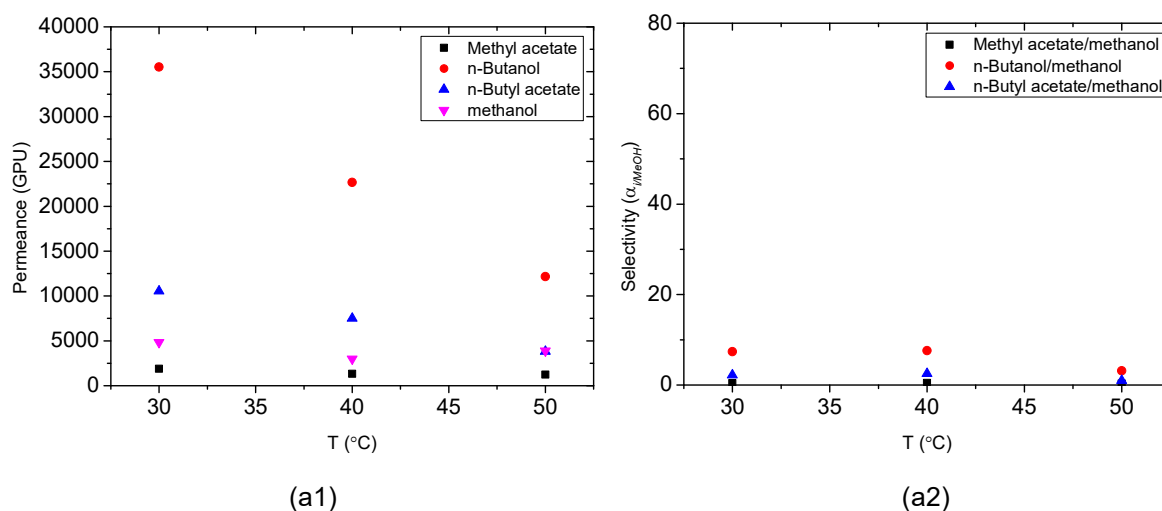


Figure 4-3. The permeance (left) and selectivity of different type of membranes for different pure compounds at different temperature, (a) 1255-30 membrane, (b) 4155-40 membrane, (c) 1255-50 membrane and (d) 4155-80 membrane

4.4 Pervaporation of mixtures

4.4.1 Effect of the feed composition

The results of transmembrane flux and separation factor for the mixture M1 and mixture M2 have been included in Appendix Figure A4.1, Figure A4.2, Figure A4.3 and Figure A4.4, respectively and the experimental results of permeance and selectivity for the mixture M1 and mixture M2 are shown in Figure 4-4 and Figure 4-5, respectively. The experimental data show a significant decrease in the permeance of the components when the temperature increases. This phenomenon can be interpreted in terms of activation energy. The activation energy of permeation has an impact on the change of the permeation behavior of membranes caused by temperature variation^{19,90}. The activation energy of diffusion is normally positive: a higher temperature enhances the diffusivity of molecules, increasing the permeation. On the other hand, the heat of solution can be negative in a sorption process: a higher temperature may cause a disadvantage for sorption. The final activation energy of permeation is defined as the contribution of these two processes. If the sorption is dominant, the activation energy is negative, leading to a decrease of permeance with an increase of temperature.



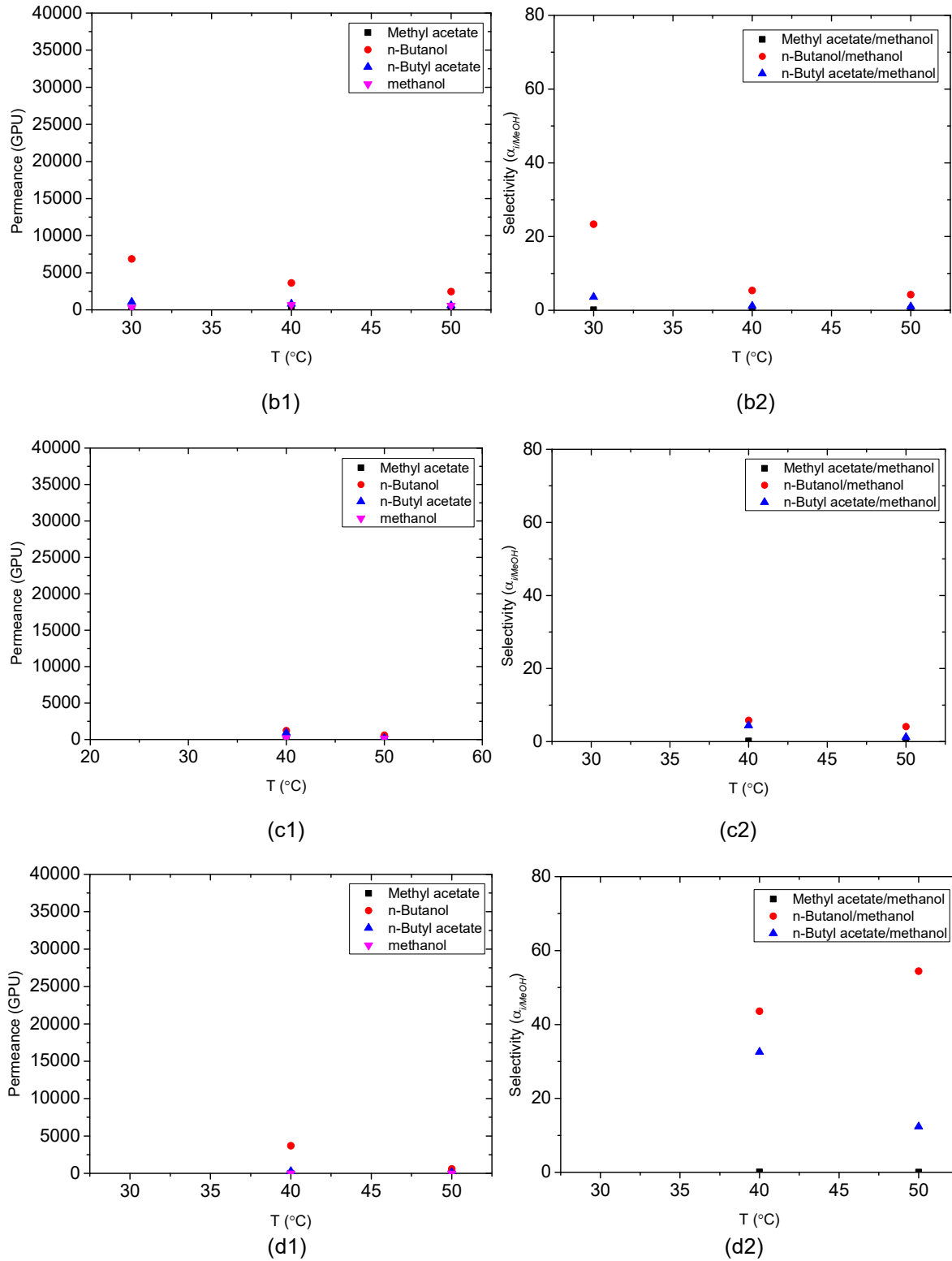
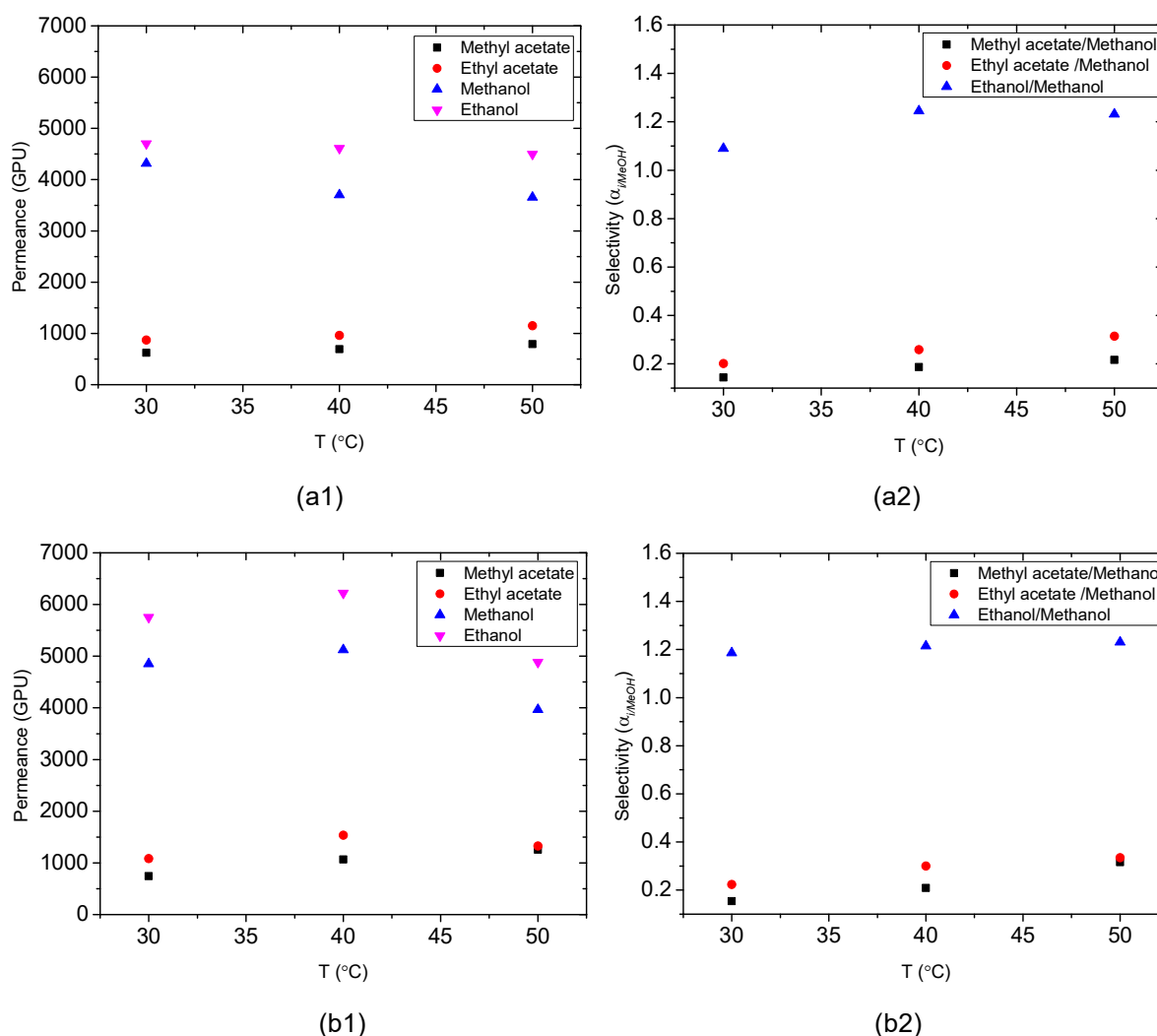


Figure 4-4. The permeance (left) and selectivity (right) of different types of membranes for mixture M1 at different temperature (a) 1255-30 membrane, (b) 4155-40 membrane, (c) 1255-50 membrane and (d) 4155-80 membrane

For the mixture M1 (Figure 4-4), several interesting observations can be inferred from the results. Firstly, butanol presents the largest permeance in spite of the highest flux of methanol. This aspect is directly related to the effect of the higher driving force that methanol has in the mixture due to a higher volatility, as indicated before. Secondly, butyl acetate presents a permeance higher than methanol in all the membranes, while a lower permeance was observed when working with pure feed solutions. A clear coupling effect of butyl acetate by the presence of other compounds is taking place. Thirdly, methyl acetate and ethyl acetate were obtained in the permeate for the membranes 1255-50 and 4155-80 when the feed solution is a multicomponent mixture, but in section 4.3, it was observed that both components did not permeate through the membranes (1255-50 and 4155-80) regardless the temperature and only alcohols did permeate through these membranes when pure solutions were considered. This result is also an indication of the presence of coupling effects among components, in which some compounds are dragging others through the membrane.



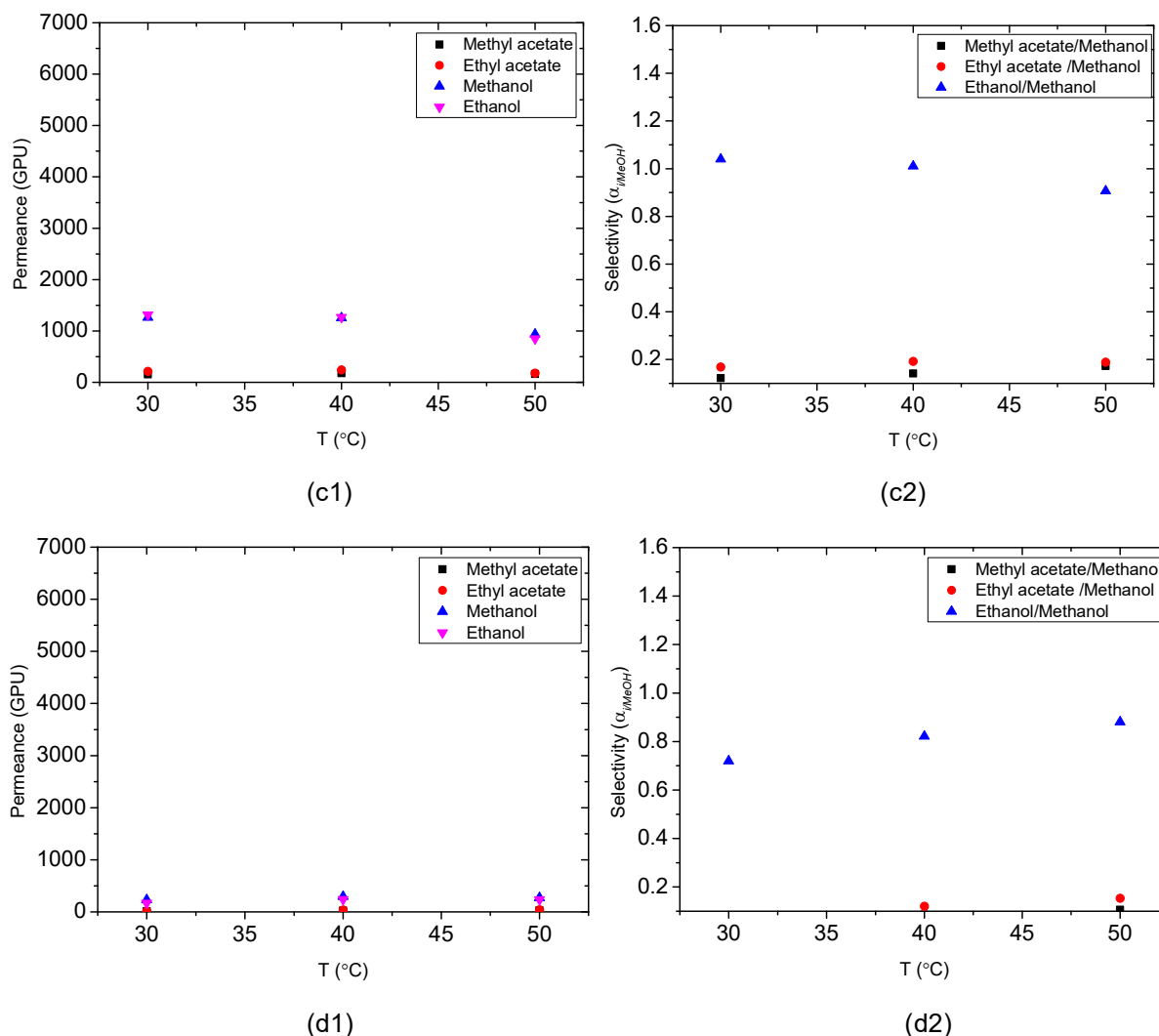


Figure 4-5. The permeance (left) and selectivity (right) of different types of membranes for the mixture M2 at different temperatures (a) 1255-30 membrane, (b) 4155-40 membrane, (c) 1255-50 membrane and (d) 4155-80 membrane

Regarding the mixture M2 (Figure 4-5), the main aspect to highlight is the dramatic increase of the permeance of ethanol when present in the multicomponent mixture. In Figure 4-3, the permeance results of the pure compound showed a much lower permeance in comparison with methanol for all the membranes. However, in the mixture, ethanol is the main permeant for the membranes 1255-30 and 4155-40, it shows a similar permeance than methanol in the membrane 1255-50, and it shows a slightly lower permeance than methanol in the membrane 4155-80; but in all cases, the permeance of ethanol in absolute values is increased in comparison with the results using pure ethanol as feed solution. The presence of other compounds is clearly enhancing the permeance of ethanol through the four studied membranes.

The coupling effects indicated above can be interpreted in terms of the Hansen solubility theory, described in section 1.3.1. A 3D representation of the Hansen solubility sphere and projection into hydrogen-polar plane and hydrogen-dispersion plane for 30 °C are shown in Figure 4-6. The 3D representation for 40 °C and 50 °C can be found in Appendix (Figure A4.5 and Figure A4.6, respectively). From the information obtained from the supplier, the active layer of the studied membranes contains polyvinyl alcohol (PVA). The membrane 4155-80 has the highest degree of crosslinking than the other membranes, followed by 1255-50, 4155-40 and 1255-30. According to the literature⁸⁴, the interaction radius (R_0) of PVA is around $10.9 \text{ MPa}^{1/2}$. From Table 4-1, it is clearly shown that the distance between alcohols to the center of polymer (PVA) solubility sphere is shorter than interaction radius, therefore, these alcohols are located in the polymer (PVA) solubility sphere. On the other hand, esters were located outside of polymer (PVA) solubility sphere. This suggests that the membrane has more affinity to alcohols than to esters. This could explain the phenomenon observed in the sorption test, in which methyl acetate and ethyl acetate have a very low sorption degree (see Figure 4-1). In the pervaporation experiments of pure feed solution, the membranes 1255-50 and 4155-80 cannot permeate methyl acetate and ethyl acetate because these membranes contain a high fraction of PVA. These two compounds are not able to dissolve into the PVA membrane. The temperature effect can be compared with the three tables (Table 4-1 (30 °C), Table A4.3 (40 °C) and Table A4.4 (50 °C) in Appendix at 30 °C, 40 °C and 50 °C, respectively.). It is observed that the solubility parameters (δ_D , δ_P and δ_H) decreased with an increase in temperature. But the R_a of all esters and PVA increases significantly, this also indicates that the increase of temperature does not enhance the solubility of esters to PVA.

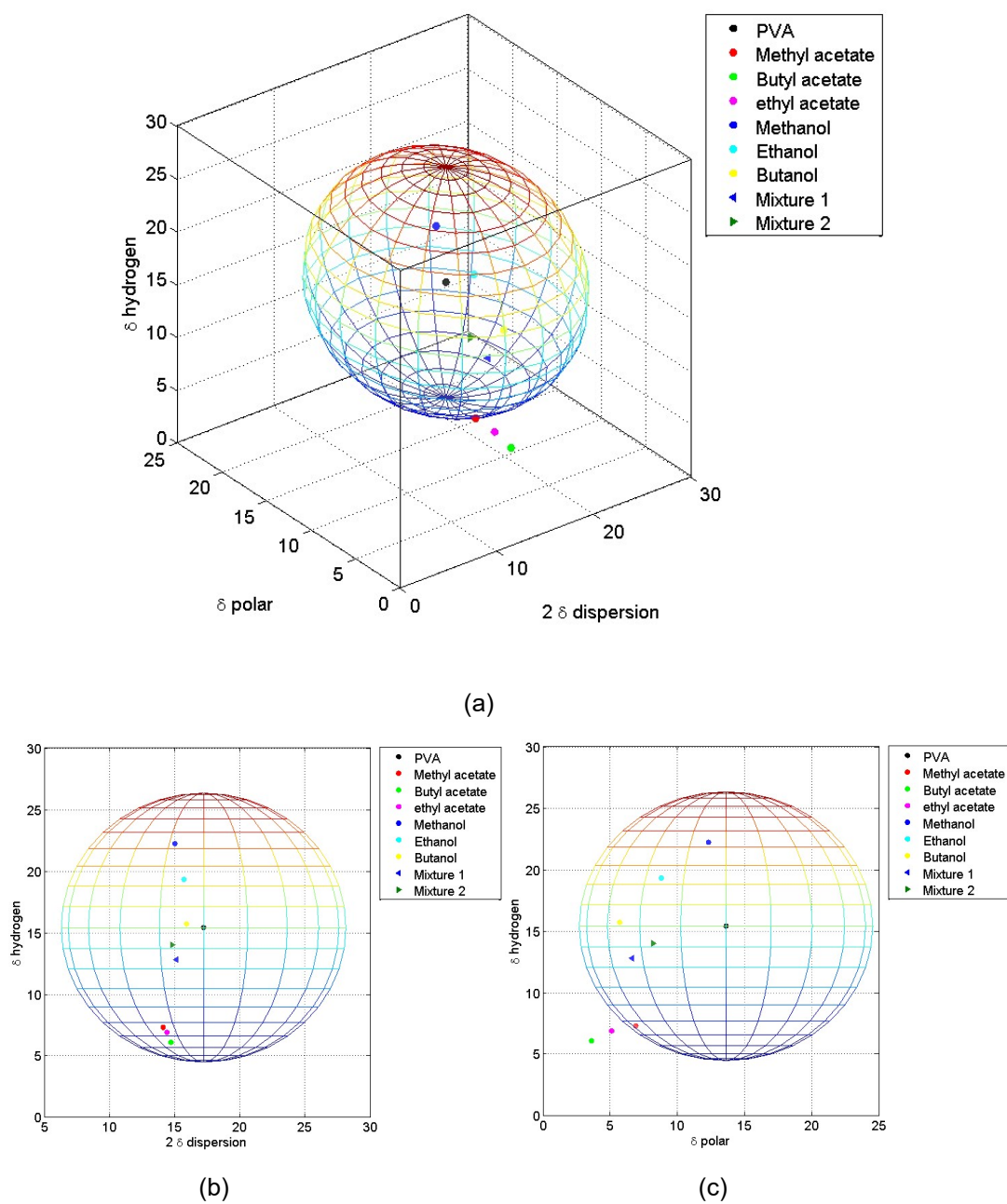


Figure 4-6. Hansen solubility sphere for PVA and pure components and mixtures at 30 °C (a) 3D representation; (b) Projection into the hydrogen-polar plane and (c) Projection into the hydrogen-dispersion plane

Table 4-1. Calculated Hansen solubility parameters of each component/mixture and R_a at 30 °C

Material	δ_D	δ_P	δ_H	R_a
PVA	17.2	13.6	15.4	
Methyl acetate	14.1	6.9	7.3	12.1
Butyl acetate	14.7	3.6	6.1	14.5
Ethyl acetate	14.4	5.1	6.9	13.2
Methanol	15.0	12.3	22.2	8.2
Butanol	15.9	5.7	15.7	8.3
Ethanol	15.7	8.8	19.3	6.9
Mixture M1	15.1	6.6	12.8	8.5
Mixture M2	14.8	8.2	14.0	7.3

Regarding the mixtures, the Hansen solubility parameters were changed according to the volume fraction of each component, calculated by equation (1-5). In Table 4-1 and Figure 4-6, it can be observed that the distance between mixture M1 and mixture M2 and the PVA sphere center is 8.5 and 7.3, respectively. Both of them are located inside the PVA solubility sphere. This indicates that both mixtures can dissolve in the PVA polymer. Consequently, all the components in the mixture can be sorbed by the membrane and then, diffuse through the membrane. Hence, it can be concluded that the sorption behavior of the polymeric membrane material changes due to the change of feed composition, which leads to the variation of the solubility of the different components into the polymer.

4.4.2 Effect of variation of the activity coefficient within the membrane

In addition to the coupling effects caused by the different solubilities of components into the membrane, which is affected by the concentration, another aspect that can affect the permeance of components is the variation of the activity coefficient of the components within the membrane⁶⁹. The interaction of permeants inside the membrane and the interaction of permeants and polymeric membrane in pervaporation process may have a strong impact on the performance of a polymeric membrane. The activity coefficient of one component can change when introducing other components or by contacting membrane materials. Thus, a positive or negative

influence can occur on the membrane performance. In this part, only the interaction of the feed compounds and the PVA polymer material are investigated, regardless of other factors such as polymer membrane structure. The experimental data of the membrane 1255-30 is applied in the analysis as example. In order to study the thermodynamic property inside the membrane by means of activity during the pervaporation process, it is assumed that the composition within the membrane is identical to the composition of permeate. The activities of the mixture in the feed solution and the mixture within the membrane were calculated according to Eq. (1-7) and they are shown in Table 4-2 for both mixture M1 and mixture M2.

Table 4-2. The activity of the mixture in the feed solution and the mixture within the membrane

Mixture 1	Methanol	Methyl acetate	Butanol	Butyl acetate
Activity within membrane (30 °C)	0.61	0.28	0.10	0.06
Activity in mixture (30 °C)	0.51	0.34	0.25	0.24
Activity within membrane (50 °C)	0.60	0.25	0.13	0.06
Activity in mixture (50 °C)	0.36	0.31	0.31	0.33
Mixture 2	Methanol	Methyl acetate	Ethanol	Ethyl acetate
Activity within membrane (30 °C)	0.61	0.22	0.29	0.11
Activity in mixture (30 °C)	0.40	0.36	0.33	0.28
Activity within membrane (50 °C)	0.57	0.23	0.31	0.13
Activity in mixture (50 °C)	0.40	0.35	0.32	0.27

In Table 4-2, the activity of each component within the membrane and in the mixture were calculated. In both mixtures, the activity of methanol was enhanced inside the membrane. This indicates that the local driving force within the membrane can be enhanced or reduced due to the interaction between permeants and polymer. One interesting observation is obtained when comparing the separation factor of the membrane 1255-30 for both mixtures. A high separation factor indicates that the component is concentrated in the permeate. It is observed that the separation factor in the mixture M1 (Appendix Figure A4.2) based on butyl acetate follows the order:

methanol>methyl acetate>butanol>1 and the separation factor in the mixture M2 (Appendix Figure A4.4) based on ethyl acetate follows the order: methanol>ethanol>methyl acetate>1. These trends follow exactly the order of activity values within the membrane, although the activity of methyl acetate in the solution is higher than that of ethanol (gray color in Table 4-2).

The results discussed above illustrate that the coupling effect can be also explained by the activity of the component within the membrane, leading to a different driving force than that produced by the feed solution. It indicates that interaction of components and membrane material is an important factor that can influence the permeation flux and composition in the permeate due to the activity variation within the membrane. In addition, the interaction between components and the membrane material as well as the swelling capability and swelling preference to certain components by the membrane material are critical factors in determining coupling effects as indicated in section 4.4.1.

There are some different findings in the application of commercial membranes on these two mixtures. The available information of the commercial membranes is that the membranes could contain less free volume with increasing of its series number (30 to 80). 4155-80 membrane can be a higher cross-link loading among these commercial membranes. Most surprisingly, in the mixture butyl acetate/methyl acetate/butanol/methanol, the experimental result shows that butanol is more favorable to permeate through the membrane. This finding was unexpected. The swelling of a solute in PVA depends on its polarity and molecular size. In the case of alcohols, polarity decreases with an increase in carbon number and methanol is more polar than another components. On the other hand, the chemical structure of alcohols contains –OH group, and esters contain =O and –O– group. PVA is a hydrophilic polymer with –OH group. Therefore, from the chemical structure, molecular size, hydrophilicity, PVA should more favorable to permeate methanol. In the work by Okuno *et al.*²⁵⁴, it is found that the permeability and selectivity of PVC membrane was affected by the molecular size of alcohols, small molecular alcohol gives a high permeation. Therefore, methanol should be more favorable to permeate through the membrane due to its small molecular size. In the literature^{19,82}, the performance of the membranes Pervap 2250-50 and Pervap 1201 made by Sulzer with a mixture of methanol/butyl acetate and methyl acetate/methanol/butanol/butyl acetate has been reported and a

similar phenomenon was observed. Although the exact information of these PVA-based commercial membranes is unknown, it is possible to deduce that this series of membranes may contain other materials, e.g. silicalite particles. In the literature²⁵⁵, such as Pervap 1070 membrane, the selective layer filled with a certain amount of silicalite particles. At a given temperature (25-65 °C), the butanol is more permeable than water due to silicalite fillers in the membrane, which have a strong affinity to butanol molecules. For this reason, the membranes can show a higher permeance for butanol. In addition, butanol and butyl acetate have a high swelling degree in these commercial membranes, this observation indicates that both of them easier to be sorbed by the membrane. The pervaporation performance of this separation system is found to be determined by this characteristics and respect to the preferential sorption is the prerequisite to the preferential permeation⁷³.

On the other hand, in the mixture ethyl acetate/methyl acetate/ethanol/methanol mixture, a quite different phenomenon was observed. The PVA membrane shows a better affinity to alcohols (methanol and ethanol) than esters (ethyl acetate and methyl acetate). However, methanol and ethanol do not show good separation because their selectivity is close to unity. The possible reason is that the methanol could swell the PVA membrane significantly. The swelling of methanol-selective membranes by methanol has been reported in the literature^{256–258}. As the liquid solvent inside the membrane increases, the relaxation of polymer chain can occur and increases the size of free volume of the PVA membrane, therefore, the membrane loses its selectivity.

4.5 Conclusions

The application of pervaporation requires the understanding of coupling effects that may take place during the separation of multicomponent mixtures. It is observed that the separation performance of two transesterification mixtures resulting from two model reactions have strong impact on this effect. Four commercial membranes containing different fractions of PVA have been studied.

Coupling is a complex phenomenon produced by the interaction among components and the interaction between components and the membrane material. This phenomenon has been observed after comparing the membrane performance with pure solvents and two quaternary mixtures. The coupling effect can be explained with

different approaches, which have been described in this work: a modification of the solubility of components in the polymer (described by the Hansen solubility approach); and the change of the components activity within the membrane.

The modification of solubility due to the presence of other components can change the membrane performance. A pure component, which can not permeate through membrane, can be obtained in the permeate when it is present in a mixture as feed solution. Therefore, it suggests that the Hansen solubility parameters of mixture should be taken into account. It is concluded that Hansen solubility parameters can be applied for predicting potential coupling effects in the separation.

The difference of activity coefficients considering the polymer and without the polymer were compared. It was found that the polymer material can enhance or reduce the activity, thereby, the driving force calculated within the polymer film is not identical to that calculated from the feed solution directly. The activity of each component within the membrane should also be analyzed in order to investigate the driving force within the membrane could be an important factor that motivates the mass transfer through the membrane.

Chapter 5. Application of pervaporation in the production of glycerol carbonate

Based on:

Wenqi Li, Ramesh Sreerangappa, Julien Estager, Jean-Christophe M. Monbaliu, Damien P. Debecker, Patricia Luis, Application of pervaporation in the bio-production of glycerol carbonate, Chemical Engineering and Processing: Process Intensification, 132 (2018) 127-136.

5.1 Introduction

The development of renewable energy sources is critical because of the energy crisis caused by the depletion of petroleum reserves and the environmental concerns associated with CO₂ emissions. The production of biodiesel is nowadays one of the most important sources of bioenergy, and it has been growing dramatically as a sulfur-free, non-toxic and biodegradable additive for fuels²³. Glycerol carbonate is an important chemical compound that can be produced from glycerol. In this work, pervaporation is proposed as the technology to separate the transesterification mixture from reaction 3 involved in the production of glycerol carbonate from glycerol and DMC. The performance of four commercial membranes is evaluated from the results of transmembrane flux, separation factor, permeance, selectivity, and a comparison with distillation via the McCabe-Thiele diagram.

In this chapter, the following scientific questions will be studied:

- Are commercial membranes able to achieve the separation of the studied transesterification mixtures?
- Does the intermolecular interaction have impact on the permeation behaviour?

5.2 Results and discussion

5.2.1 Pervaporation performance

The total transmembrane flux is shown in Figure 5-1 as a function of the temperature for the studied membranes. The partial flux of each component can be found in Figure 5-2. The overall transmembrane flux follows the trend: 1255-30>4155-40>1255-50>4155-80 for all tested temperatures. This could be an indication that the high degree of PVA polymer chain crosslinking, such as in 4155-80, leads to a decrease of the transmembrane flux. Hence, the degree of cross-linking is a more important factor than the temperature regarding to the molecule motion within the polymer.

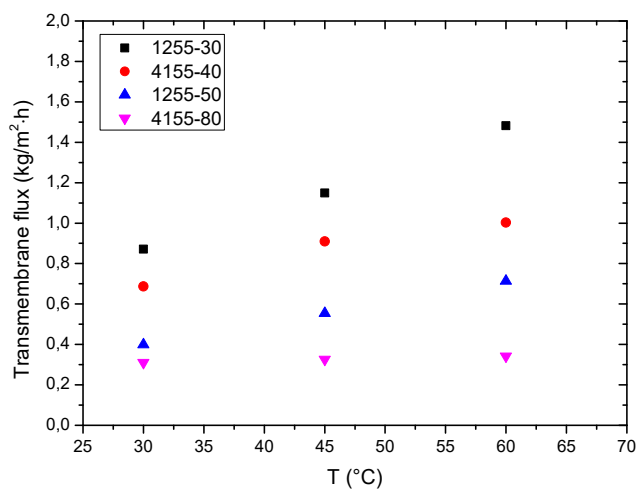


Figure 5-1. Overall transmembrane flux of each membrane at different temperatures

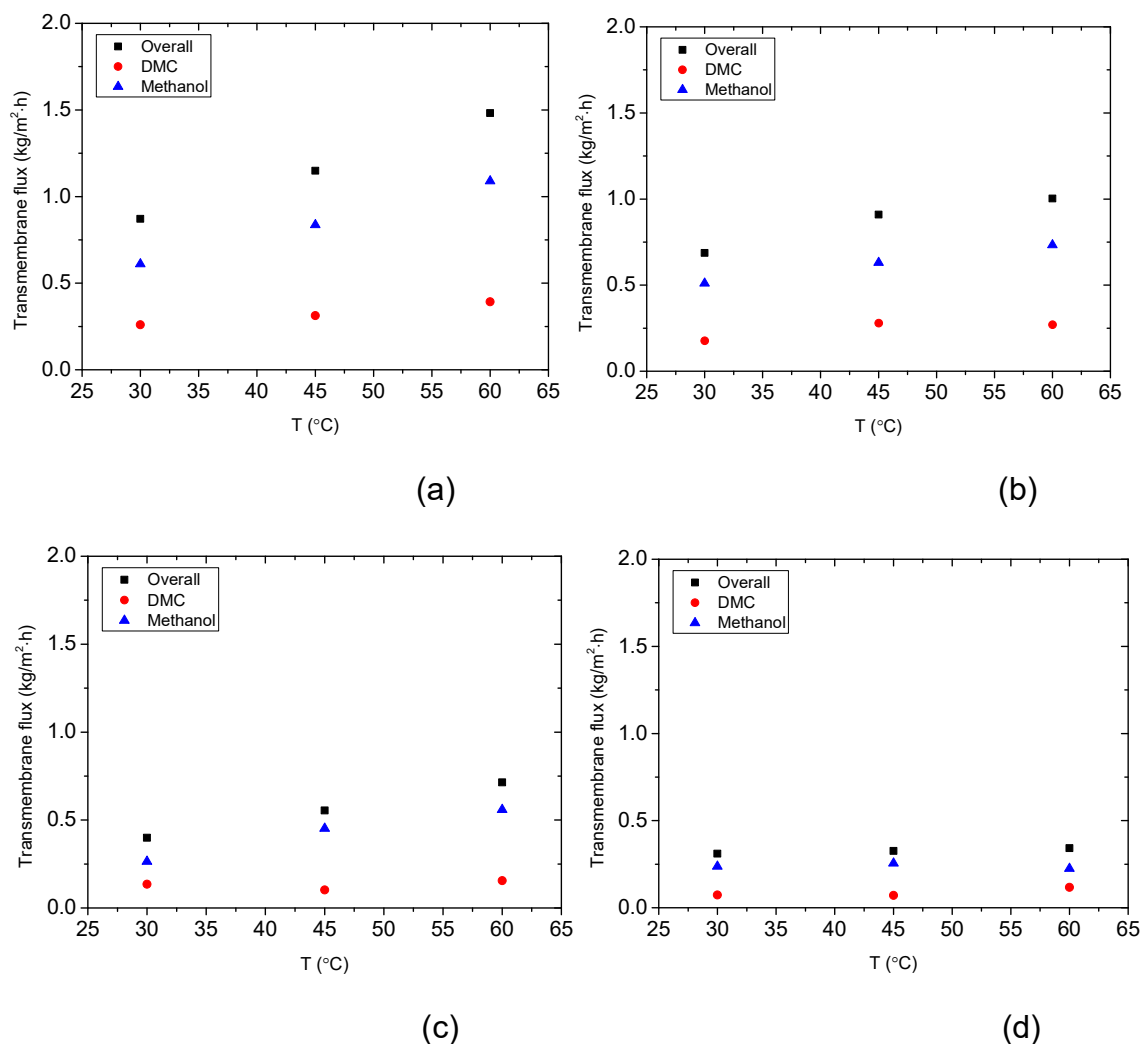


Figure 5-2. Partial flux of each component of each membrane at different temperatures: (a) membrane 1255-30 ; (b) membrane 4155-40 ; (c) membrane 1255-50, and (d) membrane 4155-80.

Glycerol and glycerol carbonate are not permeable to all these membranes (they are not detected in the permeate), meaning that only methanol and dimethyl carbonate can diffuse through membranes. In general, the partial flux of methanol is higher than that of dimethyl carbonate for all membranes. This can be interpreted by studying the driving force. In Eq. (1-13), the term representing the driving force is $(x_i \times \gamma_i \times P_i^0 - y_i \times P_p)$. In the pervaporation process, the vacuum pressure is about 12-15 mbar, and, therefore, the term $y_i P_p$ can be neglected. The vapor pressure P_i^0 plays an important role on the driving force as well as the activity coefficient γ_i . The vapor pressures P_i^0 (atm) are calculated by Aspen Plus²⁵⁹. With an increase in temperature, the vapor pressure of methanol and dimethyl carbonate increased dramatically (Table 5-1). As a result, it can be concluded that a high transmembrane flux was obtained due to a larger driving force, which is caused by a higher vapor pressure. The calculated driving force from Eq. (1-13) for different membranes and several experimental temperatures is given in Table 5-2.

Table 5-1. The vapor pressure (atm) of each component at 30 °C, 45 °C and 60 °C.

Temperature (°C)	Methanol	Glycerol	Dimethyl carbonate	Glycerol carbonate
30	0.2176	4.0467X10 ⁻⁷	0.0945	2.5165X10 ⁻⁷
45	0.4449	2.1291X10 ⁻⁶	0.1883	9.8592X10 ⁻⁶
60	0.7854	7.9620X10 ⁻⁶	0.3253	3.2775X10 ⁻⁶

Table 5-2. The driving force (atm) of methanol and dimethyl carbonate of each membrane at 30 °C, 45 °C and 60 °C.

Membranes	Temperature	Methanol	Dimethyl carbonate
1255-30	30	0.0867	0.0260
	40	0.1866	0.0593
	50	0.4038	0.1047
4155-40	30	0.0996	0.0276
	40	0.1978	0.0641
	50	0.2869	0.1243
1255-50	30	0.0853	0.0404
	40	0.1596	0.0736
	50	0.2943	0.1293
4155-80	30	0.0801	0.0376
	40	0.1702	0.0755
	50	0.2985	0.1307

Table 5-3. Activity coefficient of each component at 30 °C, 45 °C and 60 °C.

Temperature (°C)	Methanol	Glycerol	Dimethyl carbonate	Glycerol carbonate
30	1.232	1.925	1.616	1.108
45	1.223	1.885	1.575	1.100
60	1.216	1.853	1.528	1.091

In addition, glycerol and glycerol carbonate were totally not permeable due to their extremely low vapor pressure (glycerol at 60 °C: 7.96×10^{-6} atm and glycerol carbonate at 60 °C 3.85×10^{-6} atm). The activity coefficients at different temperatures were calculated by UNIFAC method; the group and group parameter in UNIFAC of studied components in this work can be found in the literature^{260,261}. The activity coefficient of

each compound is between 1.853 and 1.091 at 60 °C (Table 5-3), comparing the large variation of vapor pressure of each component at different temperature, the impact of variation of activity coefficient can be considered as very small. Therefore, the vapor pressure plays an important role on the permeation behavior.

Furthermore, the flux is clearly temperature dependent (*i.e.*, it increases when the temperature increases) except for the 4155-80 membrane. An increase of the temperature may promote the thermal motion of permeant molecules, consequently, improving the diffusion. In addition, the increase of temperature leads to an increase of the motions of polymer chains and expansion of the free volume⁹⁰. Therefore, the permeant molecules can diffuse through the cross-linked membrane easier. The temperature effect on the transmembrane flux was investigated by Eq. (1-21) and (1-22), which is presented in Figure 5-3. In Figure 5-3, it can be seen that the experimental data shows good linear relationship between $\ln J_p$ and $1/T$. It is clearly shown that the flux of 1255-30, 4155-40 and 1255-50 membranes is temperature dependent, and they have a negative permeation activation energy E_p , which indicates that the flux increases with the temperature. However, for the 4155-80 membrane, the flux shows that it is independent of temperature. This may be explained by the high cross-linking degree of this type of PVA membrane matrix, which leads to a limitation in the thermal motion of the polymer chains caused by the temperature change²⁶².

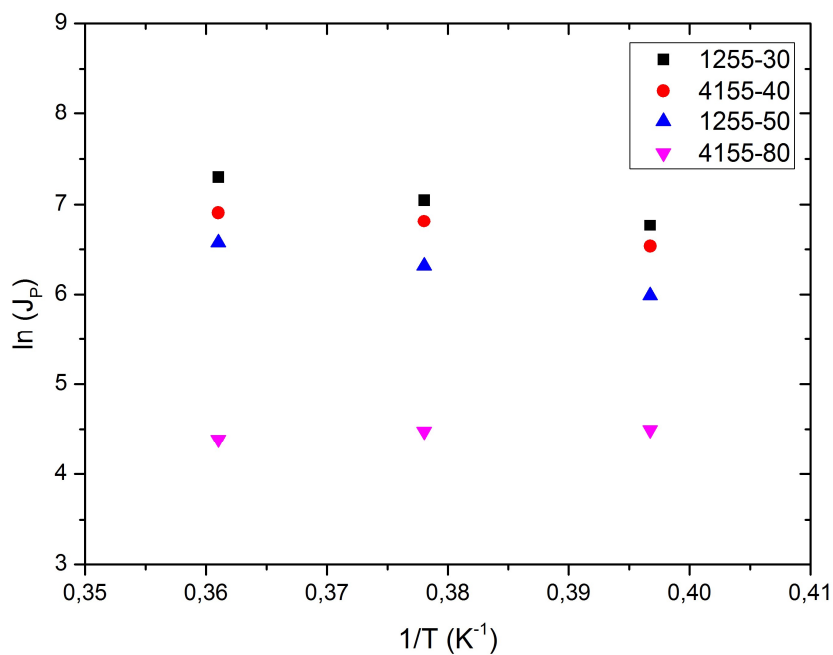


Figure 5-3. Dependence of $\ln J_p$ vs. $1/T$ of four commercial membranes

The separation factor methanol/dimethyl carbonate is shown in Figure 5-4. The results show a high separation factor for all membranes, indicating a permeate rich in methanol. The lowest separation factor is higher than 4 (1255-30 membrane at 30 °C) while the highest one is around 14 (1255-50 membrane at 45 °C).

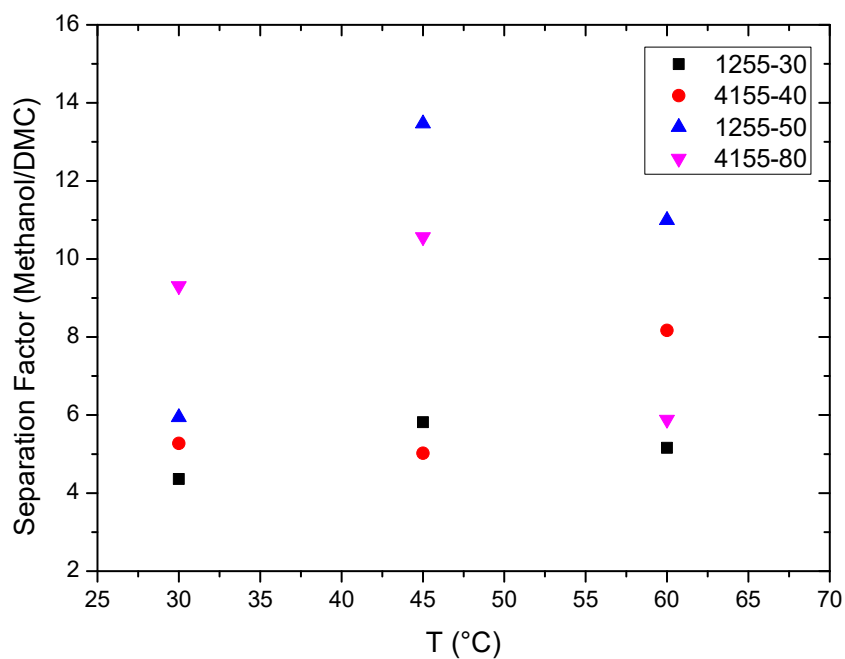


Figure 5-4. Separation factor of methanol/DMC of different types of membranes at different temperature

5.3.2 Membrane performance

The membrane performance was evaluated in terms of permeance and selectivity in order to remove the effect of the driving force of each component⁸². The results of permeance are shown in Figure 5-5. At the same temperature, the permeance of membranes follows 1255-30>4155-40>1255-50>4155-80. According to the information obtained from the supplier, the degree of crosslinking of the PVA membranes follows: 4155-80>1255-50>4155-40>1255-30; the diffusivity depends on the degree of crosslinking: a highly crosslinked polymeric membrane gives a lower diffusivity²⁶³. As a result, the molecules can diffuse through the membrane 1255-30 easier than the membrane 4155-80.

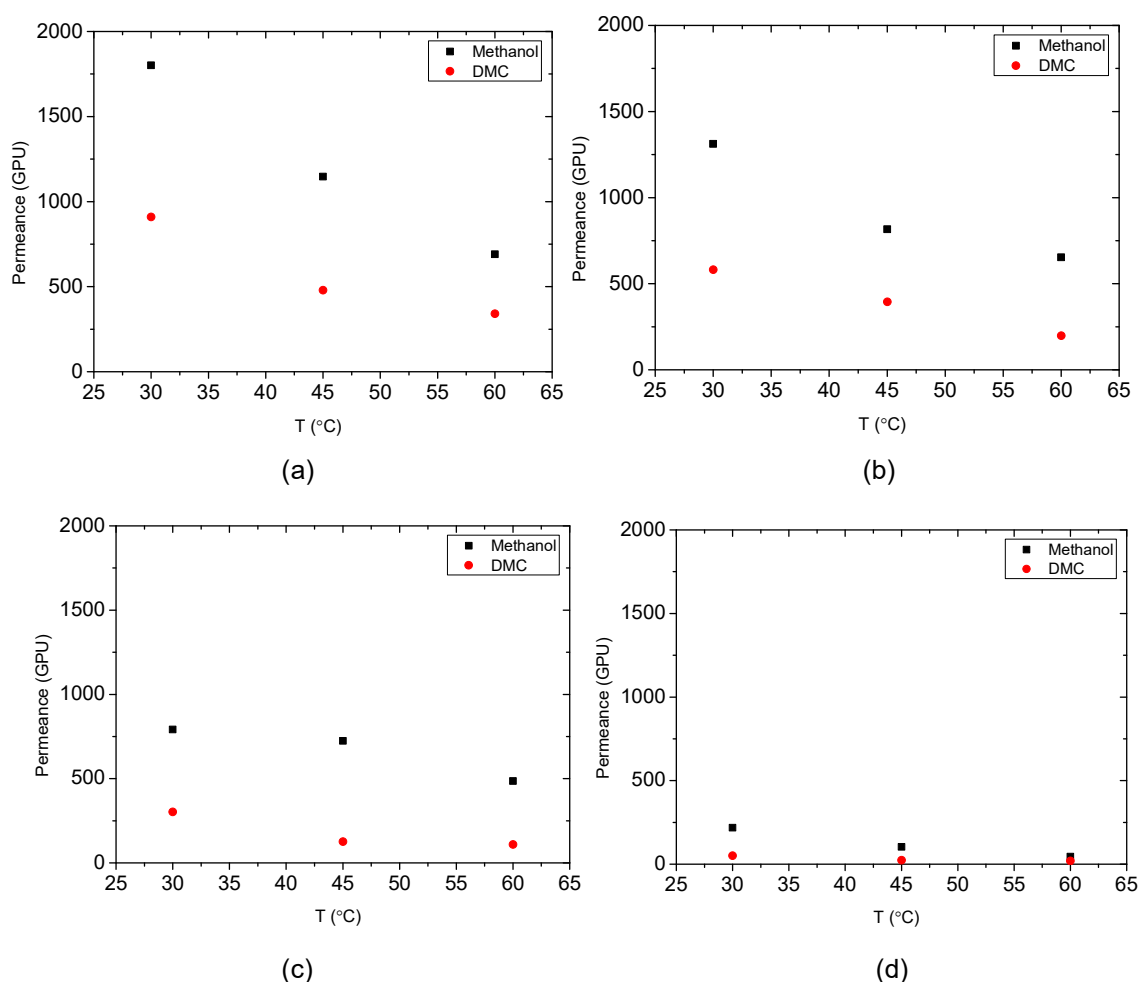


Figure 5-5. The permeance of different types of membranes at different temperature (a) 1255-30 membrane, (b) 4155-40 membrane, (c) 1255-50 membrane and (d) 4155-80 membrane

It is observed that the permeance of methanol in each membrane is always higher than the one of dimethyl carbonate, showing that the membrane has more affinity with

methanol. The functional layer of the membranes is made of polyvinyl alcohol, which contains hydroxyl functional groups. Methanol has a better affinity to PVA polymer due to its higher polarity compared to dimethyl carbonate. Hence, a high hydrogen bonding interaction with hydroxyl group can enhance the methanol permeation. On the other hand, the smaller molecular size of methanol can lead to a high permeation²⁶⁴. As a result, the permeation of methanol is higher than the one of dimethyl carbonate. Additionally, in order to predict the membrane affinity with the components in the feed solution, a preliminary study of Hansen solubility parameters was performed. (see Table 5-5). The study of the Hansen solubility parameter shows that both can be sorbed by PVA, thus, coupling effects may occur due to the sorption of components in the PVA membrane. However, methanol molecules can be sorbed by the PVA separation layer easier than dimethyl carbonate. As a consequence, more methanol molecules can diffuse through the membrane. The experimental results are in agreement with the preliminary study of the Hansen solubility parameters.

The permeance for methanol in the binary mixture methanol/DMC is lower than that obtained in the study shown in Chapter 4 due to stronger intermolecular forces between methanol/DMC mixture. The intermolecular force is presented by cohesive energy²⁶⁵. The strength of the intermolecular forces holding molecules together in the liquid can be estimated by the Hildebrand solubility parameter²⁶⁶:

$$\delta_h = \left(\frac{E_{coh}}{V_m} \right)^{1/2} = e_{coh}^{1/2} \quad (5-1)$$

where: δ_h : Hildebrand solubility parameter; E_{coh} : cohesive energy; V_m : molar volume; and e_{coh} : cohesive energy density.

The cohesive energy is calculated by the following equation²⁶⁷:

$$E_{coh} = \Delta H_{vap} - RT \quad (5-2)$$

where ΔH_{vap} is enthalpy of vaporization, R is gas constant and T is temperature.

The intermolecular forces acting between components 1 and 2, F_{12} , are assumed as follows¹²²:

$$F_{12} = (e_{coh11} \cdot e_{coh22})^{1/2} = \delta_{h1}\delta_{h2} \quad (5-3)$$

where e_{coh11} and e_{coh12} are cohesive energy densities of pure components 1 and 2, respectively.

The calculated intermolecular forces between alcohols and esters, DMC is shown in Table 5-4.

Table 5-4. The intermolecular forces (MPa) between alcohols and esters, alcohols and DMC

	Methyl acetate	Ethyl acetate	Butyl acetate	Dimethyl carbonate
Methanol	576.0	514.7	466.4	609.2
Ethanol	496.5	443.6	402.0	525.1
Butanol	464.6	415.2	376.2	491.4

Table 5-4 shows that methanol/DMC has a stronger intermolecular force than any other pairs. Therefore, it requires more energy to break the interaction between methanol and DMC. As a result, the permeances for methanol are lower than before.

Table 5-5. Calculated Hansen solubility parameters of each component/mixture and R_a

Material	δ_D	δ_P	δ_H	$\Delta\delta_{(s-p)}$
PVA	17.2	13.6	15.4	
Glycerol	17.4	12.1	29.3	13.99
Glycerol carbonate	17.9	25.5	17.4	12.15
Methanol	15.1	12.3	22.3	8.18
Dimethyl carbonate	15.5	3.9	9.7	11.75
Mixture	16.2	12.4	16.8	2.79

The selectivity (DMC/Methanol) is shown in Figure 5-6. The lowest selectivity is around 2 (1255-30 membrane at 30 °C); a value of selectivity higher than 1 indicates that the membrane is selective for methanol. It is concluded that 1255-50 membrane operated

at 45 °C is the optimal choice for the separation, both separation factor and selectivity implying a preferential permeation of methanol.

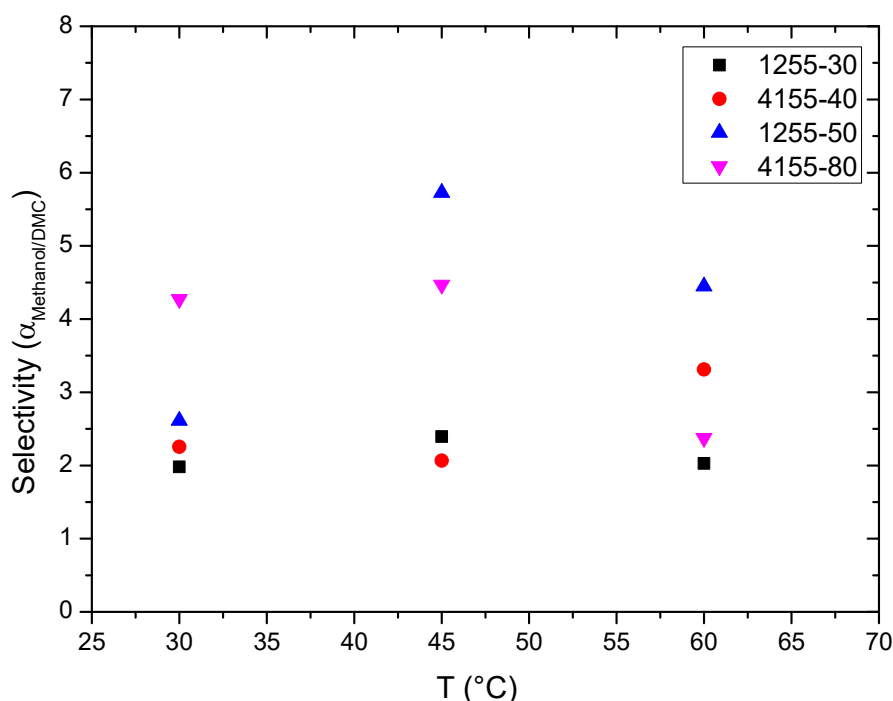


Figure 5-6. Selectivity of methanol/DMC of different types of membranes at different temperatures

Comparing Figure 5-1 and Figure 5-5, the trend of permeance does not follow the trend of transmembrane flux when the temperature increases. From Figure 5-1 and Figure 5-5, it can be seen that the transmembrane flux is increasing with temperature, however, the permeance decreases. The effect of temperature on permeance can be interpreted via the activation energy. The activation energy of permeation is calculated by the logarithmic permeance versus the inverse of the temperature. The calculated activation energy for the experiments is shown in Table 5-6. All activation energies of methanol and DMC permeation are negative (Table 5-6). The increase of temperature promotes the motion of polymer chains resulting in the expansion of the polymer free volume. Thus, it enhances the diffusion of permeant molecules through the membrane⁹¹. On the other hand, the heat of solution is the heat generated or absorbed during the sorption process, which depends on the sorption mechanisms. From Eq. (1-23), it can be concluded that the activation energy of permeation is determined by the dominant process (sorption or diffusion) which dominates. In this case, it indicates that sorption is more dominant than diffusion in the process. As a consequence, increasing

the temperature is not favorable for the component to be adsorbed by the membranes, leading to a decrease of permeance.

Table 5-6. Activation energy of methanol and DMC for the different commercial membranes

Activation energy (kJ/mol)		
Membrane	DMC	Methanol
1255-30	-27.6 ± 1.4	$-26,8 \pm 2.2$
4155-40	-30.1 ± 1.5	$-19,6 \pm 1.6$
1255-50	-28.8 ± 1.5	$-13,5 \pm 1.7$
4155-80	-27.8 ± 1.5	$-44,0 \pm 1.4$

The activation energy also affects the effect of temperature on the membrane permeation of a component. As mentioned in Section 2.3.3, and according to the solution-diffusion model, the activation energy is the sum of activation energy of diffusion and heat of solution (heat generated or absorbed during sorption process). A high activation energy means a greater energy barrier for the permeation through the membrane. If the activation energy is positive, it implies that the diffusion process is dominated. Hence, the increase of temperature is beneficial to the permeance. On the contrary, if the activation energy is negative, it indicates that the sorption process is dominated. As a result, the increase of temperature may have negative impact on the permeance if the sorption process is exothermic. From Table 5-6, it can be observed that all activation energy of DMC and methanol are negative, meaning that an increase of temperature is not in favor of the permeance of DMC and methanol.

The activation energies of DMC do not have significant differences for these four membranes. However, the activation energies of methanol decreases following the last number in the notation (related to the degree of crosslinking): 1255-50>4155-40>1255-30. The diffusion coefficient decreases with the increase of degree of crosslinking of the polymer²⁶⁸. On the other hand, since the relation of the diffusion coefficient and activation energy of diffusion follows Eq. (1-20), the activation energy of diffusion increases with the decrease of diffusion coefficient²⁶⁹. Hence, if the activation energy of sorption is the same for all membranes, the overall activation energy of methanol

decreases because the increase of activation energy of diffusion according to last notation number, which reflects the degree of crosslinking of different membranes. The membrane 4155-80 does not follow this trend since the activation energy of diffusion is much lower than for the other membranes. This membrane has a much thinner active layer (around 4.5 μm) than other types of membrane (12.3-15.5 μm). In pervaporation, the PVA membrane is partially wetted by the solution due to the swelling effect. The transport of low molecular weight permeants is not influenced by the degree of crosslinking, but it is highly affected by the equilibrium swelling ratio (the ratio of the weight of the swollen polymer to that of the dry polymer)^{270, 271}. It is concluded that the activation energy of small molecules is more sensitive to the degree of crosslinking.

Based on Figure 5-2 and Figure 5-5, it is observed that methanol shows higher values than dimethyl carbonate both in transmembrane flux and permeance. This high flux is caused by the higher vapor pressure of methanol, which leads to a higher driving force during the pervaporation transport, enhancing the transmembrane flux. Furthermore, methanol has also a higher permeance, showing that the membrane material has a greater affinity for methanol. This gives an ideal situation in which the membrane enhances the effect of the – already favored – driving force for methanol, resulting in a larger methanol flux⁸².

5.3.3 McCabe-Thiele separation diagram

In order to compare the use of pervaporation with distillation, the McCabe-Thiele separation diagram is presented in the following section for the mixture studied. In this diagram, the concentration in the vapor phase (*i.e.*, permeate in pervaporation) is plotted versus the concentration in the liquid phase (*i.e.*, retentate in pervaporation). The comparison with distillation (dark: DMC and blue: methanol points in the figure) is then straightforward. A flash distillation unit operated at 85 °C and a pressure of 1 atm is considered. Two main aspects should be considered: i) the points close to the diagonal imply similar concentration in the liquid and vapor phase, thus, no separation; and ii) if pervaporation points are not coincident to distillation points, it is due to the effect of the membrane (if the points are coincident, the separation is due to the vapor-liquid equilibrium)⁸². Figure 5-7 shows the vapor phase molar fraction of the flash equilibrium against the values for pervaporation. The comparison of pervaporation and distillation gives additional information of the merit or weakness of the membrane

separation. It is shown that the membrane separation has special advantage for separating methanol, the concentration of dimethyl carbonate (red) in the permeate after pervaporation is lower than that in the flash equilibrium (black). The presence of dimethyl carbonate in the permeate is decreased when comparing with flash equilibrium.

It is concluded that the membranes are selective to methanol and it is more concentrated in the permeate. The points are far from the diagonal, therefore, an effective separation can be achieved. In addition, the pervaporation points (red: DMC and pink: methanol) are not coincident to the distillation points (black: DMC and blue: methanol) and the pervaporation points are further away from the diagonal compared the distillation ones. This last point unambiguously proves the effect of the membrane as well as the higher efficiency of pervaporation if compared to a simple distillation.

As discussed above, pervaporation appears advantageous in comparison with flash distillation. Moreover, it is also interesting that the membranes can not permeate glycerol and glycerol carbonate completely, as only methanol and dimethyl carbonate are present in the permeate. On the other hand, different publications^{56,57,65,272} describe procedures that can achieve 97.7% - 99.93% conversion leading to a mixture containing glycerol carbonate, DMC (in excess), methanol and a only residual glycerol. By removing DMC/methanol by pervaporation instead of distillation, a glycerol carbonate of high purity – but containing the traces of glycerol – could then be obtained in a batch process. In addition, the permeate is a binary mixture of methanol and DMC with high concentration of methanol (mole fraction of methanol > 0.84) obtained from only one pervaporation stage. Other separation processes^{273,274} or other pervaporation membranes would lead to a complete separation²⁷⁵.

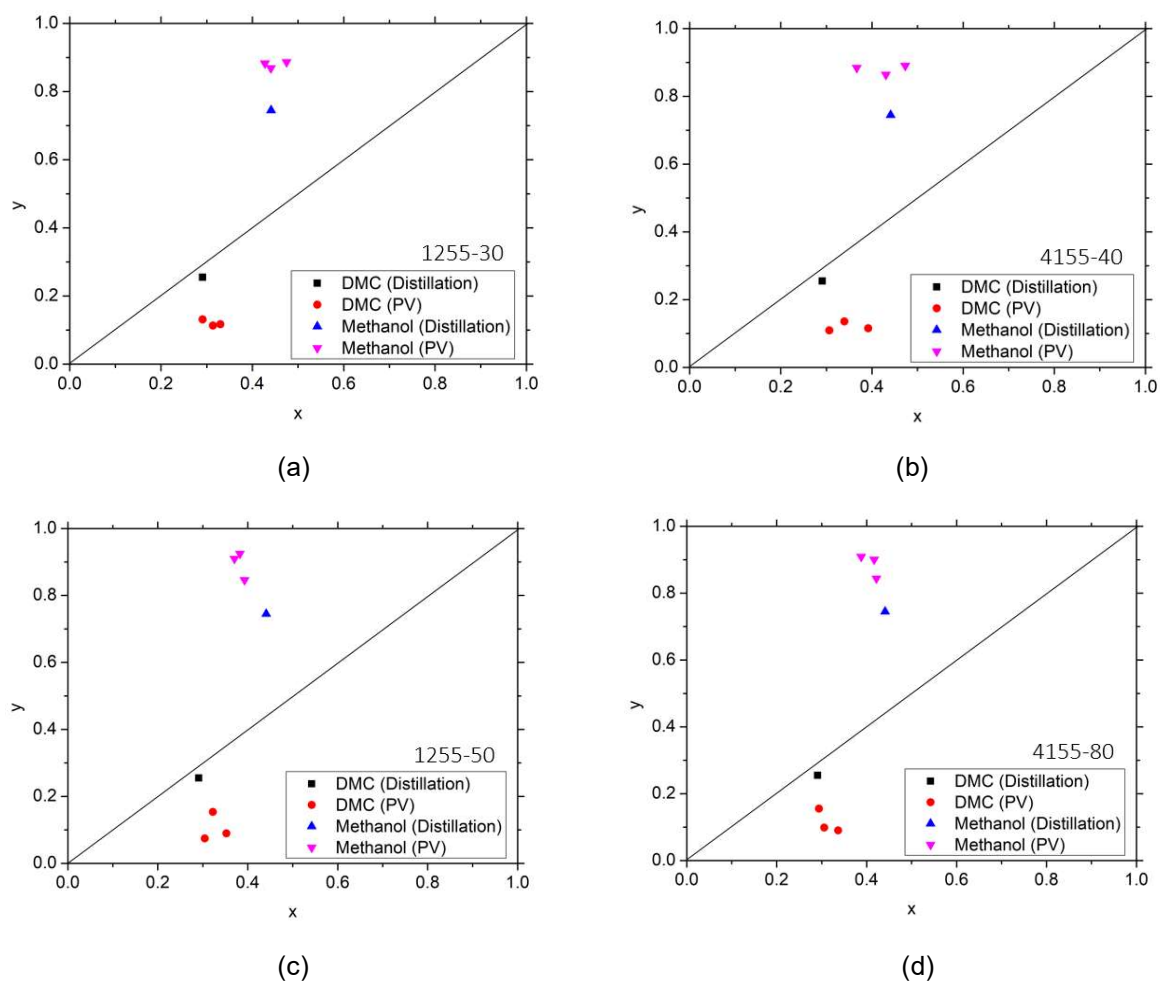


Figure 5-7. McCabe-Thiele separation diagram that shows the pervaporation selectivity for each compound using the membranes: a) 1255-30, b) 4155-40, c) 1255-50 and d) 4155-80. The axis x and y are given in molar fraction. The three points shows the effect of temperature at 30 °C, 45 °C and 60 °C. The black and blue symbols correspond to the separation obtained by simulation of flash equilibrium at 85 °C (glycerol and glycerol carbonate are not observed in the vapor phase due to their high boiling point).

5.4 Conclusions

The application of pervaporation technology to separate a quaternary transesterification mixture consisting of glycerol, dimethyl carbonate, methanol and glycerol carbonate has been investigated using four commercial membranes. Glycerol and glycerol carbonate were not detected in the permeate in the studied membranes due to their low vapor pressure. The experimental results of permeance show that the use of these membranes enhances the permeation of methanol, which is the compound that has the highest transmembrane flux and has the largest driving force.

Such a situation appears to be ideal as the membrane can operate under optimal conditions. In addition, the temperature shows great impact on the performance of membrane. When increasing the temperature, the flux increases, but the permeance decreases. Thus, working at low temperature is an advantage in terms of membrane performance.

Regarding the application of these commercial membranes for the separation of studied transesterification mixtures, the McCabe-Thiele separation diagram analysis shows that pervaporation can separate methanol more effectively than flash distillation. As a consequence, pervaporation appears to be an alternative to improve the reaction yield by removing methanol from the reaction mixture and/or to break the azeotrope (methanol and DMC) as well as to remove glycerol and glycerol carbonate.

Comparing the permeances for methanol of three transesterification mixtures, it shows that the permeances of third reaction are lower than the other two. By investigating the intermolecular forces between alcohols and esters, alcohols and DMC, it shows that methanol/DMC has the strongest intermolecular force than other pairs. It is concluded that the intermolecular interactions have impact on the permeation behaviour.

Chapter 6. Sorption and pervaporation study of methanol/dimethyl carbonate mixture with poly(etheretherketone) (PEEK-WC) membrane

Based on:

Wenqi Li, Francesco Galiano, Julien Estager, Damien P. Debecker, Jean-Christophe M. Monbaliu, Alberto Figoli, Patricia Luis, Sorption and pervaporation study of methanol/dimethyl carbonate mixture with poly(etheretherketone) (PEEK-WC) membrane, Journal of Membrane Science, 567 (2018) 303-310

6.1 Introduction

In chapter 5, it was shown that commercial membranes can not permeate glycerol and glycerol carbonate completely due to their low vapor pressure. Therefore, the separation of the permeate mixture, dimethyl carbonate and methanol, becomes an important step. In addition, the separation of DMC/methanol is an interesting topic in the chemical industry. Dimethyl carbonate (DMC) is considered a green chemical due to its biodegradability and low toxicity, and is widely applied in the chemical industry. As a low toxic intermediate, it can be used as a substitute in the pharmaceutical industry to replace more toxic solvents such as dimethyl sulfate, or in the production of important thermoplastics polycarbonate materials to replace phosgene²⁷⁶. Furthermore, it finds applications as a solvent in painting and coating industries and it is used as electrolyte for Li-ion cells^{277,278}. In the literature, different synthetic routes of DMC are reported. One of them follows a phosgene-based route to produce DMC. However, phosgene is a toxic raw material and the complementary use of NaOH during the reaction requires a high capital equipment investment for preventing corrosion²⁷⁹. DMC can be also produced by the transesterification reaction of cyclic carbonate and methanol, such as ethylene carbonate^{280–283}. Alternatively, it can be synthesized from oxidative carbonation of methanol by using copper chloride as a catalyst²⁸⁴. DMC synthesis from the alcoholysis of urea is an attractive chemical route since urea is widely available at low cost as a waste^{285,286}. This reaction proceeds by two different steps: 1) urea reacts with methanol to produce methyl carbamate; 2) methylcarbamate reacts with methanol to produce the final product DMC. Furthermore, DMC can be obtained from direct reaction of methanol and carbon dioxide (methanol carboxylation route) with the possibility of using various catalysts^{287–289}. As evidenced by literature data, it is clear that methanol participates or it is present in different synthetic routes. Therefore, the separation of DMC and methanol is of great importance in the chemical industry. However, they form an azeotrope (at 30/70 wt% DMC/methanol concentration), which makes the separation process very challenging with traditional distillation. In the literature, several alternative approaches have been proposed such as extractive distillation²⁹⁰, membrane processes^{275,291} or the use of ionic liquids as entrainers²⁹².

Different polymeric materials have been investigated in pervaporation for the separation of DMC/methanol mixture, but their application at industrial level is still limited. Modified poly ether ether ketone (poly(oxa-p-phenylene-3,3-phthalido-p-phenylene-oxy-phenylene) (PEEK-WC: WC refers to cardo group) is a polymer containing a spirolactone group with good thermal stability, mechanical properties and high resistance to chemicals due to its high glass transition temperature (225 °C)^{293,244}. Thanks to its properties, PEEK-WC membranes find wide applications in different fields such as in biomedical engineering due to their low affinity to proteins²⁹⁴ and in fuel cell applications due to their high proton conductivity and its low cost comparing with Nafion membranes²⁹⁴. In pervaporation, the performance of PEEK-WC membranes has been investigated for the separation of methanol and MTBE²⁴⁴. A high separation factor (above 250) was obtained at low concentration of methanol (1 wt%). In the application of dehydration of acetic acid, PEEK-WC membranes can achieve good separation with a value of 103 as separation factor at 50 °C with a concentration of 90 wt% of acetic acid²⁹⁵. In this work, a detailed study on sorption and pervaporation for DMC/methanol mixtures with PEEK-WC membranes is presented at different concentrations and temperatures. The coupling phenomenon during the permeation was investigated as well. The performance of the membrane was evaluated in terms of flux, separation factor, permeance and selectivity.

In this chapter, the following scientific questions will be studied:

- Applying theories based on solubility parameters to predict potential coupling effects in the separation.
- Do PEEK-based membranes have appropriate properties and high performance for the separation of the studied mixtures?

6.2 Results and discussion

6.2.1 Membrane characterization: contact angle, mechanical test and SEM analysis

PEEK-WC membranes exhibited a water contact angle of 84.96 ± 2.28 . This indicates that the PEEK-WC membrane was slightly hydrophilic. Therefore, a polar component can permeate through the membrane easier than a non-polar component.

Mechanical test results showed that the average Young's modulus of the PEEK-WC membrane was $1147.71 \pm 34.9 \text{ N/mm}^2$ with an elongation at break of $10.6\% \pm 4.6\%$. The average maximum stress was $47.76 \pm 8.28 \text{ N/mm}^2$. Comparing these results with the Young's modulus and the maximum stress of polyvinyl alcohol (PVA) ($170\text{-}360 \text{ N/mm}^2$ and $6.4 \pm 0.5 \text{ N/mm}^2$, respectively) and chitosan membranes ($4.5\text{-}5.89 \text{ N/mm}^2$ and $2.43\text{-}7 \text{ N/mm}^2$, respectively), PEEK-WC membrane shows good mechanical features^{296,297,298,299}.

SEM analysis confirmed the dense nature of prepared membranes. As observed in Figure 6-1 (a), (b) and (c), the prepared membrane is homogeneous and a dense membrane was obtained. For pervaporation separation, the transport mechanism is based on a solution-diffusion mechanism, therefore, a dense membrane is often required.

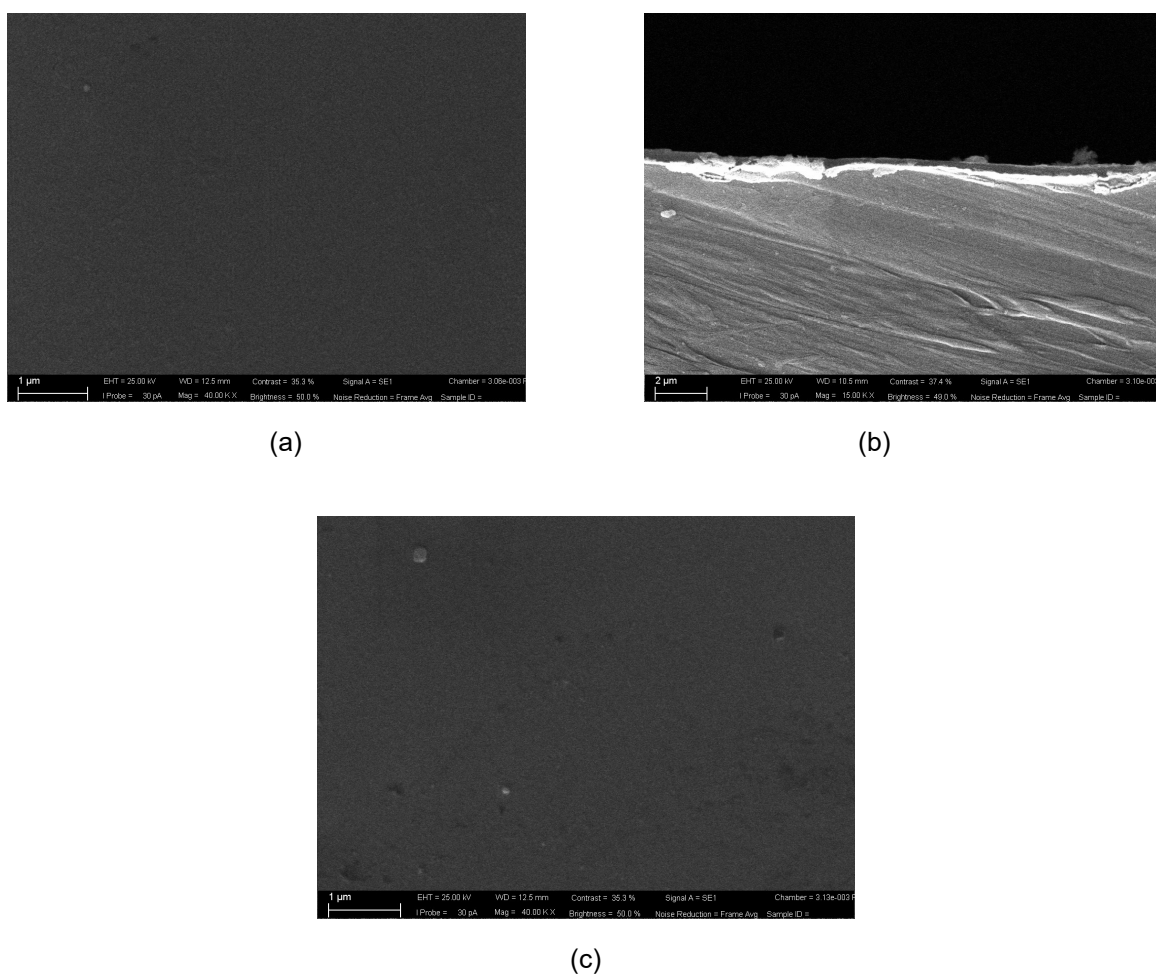


Figure 6-1. SEM image of PEEK-WC membrane. Top surface of the membrane (a) with magnification 40.00 KX; cross section (b) with magnification 15.00 KX; and bottom surface (c) with magnification 40.00 KX

6.2.2 Sorption degree measurement

The sorption degree of different concentrations of methanol/DMC solutions is shown in Figure 6-2. A decrease in sorption degree was observed when the concentration of methanol was increased in the binary mixture. The values of sorption degree of PEEK-WC in pure methanol are in agreement with the data in the literature²⁴⁴, showing values of 5%-7%. One interesting observation is that the PEEK-WC membrane is more favorable to absorb DMC than methanol. For pure DMC, the sorption degree can reach 17% and for high concentrations of DMC (0.9 molar fraction of DMC), the sorption degree is above 15%. However, the uptake of solvents into the membrane can lead to swelling effect. The swelling effect may have a negative influence on the membrane separation performance. An excessive membrane swelling leads to polymer plasticization and the polymer chain spacing increases resulting in a severe reduction of the selectivity¹¹⁶.

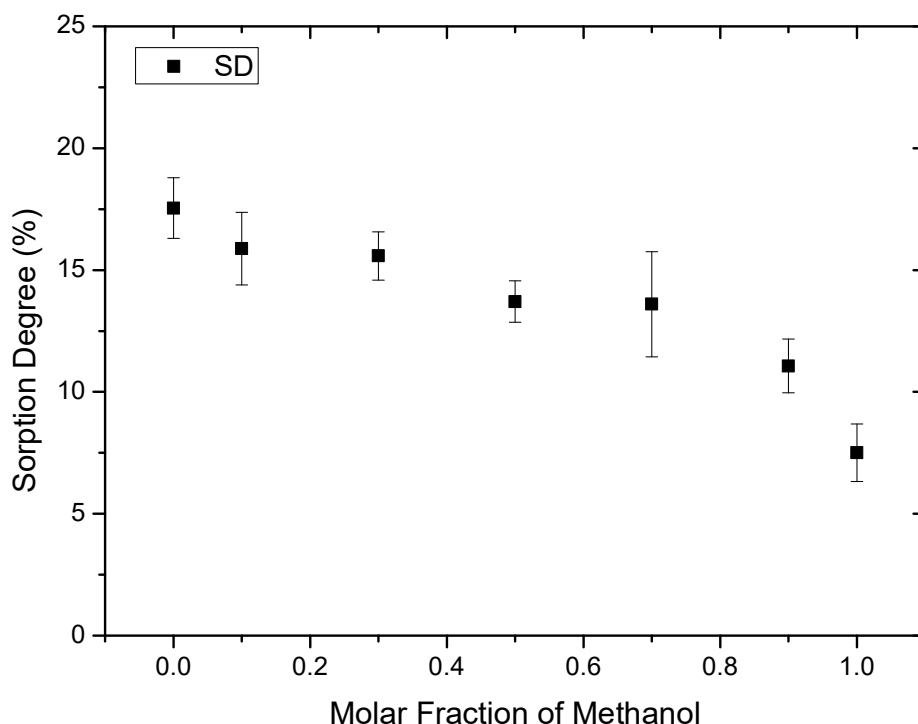


Figure 6-2. Sorption degree in different methanol/DMC mixtures.

6.2.3 Coupling effects

The data of Hansen solubility parameters of PEEK-WC, methanol, DMC and their mixtures are shown in Table 6-1. There are several approaches to estimate solubility parameters of PEEK-WC giving different results. The number in the first column

indicates the molar fraction, for example, 0.1 MeOH + 0.9 DMC means a 0.1 molar fraction of methanol and a 0.9 molar fraction of DMC in the mixture.

In the work of Zereshti *et al.*, it is stated that the solubility parameters derived from the Hoy method can be more realistic than other methods in the studying the separation of methanol/MTBE mixtures by using PEEK-WC membranes²⁴⁴. The Hoy solubility parameters also contains three parameters, which is same as Hansen solubility parameters. Hoy solubility parameters were estimated from molar attraction constants, however, Hansen solubility parameters were estimated from cohesive energy density. The three dimensional solubility vector distance (δ_t) between PEEK-WC polymer and methanol/DMC was calculated and shown in Table 6-2. From Table 6-2, it can be seen that the method applied by Hoy is not able to describe the phenomena observed in the swelling degree of methanol/DMC mixtures since pure methanol and DMC have a similar distance (8.3 methanol and 8.9 DMC, respectively) respect to the polymer solubility center. This is in contradiction with the results obtained with the swelling degree since the latter increases with the concentration of DMC in the mixture. Therefore, the solubility parameters derived from the other methods can better explain this behavior. The lower the distance polymer/solvent, the higher the compatibility between them.

Table 6-1. Solubility parameters of pure methanol, DMC and PEEK-WC at different concentrations

Material	Methods	δ_D	δ_P	δ_H	δ_t
Methanol		15.1	12.3	22.3	29.6
Dimethyl carbonate		15.5	3.9	9.7	18.7
PEEK-WC	Yamamoto ³⁰⁰	19.2	8.3	3.9	21.3
	Stefanis-Panayiotou ³⁰¹	25.5	-8	5.6	27.3
	Van Krevelen ³⁰²	18.9	2.8	6.2	20.1
	Hoy ³⁰³	16.5	11	14.6	24.6
Mixture					
0.1 MeOH + 0.9 DMC		15.5	4.3	10.3	19.1
0.3 MeOH + 0.7 DMC		15.4	5.3	11.9	20.2
0.5 MeOH + 0.5 DMC		15.4	6.6	13.8	21.7
0.7 MeOH + 0.3 DMC		15.3	8.3	16.4	23.9
0.9 MeOH + 0.1 DMC		15.2	10.7	19.9	27.3

Table 6-2. The solubility vector distance (δ_t) of different estimation methods of Hansen solubility parameters of PEEK-WC

Material	Yamamoto	Stefanis-Panayiotou	Van Krevelen	Hoy
Methanol	20.5	33.5	20.2	8.3
Dimethyl carbonate	10.4	23.6	7.7	8.9
Mixture				
0.1 MeOH + 0.9 DMC	10.6	24.0	8.1	8.2
0.3 MeOH + 0.7 DMC	11.4	24.9	9.3	6.6
0.5 MeOH + 0.5 DMC	12.6	26.3	11.1	5.0
0.7 MeOH + 0.3 DMC	14.7	28.3	13.6	4.0
0.9 MeOH + 0.1 DMC	18.1	31.3	17.5	6.0

6.2.4 Pervaporation performance

Figure 6-3 shows the impact of concentrations and temperatures on the permeation flux and separation factor. The results show that the temperature, as expected, plays a crucial role on the permeation flux. With the increase of the temperature, the flux increases. In the pervaporation process, the vacuum pressure at the permeate side was below 5 mbar, therefore, the driving force term ($x_i \times \gamma_i \times P_i^0 - y_i \times P_p$) in Eq. (1-13), $y_i \times P_p$ is near 0. As a result, the driving force depends on the activity coefficient, on the initial concentration of feed and on the vapor pressure of the components. The activity coefficient and the vapor pressure are both temperature dependent. In both factors, the variation of vapor pressures of methanol and DMC are more sensitive to the temperature change than their activity coefficients. With the increase of the temperature, the vapor pressure of methanol and DMC are increasing dramatically, leading to the increase of the driving force. As a result, the flux increases by increasing the temperature⁸². In addition, the temperature also shows an impact on the separation factor particularly at high concentration of DMC (0.9). The separation factor decreases with the increase of the temperature. A high temperature can lead to the expansion and relaxation of polymer chains and the formation of more free volume

promoting the indiscriminate transportation of molecules through the membrane^{304,305}. As a result, the separation factor decreases.

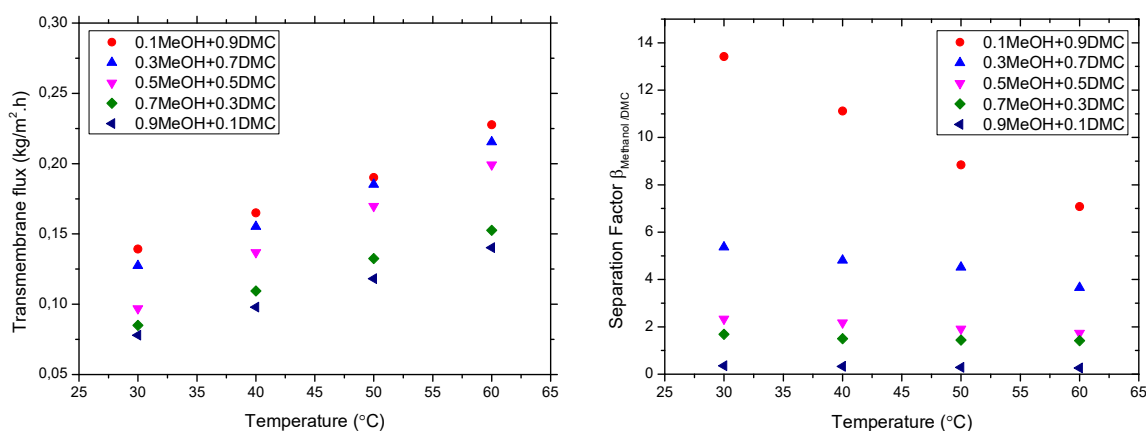


Figure 6-3. The effect of concentration and temperature on transmembrane flux and separation factor

Regarding the concentration effect, both transmembrane flux and separation factor are concentration dependent. In general, the lower concentration of methanol in the binary mixture, the higher transmembrane flux and separation factor. This could be interpreted by the variation of activity of methanol and DMC. Figure 6-4 shows the variation of activity of methanol and DMC in the mixture. The activity of methanol in the mixture increases with increasing the concentration of methanol. The methanol separation factor is higher at low concentrations and it decreases when the methanol concentration increases. In the literature, similar observations were reported²⁴⁴.

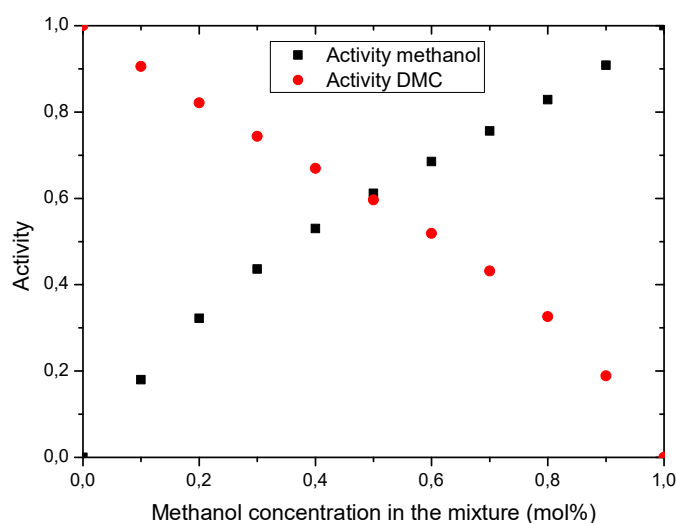


Figure 6-4. Variation of activity of methanol and DMC in their binary mixture

In the analysis of Hansen solubility, it is shown that the solubility vector distance (δ_t in Table 6-2) increases with increasing methanol concentration (except the method used by Hoy³⁰⁶). The concentration effect on the flux follows this trend. The larger the distance between the polymer and solvent, the lower the affinity between them. Therefore, the membrane flux decreases with the increase of methanol concentration. The Hansen solubility parameters give a good prediction of this phenomenon.

6.2.5 Membrane performance

The permeance and selectivity are used to describe the performance of membrane in order to eliminate the impact of the operating conditions. Figure 6-5 and Figure 6-6 show the permeance of methanol and DMC and selectivity at different temperatures and different concentrations.

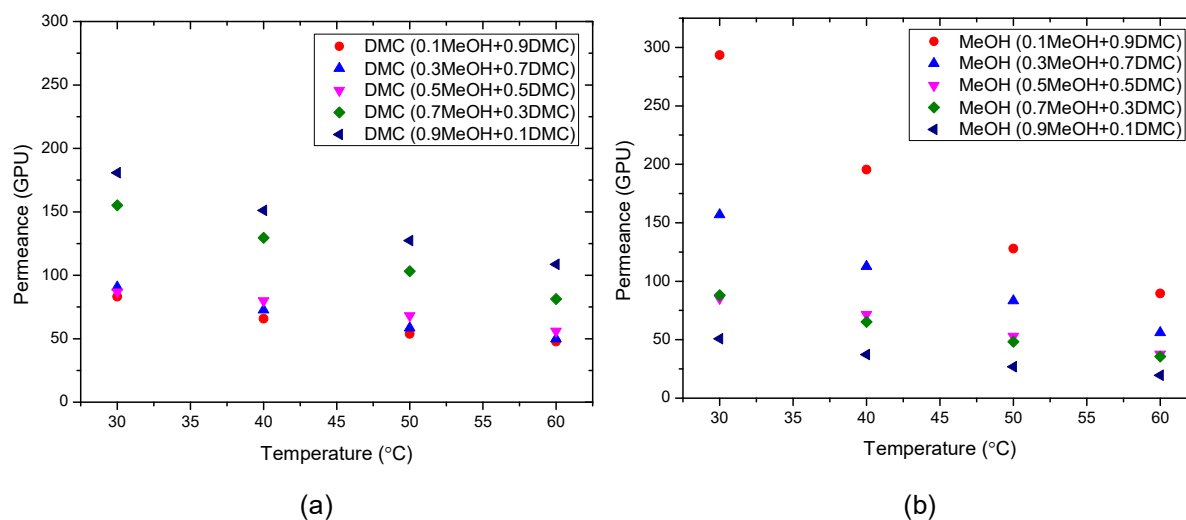


Figure 6-5. Permeance of DMC (a) and methanol (b) at different temperatures and concentrations

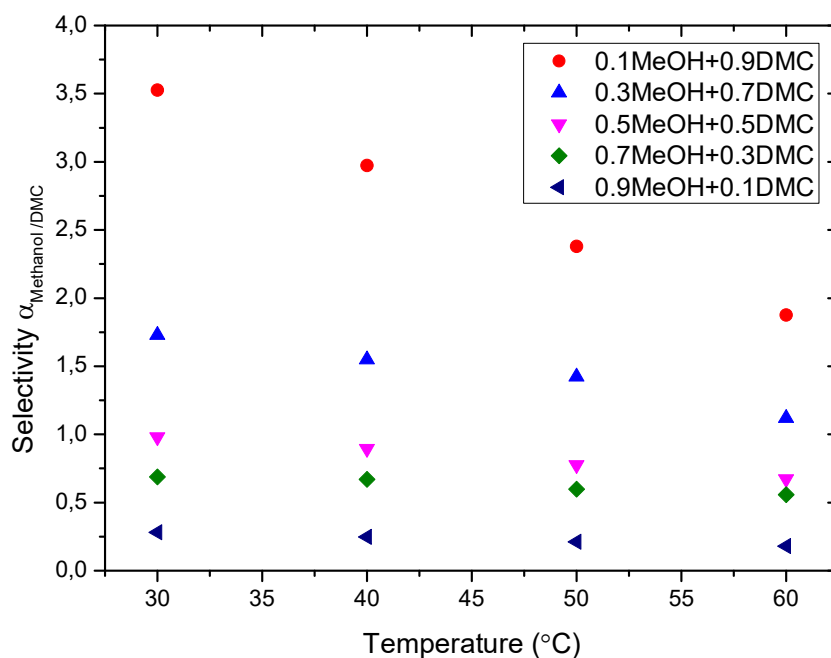


Figure 6-6. Selectivity of PEEK-WC membrane in the separation of DMC/methanol at different concentrations and temperatures

An interesting phenomenon was observed when the permeance behavior of methanol and DMC was compared with respect to the concentrations. In Figure 6-5 (a) and (b), the permeance of DMC increased with the increasing of methanol concentration. However, the permeance of methanol showed an opposite trend: a higher concentration of DMC in the binary mixture led to a higher permeance of methanol. From the experiments of swelling degree, it was found that the membrane was more prone to sorb DMC than methanol. But a preferential sorption does not give a preferential permeation at high concentration of DMC. The polarity index of methanol and DMC is 0.762 and 0.232, respectively²⁷⁸. Due to the higher polarity of methanol, the hydrophilic membranes could be more favorable to permeate methanol (instead of DMC) from the binary mixture as a consequence of the significant difference of polarity between these two components. In addition, methanol can easily diffuse through the membrane due to its smaller molecular size when compared with DMC³⁰⁷.

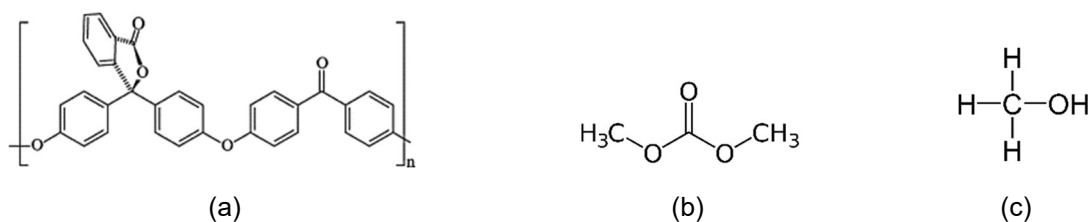


Figure 6-7. Molecular structure of (a) PEEK-WC, (b) DMC and (c) methanol

The increase of partial flux of methanol also improves the partial flux of DMC for the concentration of methanol larger than 0.5 molar fraction (See Figure A6.1), this indicates the existence of dragging effects. This can be explained intermolecular interaction. The intermolecular attraction is affected by the functional groups which contribute to dipole-dipole attractions and hydrogen bonds. From the molecular structure of polymer PEEK-WC, DMC and methanol (Figure 6-7), it can be seen that the polymer bears a ketone group which is an organic compound in which a carbonyl group ($\text{C}=\text{O}$) is bonded to two carbon atoms of the carbon backbone. A carbonyl group is polar and can generate dipole-dipole attraction with carbonyl group ($\text{C}=\text{O}$) and hydrogen bonding ($-\text{OH}$ group)^{308,309}. In studying the interactions between PEEK-WC and the two solvents, it is necessary to consider that the carbonyl group of PEEK-WC polymer generates not only dipole-dipole attractions with DMC (as DMC has a carbonyl group as well) but also generates hydrogen bonding with methanol ($-\text{OH}$ group). Moreover, the fact that both DMC and methanol have a methyl group ($-\text{CH}_3$) can lead to a weak interaction with the carbonyl groups of PEEK-WC. In the interaction between molecules, DMC and methanol contain a carbonyl and a hydroxyl group, respectively. Consequently, both molecules undergo to intermolecular interactions due to hydrogen bonding. In addition, the methyl group of methanol and carbonyl group of DMC can also generate a weak intermolecular attraction.

In Figure 6-5, the permeance of DMC decreases with the decrease of the molar fraction of methanol. At low concentration of methanol, the amount of hydroxyl groups from methanol is much lower than the carbonyl group from PEEK-WC polymer and DMC. The major competition is between carbonyl groups from PEEK-WC polymer and DMC to attract methanol (hydroxyl and methyl group). The intermolecular interaction of hydrogen bonding is stronger than dipole-dipole attraction. Therefore, methanol is more prone to interact with a PEEK-WC membrane due to hydrogen bonding formation in comparison to DMC because the interaction between the PEEK-WC membrane and

DMC is dipole-dipole attraction. As a result, methanol molecules have more opportunity to occupy the carbonyl site of PEEK-WC than DMC and, therefore, to diffuse through the membrane.

With the increase of methanol concentration, the carbonyl group of DMC can be surrounded by the methyl group of methanol due to the intermolecular attraction between the carbonyl oxygen and hydrogen atoms, the carbonyl groups are more favorable to be surrounded by the methyl groups of methanol³¹⁰. The intermolecular force between methanol and DMC has been estimated in Chapter 5 Table 5-4. It shows that these two molecules have strong intermolecular force. The dragging effect resulting from the intermolecular interaction can present in the permeation. Consequently, a strong drag effect becomes more dominant when more methanol present in the mixture. Therefore, the permeance of DMC increases with the increasing of methanol concentration in the mixture.

The result of selectivity shows that both concentration and temperature have a great influence on the membrane performance. When the concentration of methanol was larger than 50 mol%, the selectivity was below 1 (90% methanol: selectivity 0.25-0.35; 70% methanol: selectivity 0.65-0.88). This indicates that the membrane permeates DMC due to a strong dragging effect caused by the high concentration of methanol. When the concentration of methanol was 50 mol%, the selectivity was near 1. On the contrary, when the concentration of methanol was below 50 mol%, the selectivity could attain 3.5, showing that the membrane prefers to permeate methanol instead of DMC due to the higher polarity of the alcohol compared to the ester.

In Table 6-3, a literature comparison of PV performances of methanol/DMC separation of different membranes is given. The most interesting performance of the membranes here investigated with respect to literature data, is that the PEEK-WC membrane can have a good separation performance at low concentration of methanol equal to 0.1 molar fraction (3.8 wt% methanol) and at low temperature (30°C) with a separation factor of 13.4. This separation performance is better than for other membranes tested under the same conditions. This makes the process feasible when a large excess of DMC, in methanol/DMC mixtures, is encountered. For example, in the transesterification reaction of glycerol and DMC, an excess of DMC is introduced to produce glycerol carbonate and methanol as a byproduct. In the final product mixture,

a high concentration of DMC is present in the mixture with a low concentration of methanol⁵³.

Table 6-3. Comparison of pervaporation performances of methanol/DMC separation membranes in literatures

Membrane material	Feed Methanol concentration (wt%)	Temperature (°C)	Flux (g/m ² .h)	Separation Factor	Permeance	Selectivity	Ref.
Chitosan/silica	30-70	30-50	850-1265	29-49	-	-	311
Poly(vinyl alcohol)	40-70	50-40	154-510	2.8-37	-	-	312
Nano-Silica/ polydimethylsiloxane	70	40	702	3.97	-	-	313
PDMS/PVDF	72	40	487.2	3.95	~1X10 ⁴ – 8.4X10 ⁴ DMC ~2X10 ³ – 1.7X10 ⁴ MeOH	-	314
Silicotungstic acid hydrate/Chitosan	10-70	30-60	1163-1500	52-67.3	-	-	315
Chitosan hollow fiber membrane	10-90	20-50	150-500	4-24	~50-100 DMC ~720-1200 MeOH	14-17	316
Poly(acrylic acid)/poly(vinyl alcohol)	10-90	40-80	3000	1.8-13	~20-200 DMC ~80-180 MeOH	~0.2-5.8	275
Crosslinked chitosan	6-70	25-55	30-500	10-90	-	-	291
PDMS and PTMSP	9.1-80.3	40	7.2-828	1.8-4.2	~700-1800 DMC ~70-177 MeOH	-	317
PEEK-WC	3.8-96.2	30-50	78-227	0.25-13.4	~48-180 DMC ~20-293 MeOH	~0.2-3.5	This work

6.3 Conclusions

PEEK-WC membranes were prepared and studied for the pervaporation separation of the binary mixture methanol/DMC at different conditions. In the membrane swelling experiment, the results showed that the membrane can be swollen by both organics, but more in case of DMC than methanol. The swelling degree increases with the increase of DMC concentration in the DMC/methanol mixtures. The transmembrane flux increases with the temperature, but decreases with the methanol concentration mainly due the hydrophilicity of the membrane which can promote the diffusion of the more polar compound (methanol) of the binary mixture. The molecular structure has a strong impact on the membrane performance. A higher concentration of methanol can lead to a strong drag effect and to a subsequent decrease of the selectivity.

The transmembrane flux is not extraordinary high in comparison with the data reported in literature, but the separation factor (13.5) has a better performance than other membranes at low concentration of methanol (0.1 molar fraction) and at low temperature (30 °C). Moreover, the membrane showed excellent mechanical properties during the overall experimental period. Therefore, PEEK-WC membranes can be of interest to be applied in pervaporation at industrial level for breaking the azeotrope of methanol and DMC.

The solubility parameters can be applied to predict potential coupling effects, however, the methods of estimation of solubility parameters can give different results. Hence, it is important to compare the solubility parameters obtained from different methods in order to have a more accurate prediction.

Chapter 7. Pervaporation separation of methanol/dimethyl carbonate mixture by using supported ionic liquid membranes

Based on:

Wenqi Li, Cristhian Molina Fernandez, Julien Estager, Jean-Christophe M. Monbaliu, Damien P. Debecker, Patricia Luis, Application of supported ionic liquid membranes in the separation of methanol/dimethyl carbonate mixtures by pervaporation (Under preparation)

7.1 Introduction

Supported liquid membranes (SLM) have been introduced in pervaporation as potential membranes to increase selectivity and transmembrane flux due to the tuned affinity of the liquid to the target compound and the higher diffusivity through the liquid phase immobilized inside the membrane pores. In a SLM, a solvent is impregnated into a porous membrane. The transport mechanism of SLM involves three stages: 1) the molecules are sorbed from the feed solution onto the solvent in the supported liquid membrane, 2) the sorbed molecules diffuse through the membrane to the permeate side; then 3) the molecules are re-extracted to the permeate side²¹⁶. The difference of solubility and diffusion coefficients of different solutes in a liquid makes the separation process feasible since diffusion coefficients in liquids are much higher than in polymers³¹⁸. Hence, larger flux could be expected in SLMs. However, the stability issue of SLMs is the major limitation for a large scale industrial commercial application^{319,320}. The low stability of supported liquid membranes has been observed in the literature, with a loss of immobilized solvent after relative short application time, leading to a dramatic increase of flux and decrease of selectivity³²¹. Solvent evaporation, dissolution into contiguous phases and pressure gradient are the major factors leading to the loss of solvent³²². In order to solve this instability, ionic liquids have been proposed to produce the SLM, taking the name of supported ionic liquid membranes (SILMs).

Ionic liquids are organic salts containing an organic cation and an inorganic or organic anion. Ionic liquids can be designed by combining different substituents of cation and anion to modified the chemical and physical properties, such as hydrophilicity, solubility, in order to achieve a good selectivity to target component³²³. In addition, ionic liquids have high chemical and thermal stabilities and have a large temperature range (up to 400 °C) with almost zero vapor pressure²¹². Therefore, ionic liquids are considered as “green solvents” to replace volatile organic solvents in the chemical industry. Ionic liquids have wide applications in chemical reactions as catalysts or additives^{324,325,13,14,328}, extraction^{329–337}, electrolytes^{338–340}. In fluid-fluid separation processes, ionic liquids are good media for extraction. However, the high cost of synthesis of ionic liquids and the high energy consumption for re-generating ionic liquids are important factors for the limitation of application of ionic liquids in separation

processes. These shortcomings can be solved by using SILMs, supporting ionic liquids instead of organic solvents.

The SILM needs a small amount of ionic liquids to fill in the membrane pores, and the re-generation of ionic liquid for recycling is not necessary. Due to their negligible vapor pressure and high viscosity, ionic liquids in supported ionic liquid membranes can be more stable than organic solvents. In the literature, SILMs have been extensively used for gas separation, such as SO_2/CO_2 , $\text{CO}_2/\text{H}_2/\text{N}_2$, $\text{H}_2\text{S}/\text{CO}_2/\text{CH}_4$ and natural gas purification^{213,214,341–346}. The application in pervaporation is scarcer. Still, it has received increasing attention in recent years, such as the separation of transesterification reaction mixtures containing alcohols, organic acids, hydrocarbons and amines^{218,220–223,347–350}.

The use of SILMs for the separation of transesterification mixtures has been studied based on hydrophilic ionic liquids [BMIM][BF₄], [OMIM][BF₄], [BMIM][PF₆] and [OMIM][PF₆]^{222,219}. In addition, ionic liquids ([EMIM][Cl] and [BMIM][Cl]) have been investigated as entrainers for breaking the azeotrope of methanol and DMC²⁹². These two ionic liquids show their capability to eliminate the azeotrope when their molar fraction increases to a certain level, for example 0.1168 for [BMIM][Cl]. However, the application of supported ionic liquid membranes for the separation methanol/DMC mixture has not been studied. In this work, two ionic liquids were synthesized and impregnated in a porous support (PAN membrane) to prepare the corresponding SILM in order to investigate the separation performance of DMC/methanol mixtures by pervaporation.

The ionic liquids, 1-octyl-3-methylimidazole bis(tri fluoromethanesulfonyl)imide [OMIM][NTf₂] and 1-octyl-1-methylpyrrolidine bis(tri fluoromethanesulfonyl)imide [OMPyrr][NTf₂], characterized as hydrophobic ionic liquids³⁵¹, were studied and their molecular structures were presented in Figure 7-1. The ionic liquid [OMIM][NTf₂] was chosen because it has been studied extensively in the literature, such as metal ion extractions and CO₂ sorption^{351–353}. It has been studied for SILM separation for organic-organic mixtures^{219,221,223}. [OMPyrr][NTf₂] was studied in the application of metal ion extraction as well³⁵¹. However, the application of this ionic liquid for SILM is rare in literature. Therefore, both ionic liquids were chosen for the study of membrane separation on DMC/methanol mixtures. Several concentrations of binary mixtures were

studied and the performance of the membranes was evaluated in terms of flux, separation factor, permeance and selectivity.

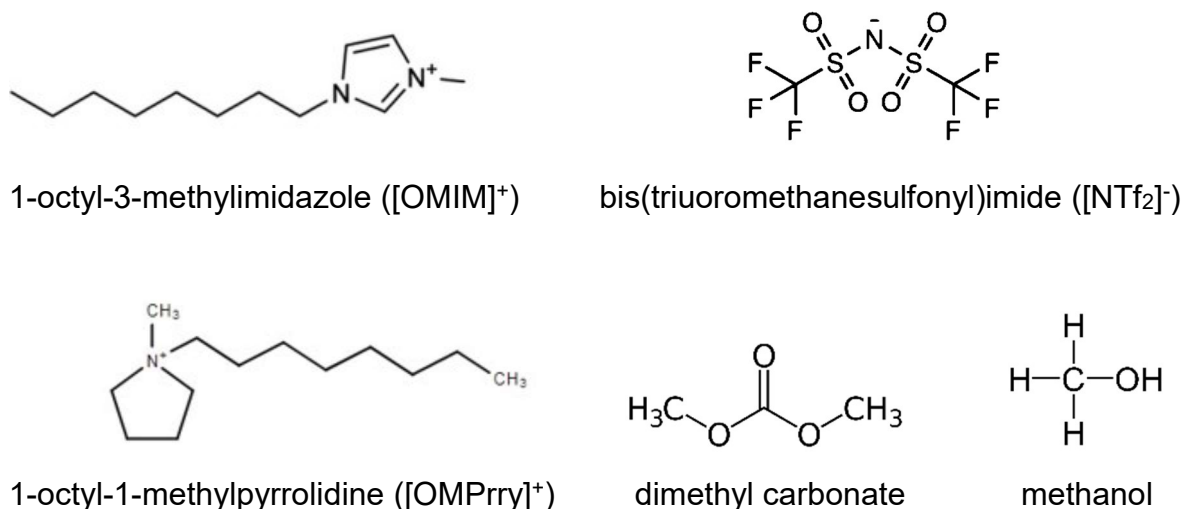


Figure 7-1. The molecular structure cations, anion and solvents

In this chapter, the following scientific question will be studied:

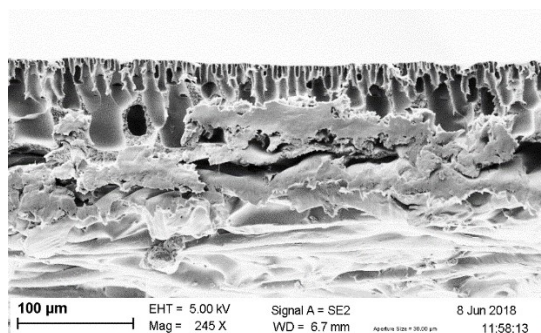
- Investigate the performance of supported ionic liquid membranes and if they have better performance comparing with available membranes in the literature for the separation of methanol/DMC?

7.2 Results and discussion

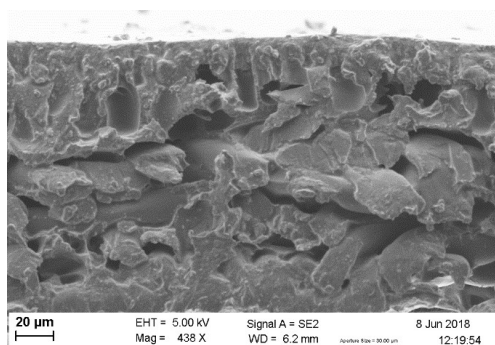
7.2.1 SEM analysis

The cross section morphology of raw PAN membrane and both prepared supported ionic liquid membranes was analyzed by SEM. The images are shown in Figure 3. Before immobilization, the regular empty pores of the raw PAN porous membrane were observed (Figure 7-2 (a)). After immobilization, both membranes are filled with ionic liquid [OMIM][NTf₂] and [OMPrpy][NTf₂] (Figure 7-2 (b1) and (c1)). When the membranes were applied for the separation process, it could be observed that some ionic liquids in the pores was washed away (Figure 7-2 (b2) and (c2)) in both supported ionic liquid membranes. However, the membranes are still capable for the separation process because only the ionic liquids at the top the pores was lost. During the experiments, it is observed that a freshly prepared supported ionic liquid membrane usually gives a high transmembrane flux. After repeating the experiments a couple of

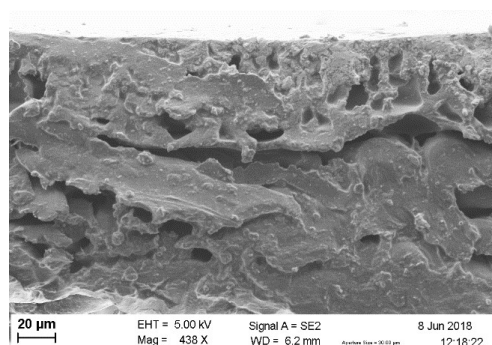
times, the flux decreased and finally became stable. The phenomena can be interpreted by the loss of ionic liquids at the top of membrane pores. When a fresh membrane was used, the interaction between the feed solution and ionic liquids was located at the surface of the supported ionic liquid membrane. When the top of ionic liquids was washed away by the feed solution, the interface of feed and ionic liquids moves to inside membrane pores.



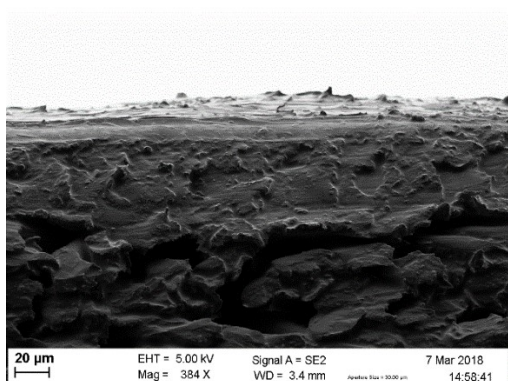
(a)



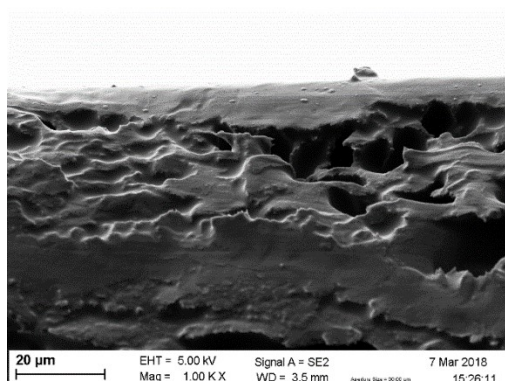
(b1)



(b2)



(c1)



(c2)

Figure 7-2. The PAN membrane before immobilization (a); immobilization of [OMIM][NTf₂] before (b1) and after (b2) experiments; immobilization of [OMPyrr][NTf₂] before (c1) and after (c2) experiments.

7.2.2 Pervaporation separation performance

The separation performance of supported ionic liquid membranes prepared with the ionic liquid [OMPyrr][NTf₂] and [OMIM][NTf₂] immobilized in PAN membranes was determined by testing different concentrations of methanol/DMC mixtures. The transmembrane flux, separation factor, permeance and selectivity of these two supported ionic liquid membranes are shown in Figure 7-3.

The separation factor and selectivity are both larger than 1. This indicates that both membranes are favorable to permeate DMC instead of methanol. The permeation behavior is highly concentration dependent. At high concentration of methanol (0.8 molar fraction), the separation factor and selectivity is only between 1.8 and 3. With the increasing of DMC concentration in the feed solution, the separation factor and selectivity increase. Both supported ionic liquid membranes can achieve a separation factor of 21 and a selectivity of 67 for [OMIM][NTf₂] and 48 for [OMPyrr][NTf₂].

Figure 7-3 (c) shows the permeance of DMC and methanol of both supported ionic liquid membranes. It reflects the interaction between ionic liquids and solvents through eliminating the impact of the driving force. Solvatochromic parameters of solvents and ionic liquids including Kamlet-Taft solvation parameters and normalized solvent polarity (E_T^N) were given in Table 7-1. The β value hydrogen bond acceptor is more influenced by anion, both ionic liquids have a low hydrogen bond acceptor, therefore, the ionic liquid is less favorable to have interaction with methanol than DMC. The hydrogen bond acceptor follows DMC > [OMPyrr][NTf₂] > [OMIM][NTf₂]. As methanol is a strong hydrogen bond donor, it could be more favorable to have a hydrogen bonding with DMC in the feed solution because DMC has a higher hydrogen bond acceptor than ionic liquids. Due to the low concentration of methanol in the feed solution, most methanol could form hydrogen bonding with DMC and be retained in the solution. This can also be seen from the molecular structure in Figure 7-1. DMC has a carbonyl group (C=O), which can generate dipole-dipole attraction with hydrogen bond (-OH group) of methanol. Therefore, the permeance of methanol of both supported ionic liquid membranes are very low at low concentration of methanol. The permeance of DMC at low methanol concentration (0.2 molar fraction of methanol) is higher for [OMPyrr][NTf₂] than for [OMIM][NTf₂]. The π^* dipolarity/polarizability of [OMPyrr][NTf₂] is smaller than that of [OMIM][NTf₂] (0.96 for [OMIM][NTf₂] and 0.73 for [OMPyrr][NTf₂]). DMC can be

more favorable to interact with [OMPyrr][NTf₂] instead of [OMIM][NTf₂] because DMC is not a high polar molecule and the π^* dipolarity/polarizability of DMC is only 0.47.

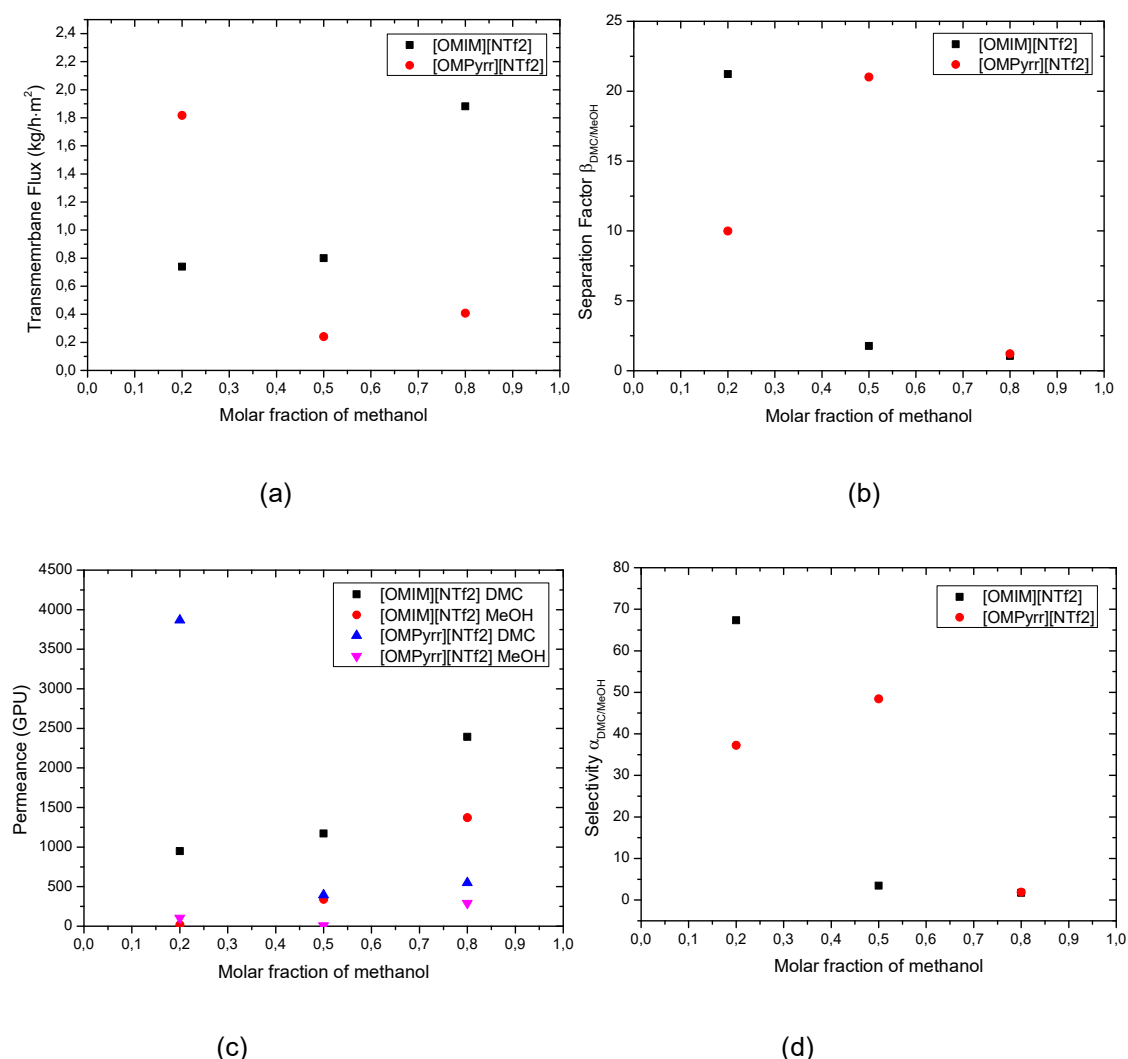


Figure 7-3. The performance of supported ionic liquid membranes based on ionic liquid [OMPyrr][NTf₂] and [OMIM][NTf₂] at 30 °C, (a) Transmembrane flux, (b) Separation factor, (c) Permeance of DMC and methanol and (d) Selectivity (DMC/methanol).

When the concentration of methanol increases, a competition between the ionic liquid and methanol for affiliating to DMC takes place. Compared to two ionic liquids, DMC is more favorable to generate a hydrogen bond with methanol. On the other hand, DMC has a strong interaction between both ionic liquids. As a result, a dragging effect takes place during the permeation, the methanol also permeate through the membrane with DMC due to hydrogen bonding interaction between them. From Figure 7-3 (c), it can be seen that the permeance of methanol in both supported ionic liquid membranes are

increased dramatically. The selectivity and separation factor have a very low value at high concentrations of methanol.

Table 7-1. Solvatochromic parameters (Kamlet-Taft solvation parameters)

Component	E_T^N	α	β	π^*	Ref.
[OMIM][NTf ₂]	0.60	0.60	0.29	0.96	354
[OMPyrr][NTf ₂]	0.651	0.80	0.08	0.73	355
Methanol	0.769	1.05	0.61	0.73	355, 356, 357
DMC	0.232	0	0.38	0.47	356, 358, 359

7.2.3 Membrane stability

The major issue of supported ionic liquid membranes is their stability due to the ionic liquid loss during the operation. Hence, a robust stability test was carried out for both supported ionic liquid membranes. The prepared membrane tested for 120 h under the concentration of 0.2 molar fraction of methanol when the transmembrane flux turns to constant. As some ionic liquids at the top of the membrane pore contacting with feed solution could lose at the beginning of the test (mentioned in section 7.2.1). The stability test is shown in Figure 7-4. The test confirms that both ionic liquids were kept in the pores of supported PAN membrane and give a stable transmembrane flux and separation factor.

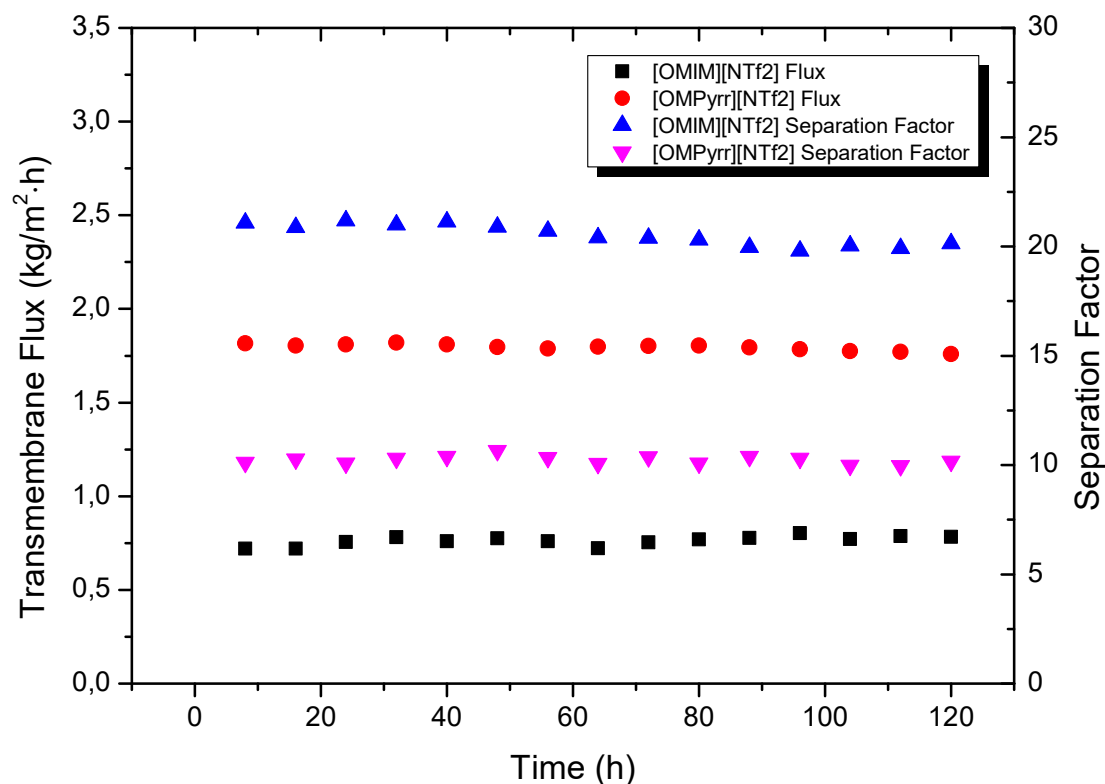


Figure 7-4. Operational stability of SILMs based on PAN membrane with supported [OMIM][NTf₂] and [OMPyrr][NTf₂] under 0.2 molar fraction of methanol at 30 °C

7.2.4 Comparison of DMC/methanol pervaporation separation in literature

A literature overview of the separation of methanol DMC mixtures by pervaporation was shown given in Table 6-3. Those results can be compared with those obtained in this work and shown in Table 7-2. Comparing with other studies, supported ionic liquid membranes have an extraordinary separation performance at 0.2 molar fraction of methanol at low temperature (30°C) with high selectivity 67 and 48 for [OMIM][NTf₂] and [OMPyrr][NTf₂] based supported ionic liquid membranes, respectively. The separation is favorable to be applied in the situation with a large excess of DMC in the binary mixture. A high purity of DMC can be recovered in the permeate and reused.

Table 7-2. Summary the performance of supported ionic liquid membranes in this work

Membrane material	Feed Methanol concentration (wt%)	Temperature (°C)	Flux (g/m ² ·h)	Separation Factor	Permeance	Selectivity	Ref.
[OMIM][NTf ₂] SILM	0.2-0.8	30	739.8	21.2	947-2400 DMC 14-1370 MeOH	1.75-67.34	This work
[OMPyrr][NTf ₂] SILM	0.2-0.8	30	1817	10.0	548-3867 DMC 8.162-290.15 MeOH	1.9-48.41	This work

7.3 Conclusions

Two supported ionic liquid membranes based on [OMIM][NTf₂] and [OMPyrr][NTf₂] ionic liquids were studied for the separation of binary mixture DMC and methanol. It is found that for high concentration of DMC (>0.8 molar fraction), the studied SILMs show a good separation performance with high selectivity comparing with available membranes in the literature. In addition, the transmembrane flux is also high (739.8 g/m²·h for [OMIM][NTf₂], 1817 g/m²·h for [OMPyrr][NTf₂]). It is concluded that supported ionic liquid membrane can have a better mass transfer due to the transport medium is liquid phase.

However, the membrane performance is highly concentration dependent. At high concentration of methanol in the mixture, the separation performance decreases due to strong dragging effect.

Chapter 8. Conclusion and Future work

8.1 Summary and general conclusions

The extraction of bio-based chemicals from renewable raw materials is important for the future in order to avoid emission of greenhouse gases from non-renewable materials and their depletion. Membrane technology, recognized as a clean technology, plays a more and more important role in separation and purification processes. Concretely, pervaporation has proved its capability for challenging separation process, such as breaking azeotropic mixtures.

In this thesis, the separation of organic mixtures from three transesterification reactions by pervaporation has been studied, applying commercial membranes from Sulzer, self-made PEEK membrane and supported ionic liquid membranes. The separation performance of those membranes was evaluated as well as the presence of coupling effects. The main conclusions of this thesis are as follows:

- Transesterification mixture from reaction 1 (methyl acetate, butyl acetate, methanol, butanol) and reaction 2 (ethyl acetate, methanol, methyl acetate and ethanol):

The commercial membranes from Sulzer containing different fractions of PVA content have been studied. It was found that these commercial membranes appear to permeate alcohols rather than esters in pure solution studies. However, the permeation performance of the membranes is quite different in mixtures. The esters could permeate through the membrane with alcohols as well. In this study, Hansen solubility approach is a useful tool not only for the materials selection and screening for the separation but also for predicting potential coupling effect in the mixture. In pervaporation, Hansen solubility parameters are applied for investigating the interaction between polymer materials and pure components. It is concluded that Hansen solubility parameters of mixture should be taken into account. Due to the different solubility property of pure component and when it is in the mixture, a modification of solubility can occur. As a result, a pure component that is not permeable by a membrane can be obtained in the permeate when it is present in a mixture as feed solution.

- Transesterification mixture from reaction 3 (glycerol, dimethyl carbonate, glycerol carbonate and methanol)

In the production of glycerol carbonate *via* application of commercial membranes, the application of pervaporation technology to separate a quaternary transesterification mixture consisting of glycerol, dimethyl carbonate, methanol and glycerol carbonate has been investigated. It was found that glycerol and glycerol carbonate are not permeable due to their extremely low vapour pressure. Only methanol and dimethyl carbonate can diffuse through the membranes and methanol is concentrated in the permeate. The temperature effect shows an opposite trend of flux and permeance. The higher the temperature, the higher the transmembrane flux. However, the permeance decreases. Therefore, working at low temperature is an advantage in terms of membrane performance assuming the trading off with the transmembrane flux. The McCabe-Thiele separation diagram analysis shows that pervaporation can separate methanol more effectively than flash distillation. Hence, pervaporation could be an alternative to improve the reaction yield by removing methanol from the reaction mixture.

- Binary mixture from reaction 3 (dimethyl carbonate and methanol)

The separation of binary mixture dimethyl carbonate and methanol was studied through self-made membrane (PEEK) and SILMs. In the application of PEEK membranes for the pervaporation separation of the binary mixture methanol/DMC, the membrane with separation factor (13.5) has a better performance than other membranes at low concentration of methanol and at low temperature (30 °C). The membrane swelling test showed that the membrane can be swollen by both organics, but more in case of DMC than methanol. Due to the hydrophilicity of the membrane, it promotes the diffusion of the more polar compound (methanol) of the binary mixture. However, the molecular interaction plays an important role at high concentration of methanol. A high concentration of methanol results in a strong dragging effect and a decrease of the selectivity. The supported ionic liquid membranes based on [OMIM][NTf₂] and [OMPyrr][NTf₂] ionic liquids were studied for the separation of binary mixture DMC and methanol. It was found that the transmembrane flux (739.8 g/m²·h) has a good performance compared to the literature. In addition, at high concentration of DMC (>0.8 molar fraction), the SILM based on [OMIM][NTf₂] shows a good separation performance with high selectivity (67). Concentration is an important factor for the separation performance; at high concentration of methanol, the separation performance decreases due to strong drag effect.

Finally, pervaporation is a good alternative to recover organic solvent from the mixture. A stand-alone pervaporation can give solutions to the separation of organic-organic mixture when the components exhibit different physical and chemical properties. However, the performance depends on the interaction between molecules and membrane materials. The intermolecular force plays an important role in pervaporation. A strong intermolecular force can lead to a strong dragging effect and result in a decrease of selectivity. Therefore, it is important to have an analysis for the molecular interactions, e.g. molecules and molecules, molecules and membrane materials. Pervaporation can achieve a good separation performance at certain conditions of temperature and feed concentration.

8.2 Future work

In Chapters 5, 6 and 7, commercial membrane, self-made PEEK membrane and supported ionic liquid membranes were studied for the separation of quaternary mixtures (glycerol, glycerol carbonate, methanol, dimethyl carbonate separated by commercial membrane) and binary mixtures (dimethyl carbonate and methanol separated by PEEK membrane and SILMs). Although the process design is out of scope for this thesis, it is still important to have a view of how these developed membranes can be applied in the separation process. Therefore, further research could be oriented towards the process design. An example is shown below for the production of glycerol carbonate.

Process design for glycerol carbonate production

The production of glycerol carbonate *via* transesterification reaction between glycerol and dimethyl carbonate has been proposed by Wang *et al*⁶⁵. The production and separation were composed by reactive distillation (CaO catalyst) and extractive distillation. In reactive distillation, glycerol and dimethyl carbonate are introduced into a reactive distillation column. At the bottom, the DMC and glycerol carbonate mixture is obtained. As glycerol carbonate has high boiling point and extremely low volatility, DMC and glycerol carbonate can be easily separated by a simple distillation. The distillate of reactive distillation column is the mixture of methanol and dimethyl carbonate. This binary mixture is introduced to extractive distillation for further separation. Hsu *et al*, compared different candidate entrainers for extractive distillation

methanol and DMC. It is found that aniline is the best solvent³⁶⁰. Then, methanol is obtained as distillate of extractive column. DMC and the solvent are obtained at the bottom of the extractive distillation column and they are separated in a recovery column. This separation flowsheet is shown in Figure 8-1.

In Chapter 5, it was shown that the glycerol and glycerol carbonate can not permeate through the commercial membrane due to their low volatility. In the literature, it is also shown that high conversion of glycerol (>95%) is possible for the transesterification glycerol and DMC. Hence, a high purity of glycerol carbonate can be obtained when DMC and methanol are removed by commercial membrane as permeate. Then, further separation of the binary mixture DMC and methanol is the key for this process.

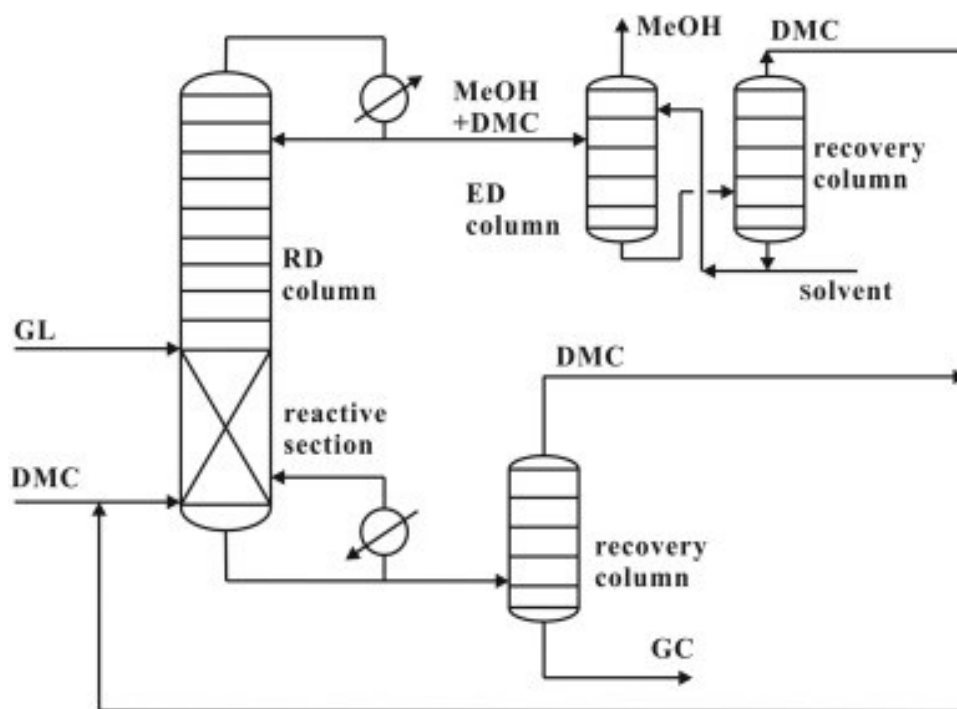


Figure 8-1 Flowsheet of the proposed reactive distillation and extractive distillation process for production of glycerol carbonate. Reprinted with permission from Wang *et al.*⁶⁵

The separation of DMC and methanol has been studied by using pressure swing distillation³⁶¹ and distillation-pervaporation hybrid process³⁶². The flowsheet of distillation-pervaporation hybrid process is shown in Figure 8-2. The 20 wt% methanol mixture was fed to the distillation and the azeotropic mixture was fed to pervaporation unit. Finally, 99 wt% DMC and 95 wt% methanol were obtained.

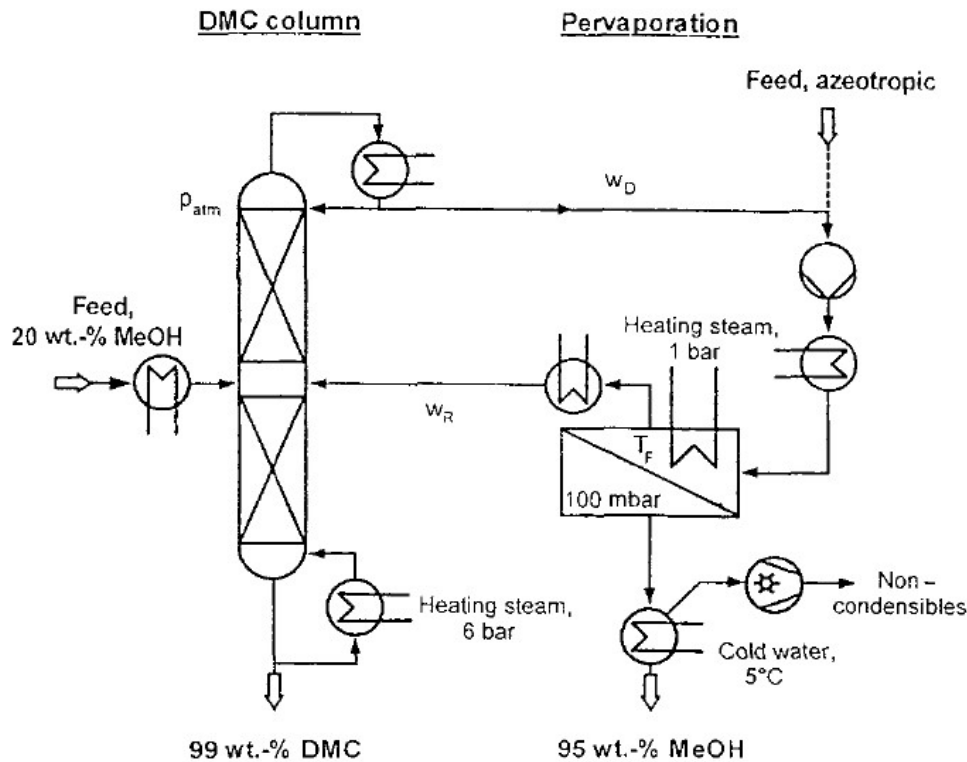


Figure 8-2. Separation of DMC/Methanol by distillation and pervaporation. Reprinted with permission from Rautenbach *et al.*³⁶²

According to the information from literature, it is proved that the hybrid process is a feasible approach for this separation. According to the results obtained in this work, the proposed flowsheet is shown in Figure 8-3.

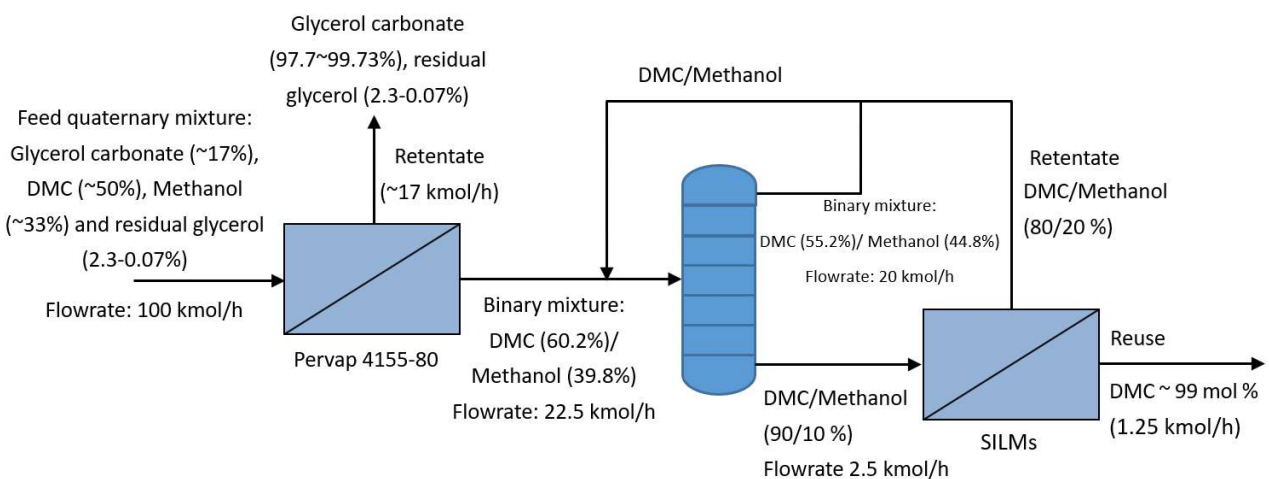


Figure 8-3. A proposed flowsheet for the production of glycerol carbonate

The quaternary mixture from reactor is fed to a stand-alone pervaporation unit, the commercial membrane can separate the mixture with two groups. In the retentate, glycerol carbonate is enriched, the purity of glycerol carbonate depends on the conversion of glycerol. In some literatures^{56,57,65,272}, the conversion of glycerol can achieve 97.7% - 99.93%. Therefore, it is possible to achieve a high purity of glycerol carbonate with just a stand-alone pervaporation unit at this stage. In the permeate, a binary mixture methanol/DMC with 39.8% molar fraction of methanol could be obtained. Then, the permeate binary mixture DMC/methanol is fed to a distillation column. The parameters of distillation are: 50 stages with 3 reflux ratio. The function of distillation column is to achieve a pre-concentrated methanol/DMC mixture with 0.9 molar fraction of DMC at the bottom. By simulation using Aspen 11, at the distillate, the composition is 44.8% methanol. This distillate is mixed with the retentate flow coming from SILMs and send back to the distillation. The mixture in the bottom of distillation transports to pervaporation unit equipped with supported ionic liquid membrane. The supported ionic liquid membrane can achieve a high purity of DMC in the permeate when the feed concentration is above 0.8 molar fraction of DMC. Finally, a high purity of DMC (98 mol%) can be recovered. The SILM based on [OMIM][NTf₂] ionic liquid has a high permeation flux, 22.5 mol/h DMC can be recovered with 1 m² membrane area.

From these results, it is concluded that applying membranes coupled with distillation to achieve high purity of glycerol carbonate product and recover high purity of DMC for reuse is possible. It is straightforward that the pre-concentration of DMC in distillation only up to 0.9 molar fraction, the energy cost of the distillation should be greatly decreased. However, a further detailed study is still necessary for the optimization of separation sequence, energy consumption analysis and installation costs. For distillation, the variation of number of stages and reflux ratio is important to achieve an economical separation performance. For pervaporation, the process costs of the variation of membrane area, heater exchange and permeate pressure must be optimized according to the concentration at each process stage. This should be done in the future.

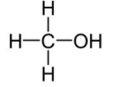
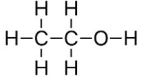
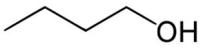
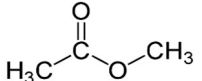
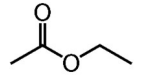
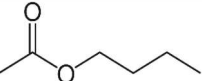
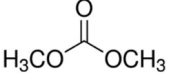
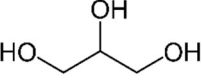
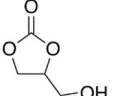
Appendices

Chapter 1

A1.1. Summarizing of the chemical structure and relevant properties of the mixture components

The chemical structure and properties of the mixture components were listed in Table A1.1 and Table A1.2

Table A1.1. The chemical structure and properties of the mixture components

Materials	Chemical Structure	Molecular Weight (g/mol)	Molar Volume (l/mol)	Boiling Point (°C at 1 atm)	Polarity (water 100)	Log ₁₀ (K _{ow})
Methanol ⁽¹⁾		32	40.4	64	76.2	-0.82
Ethanol ⁽¹⁾		46	58.7	78	65.4	-0.32
Butanol ⁽¹⁾		60	75.1	97	61.7	0.34
Methyl acetate ⁽¹⁾		74	79.8	57	29.0	0.18
Ethyl acetate ⁽¹⁾		88	98.5	77	23.0	0.73
Butyl acetate ⁽¹⁾		116	132.5	126	24.1	1.7
Dimethyl carbonate ⁽²⁾		90	84.2	90.3	23.2	0.15
Glycerol ⁽²⁾		92	73.0	290	81.2	-2.32
Glycerol Carbonate ⁽²⁾		118	84.3	110-115*	NA	-1.77

* Boiling range, 0.1 mm Hg, °C

⁽¹⁾ Lan M. Smallwood, Handbook of organic solvent properties, Butterworth-Heinemann 1996

⁽²⁾ José I. García, Héctor García-Marín and Elísabet Pires, Glycerol based solvents: synthesis, properties and applications, Green Chem. 2010, 12, 426–434

Table A1.2. Antoine equation vapor pressure constants (\log_{10} , mmHg)

Materials	A	B	C
Methanol ⁽¹⁾	8.081	1582.271	239.726
Ethanol ⁽¹⁾	8.112	1592.864	226.184
Butanol ⁽¹⁾	8.379	1788.020	227.438
Methyl acetate ⁽¹⁾	7.065	1157.63	219.726
Ethyl acetate ⁽¹⁾	7.102	1244.95	217.881
Butyl acetate ⁽¹⁾	7.028	1368.5	204
Dimethyl carbonate* ⁽²⁾	6.434	1413.00	-44.25

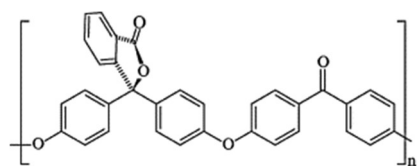
* Unit: P=kPa, T=K

⁽¹⁾ Lan M. Smallwood, Handbook of organic solvent properties, Butterworth-Heinemann 1996

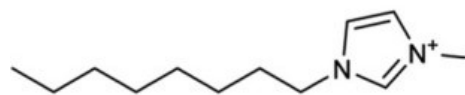
⁽²⁾ Satyajeet S. Yadav, Nilesh A. Mali, Sunil S. Joshi and Prakash V. Chavan, Isobaric Vapor–Liquid Equilibrium Data for the Binary Systems of Dimethyl Carbonate with Xylene Isomers at 93.13 kPa, J. Chem. Eng. Data 2017, 62, 2436–2442

A1.2. Summarizing of the chemical structure of membrane materials

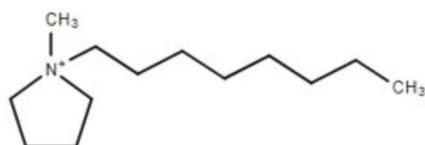
1. PEEK-WC



2. Cations: [OMIM]⁺ and [OMPyrr]⁺



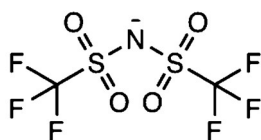
1-octyl-3-methylimidazole ([OMIM]⁺)



1-octyl-1-methylpyrrolidinium ([OMPyrr]⁺)

3. Anion

bis(trifluoromethanesulfonyl)imide ([NTf₂]⁻)



Chapter 3

A3.1. Reynolds number in the membrane cell estimation

In order to achieve turbulent flow, the Reynolds number should larger than 5000.

The kinematic viscosity of the mixture is estimated by the method proposed by Refutas (2000), which can estimate a mixture two or more liquids.

$$VBN_i = 14.534 \times \ln(\ln(v_i + 0.8)) + 10.975$$

where VBNi is Viscosity Blending Number of each component.

The VBN of mixture is then calculated:

$$VBN_{mixture} = \sum_{i=0}^N x_i \times VBN_i$$

The kinematic viscosity of the mixture can be estimated using the viscosity blending number of mixture:

$$v_{mixture} = \exp \left(\exp \left(\frac{VBN_{mixture} - 10.975}{14.534} \right) \right) - 0.8$$

In our case, the kinematic viscosity is 2.16X10-6 m2/s.

The flow velocity is 0.387 m/s for 70 L/h flow rate in our system and hydraulic diameter is 0.07 m.

Then the Reynolds number is calculated as follows:

$$Re = \frac{V_{feed\ fluid} \times D_H}{v_{mixture}} = 12550$$

Therefore, we introduce a high flow to minimize the resistance to mass transfer located at boundary layer. Hence, it is assumed that the resistance to mass transfer located at boundary layer can be negligible.

Chapter 4

A4.1. Overall average transmembrane flux of different types of membranes for mixture M1 at 30 °C, 40 °C and 50 °C

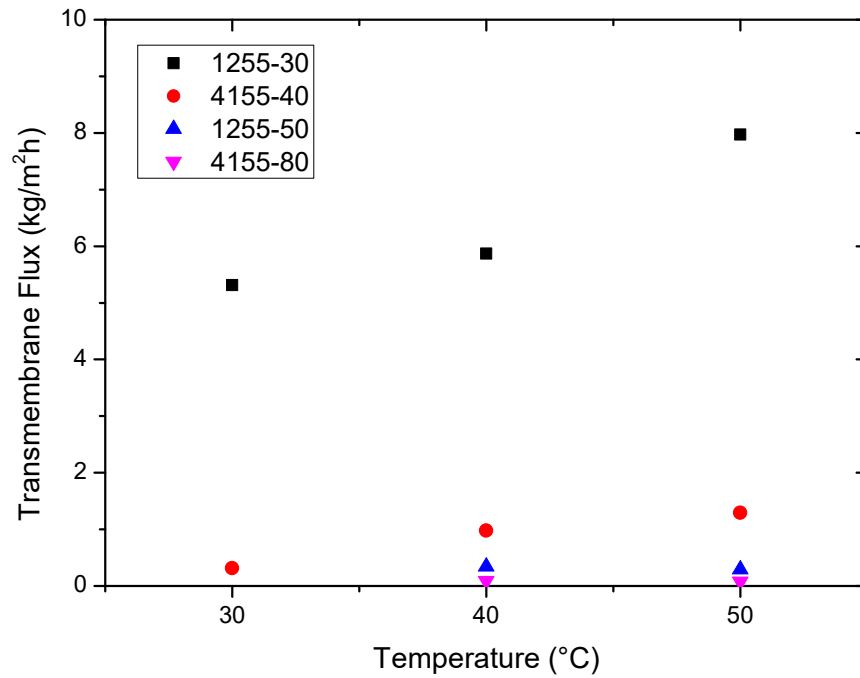


Figure A4.1. Overall average transmembrane flux of different types of membranes for mixture M1 at 30 °C, 40 °C and 50 °C

A4.2. The separation factor of different types of membranes for the mixture M1 at 30 °C, 40 °C and 50 °C; (a) 1255-30 membrane, (b) 4155-40 membrane, (c) 1255-50 membrane and (d) 4155-80 membrane

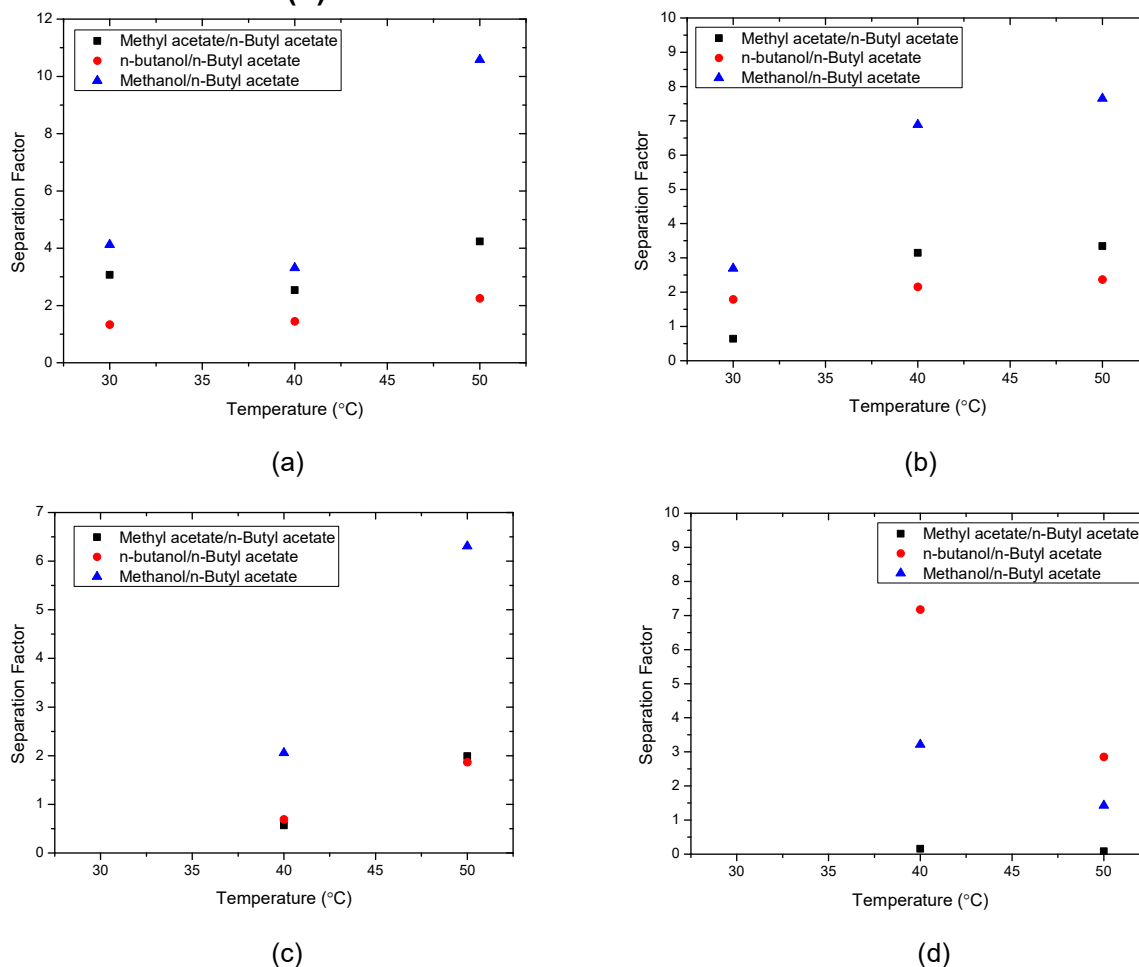


Figure A4.2. The separation factor of different types of membranes for the mixture M1 at 30 °C, 40 °C and 50 °C; (a) 1255-30 membrane, (b) 4155-40 membrane, (c) 1255-50 membrane and (d) 4155-80 membrane

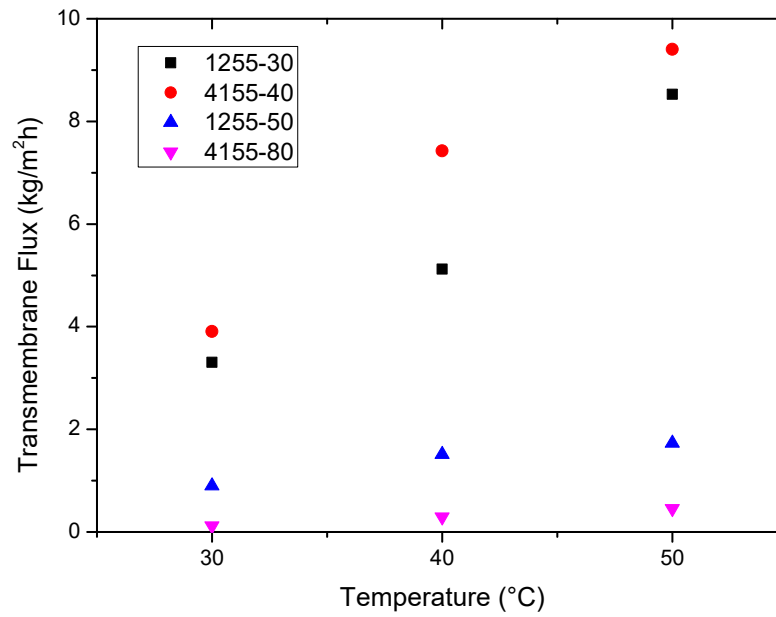
A4.3. Transmembrane flux of different types of membrane for the mixture M2 at 30°C, 40°C and 50°C

Figure A4.3. Transmembrane flux of different types of membrane for the mixture M2 at 30°C, 40°C and 50°C

A4.4. The separation factor of different types of membranes for mixture M2 at different temperature (a) 1255-30 membrane, (b) 4155-40 membrane, (c) 1255-50 membrane and (d) 4155-80 membrane

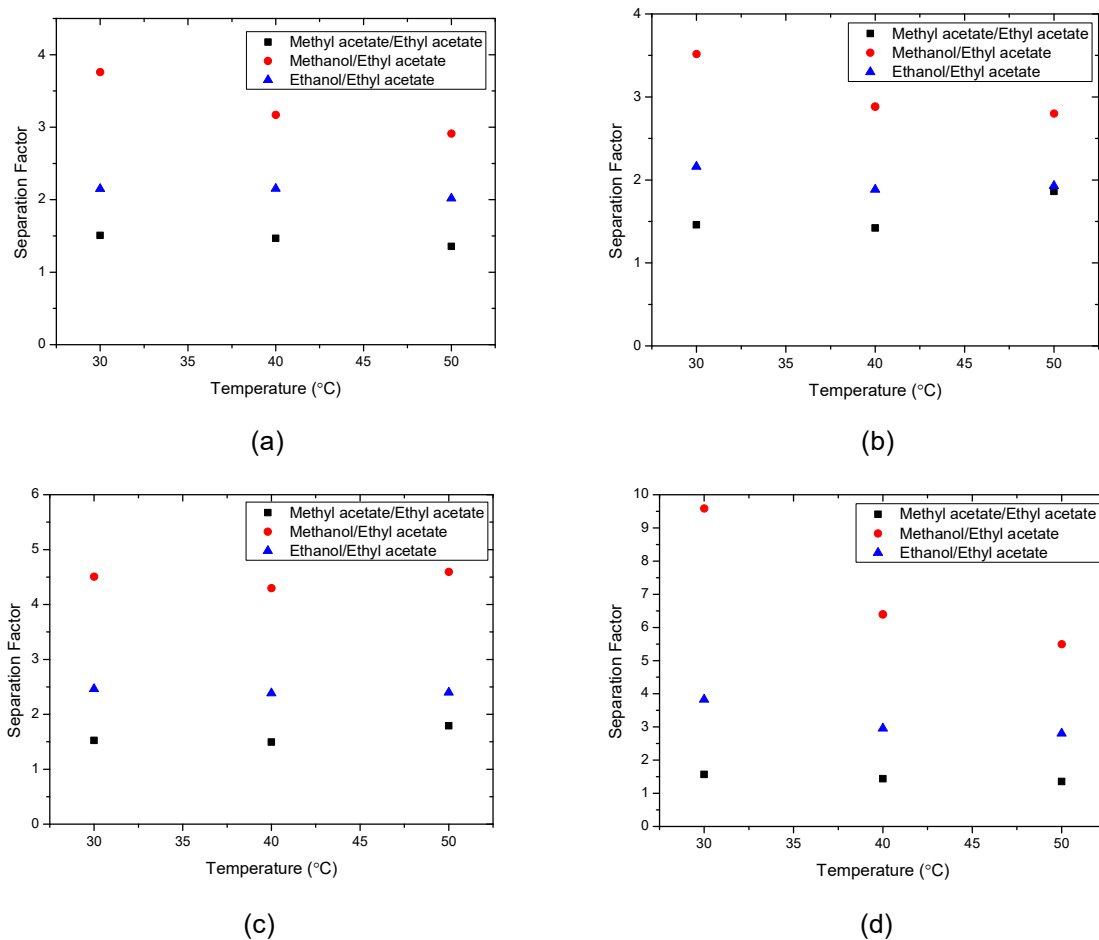


Figure A4.4. The separation factor of different types of membranes for mixture M2 at different temperature (a) 1255-30 membrane, (b) 4155-40 membrane, (c) 1255-50 membrane and (d) 4155-80 membrane

A4.5. Hansen solubility sphere for PVA and pure components and mixtures at 40 °C

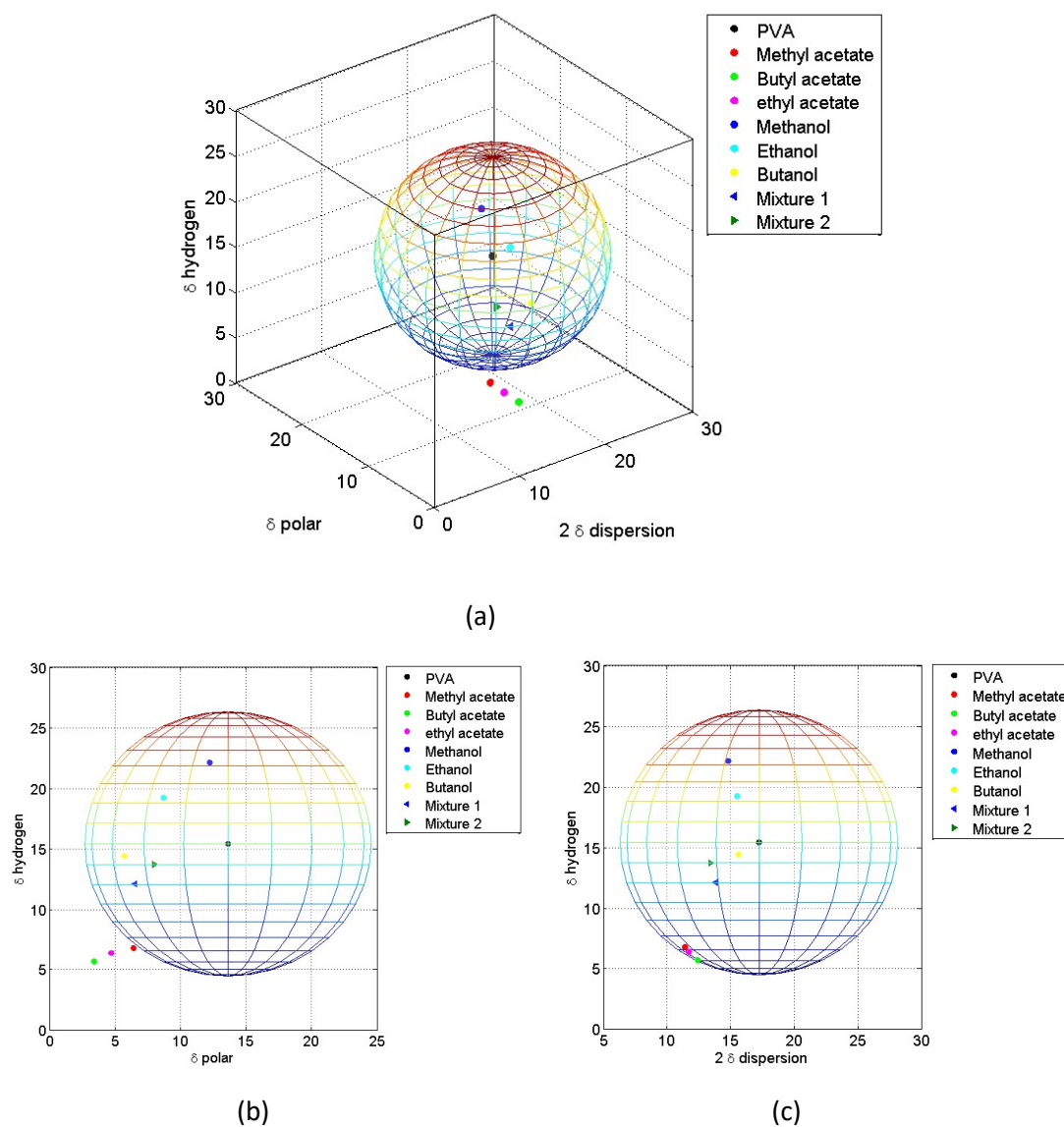


Figure A4.5. Hansen solubility sphere for PVA and pure components and mixtures at 40 °C (a) 3D representation; (b) Projection into hydrogen-polar plane and (c) Projection to hydrogen-dispersion plane

A4.6. Hansen solubility sphere for PVA and pure components and mixtures at 50 °C

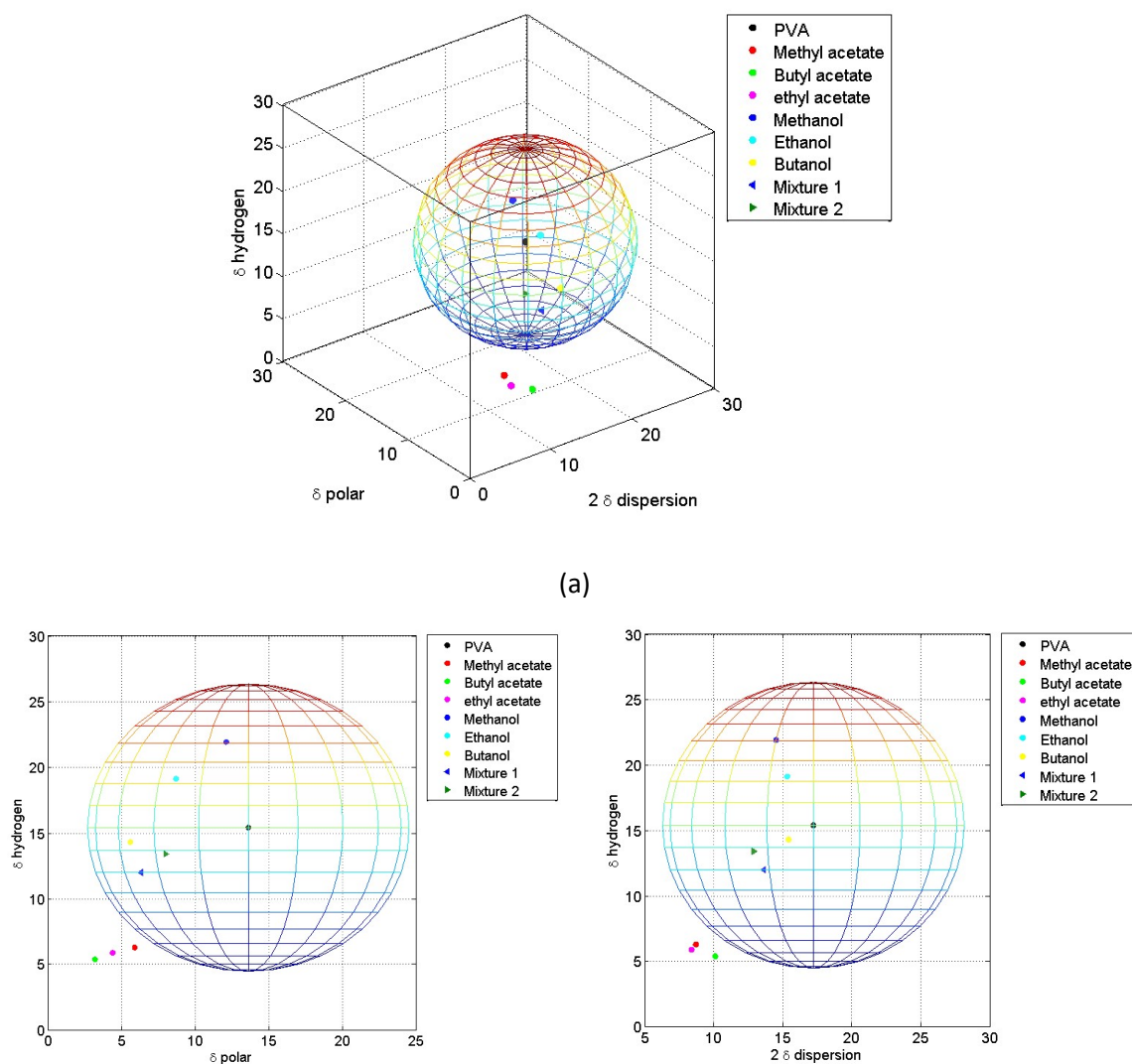


Figure A4.6. Hansen solubility sphere for PVA and pure components and mixtures at 50 °C (a) 3D representation; (b) Projection into hydrogen-polar plane and (c) Projection to hydrogen-dispersion plane

A4.7. Calculated Hansen solubility parameters of each component at 40 °C

Table A4.1. Calculated Hansen solubility parameters of each component/mixture and distance between solute and the center of the solubility sphere PVA ($\Delta\delta_{(s-p)}$) at 40 °C

Material	δ_D	δ_P	δ_H	$\Delta\delta_{(s-p)}$
PVA	17.2	13.6	15.4	
Methyl acetate	11.4	6.4	6.8	16.0
Butyl acetate	12.4	3.4	5.7	17.0
Ethyl acetate	11.7	4.7	6.4	16.7
Methanol	14.8	12.2	22.1	8.4
Butanol	15.6	5.7	14.4	8.6
Ethanol	15.5	8.7	19.2	7.1
Mixture M1	13.8	6.5	12.1	10.3
Mixture M2	13.4	8.0	13.7	9.6

A4.8. Calculated Hansen solubility parameters of each component at 50 °C**Table A4.2.** Calculated Hansen solubility parameters of each component/mixture and distance between solute and the center of the solubility sphere PVA ($\Delta\delta_{(s-p)}$) at 50 °C

Material	δ_D	δ_P	δ_H	$\Delta\delta_{(s-p)}$
PVA	17.1	13.6	15.4	
Methyl acetate	8.7	5.9	6.3	20.6
Butyl acetate	10.1	3.2	5.4	20.2
Ethyl acetate	8.9	4.4	5.9	21.0
Methanol	14.5	12.1	21.9	8.5
Butanol	15.4	5.6	14.3	8.7
Ethanol	15.3	8.7	19.1	7.23
Mixture M1	13.6	6.3	12.0	10.7
Mixture M2	12.9	8.0	13.4	10.4

Chapter 6

A6.1. Partial flux of methanol and DMC for different concentrations

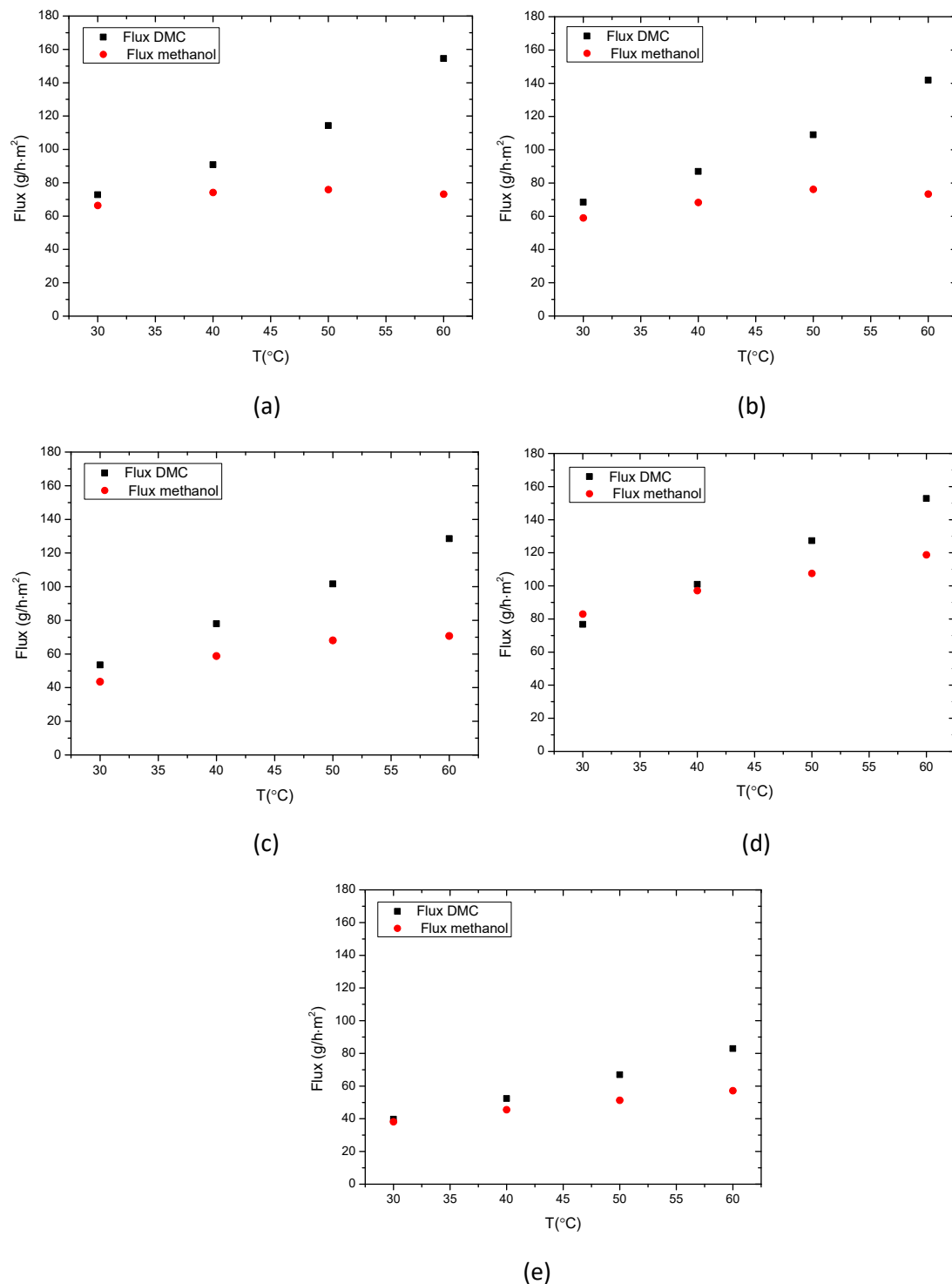


Figure A6.1. Partial flux of methanol and DMC at different concentrations, 0.1 molar fraction of methanol (a); 0.3 molar fraction of methanol (b); 0.5 molar fraction of methanol (c); 0.7 molar fraction of methanol (d) and 0.9 molar fraction of methanol (e).

Terminology

1. Membrane sorption and membrane swelling

The membrane sorption test reflects the affinity between membrane materials and the permeant molecules. It describes the stage of the membrane process in which the penetrant molecules are sorbed into the polymeric membrane until the sorption equilibrium is achieved.

The sorption of a solvent into a membrane causes intrinsic changes in membrane structure. Hence, membrane swelling is a phenomenon in which solvents diffuse into polymer chains and expand the polymer network. The degree of swelling was calculated from the difference between the wet weight M_{wet} after equilibrium sorption and the dry weight M_{dry} .

2. Permeation

In pervaporation, the permeation is the transmembrane flux through a membrane involving sorption and diffusion of permeant molecules from feed side to permeate side, relating to the driving force, e.g. concentration gradient of the permeant molecules.

References

1. Strathmann, H. Membrane separation processes. *J. Memb. Sci.* **9**, 121–189 (1981).
2. Serval, C., Roizard, D., Favre, E. & Horbez, D. Improved energy efficiency of a hybrid pervaporation/distillation process for acetic acid production: Identification of target membrane performances by simulation. *Ind. Eng. Chem. Res.* **53**, 7768–7779 (2014).
3. Nagy, E., Mizsey, P., Hancsok, J., Boldyryev, S. & Varbanov, P. Analysis of energy saving by combination of distillation and pervaporation for biofuel production. *Chem. Eng. Process. Process Intensif.* **98**, 86–94 (2015).
4. Ozdemir, S. S., Buonomenna, M. G. & Drioli, E. Catalytic polymeric membranes: Preparation and application. *Appl. Catal. A Gen.* **307**, 167–183 (2006).
5. Luis, P., Amelio, A., Vreysen, S., Calabro, V. & Van der Bruggen, B. Simulation and environmental evaluation of process design: Distillation vs. hybrid distillation-pervaporation for methanol/tetrahydrofuran separation. *Appl. Energy* **113**, 565–575 (2014).
6. Smitha, B., Suhanya, D., Sridhar, S. & Ramakrishna, M. Separation of organic-organic mixtures by pervaporation - A review. *J. Memb. Sci.* **241**, 1–21 (2004).
7. Kujawa, J., Cerneaux, S. & Kujawski, W. Removal of hazardous volatile organic compounds from water by vacuum pervaporation with hydrophobic ceramic membranes. *J. Memb. Sci.* **474**, 11–19 (2015).
8. Sert, E. & Atalay, F. S. N-Butyl acrylate production by esterification of acrylic acid with n-butanol combined with pervaporation. *Chem. Eng. Process. Process Intensif.* **81**, 41–47 (2014).
9. Rathod, A. P., Wasewar, K. L. & Sonawane, S. S. Intensification of esterification reaction of lactic acid with iso-propanol using pervaporation reactor. *Procedia Eng.* **51**, 456–460 (2013).
10. Xu, S. & Wang, Y. Novel thermally cross-linked polyimide membranes for ethanol dehydration via pervaporation. *J. Memb. Sci.* **496**, 142–155 (2015).
11. Hiwale, R. S. Industrial applications of reactive distillation: recent trends. *Int. J. Chem. React. Eng.* **2**, 1–52 (2004).
12. Van der Bruggen, B. Comprehensive Membrane Science and Engineering. *Compr. Membr. Sci. Eng.* 135–163 (2010).
13. Kita, H. Esterification of carboxylic acid with ethanol accompanied by pervaporation. *Chem. Lett.* 2025–2028 (1988).
14. Lipnizki, F., Field, R. W. & Ten, P.-K. Pervaporation-based hybrid process: a review of process design, applications and economics. *J. Memb. Sci.* **153**, 183–210 (1999).
15. Pilar Bernal, M., Coronas, J., Menéndez, M. & Santamaría, J. Coupling of reaction and separation at the microscopic level: Esterification processes in a H-ZSM-5 membrane reactor. *Chem. Eng. Sci.* **57**, 1557–1562 (2002).
16. Shah, T. N. & Ritchie, S. M. C. Esterification catalysis using functionalized membranes. *Appl. Catal. A Gen.* **296**, 12–20 (2005).

17. Aransiola, E. F., Ojumu, T. V., Oyekola, O. O., Madzimbamuto, T. F. & Ikhu-Omoregbe, D. I. O. A review of current technology for biodiesel production: State of the art. *Biomass and Bioenergy* **61**, 276–297 (2014).
18. Steinigeweg, S. & Gmehling, J. Transesterification processes by combination of reactive distillation and pervaporation. *Chem. Eng. Process. Process Intensif.* **43**, 447–456 (2004).
19. Luis, P., Degreève, J. & der Bruggen, B. Van. Separation of methanol-n-butyl acetate mixtures by pervaporation: Potential of 10 commercial membranes. *J. Memb. Sci.* **429**, 1–12 (2013).
20. Diaz, P. A. B., Kronemberger, F. de A. & Habert, A. C. A pervaporation-assisted bioreactor to enhance efficiency in the synthesis of a novel biolubricant based on the enzymatic transesterification of a castor oil based biodiesel. *Fuel* **204**, 98–105 (2017).
21. Harvianto, G. R., Ahmad, F. & Lee, M. A hybrid reactive distillation process with high selectivity pervaporation for butyl acetate production via transesterification. *J. Memb. Sci.* **543**, 49–57 (2017).
22. Meher, L. C., Vidya Sagar, D. & Naik, S. N. Technical aspects of biodiesel production by transesterification - A review. *Renew. Sustain. Energy Rev.* **10**, 248–268 (2006).
23. Abbaszaadeh, A., Ghobadian, B., Omidkhah, M. R. & Najafi, G. Current biodiesel production technologies : A comparative review. *Energy Convers. Manag.* **63**, 138–148 (2012).
24. Gargano, I. *et al.* Alkaline direct transesterification of different species of *Stichococcus* for bio-oil production. *N. Biotechnol.* **33**, 797–806 (2016).
25. Parida, S., Sahu, D. K. & Misra, P. K. Optimization of transesterification process by the application of ultrasound energy coupled with diesel as cosolvent. *J. Energy Inst.* **90**, 556–562 (2017).
26. Sivakumar, P., Anbarasu, K. & Renganathan, S. Bio-diesel production by alkali catalyzed transesterification of dairy waste scum. *Fuel* **90**, 147–151 (2011).
27. Jiménez, L., Garvín, A. & Costa-López, J. The production of butyl acetate and methanol via reactive and extractive distillation I . Chemical equilibrium, kinetics, and mass transfer Issues. *Ind. Eng. Chem. Res.* **41**, 6663–6669 (2002).
28. Kumar, V. & Satyanarayana, M. Transesterification of ethyl acetate with methanol in a tubular reactor. *Ind. Eng. Chem. Process Des. Dev.* **10**, 289–293 (1971).
29. Van De Steene, E., De Clercq, J. & Thybaut, J. W. Adsorption and reaction in the transesterification of ethyl acetate with methanol on Lewatit K1221. *J. Mol. Catal. A Chem.* **359**, 57–68 (2012).
30. Dossin, T. F., Reyniers, M. F. & Marin, G. B. Kinetics of heterogeneously MgO-catalyzed transesterification. *Appl. Catal. B Environ.* **62**, 35–45 (2006).
31. Knapp, J. P. & Doherty, M. F. New pressure-swing-distillation process for separating homogeneous azeotropic mixtures. *Ind. Eng. Chem. Res.* **23**, 346–357 (1992).
32. Modla, G. Reactive pressure swing batch distillation by a new double column system. *Comput. Chem. Eng.* **35**, 2401–2410 (2011).
33. Lam, M. K., Lee, K. T. & Mohamed, A. R. Homogeneous, heterogeneous and enzymatic catalysis for transesterification of high free fatty acid oil (waste cooking oil) to biodiesel : A review. *Biotechnol. Adv.* **28**, 500–518 (2010).

34. Luo, X., Ge, X., Cui, S. & Li, Y. Value-added processing of crude glycerol into chemicals and polymers. *Bioresour. Technol.* **215**, 144–154 (2016).
35. Quispe, C. A. G., Coronado, C. J. R. & Carvalho, J. A. Glycerol: Production, consumption, prices, characterization and new trends in combustion. *Renew. Sustain. Energy Rev.* **27**, 475–493 (2013).
36. Coronado, C. R., Carvalho, J. A., Quispe, C. A. & Sotomonte, C. R. Ecological efficiency in glycerol combustion. *Appl. Therm. Eng. J.* **63**, 97–104 (2014).
37. Teng, W. K., Ngoh, G. C., Yusoff, R. & Aroua, M. K. A review on the performance of glycerol carbonate production via catalytic transesterification: Effects of influencing parameters. *Energy Convers. Manag.* **88**, 484–497 (2014).
38. Chai, S., Wang, H., Liang, Y. & Xu, B. Sustainable production of acrolein: investigation of solid acid – base catalysts for gas-phase dehydration of glycerol. *Green Chem.* **9**, 1130–1136 (2007).
39. Godard, N. *et al.* High-yield synthesis of ethyl lactate with mesoporous Tin Silicate catalysts prepared by an aerosol-assisted Sol–Gel process. *ChemCatChem.* **9**, 2211–2218 (2017).
40. Claude, S. Research of new outlets for glycerol – recent developments in France. *Fett/Lipid.* **101**, 101–104 (1999).
41. Jitrwung, R. & Yargeau, V. Biohydrogen and bioethanol production from biodiesel-based glycerol by enterobacter aerogenes in a continuous stir tank reactor. *Int. J. Mol. Sci.* **16**, 10650–10664 (2015).
42. He, Q. S., McNutt, J. & Yang, J. Utilization of the residual glycerol from biodiesel production for renewable energy generation. *Renew. Sustain. Energy Rev.* **71**, 63–76 (2017).
43. Tshibalonza, N. N. & Monbaliu, J.-C. M. Revisiting the deoxydehydration of glycerol towards allyl alcohol under continuous-flow conditions. *Green Chem.* **19**, 3006–3013 (2017).
44. Monbaliu, J. C. M. *et al.* Effective production of the biodiesel additive STBE by a continuous flow process. *Bioresour. Technol.* **102**, 9304–9307 (2011).
45. Sonnati, M. O., Amigoni, S., Darmanin, T. & Choulet, O. Glycerol carbonate as a versatile building block for tomorrow: synthesis, reactivity, properties and applications. *Green Chem.* **15**, 283–306 (2013).
46. Tin, G., Tat, K. & Teong, K. Recent development and economic analysis of glycerol-free processes via supercritical fluid transesterification for biodiesel production. *Renew. Sustain. Energy Rev.* **31**, 61–70 (2014).
47. Aresta, M., Dibenedetto, A. & Bitonto, L. Di. New efficient and recyclable catalysts for the synthesis of di- and tri-glycerol carbonates. *RSC Adv.* **5**, 64433–64443 (2015).
48. Terence, W. T., Patti, A., Gates, W., Shaheen, U. & Sanjitha, K. Formation of glycerol carbonate from glycerol and urea catalysed by metal monoglycerolates. *Green Chem.* **15**, 1925–1931 (2013).
49. Vieville, C., Yoo, J. W., Pelet, S. & Mouloungui, Z. Synthesis of glycerol carbonate by direct carbonation of glycerol in supercritical CO₂ in the presence of zeolites and ion exchange resins. *Catal. Lett.* **60**, 245–247 (1998).
50. Cho, H., Kwon, H., Tharun, J. & Park, D. Synthesis of glycerol carbonate from ethylene carbonate and glycerol using immobilized ionic liquid catalysts. *J. Ind. Eng. Chem.* **16**, 679–683 (2010).

51. Esteban, J., Domínguez, E., Ladero, M. & Garcia-ochoa, F. Kinetics of the production of glycerol carbonate by transesterification of glycerol with dimethyl and ethylene carbonate using potassium methoxide, a highly active catalyst. *Fuel Process. Technol.* **138**, 243–251 (2015).
52. José R. Ochoa-Gómez; Olga Gómez-Jiménez-Aberasturi *et al.* Synthesis of glycerol carbonate from glycerol and dimethyl carbonate by transesterification: Catalyst screening and reaction optimization. *Appl. Catal. A Gen.* **366**, 315–324 (2009).
53. Ramesh, S. & Debecker, D. P. Room temperature synthesis of glycerol carbonate catalyzed by spray dried sodium aluminate microspheres. *Catal. Commun.* **97**, 102–105 (2017).
54. Ilham, Z. & Saka, S. Esterification of glycerol from biodiesel production to glycerol carbonate in non-catalytic supercritical dimethyl carbonate. *Springerplus* **5**, 923 (2016).
55. Stefanus, F. *et al.* CaO-catalyzed synthesis of glycerol carbonate from glycerol and dimethyl carbonate: Isolation and characterization of an active Ca species. *Applied Catal. A, Gen.* **401**, 220–225 (2011).
56. Okoye, P. U., Abdullah, A. Z. & Hameed, B. H. Glycerol carbonate synthesis from glycerol and dimethyl carbonate using trisodium phosphate. *J. Taiwan Inst. Chem. Eng.* **68**, 51–58 (2016).
57. Hu, K., Wang, H., Liu, Y. & Yang, C. KNO₃/CaO as cost-effective heterogeneous catalyst for the synthesis of glycerol carbonate from glycerol and dimethyl carbonate. *J. Ind. Eng. Chem.* **28**, 334–343 (2015).
58. Malyaadri, M., Jagadeeswaraiiah, K., Prasad, P. S. S. & Lingaiah, N. Synthesis of glycerol carbonate by transesterification of glycerol with dimethyl carbonate over Mg/Al/Zr catalysts. *Applied Catal. A, Gen.* **401**, 153–157 (2011).
59. Stefanus, F. *et al.* Synthesis of glycerol carbonate from the transesterification of dimethyl carbonate with glycerol using DABCO and DABCO-anchored Merrifield resin. *Applied Catal. B, Environ.* **165**, 642–650 (2015).
60. Bai, R., Wang, S., Mei, F., Li, T. & Li, G. Synthesis of glycerol carbonate from glycerol and dimethyl carbonate catalyzed by KF modified hydroxyapatite. *J. Ind. Eng. Chem.* **17**, 777–781 (2011).
61. Pyo, S., Park, J. H., Chang, T. & Hatti-kaul, R. Dimethyl carbonate as a Green Chemical. *Curr. Opin. Green Sustain. Chem.* **5**, 61–66(2017).
62. Stoian, D., Bansode, A., Medina, F. & Urakawa, A. Catalysis under microscope: Unraveling the mechanism of catalyst de- and re-activation in the continuous dimethyl carbonate synthesis from CO₂ and methanol in the presence of a dehydrating agent. *Catal. Today* **283**, 2–10 (2017).
63. Li, A. *et al.* Synthesis of dimethyl carbonate from methanol and CO₂ over Fe – Zr mixed oxides. *Biochem. Pharmacol.* **19**, 33–39 (2017).
64. Li, J. & Wang, T. Coupling reaction and azeotropic distillation for the synthesis of glycerol carbonate from glycerol and dimethyl carbonate. *Chem. Eng. Process. Process Intensif.* **49**, 530–535 (2010).
65. Wang, H., Pang, L., Yang, C. & Liu, Y. Production of glycerol carbonate via reactive distillation and extractive distillation: An experimental study. *Chinese J. Chem. Eng.* **23**, 1469–1474 (2015).
66. Aptel, P., Challard, N., Cuny, J. & Neel, J. Application of the pervaporation process to separate azeotropic mixtures. *J. Memb. Sci.* **1**, 271–287 (1976).

67. Feng, X. & Huang, R. Y. M. Liquid separation by membrane pervaporation: a review. *Ind. Eng. Chem. Res.* **36**, 1048–1066 (1997).
68. Wijmans, J. G. & Baker, R. W. The solution-diffusion model: a review. *J. Memb. Sci.* **107**, 1–21 (1995).
69. Ren, J. & Jiang, C. The coupling effect of the thermodynamic swelling process in pervaporation. *J. Memb. Sci.* **140**, 221–233 (1998).
70. Baker, R. W., Wijmans, J. G. & Huang, Y. Permeability, permeance and selectivity: A preferred way of reporting pervaporation performance data. *J. Memb. Sci.* **348**, 346–352 (2010).
71. Binning, R. C., Lee, R. J., Jennings, J. F. & Martin, E. C. Separation of liquid mixtures by permeation. *Ind. Eng. Chem.* **53**, 45–50 (1961).
72. Kedem, O. The role of coupling in pervaporation. *J. Memb. Sci.* **47**, 277–284 (1989).
73. Mulder, M. H. V., Franken, T. & Smolders, C. A. Preferential sorption versus preferential permeability in pervaporation. *J. Memb. Sci.* **22**, 155–173 (1985).
74. Uragami, T. *et al.* Pervaporation characteristics in removal of benzene from water through Polystyrene-Poly (Dimethylsiloxane) IPN membranes. *Mater. Sci. Appl.* **02**, 169–179 (2011).
75. Mulder, M. H. V., Kruit, F. & Smolders, C. A. Separation of isomeric xylenes by pervaporation through cellulose ester membranes. *J. Memb. Sci.* **11**, 349–363 (1982).
76. Shaban, I. Separation of binary, ternary and multicomponent organic/water mixtures. *Gas Sep. Purif.* **9**, 75–79 (1995).
77. Mulder, M. H. V., Franken, T. & Smolders, C. A. Preferential sorption versus preferential permeability in pervaporation. *J. Memb. Sci.* **22**, 155–173 (1985).
78. Shelden, R. A. & Thompson, E. V. Dependence of diffusive permeation rates and selectivities on upstream and downstream pressures IV. computer simulation of nonideal systems. *J. Memb. Sci.* **19**, 39–49 (1984).
79. Karlsson, H. O. E. & Tragardh, G. Aroma compound recovery with pervaporation - the effect of high ethanol concentrations. *J. Memb. Sci.* **91**, 189–198 (1994).
80. She, M. & Hwang, S. Effects of concentration, temperature, and coupling on pervaporation of dilute flavor organics. *J. Memb. Sci.* **271**, 16–28 (2006).
81. Raisi, A. & Aroujalian, A. Aroma compound recovery by hydrophobic pervaporation: The effect of membrane thickness and coupling phenomena. *Sep. Purif. Technol.* **82**, 53–62 (2011).
82. Luis, P. & Van Der Bruggen, B. The driving force as key element to evaluate the pervaporation performance of multicomponent mixtures. *Sep. Purif. Technol.* **148**, 94–102 (2015).
83. Hansen, C. M. 50 Years with solubility parameters — past and future. *Prog. Org. Coat.* **51**, 77–84 (2004).
84. Hansen, C. M. Hansen Solubility Parameters - A User's Handbook. (CRC Press, 2007).
85. Barton, A. F. M. Solubility Parameters. *Chem. Rev.* **75**, 731–753 (1975).
86. Li, W. & Luis, P. Understanding coupling effects in pervaporation of multi-component mixtures. *Sep. Purif. Technol.* **197**, 95–106 (2018).

87. Foroutan, M. & Khomami, M. H. Quaternary (liquid+liquid) equilibria of aqueous two-phase poly(ethylene glycol), poly (DMAM–TBAM), and KH_2PO_4 : Experimental and generalized Flory – Huggins theory. *J. Chem. Thermodyn.* **41**, 604–609 (2009).
88. Dolan, D. A., Sherman, D. A., Atkin, R. & Warr, G. G. Kamlet–Taft Solvation Parameters of Solvate Ionic Liquids. *ChemPhysChem* **17**, 3096–3101 (2016).
89. Klopffer, M. H. & Flaconnèche, B. Transport Properties of Gases in Polymers: Bibliographic Review. *Oil gas sci. technol.* **56**, 223–244 (2001).
90. Jyoti, G., Keshav, A. & Anandkumar, J. Review on pervaporation: theory, membrane performance and application to intensification of esterification reaction. *J. Eng.* **2015**, 24 (2015).
91. Aminabhavi, M. & Phayde, H. T. S. Sorption/diffusion of aliphatic esters into tetrafluoroethylene/propylene copolymeric membranes in the temperature interval from 25 to 70 °C. *Eur. Polym. J.* **32**, 1117–1126 (1996).
92. Overington, A. R., Wong, M., John, A. & Ferreira, L. B. Estimation of mass transfer rates through hydrophobic pervaporation membranes. *Sep. Sci. Technol.* **44**, 787–816 (2009).
93. Lu, Y., Nakicenovic, N., Visbeck, M. & Stevance, A.-S. Five priorities for the UN Sustainable Development Goals. *Nature* **520**, 432–433 (2015).
94. Abbasi, T., Premalatha, M. & Abbasi, S. A. The return to renewables: Will it help in global warming control? *Renew. Sustain. Energy Rev.* **15**, 891–894 (2011).
95. Louwen, A., van Sark, W. G. J. H. M., Faaij, A. P. C. & Schropp, R. E. I. Re-assessment of net energy production and greenhouse gas emissions avoidance after 40 years of photovoltaics development. *Nat. Commun.* **7**, 13728 (2016).
96. Patel, M. *et al.* Carbon dioxide emissions from non-energy use of fossil fuels: Summary of key issues and conclusions from the country analyses. *Resour. Conserv. Recycl.* **45**, 195–209 (2005).
97. Shen, L., Haufe, J., Patel, M. K. & Science, G. Product overview and market projection of emerging bio-based plastics. *s.l. Utrechr Univ.* (2009).
98. Edenhofer, O. *et al.* IPCC, 2011: Summary for Policymakers. In: IPCC Special Report on Renewable Energy Sources and Climate Change Mitigation. *Cambridge University Press* (2011). doi:10.5860/CHOICE.49-6309
99. Raschka, A. & Carus, M. Industrial material use of biomass Basic data for Germany, Europe and the world Industrial material use of biomass Basic data for Germany, Europe and the world. *First part Rep. R&D Proj. “Environmental Innov. Policy more Effic. Resour. use Clim. Prot. through Sustain. Mater. use biomass”*, Ger. nova-Institute GmbH 28 (2012).
100. Vassilev, S. V & Vassileva, C. G. A new approach for the combined chemical and mineral classification of the inorganic matter in coal 1. Chemical and mineral classification systems. *Fuel* **88**, 235–245 (2009).
101. B. Jonathan Moncada , M. Valentina Aristizábal , C. Carlos A. Design strategies for sustainable biorefineries. *Biochem. Eng. J.* **116**, 122–134 (2016).
102. Cherubini, F. The biorefinery concept: Using biomass instead of oil for producing energy and chemicals. *Energy Convers. Manag.* **51**, 1412–1421 (2010).
103. Mulder, M. Membrane Processes in Separation and Purification. Springer 445–475 (1994).

104. Shao, P. & Huang, R. Y. M. Polymeric membrane pervaporation. *J. Memb. Sci.* **287**, 162–179 (2007).
105. Abels, C., Carstensen, F. & Wessling, M. Membrane processes in biorefinery applications. *J. Memb. Sci.* **444**, 285–317 (2013).
106. Vane, L. M. A review of pervaporation for product recovery from biomass fermentation processes. *J. Chem. Technol. Biotechnol.* **80**, 603–629 (2005).
107. Okada, T. & Matsuura, T. A new transport model for pervaporation. *J. Memb. Sci.* **59**, 133–150 (1991).
108. H. K. Lonsdale. The growth of membrane technology. *J. Memb. Sci.* **10**, 81–181 (1982).
109. Mulder, M. H. V. & Smolders, C. A. On the mechanism of separation of ethanol/water mixtures by pervaporation I. Calculations of concentration profiles. *J. Memb. Sci.* **17**, 289–307 (1984).
110. Greenlaw, F. W., Prince, W. D., Shelden, R. a. & Thompson, E. V. Dependence of diffusive permeation rates by upstream and downstream pressures II. Two component permeant. *J. Memb. Sci.* **2**, 333–346 (1977).
111. Gugliuzza, A. Membrane Swelling. in *Encyclopedia of Membranes* (eds. Drioli, E. & Giorno, L.) 1–2 Springer Berlin Heidelberg, 2015. doi:10.1007/978-3-642-40872-4_720-6
112. Liu, G. *et al.* Pervaporation performance comparison of hybrid membranes filled with two-dimensional ZIF-L nanosheets and zero-dimensional ZIF-8 nanoparticles. *J. Memb. Sci.* **523**, 185–196 (2017).
113. Zhao, J. *et al.* Fabrication of ultrathin membrane via layer-by-layer self-assembly driven by hydrophobic interaction towards high separation performance. *ACS Appl. Mater. Interfaces* **5**, 13275–13283 (2013).
114. Immergut, E. H. & Mark, H. F. Principles of Plasticization. in *Plasticization and Plasticizer Processes*. ACS Publications 1–26 (1965). doi:10.1021/ba-1965-0048.ch001
115. Yeom, C. K. & Lee, K. H. Pervaporation separation of water-acetic acid mixtures through poly(vinyl alcohol) membranes crosslinked with glutaraldehyde. *J. Memb. Sci.* **109**, 257–265 (1996).
116. Cao, S., Shi, Y. & Chen, G. Permeation behaviour in cellulose triacetate dense membrane during pervaporation separation of methanol/methyl tert- butyl ether mixture. *Polym. Int.* **215**, 209–215 (2000).
117. Franklin, P. M., Koshland, C. P., Lucas, D. & Sawyer, R. F. Evaluation of combustion by-products of MTBE as a component of reformulated gasoline. *Chemosphere* **42**, 861–872 (2001).
118. Qiao, X. & Chung, T. S. Fundamental characteristics of sorption, swelling, and permeation of P84 Co-polyimide membranes for pervaporation dehydration of alcohols. *Ind. Eng. Chem. Res.* **44**, 8938–8943 (2005).
119. Touchal, S., Roizard, D. & Perrin, L. Pervaporation properties of polypyrrolidinone-based membranes for EtOH/ETBE mixtures separation. *J. Appl. Polym. Sci.* **99**, 3622–3630 (2006).
120. Guo, Z. & Hu, C. Pervaporation of organic liquid/water mixtures through a novel silicone copolymer membrane. *Chinese Sci. Bull.* **43**, 487–490 (1998).

121. Mangaraj, D., Patra, S., Rashid, S. Cohesive energy densities of high polymers Part II. Cohesive energy densities of Polyacrylates and Polymethacrylates from swelling measurements. *Macromol. Chem. Phys.* **65**, 39–46 (1963).
122. Yamaguchi, T., Nakao, S. & Kimura, S. Solubility and pervaporation properties of the filling-polymerized membrane prepared by plasma-graft polymerization for pervaporation of organic-liquid mixtures. *Ind. Eng. Chem. Res.* **31**, 1914–1919 (1992).
123. Deng, W., Wang, Y. & Yan, N. Production of organic acids from biomass resources. *Curr. Opin. Green Sustain. Chem.* **2**, 54–58 (2016).
124. De Clercq, R. *et al.* Titania-Silica catalysts for lactide production from renewable alkyl lactates: structure-activity relations. *ACS Catal.* (2018). doi:10.1021/acscatal.8b02216
125. Baudot, A. & Marin, M. Pervaporation of aroma compounds: comparison of membrane performances with vapour-liquid equilibria and engineering aspects of process improvement restored. *Food Bioprod. Process.* **75**, 117–142 (1997).
126. Lipnizki, F., Hausmanns, S. & Field, R. W. Influence of impermeable components on the permeation of aqueous 1-propanol mixtures in hydrophobic pervaporation. *J. Memb. Sci.* **228**, 129–138 (2004).
127. Overington, A. R., Wong, M. & Harrison, J. A. Effect of feed pH and non-volatile dairy components on flavour concentration by pervaporation. *J. Food Eng.* **107**, 60–70 (2011).
128. Matsuda, H. *et al.* Preparation of silicalite pervaporation membrane with ethanol permselectivity by a 2-step hydrothermal synthesis. *Sep. Sci. Technol.* **36**, 3305–3310 (2001).
129. Ikegami, T. *et al.* Stabilization of bioethanol recovery with silicone rubber-coated ethanol-permselective silicalite membranes by controlling the pH of acidic feed solution. *J. Chem. Technol. Biotechnol.* **80**, 381–387 (2005).
130. Zhang, S. *et al.* Pervaporation dehydration of binary and ternary mixtures of n-butyl acetate , n-butanol and water using PVA-CS blended membranes. *Sep. Purif. Technol.* **173**, 314–322 (2017).
131. Adymkanov, S. V. *et al.* Pervaporation of alcohols through highly permeable PIM-1 polymer films. *Polym. Sci. Ser. A* **50**, 444–450 (2008).
132. Pulyalina, A. Y. *et al.* Ethanol purification from methanol via pervaporation using polybenzoxazineimide membrane. *Fuel Process. Technol.* **139**, 178–185 (2015).
133. Ma, J. *et al.* Intensifying esterification reaction between lactic acid and ethanol by pervaporation dehydration using chitosan – TEOS hybrid membranes. *Chem. Eng. J.* **155**, 800–809 (2009).
134. Brun, J. P., Bulvestre, G., Kergreis, A. & Guillou, M. Hydrocarbons separation with polymer membranes. I. Butadiene-isobutene separation with nitrile rubber membranes. *J. Appl. Polym. Sci.* **18**, 1663–1683 (1974).
135. Kruger, J. S., Dong, T., Beckham, G. T. & Biddy, M. J. Integrated conversion of 1-butanol to 1,3-butadiene. *RCS Adv.* **8**, 24068–24074 (2018).
136. Vidra, A. & Németh, Á. Bio-produced Acetic Acid: A Review. *Period. Polytech. Chem. Eng.* **62**, 245–256 (2018).

137. Koops, G. H., Nolten, J. A. M., Mulder, M. H. V. & Smolders, C. A. Selectivity as a function of membrane thickness: Gas separation and pervaporation. *J. Appl. Polym. Sci.* **53**, 1639–1651 (1994).
138. Qunhui, G., Ohya, H. & Negishi, Y. Investigation of the permselectivity of chitosan membrane used in pervaporation separation II. Influences of temperature and membrane thickness. *J. Memb. Sci.* **98**, 223–232 (1995).
139. Passaglia, E. Crazes and Fracture. *J. Phys. Chem. Solids* **48**, 1075–1100 (1987).
140. Ray, S. K., Sawant, S. B., Joshi, J. B. & Pangarkar, V. G. Dehydration of acetic acid by pervaporation. *J. Memb. Sci.* **138**, 1–17 (1998).
141. Kanti, P., Srigowri, K., Madhuri, J., Smitha, B. & Sridhar, S. Dehydration of ethanol through blend membranes of chitosan and sodium alginate by pervaporation. *Sep. Purif. Technol.* **40**, 259–266 (2004).
142. Sridhar, S., Srinivasan, T., Virendra, U. & Khan, A. A. Pervaporation of ketazine aqueous layer in production of hydrazine hydrate by peroxide process. *Chem. Eng. J.* **94**, 51–56 (2003).
143. Villaluenga, J. P. G., Khayet, M., Godino, P., Seoane, B. & Mengual, J. I. Analysis of the membrane thickness effect on the pervaporation separation of methanol/methyl tertiary butyl ether mixtures. *Sep. Purif. Technol.* **47**, 80–87 (2005).
144. Schaetzel, P., Vauclair, C., Luo, G. & Nguyen, Q. T. The solution – diffusion model order of magnitude calculation of coupling between the fluxes in pervaporation. *J. Memb. Sci.* **191**, 103–108 (2001).
145. Longo, M. A. & Sanromán, M. A. Production of food aroma compounds: microbial and enzymatic methodologies. *Food Technol. Biotechnol.* **3**, 335–353 (2006).
146. Raisi, A., Aroujalian, A. & Kaghazchi, T. A predictive mass transfer model for aroma compounds recovery by pervaporation. *J. Food Eng.* **95**, 305–312 (2009).
147. Mafi, A., Raisi, A., Hatam, M. & Aroujalian, A. A comparative study on the free volume theories for diffusivity through polymeric membrane in pervaporation process. *J. Appl. Polym. Sci.* **131**, 1–12 (2014).
148. Nagel, C. *et al.* Free volume distributions in glassy polymer membranes: comparison between molecular modeling and experiments. *Macromolecules* **33**, 2242–2248 (2000).
149. Fritsch, D., Strunskus, T. & Faupel, F. Free volume and transport properties in highly selective polymer membranes. *Macromolecules* **35**, 2071–2077 (2002).
150. Hodge, R. M., Bastow, T. J., Edward, G. H., Simon, G. P. & Hill, A. J. Free volume and the mechanism of plasticization in water-swollen poly(vinyl alcohol). *Macromolecules* **29**, 8137–8143 (1996).
151. Petzetakis, N. *et al.* Membranes with artificial free-volume for biofuel production. *Nat Commun* **6**, 7529 (2015).
152. Shi, G. M., Chen, H., Jean, Y. C. & Chung, T. S. Sorption, swelling, and free volume of polybenzimidazole (PBI) and PBI/zeolitic imidazolate framework (ZIF-8) nano-composite membranes for pervaporation. *Polym. (United Kingdom)* **54**, 774–783 (2013).
153. Li, C. L. *et al.* Study on the influence of the free volume of hybrid membrane on pervaporation performance by positron annihilation spectroscopy. *J. Memb. Sci.* **313**, 68–74 (2008).

154. Satyanarayana, S. V., Subrahmanyam, V. S., Verma, H. C., Sharma, A. & Bhattacharya, P. K. Application of positron annihilation: Study of pervaporation dense membranes. *Polymer (Guildf)*. **47**, 1300–1307 (2006).
155. Robeson, L. M. Correlation of separation factor versus permeability for polymeric membranes. *J. Memb. Sci.* **62**, 165–185 (1991).
156. Merkel, T. C. *et al.* Ultrapervaporation, reverse-selective nanocomposite membranes. *Science* **296**, 519–522 (2002).
157. Huang, Z., Guan, H. M., Tan, W. L., Qiao, X. Y. & Kulprathipanja, S. Pervaporation study of aqueous ethanol solution through zeolite-incorporated multilayer poly(vinyl alcohol) membranes: Effect of zeolites. *J. Memb. Sci.* **276**, 260–271 (2006).
158. Ting, S. S. T., Tomasko, D. L., Foster, N. R. & Macnaughton, S. J. Solubility of naproxen in supercritical carbon dioxide with and without cosolvents. *Ind. Eng. Chem.* **32**, 1471–1481 (1993).
159. Finneran, I. A., Carroll, P. B., Allodi, M. A. & Blake, G. A. Hydrogen bonding in the ethanol-water dimer. *Phys. Chem. Chem. Phys.* **17**, 24210–24214 (2015).
160. Sommer, S. & Melin, T. Performance evaluation of microporous inorganic membranes in the dehydration of industrial solvents. *Chem. Eng. Process. Process Intensif.* **44**, 1138–1156 (2005).
161. Ten Elshof, J. E., Abadal, C. R., Sekulić, J., Chowdhury, S. R. & Blank, D. H. A. Transport mechanisms of water and organic solvents through microporous silica in the pervaporation of binary liquids. *Microporous Mesoporous Mater.* **65**, 197–208 (2003).
162. Koops, G. H., Nolten, J. A. M., Mulder, M. H. V. & Smolders, C. A. Selectivity as a function of membrane thickness: Gas separation and pervaporation. *J. Appl. Polym. Sci.* **53**, 1639–1651 (1994).
163. Carbone-Lorraine L. Industrial Applications of Pervaporation. In: Turner M.K. (eds) *Effective Industrial Membrane Processes: Benefits and Opportunities*. 281–293 (Springer, Dordrecht, 1991). doi:10.1007/978-94-011-3682-2
164. Wang, Y., Shung, T. & Gruender, M. Sulfonated polybenzimidazole membranes for pervaporation dehydration of acetic acid. *J. Memb. Sci.* **415–416**, 486–495 (2012).
165. Brinker, C. J. & Scherer, G. W. *Sol-gel science: the physics and chemistry of sol-gel processing*. Acad. Press (1990).
166. Tsuru, T., Wada, S. I., Izumi, S. & Asaeda, M. Silica-zirconia membranes for nanofiltration. *J. Memb. Sci.* **149**, 127–135 (1998).
167. Asaeda, M., Yang, J. & Sakou, Y. Porous Silica-Zirconia (50%) membranes for pervaporation of iso-propyl Alcohol (IPA)/water mixtures. *J. Chem. Eng. Japan* **35**, 365–371 (2002).
168. Wang, J., Kanezashi, M., Yoshioka, T. & Tsuru, T. Effect of calcination temperature on the PV dehydration performance of alcohol aqueous solutions through BTESE-derived silica membranes. *J. Memb. Sci.* **415–416**, 810–815 (2012).
169. Asaeda, M., Ishida, M. & Waki, T. Pervaporation of aqueous organic acid solutions by porous ceramic membranes. *J. Chem. Eng. Japan* **38**, 336–343 (2005).
170. Kitao, S. & Asaeda, M. Separation of organic acid/water mixtures by thin porous silica membrane. *J. Chem. Eng. JPN.* **23**, 367–370 (1990).

171. Tsuru, T., Sasaki, A., Kanezashi, M. & Yoshioka, T. Pervaporation of methanol/dimethyl carbonate using SiO₂ membranes with nano-tuned pore sizes and surface chemistry. *AIChE J.* **57**, 2079–2089 (2011).
172. Nunes, S. P. & Peinemann, K.-V. Membrane technology in the chemical industry. *WILEY-VCH* (2006).
173. Hasegawa, Y., Nagase, T., Kiyozumi, Y., Hanaoka, T. & Mizukami, F. Influence of acid on the permeation properties of NaA-type zeolite membranes. *J. Memb. Sci.* **349**, 189–194 (2010).
174. Zhu, M. H., Kumakiri, I., Tanaka, K. & Kita, H. Dehydration of acetic acid and esterification product by acid-stable ZSM-5 membrane. *Microporous Mesoporous Mater.* **181**, 47–53 (2013).
175. Huang, R., Chen, G., Sun, M. & Gao, C. Preparation and characterization of quaterinized chitosan/poly(acrylonitrile) composite nanofiltration membrane from anhydride mixture cross-linking. *Sep. Purif. Technol.* **58**, 393–399 (2008).
176. Jin, H. *et al.* Conversion of xylose into furfural in a MOF-based mixed matrix membrane reactor. *Chem. Eng. J.* **305**, 12–18 (2016).
177. Liu, X. *et al.* Metal – organic framework ZIF-8 nanocomposite membrane for efficient recovery of furfural via pervaporation and vapor permeation. *J. Memb. Sci.* **428**, 498–506 (2013).
178. Blume, I., Wijmans, J. G. & Baker, R. W. The separation of dissolved organics from water by pervaporation. *J. Memb. Sci.* **49**, 253–286 (1990).
179. Hu, X.-D., Jenkins, S. E., Min, B. G., Polk, M. B. & Kumar, S. Rigid-rod polymers: Synthesis, Processing, Simulation, Structure, and Properties. *Macromol. Mater. Eng.* **288**, 823–843 (2003).
180. Tullos, G. L., Powers, J. M., Jeskey, S. J. & Mathias, L. J. Thermal conversion of hydroxy-containing imides to benzoxazoles: polymer and model compound study. *Macromolecules* **32**, 3598–3612 (1999).
181. Tullos, G. L. & Mathias, L. J. Unexpected thermal conversion of hydroxy-containing polyimides to polybenzoxazoles. *Polymer (Guildf)*. **40**, 3463–3468 (1999).
182. Jullok, N., Luis, P., Degreve, J. & Van der Bruggen, B. A cascaded pervaporation process for dehydration of acetic acid. *Chem. Eng. Sci.* **105**, 208–212 (2014).
183. Zhu, M. H., Kumakiri, I., Tanaka, K. & Kita, H. Dehydration of acetic acid and esterification product by acid-stable ZSM-5 membrane. *Microporous Mesoporous Mater.* **181**, 47–53 (2013).
184. Jullok, N. *et al.* Effect of silica nanoparticles in mixed matrix membranes for pervaporation dehydration of acetic acid aqueous solution: Plant-inspired dewatering systems. *J. Clean. Prod.* **112**, 4879–4889 (2016).
185. Chen, J. H. *et al.* Pervaporation dehydration of acetic acid using polyelectrolytes complex (PEC)/ 11-phosphotungstic acid hydrate (PW 11) hybrid membrane. *J. Memb. Sci.* **429**, 206–213 (2013).
186. Zhang, W., Xu, Y., Yu, Z., Lu, S. & Wang, X. Separation of acetic acid/water mixtures by pervaporation with composite membranes of sodium alginate active layer and microporous polypropylene substrate. *J. Memb. Sci.* **451**, 135–147 (2014).
187. Sanoa, T., Ejiri, S., Yamada, K. & Kawakami, Y. Separation of acetic acid-water mixtures by pervaporation through silicalite membrane. *J. Memb. Sci.* **123**, 225–233 (1997).

188. Xu, Y. M., Le, N. L., Zuo, J. & Chung, T. S. Aromatic polyimide and crosslinked thermally rearranged poly(benzoxazole-co-imide) membranes for isopropanol dehydration via pervaporation. *J. Memb. Sci.* **499**, 317–325 (2016).
189. Hassan Hassan Abdellatif, F. *et al.* Bio-based membranes for ethyl tert-butyl ether (ETBE) bio-fuel purification by pervaporation. *J. Memb. Sci.* **524**, 449–459 (2017).
190. Jin, H. *et al.* Conversion of xylose into furfural in a MOF-based mixed matrix membrane reactor. *Chem. Eng. J.* **305**, 12–18 (2016).
191. Ghosh, U. K., Pradhan, N. C. & Adhikari, B. Separation of furfural from aqueous solution by pervaporation using HTPB-based hydrophobic polyurethaneurea membranes. *Desalination* **208**, 146–158 (2007).
192. Smitha, B., Dhanuja, G. & Sridhar, S. Dehydration of 1,4-dioxane by pervaporation using modified blend membranes of chitosan and nylon 66. *Carbohydr. Polym.* **66**, 463–472 (2006).
193. Ray, S. & Ray, S. K. Dehydration of tetrahydrofuran (THF) by pervaporation using crosslinked copolymer membranes. *Chem. Eng. Process. Process Intensif.* **47**, 1620–1630 (2008).
194. Chandane, V. S., Rathod, A. P. & Wasewar, K. L. Enhancement of esterification conversion using pervaporation membrane reactor. *Resour. Technol.* **2**, S47–S52 (2016).
195. Delgado, P., Sanz, M. T., Beltrán, S. & Alberto, L. Ethyl lactate production via esterification of lactic acid with ethanol combined with pervaporation. *Chem. Eng. J.* **165**, 693–700 (2010).
196. Ma, J. *et al.* Intensifying esterification reaction between lactic acid and ethanol by pervaporation dehydration using chitosan – TEOS hybrid membranes. *Chem. Eng. J.* **155**, 800–809 (2009).
197. Zhang, W. *et al.* Mixed matrix membranes incorporated with polydopamine-coated metal-organic framework for dehydration of ethylene glycol by pervaporation. *J. Memb. Sci.* **527**, 8–17 (2017).
198. Guo, R., Ma, X., Hu, C. & Jiang, Z. Novel PVA e silica nanocomposite membrane for pervaporative dehydration of ethylene glycol aqueous solution. *Polymer* **48**, 2939–2945 (2007).
199. Hu, C., Li, B., Guo, R., Wu, H. & Jiang, Z. Pervaporation performance of chitosan – poly (acrylic acid) polyelectrolyte complex membranes for dehydration of ethylene glycol aqueous solution. *Sep. Purif. Technol.* **55**, 327–334 (2007).
200. Sun, D., Yang, P., Sun, H. & Li, B. Preparation and characterization of cross-linked poly (vinyl alcohol)/hyperbranched polyester membrane for the pervaporation dehydration of ethylene glycol solution. *Eur. Polym. J.* **62**, 155–166 (2015).
201. Wu, D. *et al.* Thin film composite membranes comprising of polyamide and polydopamine for dehydration of ethylene glycol by pervaporation. *J. Memb. Sci.* **493**, 622–635 (2015).
202. Falbo, F. *et al.* Organic/organic mixture separation by using novel ECTFE polymeric pervaporation membranes. *Polymer (Guildf)*. **98**, 110–117 (2016).
203. Cao, B., Hinode, H. & Kajiuchi, T. Permeation and separation of styrene/ethylbenzene mixtures through cross-linked poly (hexamethylene sebacate) membranes. **156**, 43–47 (1999).
204. Kanjilal, B., Noshadi, I., Mccutcheon, J. R., Asandei, A. D. & Parnas, R. S. Allylcyclohexylamine functionalized siloxane polymer and its phase separated blend as pervaporation membranes

- for 1, 3-propanediol enrichment from binary aqueous mixtures. *J. Memb. Sci.* **486**, 59–70 (2015).
205. Rajagopalan, N. & Cheryan, M. Pervaporation of grape juice aroma. *J. Memb. Sci.* **104**, 243–250 (1995).
206. Delgado, P., Sanz, M. T. & Beltrán, S. Pervaporation of the quaternary mixture present during the esterification of lactic acid with ethanol. *J. Memb. Sci.* **332**, 113–120 (2009).
207. Moulik, S., Nazia, S., Vani, B. & Sridhar, S. Pervaporation separation of acetic acid/water mixtures through sodium alginate/polyaniline polyion complex membrane. *Sep. Purif. Technol.* **170**, 30–39 (2016).
208. Benedict, D. J., Parulekar, S. J. & Tsai, S. Pervaporation-assisted esterification of lactic and succinic acids with downstream ester recovery. *J. Memb. Sci.* **281**, 435–445 (2006).
209. Unlu, D., Ilgen, O. & Hilmioglu, N. D. Reactive separation system for effective upgrade of levulinic acid into ethyl levulinate. *Chem. Eng. Res. Des.* **118**, 248–258 (2016).
210. Lue, S. J. & Liaw, T. Separation of xylene mixtures using polyurethane – zeolite composite membranes. *Desalination* **193**, 137–143 (2006).
211. Kahya, S., Kondolot, E. & Oya, S. Sodium alginate/poly(vinyl alcohol) alloy membranes for the pervaporation, vapour permeation and vapour permeation with temperature difference separation of dimethylformamide/water mixtures: A comparative study. *Vacuum* **84**, 1092–1102 (2010).
212. Brennecke, J. F. & Maginn, E. J. Ionic liquids: Innovative fluids for chemical processing. *AIChE J.* **47**, 2384–2389 (2001).
213. Karkhanechi, H., Salmani, S. & Asghari, M. A review on gas separation applications of supported ionic liquid membranes. *ChemBioEng Rev.* **2**, 290–302 (2015).
214. Althuluth, M. *et al.* Natural gas purification using supported ionic liquid membrane. *J. Memb. Sci.* **484**, 80–86 (2015).
215. Way, J. D. Chemical separations with liquid membranes. *J. Liq. Chromatogr. Relat. Technol.* **21**, 1073–1076 (1998).
216. Lozano, L. J. *et al.* Recent advances in supported ionic liquid membrane technology. *J. Memb. Sci.* **376**, 1–14 (2011).
217. Wang, J. *et al.* Recent development of ionic liquid membranes. *Green Energy Environ.* **1**, 43–61 (2016).
218. Hernández-Fernández, F. J. *et al.* A novel application of supported liquid membranes based on ionic liquids to the selective simultaneous separation of the substrates and products of a transesterification reaction. *J. Memb. Sci.* **293**, 73–80 (2007).
219. de los Ríos, A. P. *et al.* Prediction of the selectivity in the recovery of transesterification reaction products using supported liquid membranes based on ionic liquids. *J. Memb. Sci.* **307**, 225–232 (2008).
220. de los Ríos, A. P. *et al.* On the importance of the nature of the ionic liquids in the selective simultaneous separation of the substrates and products of a transesterification reaction through supported ionic liquid membranes. *J. Memb. Sci.* **307**, 233–238 (2008).
221. Hernández-Fernández, F. J., de los Ríos, A. P., Tomás-Alonso, F., Gómez, D. & Vllora, G. Improvement in the separation efficiency of transesterification reaction compounds by the

- use of supported ionic liquid membranes based on the dicyanamide anion. *Desalination* **244**, 122–129 (2009).
222. de los Ríos, A. P., Hernández-Fernández, F. J., Rubio, M., Gómez, D. & Villora, G. Highly selective transport of transesterification reaction compounds through supported liquid membranes containing ionic liquids based on the tetrafluoroborate anion. *Desalination* **250**, 101–104 (2010).
223. Hernández-Fernández, F. J. *et al.* Integrated reaction/separation processes for the kinetic resolution of rac-1-phenylethanol using supported liquid membranes based on ionic liquids. *Chem. Eng. Process. Process Intensif.* **46**, 818–824 (2007).
224. Françoisse, O. & Thyron, F. C. Kinetics and mechanism of ethyl tert-butyl ether liquid-phase synthesis. *Chem. Eng. Process.* **30**, 141–149 (1991).
225. Ortiz, I., Alonso, P. & Urtiaga, A. Pervaporation of azeotropic mixtures ethanol/ethyl tert-butyl ether: Influence of membrane conditioning and operation variables on pervaporation flux. *Desalination* **149**, 67–72 (2002).
226. Norkobilov, A., Gorri, D. & Ortiz, I. Comparative study of conventional, reactive-distillation and pervaporation integrated hybrid process for ethyl tert-butyl ether production. *Chem. Eng. Process. Process Intensif.* **122**, 434–446 (2017).
227. Harvianto, G. R., Ahmad, F. & Lee, M. A thermally coupled reactive distillation and pervaporation hybrid process for n-butyl acetate production with enhanced energy efficiency. *Chem. Eng. Res. Des.* **124**, 98–113 (2017).
228. Figueroa Paredes, D. A. *et al.* Screening of pervaporation membranes for the separation of methanol-methyl acetate mixtures: An approach based on the conceptual design of the pervaporation-distillation hybrid process. *Sep. Purif. Technol.* **189**, 296–309 (2017).
229. Fontalvo, J. & Keurentjes, J. T. F. A hybrid distillation-pervaporation system in a single unit for breaking distillation boundaries in multicomponent mixtures. *Chem. Eng. Res. Des.* **99**, 158–164 (2015).
230. Cai, D. *et al.* Biobutanol from sweet sorghum bagasse hydrolysate by a hybrid pervaporation process. *Bioresour. Technol.* **145**, 97–102 (2013).
231. Ujor, V., Agu, C. V., Gopalan, V. & Ezeji, T. C. Allopurinol-mediated lignocellulose-derived microbial inhibitor tolerance by *Clostridium beijerinckii* during acetone–butanol–ethanol (ABE) fermentation. *Appl. Microbiol. Biotechnol.* **99**, 3729–3740 (2015).
232. Delgado, P., Sanz, M. T., Beltrán, S. & Alberto, L. Ethyl acetate production via esterification of lactic acid with ethanol combined with pervaporation. *Chem. Eng. J.* **165**, 693–700 (2010).
233. Assabumrungrat, S., Kiatkittipong, W., Praserttham, P. & Goto, S. Simulation of pervaporation membrane reactors for liquid phase synthesis of ethyl tert-butyl ether from tert-butyl alcohol and ethanol. *Catal. Today* **79–80**, 249–257 (2003).
234. Feng, X. & Huang, R. Y. M. Studies of a membrane reactor: Esterification facilitated by pervaporation. *Chem. Eng. Sci.* **51**, 4673–4679 (1996).
235. Domingues, L., Recasens, F. & Larrayoz, M. A. Studies of a pervaporation reactor: Kinetics and equilibrium shift in benzyl alcohol acetylation. *Chem. Eng. Sci.* **54**, 1461–1465 (1999).
236. Sanz, M. T. & Gmehling, J. Esterification of acetic acid with isopropanol coupled with pervaporation Part I: Kinetics and pervaporation studies. *Chem. Eng. J.* **123**, 1–8 (2006).

237. Ameri, E. & Moheb, A. Using PERVAP 2201 membrane in vapor permeation facilitated isopropyl propionate production through esterification reaction. *Iran. J. Chem. Eng.* **9**, 14-21 (2012).
238. Chandane, V. S., Rathod, A. P. & Wasewar, K. L. Coupling of in-situ pervaporation for the enhanced esterification of propionic acid with isobutyl alcohol over cenosphere based catalyst. *Chem. Eng. Process. Process Intensif.* **119**, 16–24 (2017).
239. Rathod, A. P., Wasewar, K. L. & Sonawane, S. S. Enhancement of esterification reaction by pervaporation reactor: An intensifying approach. *Procedia Eng.* **51**, 330–334 (2013).
240. Sanz, M. T. & Gmehling, J. Esterification of acetic acid with isopropanol coupled with pervaporation. Part II. Study of a pervaporation reactor. *Chem. Eng. J.* **123**, 9–14 (2006).
241. Kim, K.-J., Lee, S.-B. & Han, N.-W. Effect of the degree of crosslinking on properties of poly(vinyl alcohol) membranes. *Polym. J.* **25**, 1295–1302 (1993).
242. Rudra, R., Kumar, V. & Kundu, P. P. Acid catalysed cross-linking of poly vinyl alcohol (PVA) by glutaraldehyde: effect of crosslink density on the characteristics of PVA membranes used in single chambered microbial fuel cells. *RSC Adv.* **5**, 83436–83447 (2015).
243. Figueiredo, K. C. S., Alves, T. L. M. & Borges, C. P. Poly(vinyl alcohol) films crosslinked by glutaraldehyde under mild conditions. *J. Applied Polym. Sci.* **111**, 3074–3080 (2009).
244. Zereshti, S. *et al.* Pervaporation separation of MeOH/MTBE mixtures with modified PEEK membrane: Effect of operating conditions. *J. Memb. Sci.* **371**, 1–9 (2011).
245. Broens, L., Altena, F. W., Smolders, C. A. & Koenhen, D. M. Asymmetric membrane structures as a result of phase separation phenomena. *Desalination* **32**, 33–45 (1980).
246. Cornelissen, E. R., Van den Boomgaard, Th., & Strathmann, H. Physicochemical aspects of polymer selection for ultrafiltration and microfiltration membranes. *Colloids Surfaces A Physicochem. Eng. Asp.* **138**, 283–289 (1998).
247. Feng, X. & Huang, R. Y. M. Concentration polarization in pervaporation separation processes. *J. Memb. Sci.* **92**, 201–208 (1994).
248. Kuila, S. B. & Ray, S. K. Separation of isopropyl alcohol – water mixtures by pervaporation using copolymer membrane: Analysis of sorption and permeation. *Chem. Eng. Res. Des.* **91**, 377–388 (2012).
249. Vasenin, R. M. Kinetics of swelling of polymers. *Polym. Sci.* **6**, 624–629 (1964).
250. Mulder, M. Basic Principles of Membrane Technology. (Netherland: Kluwer academic publishers, 1996).
251. Soltane, H. Ben, Roizard, D. & Favre, E. Study of the rejection of various solutes in OSN by a composite polydimethylsiloxane membrane: Investigation of the role of solute affinity. *Sep. Purif. Technol.* **161**, 193–201 (2016).
252. Vasenin, R. M. Kinetics of swelling of polymers. *Polym. Sci. (USSR)* 624–629 (1964).
253. Baker, R. W., Wijmans, J. G. & Huang, Y. Permeability, permeance and selectivity: A preferred way of reporting pervaporation performance data. *J. Memb. Sci.* **348**, 346–352 (2010).
254. Okuno, H., Morimoto, K., Uragami, T., Chemistry, A. & Branch, C. Permselectivities of poly(vinyl chloride) membrane for binary alcohol mixtures in pervaporation. *Polym. Bull.* **28**, 683–687 (1992).

255. Fouad, E. A. & Feng, X. Pervaporative separation of n-butanol from dilute aqueous solutions using silicalite-filled poly(dimethyl siloxane) membranes. *J. Memb. Sci.* **339**, 120–125 (2009).
256. Gorri, D., Ibáñez, R. & Ortiz, I. Comparative study of the separation of methanol-methyl acetate mixtures by pervaporation and vapor permeation using a commercial membrane. *J. Memb. Sci.* **280**, 582–593 (2006).
257. Mandal, S. & Pangarkar, V. G. Separation of methanol – benzene and methanol – toluene mixtures by pervaporation: effects of thermodynamics and structural phenomenon. *J. Memb. Sci.* **201**, 175–190 (2002).
258. Marx, S., Gryp, P. Van Der, Neomagus, H., Everson, R. & Keizer, K. Pervaporation separation of methanol from methanol/tert-amyl methyl ether mixtures with a commercial membrane. *J. Memb. Sci.* **209**, 353–362 (2002).
259. Esteban, J., Ladero, M., Molinero, L. & García-ocha, F. Liquid – liquid equilibria for the ternary systems DMC – methanol – glycerol , DMC – glycerol carbonate – glycerol and the quaternary system DMC – methanol – glycerol carbonate – glycerol at catalytic reacting temperatures. *Chem. Eng. Res. Des.* **92**, 2797–2805 (2014).
260. Li, J. & Wang, T. Chemical equilibrium of glycerol carbonate synthesis from glycerol. *J. Chem. Thermodyn.* **43**, 731–736 (2011).
261. Fredenslund, A., Gmehling, J. & Rasmussen, P. Vapor-Liquid Equilibria using UNIFAC. A Group-Contribution Method. (Elsevier Scientific Pub. Co., New York, 1977).
262. Liu, J., Ma, Y., Hu, K., He, H. & Shao, G. Pervaporation separation of isopropanol/benzene mixtures using inorganic-organic hybrid membranes. *J. Appl. Polym. Sci.* **117**, 2464–2471 (2010).
263. George, S. C. & Thomas, S. Transport phenomena through polymeric systems. *Prog. Polym. Sci.* **26**, 985–1017 (2001).
264. Villaluenga, J. P. G., Khayet, M., Godino, P., Seoane, B. & Mengual, J. I. Pervaporation of Toluene/Alcohol Mixtures through a Coextruded Linear Low-Density Polyethylene Membrane. *Ind. Eng. Chem. Res.* **42**, 386–391 (2003).
265. Hansen, M. The universality of the solubility parameter. *Ind. Eng. Chem. Prod. Res. Dev.* **8**, 2–11 (1969).
266. Mulder, M. H. V, Kruit, F. & Smolders, C. A. Separation of isomeric xylenes by pervaporation through cellulose ester membranes. *J. Memb. Sci.* **11**, 349–363 (1982).
267. Belmares, M. *et al.* Hildebrand and hansen solubility parameters from molecular dynamics with applications to electronic nose polymer sensors. *J. Comput. Chem.* **25**, 1814–1826 (2004).
268. Garcia, O., Trigo, R. M., Blanco, M. D. & Teijón, J. M. Influence of degree of crosslinking on 5-fluorouracil release from poly(2-hydroxyethyl methacrylate) hydrogels. *Biomaterials* **15**, 689–694 (1994).
269. Welle, F. & Franz, R. Diffusion coefficients and activation energies of diffusion of low molecular weight migrants in Poly(ethylene terephthalate) bottles. *Polym. Test.* **31**, 93–101 (2012).
270. Stringer, J. L. & Peppas, N. A. Diffusion of small molecular weight drugs in radiation-crosslinked poly(ethylene oxide) hydrogels. *J. Control. Release* **42**, 195–202 (1996).

271. Gudeman, L. F. & Peppas, N. A. Preparation and characterization of pH-sensitive, interpenetrating networks of poly(vinyl alcohol) and poly(acrylic acid). *J. Appl. Polym. Sci.* **55**, 919–928 (1995).
272. Wang, S. *et al.* General Synthesis of glycerol carbonate from glycerol and dimethyl carbonate catalyzed by calcined silicates. *Appl. Catal. A, Gen.* **542**, 174–181 (2017).
273. Wei, H. *et al.* Design and control of dimethyl carbonate – methanol separation via pressure-swing distillation. *Ind. Eng. Chem. Res.* **52**, 11463–11478 (2013).
274. Hu, C. C. & Cheng, S. H. Development of alternative methanol/dimethyl carbonate separation systems by extractive distillation — A holistic approach. *Chem. Eng. Res. Des.* **127**, 189–214 (2017).
275. Wang, L., Li, J., Lin, Y. & Chen, C. Separation of dimethyl carbonate/methanol mixtures by pervaporation with poly (acrylic acid)/ poly (vinyl alcohol) blend membranes. *J. Memb. Sci.* **305**, 238–246 (2007).
276. Ono, Y. Dimethyl carbonate for environmentally benign reactions. *Catal. Today* **35**, 15–25 (1997).
277. Shiao, H. Ž. A., Chua, D., Lin, H., Slane, S. & Salomon, M. Low temperature electrolytes for Li-ion PVDF cells. *J. Power Sources* **87**, 167–173 (2000).
278. Pyo, S. H., Park, J. H., Chang, T. S. & Hatti-Kaul, R. Dimethyl carbonate as a green chemical. *Curr. Opin. Green Sustain. Chem.* **5**, 61–66 (2017).
279. Aresta, M. & Galatola, M. Life cycle analysis applied to the assessment of the environmental impact of alternative synthetic processes. The dimethylcarbonate case: part 1. *J. Clean. Prod.* **7**, 181–193 (1999).
280. Kumar, P., Kaur, R., Verma, S., Srivastava, V. C. & Mishra, I. M. The preparation and efficacy of SrO/CeO₂ catalysts for the production of dimethyl carbonate by transesterification of ethylene carbonate. *Fuel* **220**, 706–716 (2018).
281. Zheng, H., Hong, Y., Xu, J., Xue, B. & Li, Y. X. Transesterification of ethylene carbonate to dimethyl carbonate catalyzed by CeO₂ materials with various morphologies. *Catal. Commun.* **106**, 6–10 (2018).
282. Gandara-Loe, J., Jacobo-Azuara, A., Silvestre-Albero, J., Sepúlveda-Escribano, A. & Ramos-Fernández, E. V. Layered double hydroxides as base catalysts for the synthesis of dimethyl carbonate. *Catal. Today* **296**, 254–261 (2017).
283. Du, G. F. *et al.* N-heterocyclic carbene catalyzed synthesis of dimethyl carbonate via transesterification of ethylene carbonate with methanol. *J. Saudi Chem. Soc.* **19**, 112–115 (2015).
284. Romano, U., Tesel, R., Massi Mauri, M. & Rebora, P. Synthesis of dimethyl carbonate from methanol, carbon monoxide, and oxygen catalyzed by copper compounds. *Ind. Eng. Chem. Prod. Res. Dev.* **19**, (1980).
285. Hou, Z. *et al.* High-yield synthesis of dimethyl carbonate from the direct alcoholysis of urea in supercritical methanol. *Chem. Eng. J.* **236**, 415–418 (2014).
286. Wu, X. *et al.* Synthesis of dimethyl carbonate by urea alcoholysis over Zn/Al bi-functional catalysts. *Appl. Catal. A Gen.* **473**, 13–20 (2014).

287. Wu, X. L., Meng, Y. Z., Xiao, M. & Lu, Y. X. Direct synthesis of dimethyl carbonate (DMC) using Cu-Ni/VSO as catalyst. *J. Mol. Catal. A Chem.* **249**, 93–97 (2006).
288. Jiang, C. *et al.* Synthesis of dimethyl carbonate from methanol and carbon dioxide in the presence of polyoxometalates under mild conditions. *Appl. Catal. A Gen.* **256**, 203–212 (2003).
289. Aresta, M. *et al.* Cerium(IV)oxide modification by inclusion of a hetero-atom: A strategy for producing efficient and robust nano-catalysts for methanol carboxylation. *Catal. Today* **137**, 125–131 (2008).
290. Liu, W., Wong, D. S., Wang, S. & Hsu, H. Effect of mass transfer on the design of an extractive distillation process for separating DMC and methanol. *J. Taiwan Inst. Chem. Eng.* **60**, 205–212 (2016).
291. Won, W., Feng, X. & Lawless, D. Separation of dimethyl carbonate/methanol/water mixtures by pervaporation using crosslinked chitosan membranes. *Sep. Purif. Technol.* **31**, 129–140 (2003).
292. Zhang, Z. *et al.* Separation of methanol dimethyl carbonate azeotropic mixture using ionic liquids as entrainers. *Fluid Phase Equilib.* **435**, 98–103 (2017).
293. Gordano, A., Clarizia, G., Torchia, A., Trotta, F. & Drioli, E. New membranes from PEEK-WC and its derivatives. *Desalination* **145**, 47–52 (2002).
294. De Bartolo, L. *et al.* Novel PEEK-WC membranes with low plasma protein affinity related to surface free energy parameters. *J. Mater. Sci. Mater. Med.* **15**, 877–883 (2004).
295. Chen, J. H., Liu, Q. L., Zhu, A. M., Fang, J. & Zhang, Q. G. Dehydration of acetic acid using sulfonation cardo polyetherketone (SPEK-C) membranes. *J. Memb. Sci.* **308**, 171–179 (2008).
296. Hemeda, O. M., Hemeda, D. M. & Said, M. Z. Some physical properties of pure and doped polyvinyl alcohol under applied stress. *Mech. Time-Dependent Mater.* **7**, 251–268 (2003).
297. Kienzle-Sterzer, C. A., Rodriguez-Sanchez, D. & Rha, C. Mechanical properties of chitosan films: Effect of solvent acid. *Die Makromol. Chemie* **183**, 1353–1359 (1982).
298. Mohammad Mahdi Dadfar, S., Kavooosi, G. & Mohammad Ali Dadfar, S. Investigation of mechanical properties, antibacterial features, and water vapor permeability of polyvinyl alcohol thin films reinforced by glutaraldehyde and multiwalled carbon nanotube. *Polym. Compos.* **35**, 1736–1743 (2014).
299. Le, H. R., Qu, S., Mackay, R. E. & Rothwell, R. Fabrication and mechanical properties of chitosan composite membrane containing hydroxyapatite particles. *J. Adv. Ceram.* **1**, 66–71 (2012).
300. Abbott, S., Hansen, C. M. & Yamamoto, H. Hansen solubility parameters in practice complete with eBook, software and data. (Hoersholm Denmark: www.hansen-solubility.com, 2013).
301. Stefanis, E. & Panayiotou, C. Prediction of hansen solubility parameters with a new group-contribution method. *Int. J. Thermophys.* **29**, 568–585 (2008).
302. Wu, H. L., Ma, C. C. M., Li, C. H. & Chen, C. Y. Swelling behavior and solubility parameter of sulfonated poly(ether ether ketone). *J. Polym. Sci. Part B Polym. Phys.* **45**, 1390–1398 (2007).
303. Ravindra, R., Krovvidi, K. R. & Khan, A. A. Solubility parameter of chitin and chitosan. *Carbohydr. Polym.* **36**, 121–127 (1998).
304. Burshe, M. C., Sawant, S. B. & Pangarkar, V. G. Dehydration of glycerine-water mixtures by pervaporation. *J. Am. Oil Chem. Soc.* **76**, 209–214 (1999).

305. Guo, W. F., Chung, T. & Matsuura, T. Pervaporation study on the dehydration of aqueous butanol solutions: a comparison of flux vs. permeance, separation factor vs. selectivity. *J. Memb. Sci.* **245**, 199–210 (2004).
306. Hoy, K. L. Solubility parameter as a design parameter for water-borne polymers and coatings. *J. Coat. Fabr.* **19**, 53–67 (1989).
307. Smuleac, V., Wu, J., Nemser, S., Majumdar, S. & Bhattacharyya, D. Novel perfluorinated polymer-based pervaporation membranes for the separation of solvent/water mixtures. *J. Memb. Sci.* **352**, 41–49 (2010).
308. Schuster, P. Studies on hydrogen bonding: The interaction between carbonyl and hydroxyl groups. *Int. J. Quantum Chem.* **3**, 851–871 (1969).
309. Cheong, W. J., Keum, Y. I. & Ko, J. H. The hydroxyl group-solvent and carbonyl group-solvent specific interactions for some selected solutes including positional isomers in acetonitrile/water mixed solvents monitored by HPLC. *Bull. Korean Chem. Soc.* **23**, 65–70 (2002).
310. Reddy, S. K. & Balasubramanian, S. Liquid dimethyl carbonate: A quantum chemical and molecular dynamics study. *J. Phys. Chem. B* **116**, 14892–14902 (2012).
311. Chen, J. H., Liu, Q. L., Fang, J., Zhu, A. M. & Zhang, Q. G. Composite hybrid membrane of chitosan-silica in pervaporation separation of MeOH/DMC mixtures. *J. Colloid Interface Sci.* **316**, 580–588 (2007).
312. Wang, L., Li, J., Lin, Y. & Chen, C. Crosslinked poly(vinyl alcohol) membranes for separation of dimethyl carbonate/methanol mixtures by pervaporation. *Chem. Eng. J.* **146**, 71–78 (2009).
313. Wang, L., Han, X., Li, J., Zhan, X. & Chen, J. Hydrophobic nano-silica/polydimethylsiloxane membrane for dimethylcarbonate-methanol separation via pervaporation. *Chem. Eng. J.* **171**, 1035–1044 (2011).
314. Zhou, H., Lv, L., Liu, G., Jin, W. & Xing, W. PDMS/PVDF composite pervaporation membrane for the separation of dimethyl carbonate from a methanol solution. *J. Memb. Sci.* **471**, 47–55 (2014).
315. Chen, J. H., Liu, Q. L., Zhu, A. M., Zhang, Q. G. & Fang, J. Pervaporation separation of MeOH/DMC mixtures using STA/CS hybrid membranes. *J. Memb. Sci.* **315**, 74–81 (2008).
316. Xiao, T. *et al.* Preparation of Asymmetric Chitosan Hollow Fiber Membrane and Its Pervaporation Performance for Dimethyl Carbonate/Methanol Mixtures. *J. Applied Polym. Sci.* **115**, 2875–2882 (2010).
317. Vopička, O., Pilnáček, K. & Friess, K. Separation of methanol-dimethyl carbonate vapour mixtures with PDMS and PTMSP membranes. *Sep. Purif. Technol.* **174**, 1–11 (2017).
318. Bartsch, R. A., Way, J. D., Galier, S., Savignac, J. & Roux-de Balman, H. Chemical separations with liquid membranes: an overview. *ACS Symp. Ser.* **642**, 1–8 (1996).
319. Kazemi, P., Peydayesh, M., Bandegi, A., Mohammadi, T. & Bakhtiari, O. Stability and extraction study of phenolic wastewater treatment by supported liquid membrane using tributyl phosphate and sesame oil as liquid membrane. *Chem. Eng. Res. Des.* **92**, 375–383 (2014).
320. Teramoto, M. *et al.* An attempt for the stabilization of supported liquid membrane. *Sep. Purif. Technol.* **21**, 137–144 (2000).

321. Van De Voorde, I., Pinoy, L. & De Ketelaere, R. F. Recovery of nickel ions by supported liquid membrane (SLM) extraction. *J. Memb. Sci.* **234**, 11–21 (2004).
322. Takeuchi, H., Takahashi, K. & Goto, W. Some observations liquid membranes on the stability of supported. *J. Memb. Sci.* **34**, 19–31 (1987).
323. Plechkova, N. V. & Seddon, K. R. Applications of ionic liquids in the chemical industry. *Chem. Soc. Rev.* **37**, 123–150 (2008).
324. Conrad Zhang, Z. Catalysis in Ionic Liquids. *Adv. Catal.* **49**, 153–237 (2006).
325. Hubbard, C. D., Illner, P. & Van Eldik, R. Understanding chemical reaction mechanisms in ionic liquids: Successes and challenges. *Chem. Soc. Rev.* **40**, 272–290 (2011).
326. Fehér, E. *et al.* Enzymatic production of isoamyl acetate in an ionic liquid-alcohol biphasic system. *J. Mol. Catal. B Enzym.* **50**, 28–32 (2008).
327. Toral, A. R. *et al.* Cross-linked *Candida antarctica* lipase B is active in denaturing ionic liquids. *Enzyme Microb. Technol.* **40**, 1095–1099 (2007).
328. Rios, A. P. d. los, Hernandez-Fernandez, F. J., Rubio, M., Gomez, D. & Villora, G. Stabilization of native penicillin G acylase by ionic liquids. *J. Chem. Technol. Biotechnol.* **82**, 190–195 (2007).
329. Dietz, M. L. Ionic liquids as extraction solvents: Where do we stand? *Sep. Sci. Technol.* **41**, 2047–2063 (2006).
330. Ventura, S. P. M. *et al.* Ionic-Liquid-Mediated Extraction and Separation Processes for Bioactive Compounds: Past, Present, and Future Trends. *Chem. Rev.* **117**, 6984–7052 (2017).
331. Fischer, L. *et al.* Ionic liquids for extraction of metals and metal containing compounds from communal and industrial waste water. *Water Res.* **45**, 4601–4614 (2011).
332. Passos, H., Freire, M. G. & Coutinho, J. A. P. Ionic liquid solutions as extractive solvents for value - added compounds from biomass. *Green Chem.* **16**, 4786–4815 (2014).
333. Poole, C. F. & Poole, S. K. Extraction of organic compounds with room temperature ionic liquids. *J. Chromatogr. A* **1217**, 2268–2286 (2010).
334. Chun, S., Dzyuba, S. V. & Bartsch, R. A. Influence of structural variation in room-temperature ionic liquids on the selectivity and efficiency of competitive alkali metal salt extraction by a crown ether. *Anal. Chem.* **73**, 3737–3741 (2001).
335. Wei, G. T., Yang, Z. & Chen, C. J. Room temperature ionic liquid as a novel medium for liquid/liquid extraction of metal ions. *Anal. Chim. Acta* **488**, 183–192 (2003).
336. Zhao, H., Xia, S. & Ma, P. Use of ionic liquids as ‘green’ solvents for extractions. *J. Chem. Technol. Biotechnol.* **80**, 1089–1096 (2005).
337. Kumar, A., Thakur, A. & Panesar, P. S. Lactic acid extraction using environmentally benign Green emulsion ionic liquid membrane. *J. Clean. Prod.* **181**, 574–583 (2018).
338. Menne, S., Pires, J., Anouti, M. & Balducci, A. Protic ionic liquids as electrolytes for lithium-ion batteries. *Electrochem. commun.* **31**, 39–41 (2013).
339. Moreno, M. *et al.* Ionic Liquid Electrolytes for Safer Lithium Batteries. *J. Electrochem. Soc.* **164**, A6026–A6031 (2017).
340. Ding, J. *et al.* Use of ionic liquids as electrolytes in electromechanical actuator systems based on inherently conducting polymers. *Chem. Mater.* **15**, 2392–2398 (2003).

341. Liu, Z., Liu, C., Li, L., Qin, W. & Xu, A. CO₂ separation by supported ionic liquid membranes and prediction of separation performance. *Int. J. Greenh. Gas Control* **53**, 79–84 (2016).
342. Cserjési, P., Nemestóthy, N. & Bélafi-Bakó, K. Gas separation properties of supported liquid membranes prepared with unconventional ionic liquids. *J. Memb. Sci.* **349**, 6–11 (2010).
343. Zhang, X. *et al.* Selective separation of H₂S and CO₂ from CH₄ by supported ionic liquid membranes. *J. Memb. Sci.* **543**, 282–287 (2017).
344. Jiang, Y.-Y. *et al.* SO₂ gas separation using supported ionic liquid membranes. *J. Phys. Chem. B* **111**, 5058–5061 (2007).
345. Ilyas, A. *et al.* Supported protic ionic liquid membrane based on 3-(trimethoxysilyl)propan-1-aminium acetate for the highly selective separation of CO₂. *J. Memb. Sci.* **543**, 301–309 (2017).
346. Sasikumar, B., Arthanareeswaran, G. & Ismail, A. F. Recent progress in ionic liquid membranes for gas separation. *J. Mol. Liq.* **266**, 330–341 (2018).
347. Zhang, F., Sun, W., Liu, J., Zhang, W. & Ren, Z. Extraction separation of toluene/cyclohexane with hollow fiber supported ionic liquid membrane. *Korean J. Chem. Eng.* **31**, 1049–1056 (2014).
348. Izák, P., Ruth, W., Fei, Z., Dyson, P. J. & Kragl, U. Selective removal of acetone and butan-1-ol from water with supported ionic liquid-polydimethylsiloxane membrane by pervaporation. *Chem. Eng. J.* **139**, 318–321 (2008).
349. Izák, P., Köckerling, M. & Kragl, U. Solute transport from aqueous mixture through supported ionic liquid membrane by pervaporation. *Desalination* **199**, 96–98 (2006).
350. Matsumoto, M., Inomoto, Y. & Kondo, K. Selective separation of aromatic hydrocarbons through supported liquid membranes based on ionic liquids. *J. Memb. Sci.* **246**, 77–81 (2005).
351. Papaiconomou, N., Billard, I. & Chainet, E. Extraction of iridium(IV) from aqueous solutions using hydrophilic/hydrophobic ionic liquids. *RSC Adv.* **4**, 48260–48266 (2014).
352. Génand-Pinaz, S., Papaiconomou, N. & Leveque, J. M. Removal of platinum from water by precipitation or liquid-liquid extraction and separation from gold using ionic liquids. *Green Chem.* **15**, 2493–2501 (2013).
353. Gonzalez-Miquel, M., Bedia, J., Palomar, J. & Rodriguez, F. Solubility and diffusivity of CO₂ in [hxmim][NTf₂], [omim][NTf₂], and [dcmim][NTf₂] at T = (298.15, 308.15, and 323.15) K and pressures up to 20 bar. *J. Chem. Eng. Data* **59**, 212–217 (2014).
354. Ab Rani, M. A. *et al.* Understanding the polarity of ionic liquids. *Phys. Chem. Chem. Phys.* **13**, 16831–16840 (2011).
355. Khupse, N. D. & Kumar, A. Contrasting thermosolvatochromic trends in pyridinium-, pyrrolidinium-, and phosphonium-based ionic liquids. *J. Phys. Chem. B* **114**, 376–381 (2010).
356. García, J. I., García-marín, H. & Pires, E. Glycerol based solvents: synthesis, properties and applications. *Green Chem.* **12**, 426–434 (2010).
357. Crowhurst, L., Falcone, R., Lancaster, N. L., Llopis-Mestre, V. & Welton, T. Using Kamlet-Taft solvent descriptors to explain the reactivity of anionic nucleophiles in ionic liquids. *J. Org. Chem.* **71**, 8847–8853 (2006).
358. Kamlet, M. J., Abboud, J.-L. M., Abraham, M. H. & Taft, R. W. Linear solvation energy relationships. 23. A comprehensive collection of the solvatochromic parameters, π^* , α , β ,

- and β , and some methods for simplifying the generalized solvatochromic equation Solvatochromic Equation. *J. Org. Chem* **48**, 2877–2887 (1983).
359. Laurence, C., Nicolet, P., Dalati, M. T., Abboud, J.-L. M. & Notario, R. The empirical treatment of solvent-solute interactions: 15 Years of π^* . *J. Phys. Chem.* **98**, 5807–5816 (1994).
360. Hsu, K. Y., Hsiao, Y. C. & Chien, I. L. Design and control of dimethyl carbonate-methanol separation via extractive distillation in the dimethyl carbonate reactive-distillation process. *Ind. Eng. Chem. Res.* **49**, 735–749 (2010).
361. Zhang, Q., Peng, J. & Zhang, K. Separation of an azeotropic mixture of dimethyl carbonate and methanol via partial heat integration pressure swing distillation. *Asia-Pac. J. Chem. Eng.* 50–64 (2017).
362. Rautenbach, R., Knauf, R., Struck, A. & Vier, J. Simulation and design of membrane plants with AspenPlus. *Chem. Eng. Technol.* **19**, 391–397 (1996).

Curriculum Vitae

Wenqi Li

Université catholique de Louvain, Belgium

SST/IMMC - Institute of Mechanics, Materials and Civil Engineering (iMMC)

IMAP - Materials and process engineering (IMAP)

Place Sainte Barbe 2 bte L5.02.02 à 1348 Louvain-la-Neuve

E-mail : wenqi.li@uclouvain.be; xiaobawang@gmail.com



EDUCATION

Sept. 2014 – 2018 PhD candidate in Science of Engineering and Technology

Université catholique de Louvain, Belgium

Sept. 2011 – Sept. 2014 Master of Chemical Engineering

Katholieke Universiteit Leuven

Sept. 2009 – Sept. 2011 Master of Materials Engineering

Katholieke Universiteit Leuven

PUBLISHED ARTICLES IN PEER-REVIEWED INTERNATIONAL JOURNALS

Wenqi Li, Francesco Galiano, Julien Estager, Damien P. Debecker, Jean-Christophe M. Monbaliu, Alberto Figoli, Patricia Luis, Sorption and pervaporation study of methanol/dimethyl carbonate mixture with poly(etheretherketone) (PEEK-WC) membrane Journal of Membrane Science, 567, 303-310, 2018

Wenqi Li, Ramesh Sreerangappa, Julien Estager, Jean-Christophe M. Monbaliu, Damien P. Debecker, Patricia Luis, Application of pervaporation in the bio-production of glycerol carbonate, Chemical Engineering and Processing: Process Intensification, 132, 127-136, 2018

Wenqi Li, Patricia Luis, Understanding coupling effects in pervaporation of multi-component mixtures, Separation and Purification Technology, 197, 95-106, 2018.

Wenqi Li, Bart Van der Bruggen, Patricia Luis, Recovery of Na₂SO₄ and Na₂CO₃ from mixed solutions by membrane crystallization, Chemical Engineering Research and Design, 106, 315 - 326, 2016.

Jeffrey G. Tait, Tamara Merckx, **Wenqi Li**, Cindy Wong, Robert Gehlhaar, David Cheyns, Mathieu Turbiez, Paul Heremans, Determination of Solvent Systems for Blade Coating Thin Film Photovolatics, Advanced Functional Materials, 2015.

Wenqi Li, Bart Van der Bruggen, Patricia Luis, Integration of reverse osmosis and membrane crystallization for sodium sulphate recovery, Chemical Engineering and Processing: Process Intensification, 85, 57–68, 2014.

ARTICLES UNDER PREPARATION/SUBMITTED IN PEER-REVIEWED INTERNATIONAL JOURNALS

Wenqi Li, Cristhian Molina Fernandez, Julien Estager, Jean-Christophe M. Monbaliu, Damien P. Debecker, Patricia Luis, Application of supported ionic liquid membranes in the separation of methanol/dimethyl carbonate mixtures by pervaporation (Under preparation)

Wenqi Li, Julien Estager, Jean-Christophe M. Monbaliu, Damien P. Debecker, Patricia Luis, Separation of bio-based chemicals using pervaporation: a review. Membranes (Submitted)

Romarc G  rardy, Julien Estager, **Wenqi Li**, Patricia Luis, Damien P. Debecker, Jean-Christophe M. Monbaliu, Continuous Flow Upgrading of Chemicals Derived from Biomass, Chemical Reviews (Under preparation)

INTERNATIONAL CONFERENCES

Wenqi Li, Bart Van der Bruggen, Patricia Luis, Integration of reverse osmosis and membrane crystallization for sodium sulphate recovery, Membrane Distillation and Innovating Membrane Operations in Desalination and Water Reuse (2IWMD2015), Ravello, July 1st - 4th, 2015, Italy. (Oral Presentation)

Wenqi Li, Bart Van der Bruggen, Patricia Luis; Enhancing transesterification reactions by pervaporation. International conferences "Green Chemistry and white biotechnology", 12th – 13th May 2016, Gembloux, Belgium. (Poster presentation)

Wenqi Li, Bart Van der Bruggen, Patricia Luis; Transesterification mixtures separation by pervaporation process using commercial membranes. 2016 EMS Summer School on "Membranes and Membrane Processes Design", 26th June – 1st July 2016, Bertinoro, Italy. (Poster presentation)

Wenqi Li, Bart Van der Bruggen, Patricia Luis; Coupling effects in pervaporation of multi-component mixtures. Journée Jeunes Chercheurs 2016, 6th October, Louvain-la-Neuve, Belgium. (Poster presentation)

Wenqi Li, Ramesh Sreerangappa, Julien Estager, Damien Debecker, Patricia Luis; Application of pervaporation in the production of glycerol carbonate. 3rd edition of international conferences "Green Chemistry and white biotechnology: Industry of the future", 22th – 23th May 2017, University Mons.

Wenqi Li, Patricia Luis; Understanding coupling effects in pervaporation of multi-component mixtures by Hansen Solubility Parameters. 5th International Scientific Conference on Pervaporation, Vapor Permeation and Membrane Distillation, 2017, 20-23th June, Torun, Poland. (Oral Presentation)

Wenqi Li, Francesco Galiano, Figoli Alberto, Julien Estager, Damien Debecker, Patricia Luis; Membrane separation for methanol/dimethyl carbonate mixture. International conferences "Green Chemistry and white biotechnology", 23th – 24th May 2018, Louvain-la-Neuve. (Poster presentation)

Wenqi Li, Francesco Galiano, Figoli Alberto, Julien Estager, Damien Debecker, Patricia Luis; Sorption and pervaporation study of methanol/dimethyl carbonate mixture with poly(etheretherketone) (PEEK) membrane. Euromembrane 2018, 9th – 13th July, 2018. Valencia Spain. (Poster presentation)